

Dissertation zur Erlangung des Doktorgrades  
der Fakultät für Chemie und Pharmazie  
der Ludwig-Maximilians-Universität München

***Matching Phosphorus and  
Chalcogens  
– New Chemistry with Old  
Elements***

*Synthesis of Unusual Anions and Small  
Molecules*

vorgelegt von

Christiane Rotter

aus

Augsburg

**2009**

### **Erklärung**

Diese Dissertation wurde im Sinne von § 13 Abs. 3 bzw. 4 der Promotionsordnung vom 29. Januar 1998 von Herrn Professor Konstantin Karaghiosoff betreut.

### **Ehrenwörtliche Versicherung**

Diese Dissertation wurde selbstständig, ohne unerlaubte Hilfe erarbeitet.

München, am 24.11.2009

---

Christiane Rotter

Dissertation eingereicht am: 24.11.2009

1. Gutachter: Prof. Dr. Konstantin Karaghiosoff

2. Gutachter: Prof. Dr. Thomas M. Klapötke

Mündliche Prüfung am: 11.12.2009

# Danksagung

***Keine Schuld ist dringender, als die, DANKE zu sagen.***

(Marcus Tullius Cicero)

Und diese Schuld möchte ich hiermit begleichen, denn ohne die fachliche, finanzielle und moralische Unterstützung vieler Personen, wäre die Anfertigung der vorliegenden Arbeit nicht möglich gewesen: **V I E L E N D A N K ...**

... meinem Doktorvater, **HERRN PROF. DR. KONSTANTIN KARAGHIOSOFF**, für die Geduld, den fachlichen Rat und das andauernde Interesse an meiner Arbeit.

... **HERRN PROF. DR. THOMAS M. KLAPÖTKE**, für die freundliche Aufnahme in den Arbeitskreis, die fortwährende Unterstützung in jedweder Form, das fachliche Interesse, und die exzellenten Berechnungen.

... meiner **FAMILIE** und meinem **FREUND**, die mich sowohl moralisch, als auch finanziell andauernd unterstützten, und mich immer wieder motiviert haben weiterzumachen.

... **DR. F. XAVER STEEMANN, NORBERT MAYR** und **RICHARD MOLL**, die mir mit Rat und Tat, vor allem in der anstrengenden Schlusszeit, zur Seite gestanden sind, und immer ein offenes Ohr für meine Probleme hatten.

... meinen Praktikanten, **STEFANIE SCHÖNBERGER, MIRIJAM KOHLER, JOWITA HUMIN, CAMILLA EVANGELISTI** (ihr ein besonderer Dank auch für die Berechnungen), **SEBASTIAN GEBLER, KATRIN BEIMLER**, sowie **ALBERTO MAULU**, die durch ihr großartiges Engagement wertvolle Ergebnisse für diese Arbeit beigetragen haben.

... meinen Laborkollegen aus D 3.103, **ALEXANDER PENGER, STEFAN HUBER, SUSANNE SCHEUTZOW**, und vor allem **KARIN LUX** (die mir nicht nur während der Promotionszeit zur Seite gestanden hat) für das entspannte Arbeitsklima.

... **DR. JÖRG STIERSTORFER, WOLFGANG BETZL, DR. F. XAVER STEEMANN** und **DANIEL MAXIEN** die meine Arbeit Korrektur gelesen haben.

... **LEO BERLINGER**, für die Gestaltung des Titelbildes.

... **DR. OLIVER SCHÖN**, für die angeregten Diskussionen, und fortwährende Unterstützung.

... dem gesamten Arbeitskreis Klapötke für die freundliche Atmosphäre.



## TABLE OF CONTENT

### **PHOSPHORUS THE LIVING ELEMENT** **13**

---

#### **RESEARCH OBJECTIVES** **19**

---

1	Thiophosphates $P_n S_m^{x-}$	20
2	Selenophosphates $P_n Se_m^{x-}$	20
3	Tellurophosphates $P_n Te_m^{x-}$	20

### **THE TRUTH ABOUT TRITHIOMETAPHOSPHATE $PS_3^-$ - THE HISTORY OF A FORBIDDEN ANION** **21**

---

1	Introduction	22
2	Results and Discussion	26
2.1	Synthesis of $[nBu_4N]_2[P_2S_6] \cdot THF$ (1) and $[Ph_4P]_2[P_2S_6]$ (2)	26
2.2	$^{31}P$ NMR spectroscopic investigation	30
2.3	Computational results	33
2.4	Chemical behavior of $PS_3^-$	38
2.5	Adduct formation	38
2.6	Comparison of the structures of the adduct stabilized trithiometaphosphate $PS_3^-$	44
3	Conclusion	45
4	Experimental Section	46

### **THE TRISELENOMETAPHOSPHATE ANION $PSe_3^-$ : A SYNTHETIC CHALLENGE** **49**

---

1	Introduction	50
2	Syntheses	51

3	Crystal and Molecular Structure of [pyH][pyPSe <sub>3</sub> ] (1)	54
4	Comparison of the structures of [pyH][pyPS <sub>3</sub> ] and [pyH][pyPSe <sub>3</sub> ]	56
5	Quantum chemical calculation	57
6	Conclusion	61
7	Experimental Section	62

## **ON THE EXISTENCE OF DICHALCOGENOPHOSPHORYL**

### **MONOHALOGENIDES PCh<sub>2</sub>X (Ch = S, Se, Te; X = Cl, Br, I) 65**

1	The Problem with $\sigma^3\lambda^5$ Phosphorus	66
2	New route to pyPCh <sub>2</sub> X (Ch = S, Se, Te; X = Cl, Br, I)	69
3	Reactions of PX <sub>3</sub> with Na <sub>2</sub> S <sub>2</sub> (X = Cl, Br, I)	69
3.1	Reaction of PCl <sub>3</sub> and Na <sub>2</sub> S <sub>2</sub>	69
3.2	Reaction of PBr <sub>3</sub> and Na <sub>2</sub> S <sub>2</sub>	70
3.3	Reaction of PI <sub>3</sub> and Na <sub>2</sub> S <sub>2</sub>	71
4	Reaction of PX <sub>3</sub> with Na <sub>2</sub> Se <sub>2</sub> (X = Cl, Br, I)	71
4.1	Reaction of PCl <sub>3</sub> with Na <sub>2</sub> Se <sub>2</sub>	71
4.2	Reaction of PBr <sub>3</sub> with Na <sub>2</sub> Se <sub>2</sub>	73
4.3	Reaction of PI <sub>3</sub> with Na <sub>2</sub> Se <sub>2</sub>	74
4.4	Reaction of PI <sub>3</sub> with Na <sub>2</sub> Te <sub>2</sub>	74
5	Conclusion	75
6	Experimental Section	76

### **BINARY NEUTRAL PHOSPHORUS SULFIDES py<sub>2</sub>P<sub>2</sub>S<sub>5</sub> AND py<sub>2</sub>P<sub>2</sub>S<sub>7</sub> 79**

1	Introduction	80
2	Results and Discussion	81
3	Quantum chemical calculations	86
4	Conclusion	88
5	Experimental Section	89

**SOME NEWS ABOUT  $P_2S_8^{2-}$  **93****

1	Introduction	94
2	Results and Discussion	95
3	Conclusion	98
4	Experimental Section	99

**STRUCTURAL AND NMR SPECTROSCOPIC INVESTIGATIONS OF  
CHAIR AND TWIST CONFORMERS OF THE  $P_2Se_8^{2-}$  ANION **103****

1	Introduction	104
2	Syntheses	104
3	$^{31}P$ and $^{77}Se$ NMR Spectroscopy of the $P_2Se_8^{2-}$ Anion	105
3.1	$^{31}P$ NMR Spectra of chair- $P_2Se_8^{2-}$	106
3.2	$^{31}P$ NMR spectra of twist- $P_2Se_8^{2-}$	107
3.3	$^{77}Se$ NMR Spectrum of twist – and chair- $P_2Se_8^{2-}$	107
4	Crystal and Molecular Structures of $P_2Se_8^{2-}$ Salts	109
4.1	$[Li(py)_4]_2[P_2Se_8]$ (1)	109
4.2	$[nBu_4N]_2[P_2Se_8] \cdot 2MeCN$ (2)	111
4.3	$[bmim]_2[P_2Se_8]$ (3)	112
4.4	$[Li(MeCN)_4]_2[P_2Se_8]$ (4): First Structure of twist- $P_2Se_8^{2-}$	114
4.5	Comparison of the Structures of $P_2Se_8^{2-}$ Salts	116
5	Computational Results	117
6	Conclusion	122
7	Experimental Section	123

## **A WATERSTABLE SELENOPHOSPHATE ANION: $P_2Se_6^{4-}$ \_\_\_\_\_ 129**

1	Introduction	130
2	Syntheses	131
3	$[pyH]_4[P_2Se_6] \cdot H_2O$ (2)	132
4	$^{31}P$ and $^{77}Se$ Heteronuclear NMR Spectroscopy	134
5	Conclusion	136
6	Experimental Section	137

## **A NEW SYNTHESIS AND CRYSTAL STRUCTURE OF THE OLD**

### **HEXATHIOHYPODIPHOSPHATE $P_2S_6^{4-}$ \_\_\_\_\_ 141**

1	Introduction	142
2	$[py_2Li]_4[P_2S_6] \cdot 2 py$	143
3	Comparison of the structures of $[py_2Li]_4[P_2S_6] \cdot 2py$ and the corresponding selenium compound $[py_2Li]_4[P_2Se_6] \cdot 2 py$	145
4	Conclusion	147
5	Experimental Section	148

### **PHOSPHORUS RICH SELENOPHOSPHATES \_\_\_\_\_ 151**

1	Introduction	152
2	A New Route to Phosphorus Rich Selenophosphate Anions $P_nSe_m^{x-}$	153
3	Reaction of $P_4$ with $P_4Se_7^{2-}$	153
5	Reaction of $P_4$ with $P_4Se_3$ and $Na_2Se_2$	157

### **TRIS(PENTAFLUOROPHENYLSELENO)PHOSPHINE $(C_6F_5Se)_3P$ \_\_\_\_\_ 161**

1	Introduction	162
2	Results and Discussion	163
3	Conclusions	165
4	Experimental Section	166

## **DO BINARY PHOSPHORUS TELLURIUM ANIONS EXIST? 167**

1	Introduction	168
2	Synthesis and NMR analysis of $P_4Te_2^{2-}$	169
3	Quantum chemical calculations	174
4	Are there more phosphorus-tellurium anions?	175
5	Conclusion	177
6	Experimental Section	178

## **SOME UNEXPECTED COMPOUNDS IN THE REACTION OF WHITE PHOSPHORUS, LITHIUM AND TELLURIUM 179**

1	Introduction	180
2	Results and Discussion	180
3	Conclusion	189
4	Experimental Section	190
4.1	Syntheses of new P-Te anions outgoing from the elements	191
4.2	Syntheses of $(N-MeIm)_2P_4Li_2$	191
4.3	Syntheses of $(N-MeIm)_2PLi$	192
4.4	Reaction of $(N-MeIm)_2PLi$ with tellurium	193

## **CONCLUSION 195**

1	$\sigma^3\lambda^5$ - An unusual bonding situation for the phosphorus atom	195
2	Alternative syntheses for chalcogenophosphates	196
3	New fields of chalcogenophosphate chemistry	196
	- a first insight into P, Te anions	196





Matching Phosphorus and Chalcogens  
-New Chemistry with Old Elements-

Synthesis of Unusual Anions and Small Molecules

Christiane Rotter



# CHAPTER I

---

## Phosphorus the Living Element

Mit Eifer hab' ich mich der Studien beflissen;  
Zwar weiß ich viel, doch möcht' ich alles wissen  
Goethe, Faust I

This citation is most probable the motivation of every chemist to make chemical research. It is the inquisitiveness to discover, learn about and understand new, exciting fields of chemistry.

One of the most fascinating elements is phosphorus, due to its versatile chemistry and properties.

Phosphorus was discovered by the alchemist, researched by the early chemists, exploited by the industrialists of the nineteenth century and abused by the combatants of the twentieth.<sup>1</sup>

Elemental white (or yellow) phosphorus was accidentally discovered by Henning Brandt 1669 in Hamburg. Brandt searched for the philosopher's stone, like every alchemist at that time. He dried urine in a glass vessel and added then some charcoal. After heating the vessel glowing fumes appeared and a liquid, which bursts into flames immediately when having contact with air, dripped out of the vessel opening – white phosphorus has been prepared for the first time.<sup>1</sup>

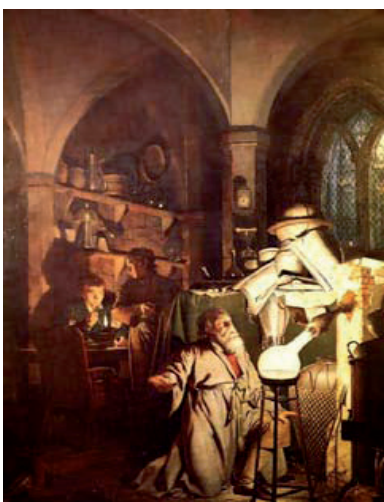


Figure 1. The Alchemist in Search of the Philosopher's Stone, by Joseph Wright of Derby, 1771.

---

<sup>1</sup> Emsley, J. *The Sordid Tale of Murder, Fire and Phosphorus – The 13<sup>th</sup> Element*, John Wiley & Sons, Inc., New York, 2000.

Since that, phosphorus fascinated the chemists because of its incomparable properties. The glow of phosphorus gave the element its name: it originates from the greek word *phosphoros*, which means *light bringing*. Due to its glow phosphorus was believed to have healing powers, so it was widely used as medicine for almost every disease. But since white phosphorus is poisonous and may cause death, no one could ever be cured from any suffering, so suffering was most probable alleviated and definitely shortened, however.

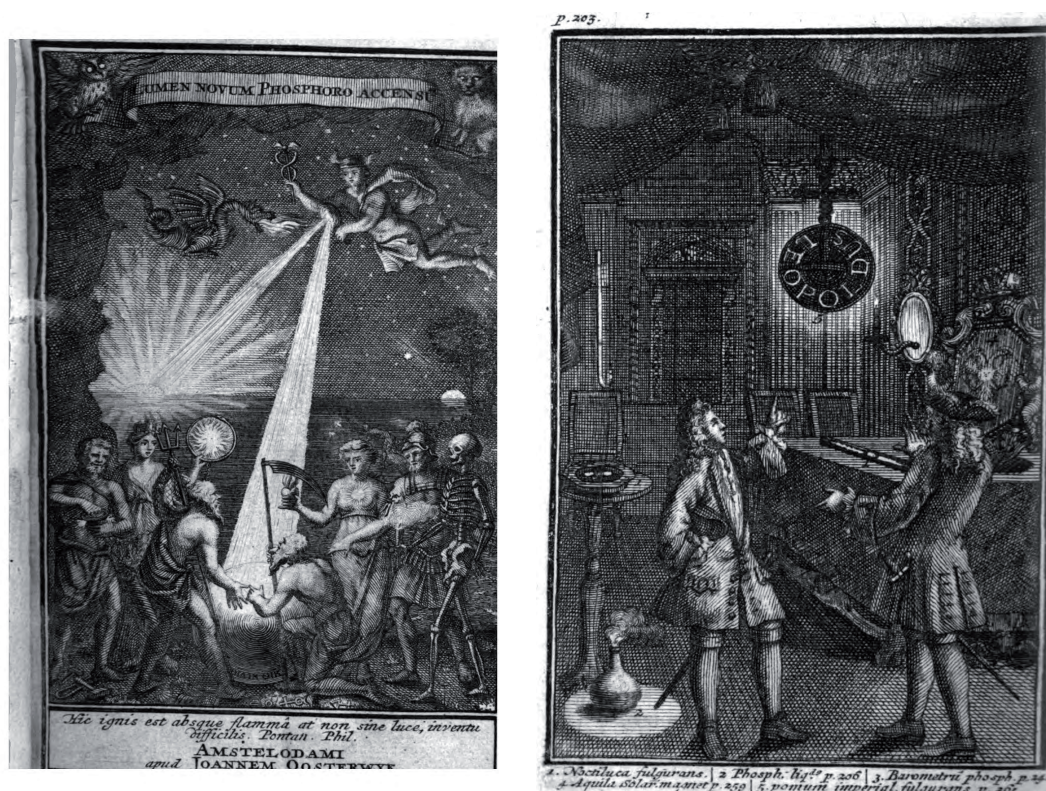


Figure 2. Title page of Johann Heinrich Cohausen's book about phosphorus, 1717 (left) and illustration in the same book (right). It demonstrates that it was believed the glow was made by supernatural powers.

White phosphorus brought light to the people in the 18<sup>th</sup> century in the truest sense of the word in terms of friction matches called *Lucifers*. In times where only flint and tinder could be used to make fire the Lucifer matches were considered as blessing as it was now possible to light fire everywhere. Nevertheless the other side of the coin was called *Phossy Jaw* – a serious disease causing the degradation of the jaw bone.



Figure 3. Lucifer matches which could be struck everywhere.

The match-makers suffered from phossy jaw, especially those who dipped the matches. But it was not before the 2<sup>nd</sup> world war white phosphorus got disrepute due to its use in phosphorus bombs, which cause bad injuries and painful death.

So deadly phosphorus in its elemental form can be, so essential are phosphorus compounds for living organism, especially the phosphate moiety plays a major role as it is the limiting factor for life itself, being part of the DNA and ATP.

We may be able to substitute nuclear power for coal, and plastics for wood, and yeast for meat, and friendliness for isolation – but for phosphorus there is neither substitute nor replacement.<sup>2</sup>

In the form of detergents and food additives phosphate compounds make our daily life easier. Of particular importance is the role of phosphate compounds as fertilizers as the natural availability of phosphate is the most important growth factor of plants. Only with the invention of phosphate fertilizers it is possible to yield a large crop.

Recently a very special phosphate, the lithium iron phosphate  $\text{LiFePO}_4$  attracts more and more attention, as its application as cathode material in highly efficient lithium ion accumulators is much appreciated.<sup>3</sup>

Life can multiply until all the phosphorus has gone and then there is an inexorable halt which nothing can prevent.<sup>2</sup>

<sup>2</sup> Asimov, I. *Asimov on Chemistry*, Macdonald & Jane's, London, 1975.

<sup>3</sup> Padhi, A. K.; Nanjundaswamy, K. S.; Goodenough, J. B. *J. Electrochem. Soc.* 1997, 144(4), 1188.

Consequently, oxophosphates  $P_nO_m^{x-}$  are very well investigated and represent an integral part in chemistry textbooks. In contrast chalcogenophosphates  $P_nCh_m^{x-}$  containing the heavier chalcogens sulfur, selenium and tellurium are much less investigated and therefore still represent a challenge in the field of inorganic chemistry. Indeed only a limited number of thiophosphate anions  $P_nS_m^{x-}$  and only a few selenophosphate anions  $P_nSe_m^{x-}$  have been described in the literature so far.<sup>4</sup> In the case of tellurophosphate anions only one example has been described in literature. Mewis et al. found in crystalline  $BaP_4Te_2$ .<sup>5</sup> Considering only the selenophosphates  $P_nSe_m^{x-}$  many contributions to these compounds originate from the groups of Kanatzidis and Dorhout.<sup>6</sup>

The increasing interest in metal chalcogenophosphates with the heavier chalcogens sulfur and selenium due to their interesting material properties like ion conductivity<sup>3</sup> or optoelectrical<sup>7</sup> properties stimulates the search for new and in particular phosphorus rich chalcogenophosphate anions. The classical syntheses of metal chalcogenophosphates are mainly the domain of solid state chemistry. They involve reactions at high temperatures in the melt, under hydrothermal conditions or using polychalcogenide fluxes.<sup>4,5,6</sup> So there is a need to investigate new syntheses routes under kinteical conditions.

In our research work group a new method to synthesize chalcogenophosphates has been developed outgoing from easily available educts in solution at ambient temperature or below, thus making the formation of metastable chalcogenophosphate anions possible.<sup>8</sup> Remarkably the thio- and selenophosphates show a much larger structural diversity than the oxophosphates. Especially concerning the selenophosphates, structural motives can be found like in polyphosphides or neutral binary phosphorus selenides.

The use of organic cations like  $Ph_4P^+$  or  $nBu_4N^+$  makes it possible to isolate the chalcogenophosphate anions in the solid state. The yielded salts are soluble in common organic solvents thus opens up the possibility to investigate the further chemistry of those compounds.

<sup>4</sup> (a) Klingen, W.; Ott, R.; Hahn, H. Z. *Anorg. Allg. Chem.*, **1973**, 396, 271. (b) Krause, W.; Falius, H. Z. *Anorg. Allg. Chem.*, **1983**, 496, 80. (c) Chan, B. C.; Hess, R. F.; Feng, P. L.; Abney, K. D.; Dorhout, P. K. *Inorg. Chem.*, **2005**, 44, 2106, and references therein.

<sup>5</sup> Mewis, A.; Jörgens, S.; Johrendt, D. *Chem. Eur. J.*, **2003**, 9, 2405.

<sup>6</sup> (a) Chung, I.; Karst, A. L.; Weliky, D.; Kanatzidis, M. G. *Inorg. Chem.* **2006**, 45, 2785. (b) Chung, I.; Malliakas, C. D.; Jang, J. I.; Canlas, C. G.; Weiky, D. P.; Kanatzidis, M. G. *J. Am. Chem. Soc.* **2009**, 129(48), 14996. (c) Chung, I.; Karst, A. L.; Weliky, C. G.; Kanatzidis, M. G. *Inorg. Chem.* **2004**, 43, 2785. (d) Briggs Piccoli, P. M.; Abney, K. D.; Schoonover, J. R.; Dorhout, P. K. *Inorg. Chem.* **2000**, 39, 2970. (e) Chan, B. C.; Hess, R. F.; Feng, P. L.; Abney, K. D.; Dorhout, P. K. *Inorg. Chem.* **2005**, 44(6), 2106.

<sup>7</sup> Galdámez, A.; Manríquez, V.; Kasaneva, J.; Avila, R. E. *Mater. Res. Bull.* **2003**, 38, 1063.

<sup>8</sup> (a) Schuster, M. *dissertation*, LMU Munich, **1999**. (b) Schuster, M.; Karaghiosoff, K. *Phosphorus, Sulfur Silicon and Relat. Elem.* **2001**, 168, 117. (c) Rotter, C.; Schuster, M.; Kidik, M.; Schön, O.; Klapötke, T. M.; Karaghiosoff, K. *Inorg. Chem.* **2008**, 47, 1663.

---

Although the chalcogenophosphate chemistry is an already established field of research among phosphorus chemistry, there is still a big lack of knowledge concerning the following points:

- *Small molecules with a central phosphorus atom in unusual bonding situations (e.g.  $\sigma^3\lambda^5$  or  $\sigma^2\lambda^3$ ) are rarely described and even much less explored concerning stability, reactivity and bonding situation*
- *Analogies and differences to the nitrogen chemistry should be examined*
- *As phosphorus containing compounds which are analogue to nitrogen-chalcogen-compounds are forbidden by the double bond rule and by the classical chemical view of the world, it is a particular challenge for a phosphorus chemist to investigate this special, unanswered topic of phosphorus chemistry*
- *Nevertheless, scientific research should also always result in contributions to solution of daily life problems. So it is important to gain knowledge about the syntheses of compounds which could find practical applications*

The above mentioned considerations are the starting point for the idea and concept of the following thesis. The formulated goals listed below should be received within this thesis.



## CHAPTER II

---

### Research Objectives



*Main research objectives of the present thesis are the development of synthetic procedures to prepare and isolate new simple neutral and anionic phosphorus chalcogen species. Their identity should be established by means of heteronuclear ( $^{31}\text{P}$ ,  $^{77}\text{Se}$ ,  $^{125}\text{Te}$ ) NMR spectroscopy and single crystal X-ray diffraction. Their chemical properties should be investigated. The investigations should enable us to compare in detail the chemistry of N-O compounds with the heavier homologues P-S(Se, Te). Quantum chemical calculations (in collaboration with Prof. Thomas M. Klapötke and Camilla Evangelisti, B. Sc.) should help us to understand analogies and differences.*

### 1 Thiophosphates $P_nS_m^{x-}$

It was planned to put light on the mystery around the  $PS_3^-$  anion. Does it really exist and is it in deed a “heavy nitrate”, or does it show completely different properties? For this synthesis of a salt containing the  $PS_3^-$  anion and NMR spectroscopical investigations concerning the reaction behaviour in basic solvents should be carried out. In addition, the formation and reaction behaviour of the corresponding dimer  $P_2S_6^{2-}$  and trimer  $P_3S_9^{3-}$  should be investigated. At the same time, quantum chemical calculations should be made to help to explain the experimental results obtained.

In addition, the investigations should be extended to neutral compounds like  $P_2S_5$  or  $PS_2Cl$ , which have the same interesting bonding situation for the central phosphorus atom ( $\sigma^3\lambda^5$ ) like in case of the  $PS_3^-$  anion. Does the change from an anionic species to neutral affect the stability of these compounds?

### 2 Selenophosphates $P_nSe_m^{x-}$

The investigations on  $PS_3^-$  (see above) should be extended to the corresponding selenium derivative  $PSe_3^-$ . Which analogies and differences can be observed for the two systems? The planned investigations includes the development of a synthesis for  $PSe_3^-$  salts, the possible isolation of acid-base adducts and again the elucidation of the bonding situation by means of quantum chemical calculations.

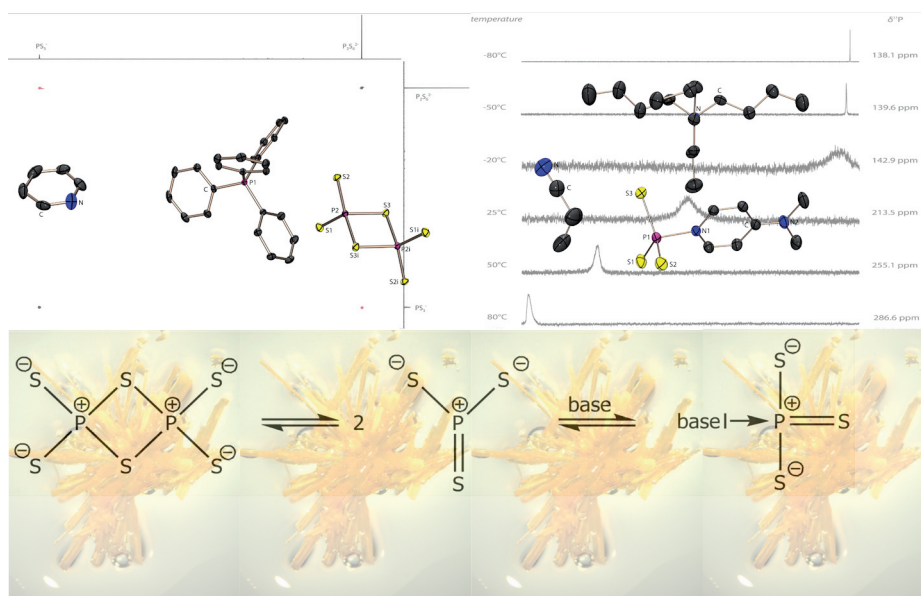
In addition, the syntheses of new phosphorus rich selenophosphates as well as of new soluble salts of selenium rich selenophosphates should be attempted.

### 3 Tellurophosphates $P_nTe_m^{x-}$

A particular intriguing question regards the existence of unstable soluble tellurophosphates. This point represents a central objective of the present thesis. Do phosphorus-tellurium anions exist at all? Different synthetic strategies, e. g. starting from the elements ( $P_4$ , Li, Te), should be attempted, in order to give an answer to this challenging question.

## CHAPTER III

### The Truth about Trithiometaphosphate $PS_3^-$ - the History of a Forbidden Anion



Two new salts containing the  $P_2S_6^{2-}$  anion have been prepared as well as a new salt of the donor-stabilized monotrithiometaphosphate  $PS_3^-$  starting from  $P_4S_3$ ,  $Na_2S_2$  and elemental sulfur in common organic solvents like THF or acetonitrile.  $^{31}P$ ,  $^{31}P$  EXSY NMR spectroscopy was used to proof the existence of free monomeric trithiometaphosphate anion in solution, and to determine its  $^{31}P$  NMR chemical shift, as well as the one of  $P_2S_6^{2-}$ . Temperature dependent  $^{31}P$  NMR spectroscopy was used to reveal the equilibrium between the adduct stabilized monomeric trithiometaphosphate and the free monomeric trithiometaphosphate in solution. Quantum chemical calculations were performed to elucidate the bonding situation in the trithiometaphosphate  $PS_3^-$  and the formation of the dimeric ( $P_2S_6^{2-}$ ) and trimeric ( $P_3S_9^{3-}$ ) trithiometaphosphate in solution.

## 1 Introduction

Binary nitrogen-oxygen anions are well known and represent an integral part of every textbook of inorganic chemistry.<sup>1</sup> The most prominent exponent of representative species with the general formula  $\text{PnCh}_3^-$  ( $\text{Pn} = \text{N, P}$ ;  $\text{Ch} = \text{O, S, Se}$ ) is the nitrate anion  $\text{NO}_3^-$ , which has a trigonal planar structure. Oligomers of  $\text{NO}_3^-$  are not known. Besides the trigonal planar  $\text{NO}_3^-$  molecule a structural isomer, the unstable peroxyxynitrite consisting of a bent ONOO chain is known (Scheme 2).

On introduction of sulfur in place of oxygen in  $\text{NO}_3^-$ , the corresponding  $\text{NS}_3^-$  anion does not adopt a trigonal planar structure like  $\text{NO}_3^-$  but has the structure of trithiooxyxynitrite, consisting of a bent SNSS chain (Scheme 2). A  $\text{NSe}_3^-$  compound is still not described in literature.

The situation changes drastically if nitrogen is replaced by the higher homologue phosphorus. Due to the low tendency of the elements of the third period to form double bonds, small anions consisting of a central phosphorus atom in a low coordination number CN ( $\text{CN} = 2-3$ ) are less favored. Stable cyclic oligomers are formed which could be isolated as metal salts.

A monomeric trioxometaphosphate  $\text{PO}_3^-$  is only known as reactive intermediate in the gas phase: instead cyclic oligomers  $(\text{PO}_3^-)_n$  ( $n = 3-8$ ) are thermodynamically and structurally favored.<sup>1,2,3,4,5</sup> In case of trithioxyxynitrite anion  $\text{PS}_3^-$ , the corresponding dimer, trimer and tetramer  $(\text{PS}_3^-)_n$  ( $n = 2-4$ ) are described in literature.

6,7,8,9,10

<sup>1</sup> Holleman, A.; Wiberg, E.; Wiberg, N. *Lehrbuch der Anorganischen Chemie* 102<sup>nd</sup> edition, **2007**, Walter de Gruyter, Berlin – New York.

<sup>2</sup> Henchman, M.; Viggiano, A. A.; Paulsen, J. F.; Freedman, A.; Wormhoudt, J. J. *Am. Chem. Soc.* **1985**, *107*(5), 265-266.

<sup>3</sup> Westheimer, F. H. *Chem. Rev.* **1981**, *81*, 313-326.

<sup>4</sup> Meisel, M. *Multiple Bonds and Low Coordination in Phosphorus Chemistry*, Georg Thieme Verlag, Ed.: M. Regitz, O. J. Scherer, Stuttgart, **1990**, 415-442.

<sup>5</sup> Binnewies, M.; Schnöckel, H. *Chem. Rev.* **1990**, *90*, 321-330.

<sup>6</sup> Roesky, H. W.; Ahlrichs, R.; Brode, S. *Angew. Chem.* **1986**, *98*, 91-93.

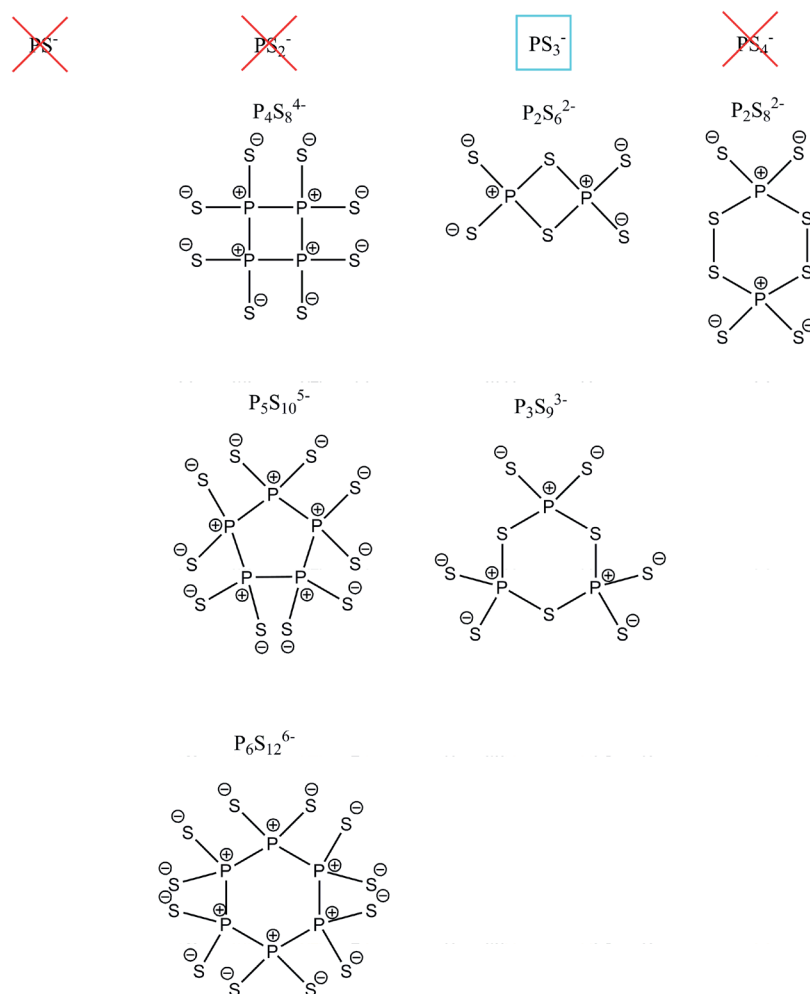
<sup>7</sup> a) Gjikaj, M.; Ehrhardt, C.; Brockner, W. *Z. Naturforsch.* **2006**, *61b*(9), 1049-1053. b) Gjikaj, M.; Brockner, W. *Z. Anorg. Allg. Chem.* **2006**, *632*(2), 279-283. c) Dimitrov, A.; Hartwich, I.; Ziemer, B.; Heidemann, D.; Meisel, M. *Z. Anorg. Allg. Chem.* **2005**, *631*(12), 2439-2444. d) Gjikaj, M.; Brockner, W. *Vibr. Spec.* **2005**, *39*(2), 262-265. e) Gjikaj, M.; Adam, A.; Diewel, M.; Brockner, W. *Kristallograph.* **2005**, *220*(1), 67-68. f) Angenault, J.; Cieren, X.; Wallez, G.; Quarton, M. *J. Solid State Chem.* **2000**, *153*(1), 55-65. g) Salmon, P. S.; Xin, S.; Fischer, H. E. *Phys. Rev.* **1998**, *58B*(10), 6115-6123. h) Menzel, F.; Brockner, W.; Ystenes, M. *Vibrational Spec.* **1997**, *14*(1), 59-70. i) Voroshilov, Y. V.; Potorii, M. V.; Gebesh, V. Y. *Neorganicheskie Materialy* **1994**, *30*(4), 479-483. j) Menzel, F.; Brockner, W.; Ystenes, M. *J. Mol. Struct.* **1993**, *294*, 53-56. k) Andrae, H.; Blachnik, R. *J. Alloys Compd.* **1992**, *189*(2), 209-215. l) Lathrop, D.; Franke, D.; Maxwell, R.; Tepe, T.; Flesher, R.; Zhang, Z.; Eckert, H. *Solid State Nucl. Magn. Reson.* **1992**, *1*(2), 73-83. m) Ystenes, M.; Brockner, W.; Menzel, F. *Z. Naturforsch.* **1992**, *47a*(4), 614-618. n) Andrae, H.; Blachnik, R. *J. Thermal Anal.* **1989**, *35*(2), 595-607. o) Ohse, L.; Brockner, W. *Z. Naturforsch.* **1988**, *43*(5), 494-496. p) Jandali, M. Z.; Eulenberger, G.; Hahn, H. *Z. Anorg. Allg. Chem.* **1985**, *530*, 144-154. q) Brockner, W.; Becker, R.; Eisenmann, B.; Schaefer, H. *Z. Anorg. Allg. Chem.* **1985**, *520*, 51-58. r) Becker, R.; Brockner, W. *Z. Naturforsch.* **1984**, *39A*(11), 1120-1121. s) Toffoli, P.; Khodadad, P.; Rodier, N. *Acta Crystallogr.* **1978**, *B34*(12), 3561-3564.

<sup>8</sup> a) Hanko, J. A.; Kanatzidis, M. G. *J. Solid State Chem.* **2000**, *151*(2), 326-329. b) Hanko, J. A.; Sayettat, J.; Jobic, S.; Brec, R.; Kanatzidis, M. G. *Chem. Mater.* **1998**, *10*(10), 3040-3049. c) Wolf, G. U.; Meisel, M. *Z. Anorg. Allg. Chem.* **1982**, *494*, 49-54.

<sup>9</sup> Evain, M.; Brec, R.; Ouyard, G.; Rouxel, J. *Mat. Res. Bull.* **1984**, *19*, 41-48.

<sup>10</sup> Karaghiosoff, K.; Schuster, M. *Phosphorus, Sulfur Silicon Relat. Elem.* **2001**, *168*, 117-122.

The anion  $\text{PS}_4^-$  does not exist, in contrast to the corresponding dimer  $\text{P}_2\text{S}_8^{2-}$  (Scheme 1). The same situation could be found for the anion  $\text{PS}_2^-$ . The twofold coordination of the phosphorus atom is avoided by forming the annular oligomers  $\text{P}_4\text{S}_8^{4-}$ ,  $\text{P}_5\text{S}_{10}^{5-}$  and  $\text{P}_6\text{S}_{12}^{6-}$ .



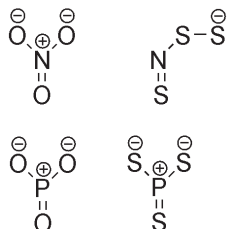
Scheme 1. Binary phosphorus-sulfur anions.

<sup>1</sup> a) Dastychova, L.; Sotolarova, M.; Dastych, D.; Taraba, J.; Necas, M.; Prihoda, J. *Polyhedron* **2007**, *26*(15), 4250-4256. b) Katrusiak, A. J. *Mol. Struct.* **1999**, *474*, 125-133. c) Falius, H.; Schliephake, A.; Schomburg, D. Z. *Anorg. Allg. Chem.* **1992**, *611*, 141-148. d) Jones, P. G.; Weinkauff, A. *Acta Crystallogr.* **1991**, *C47*(3), 686-687. e) Micu-Semeniuc, R.; Popse, S.; Haiduc, I. *Rev. Roum. Chim.* **1983**, *28*(6), 605-614. f) Minshall, P. C.; Sheldrick, G. M. *Acta Crystallogr.* **1978**, *B34*(4), 1378-1380.

<sup>2</sup> a) Badeeva, E. K.; Krivolapov, D. B.; Gubaidullin, A. T.; Litvinov, I. A.; Batyeva, E. S.; Sinyashin, O. G. *Mendeleev Commun.* **2005**, *1*, 22-23. b) Falius, H.; Schliephake, A. B. *Inorg. Synth.* **1989**, *25*, 5-7. c) Buerger, H.; Pawelke, G.; Falius, H. *Spectrochim. Acta* **1981**, *37A*(9), 753-755. d) Falius, H.; Krause, W.; Sheldrick, W. S. *Angew. Chem.* **1981**, *93*(1), 121-122.

<sup>3</sup> Krause W.; Falius, H. Z. *Allg. Anorg. Chem.* **1983**, *496*, 80-93.

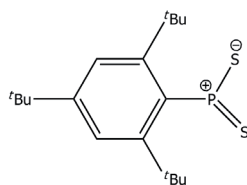
The compound of our interest is the trithiometaphosphate anion  $\text{PS}_3^-$ , which is structurally analogue to the well known nitrate anion  $\text{NO}_3^-$  (Scheme 2).



**Scheme 2.** Lewis formula of  $\text{NO}_3^-$ ,  $\text{NS}_3^-$ ,  $\text{PO}_3^-$  and  $\text{PS}_3^-$ .

But why is the trithiometaphosphate anion  $\text{PS}_3^-$  so unusual compared to the  $\text{NO}_3^-$  anion?

In order to answer this question, we have to have a closer look at the bonding situation of the central phosphorus atom, which is in an unusual bonding situation. The coordination of the central phosphorus atom in  $\text{PS}_3^-$  is planar. The phosphorus center has the formal oxidation state +V, but is only threefold coordinated and has therefore an unsaturated coordination sphere. One possibility to stabilize compounds with such a central phosphorus atom was investigated by Yoshifuji et al.<sup>4,5</sup> They could show that big bulky substituents can stabilize a  $\sigma^3\lambda^5$  phosphorus atom.

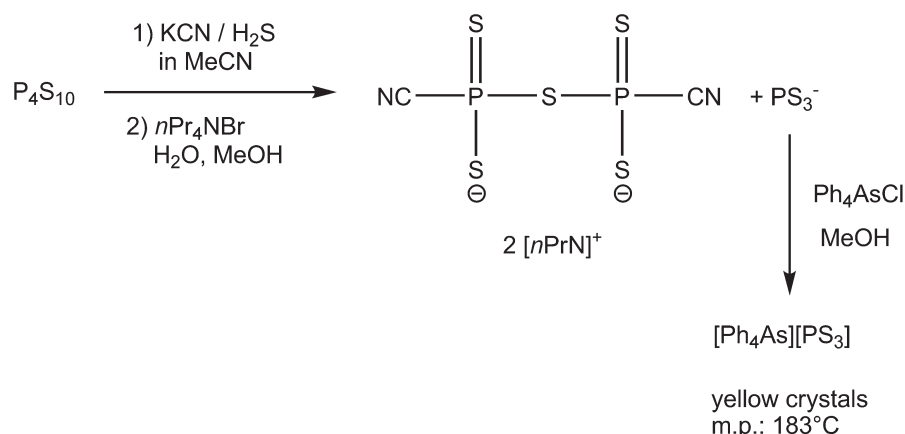


**Scheme 3.** Example for a dithioxophosphorane stabilized with the bulky substituent supermesityl.

But this sterical protection is missing in the  $\text{PS}_3^-$  anion. Due to this reason, the synthesis of the trithiometaphosphate anion  $\text{PS}_3^-$  is a very appealing preparative challenge. Obviously, Roesky and coworkers had the same idea and tried to find an answer for the problem.<sup>6</sup> They investigated the nucleophilic degradation of  $\text{P}_4\text{S}_{10}$  with  $\text{KCN}/\text{H}_2\text{S}$  in acetonitrile which resulted in the formation of the  $(\text{NCPS}_2)_2\text{S}^{2-}$  anion, isolated as the  $n\text{Pr}_4\text{N}^+$  salt on addition of  $n\text{Pr}_4\text{NBr}$  in  $\text{H}_2\text{O}/\text{MeOH}$  (Scheme 4).

<sup>4</sup> Yoshifuji, M.; Toyota, K.; Ando, K.; Inamoto, N. *Chemistry Lett.*, **1984**, 317-318.

<sup>5</sup> Yoshifuji, M.; Sangu, S.; Kamijo, K.; Toyota, K. *Chem. Ber.* **1996**, *129*, 1049.



**Scheme 4.** Synthesis and isolation of the trithiometaphosphate anion  $\text{PS}_3^-$  by Roesky et al.

On further addition of  $\text{Ph}_4\text{AsCl}$  in methanol yellow crystals formed, which the authors claim to be the tetraphenylarsonium salt of the trithiometaphosphate anion  $[\text{Ph}_4\text{As}][\text{PS}_3]$ . Evidence is provided in form of elemental analysis, mass spectra and  $^{31}\text{P}$  NMR spectra ( $\delta^{31}\text{P} = 52.3$  ppm).

But there are some problems which raise some doubts about the correctness of the result: Roesky et al. claimed that it was not possible to solve the crystal structure for sure due to a disorder of the anion. In addition, they used water and methanol as reaction medium, but to our knowledge and experiences with thiophosphates in general, this kind of compounds are unlikely to be stable or preparable in water as they are extremely sensitive towards moisture and oxidation. But the most important hint that Roesky et al. could probably be wrong is the reported  $^{31}\text{P}$  NMR chemical shift of 52.3 ppm. For a  $\sigma^3\lambda^5$  phosphorus atom, a  $^{31}\text{P}$  NMR resonance at much lower field is to be expected comparable to the ones reported by Yoshifuji et al. for thiooxophosphoranes at about  $\delta^{31}\text{P} = 300$ .<sup>14,15</sup>

Nevertheless, the corresponding cyclic oligomers  $\text{P}_2\text{S}_6^{2-}$ ,  $\text{P}_3\text{S}_9^{3-}$  and  $\text{P}_4\text{S}_{12}^{4-}$  are described in literature for sure.<sup>7,8,9</sup> Most of the contributions to the investigation of the monomeric and dimeric trithiometaphosphate  $\text{PS}_3^-$  and  $\text{P}_2\text{S}_6^{2-}$  originate from the group of Brockner.<sup>7</sup>

## 2 Results and Discussion

### 2.1 Synthesis of $[n\text{Bu}_4\text{N}]_2[\text{P}_2\text{S}_6] \cdot \text{THF}$ (**1**) and $[\text{Ph}_4\text{P}]_2[\text{P}_2\text{S}_6]$ (**2**)

$\text{PS}_3^-$  was accessible by the reaction of  $\text{P}_4\text{S}_3$  with  $\text{Na}_2\text{S}_2$  and  $\text{S}_8$  in THF as developed in course of this work (Scheme 5).<sup>6</sup>



Scheme 5. Synthesis of  $\text{PS}_3^-$  in solution.

After adding  $n\text{Bu}_4\text{Br}$  to the reaction solution, yellow rod shaped crystals could be obtained (Figure 1).



Figure 1. Crystals of  $[n\text{Bu}_4\text{N}]_2[\text{P}_2\text{S}_6] \cdot \text{THF}$  (**1**).

Interestingly, the anion of the compound obtained is formed by the cyclic dimer  $\text{P}_2\text{S}_6^{2-}$  of the trithiometaphosphate anion (Figure 2). The geometry of the anion  $\text{P}_2\text{S}_6^{2-}$  does not differ from those reported in literature. It consists of a planar four-membered ring formed by two phosphorus and two sulfur atoms. Four further sulfur atoms are bonded exocyclic to the two phosphorus atoms standing orthogonal to the ring plane. The averaged endocyclic P-S distance is 214.9(1) pm while the averaged exocyclic P-S distance is shorter with 196.4(1) pm. Both central phosphorus atoms are distorted tetrahedrally surrounded by four sulfur atoms. The averaged angles are  $\text{S}_{\text{exo}}-\text{P}-\text{S}_{\text{exo}}$  116.6(1)°,  $\text{S}_{\text{exo}}-\text{P}-\text{S}_{\text{endo}}$  111.6(1)°,  $\text{S}_{\text{endo}}-\text{P}-\text{S}_{\text{endo}}$  90.9(1)° and  $\text{P}-\text{S}_{\text{endo}}-\text{P}$  88.9(1)°. Selected parameters of the structure are given in Table 1.

One complete  $\text{P}_2\text{S}_6^{2-}$  anion can be observed within the unit cell together with two  $\text{P}_2\text{S}_6^{2-}$  anions which lie on an inversion center and therefore are in half generated by symmetry. That is the reason why only four cations are shown in the molecular structure of **1** (Figure 2).

<sup>6</sup> Karaghiosoff, K.; Schuster, M. *Phosphorus, Sulfur Silicon Relat. Elem.* **2001**, *168*, 117-122.

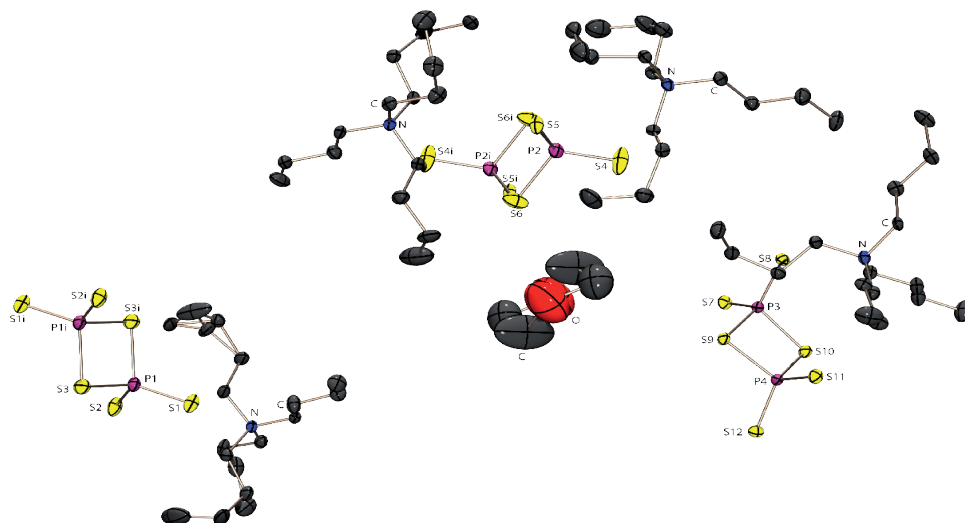
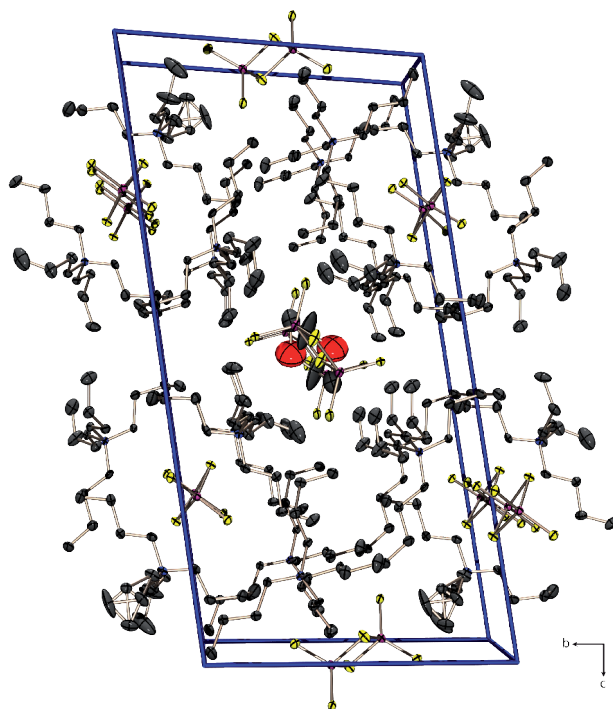


Figure 2. Molecular structure of  $[n\text{Bu}_4\text{N}]_2[\text{P}_2\text{S}_6] \cdot \text{THF}$ . Thermal ellipsoids of all non hydrogen atoms are drawn at the 50 % probability level; hydrogen atoms are omitted for clarity. View orthogonal to  $c$  axis;  $i = -x, 2-y, 2-z$ ;  $ii = 1-x, 1-y, 2-z$ .

Table 1. Selected bond lengths (pm) and angles ( $^\circ$ ) of 1;  $i = -x, 2-y, 2-z$ ;  $ii = 1-x, 1-y, 2-z$ .

Distances [pm]				Angles [ $^\circ$ ]			
P1-S1	196.8(1)	P3-S7	197.0(1)	S1-P1-S2	116.3(1)	S7-P3-S8	117.0(1)
P1-S2	196.7(1)	P3-S8	196.8(1)	S2-P1-S3	111.3(1)	S8-P3-S9	113.0(1)
P1-S3	214.9(1)	P3-S9	214.7(1)	S3-P1-S1	111.7(1)	S9-P3-S7	110.4(1)
P1-S3( <i>i</i> )	213.9(1)	P3-S10	214.8(1)	S1-P1-S3( <i>i</i> )	111.5(1)	S7-P3-S10	110.8(1)
P2-S4	196.8(1)	P4-S9	214.7(1)	S2-P1-S3( <i>i</i> )	112.2(1)	S8-P3-S10	111.7(1)
P2-S5	196.1(1)	P4-S10	214.8(1)	S3-P1-S3( <i>i</i> )	91.1(1)	S9-P3-S10	91.0(1)
P2-S6	213.9(1)	P4-S11	197.2(1)	P1( <i>i</i> )-S3-P1	88.9(1)	P4-S10-P3	88.5(1)
P2-S6( <i>ii</i> )	214.4(1)	P4-S12	196.8(1)	S4-P2-S5	117.1(1)	P4-S9-P3	88.4(1)
				S5-P2-S6	112.8(1)	S11-P4-S12	116.4(1)
				S6-P2-S4	111.3(1)	S12-P4-S9	111.0(1)
				S4-P2-S6( <i>ii</i> )	111.0(1)	S9-P4-S11	111.2(1)
				S5-P2-S6( <i>ii</i> )	110.9(1)	S11-P4-S10	112.4(1)
				S6-P2-S6( <i>ii</i> )	90.8(4)	S12-P4-S10	112.2(1)
				P2( <i>ii</i> )-S6-P2	89.2(1)	S9-P4-S10	91.0(1)



**Figure 3.** Unit cell of **1**. View along  $a$  axis. Ellipsoids are drawn at 50 % probability level. Hydrogen atoms are omitted for clarity.

Yellow block shaped crystals of  $[\text{Ph}_4\text{P}]_2[\text{P}_2\text{S}_6] \cdot 2 \text{ py}$  (**2**) were isolated after the addition of tetraphenylphosphonium bromide to a solution containing  $\text{P}_4\text{S}_3$ ,  $\text{Na}_2\text{S}_2$  and elemental sulfur in pyridine. Compound **2** crystallizes in the monoclinic space group  $P2_1/c$  with four formula units in the unit cell.

The  $\text{P}_2\text{S}_6^{2-}$  anion lies on a crystallographic inversion center which is located in the middle of the four-membered ring; therefore half of the anion is generated by symmetry. The four-membered ring consisting of both phosphorus atoms P2 and P2( $i$ ) and two sulfur atoms S3 and S3( $i$ ) has a angle sum of  $360^\circ$  and is therefore planar. The exocyclic bonded sulfur atoms are arranged orthogonal to the ring plane. The P-S bond lengths to the exocyclic sulfur atoms are 198.2(1) pm (P2-S1) and 196.4(1) pm (P2-S2) and therefore within a P-S single bond and a P=S double bond found in phosphorus(V) compounds.<sup>1,14,15</sup> The endocyclic P-S distances correspond with 215.9(1) pm (P2-S3) and 214.3(1) pm (P2( $i$ )-S3) to P-S single bonds. The phosphorus atom is surrounded in a distorted tetrahedral arrangement by four sulfur atoms. The endocyclic S3-P2-S3( $i$ ) angle is  $91.5(1)^\circ$ , whereas the exocyclic S-P-S angles range from  $110.0^\circ$  to  $118.7^\circ$ . The angle at the endocyclic sulfur atom P2-S3-P2( $i$ ) is  $88.5(1)^\circ$ . Selected structural parameters for the  $\text{P}_2\text{S}_6^{2-}$  anion in compound **2** are given in Table 1.

Four  $P_2S_6^{2-}$  anions are located on planes parallel to the  $ab$  – and  $ac$  plane. The anions and cations are staggered separately along the  $a$  axis. There are no significant interactions in the structure than the electrostatic attraction between cations and anions. The pyridine solvent molecules are located between the cations. The position of the nitrogen atom in pyridine can exactly be determined.

Table 2. Selected bond lengths (pm) and angles ( $^\circ$ ) of  $[Ph_4P]_2[P_2S_6] \cdot py$  (2);  $i = 1-x, -y, 1-z$ .

Bond lengths [pm]		Bond angles [ $^\circ$ ]		Torsion angles [ $^\circ$ ]	
S1-P2	198.2(1)	P2-S3-P2(i)	88.5(1)	P2(i)-S3-P2-S2	112.7(1)
S2-P2	196.4(1)	S3-P2-S3(i)	91.5(1)	P2(i)-S3(i)-P2-S2	-112.1(1)
S3-P2	215.9(1)	S2-P2-S3(i)	110.7(1)	P2(i)-S3(i)-P2-S1	113.6(1)
S3-P2(i)	214.3(1)	S2-P2-S3	110.0(1)	P2(i)-S3-P2-S1	-113.7(1)
		S1-P2-S3	111.3(1)	P2(i)-S3(i)-P2-S3	0.0(1)
		S1-P2-S3(i)	111.4(1)	P2(i)-S3-P2-S3(i)	0.0(1)
		S1-P2-S2	118.7(1)		

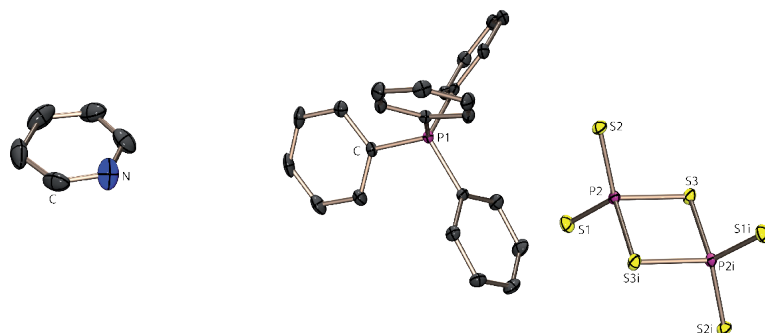


Figure 4. Molecular structure of  $[Ph_4P]_2[P_2S_6] \cdot py$  (2) in the solid state. Thermal ellipsoids are set at the 50 % probability level; hydrogen atoms are omitted for clarity. View along  $a$  axis;  $i = 1-x, -y, 1-z$ .

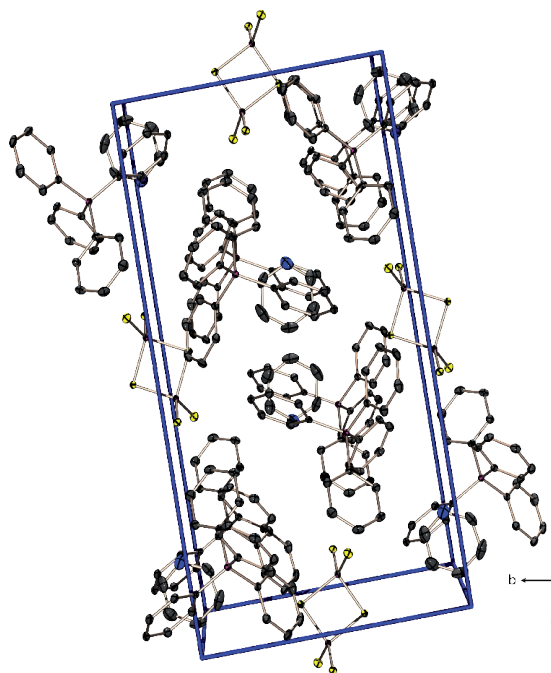


Figure 5. Crystal structure of  $[\text{Ph}_4\text{P}]_2[\text{P}_2\text{S}_6] \cdot \text{py}$  (2). View of the unit cell along the  $a$  axis; ellipsoids are drawn at the 50 % probability level. Hydrogen atoms are omitted for clarity.

## 2.2 $^{31}\text{P}$ NMR spectroscopic investigation

Brockner et al.<sup>7</sup> used high temperature syntheses starting from the elements phosphorus, sulfur and metals yielding solids, which are insoluble in common solvents. In case of  $\text{Na}_2\text{P}_2\text{S}_6$  and  $\text{K}_2\text{P}_2\text{S}_6$ , they succeeded in dissolving the solids in acetonitrile by adding crown ethers. Nevertheless, the compounds were characterized mostly using X-ray diffraction methods and Raman spectroscopy. Brockner et al. found that the formed anion was  $\text{P}_2\text{S}_6^{2-}$  in all cases. Interestingly, the Raman spectrum of a molten alkali bromide- $\text{Tl}_2\text{P}_2\text{S}_6$  mixture measured at different temperatures indicated that the  $\text{P}_2\text{S}_6^{2-}$  anion dissociates into the monomeric trithiometaphosphate anion  $\text{PS}_3^-$ . Brockner et al. were therefore the first, who postulated an equilibrium between the  $\text{P}_2\text{S}_6^{2-}$  anion and the  $\text{PS}_3^-$  anion.<sup>7</sup>

As  $[\text{nBu}_4\text{N}]_2[\text{P}_2\text{S}_6] \cdot \text{THF}$  is soluble in common polar solvents like pyridine, acetonitrile or propionitrile, it was now possible to determine the  $^{31}\text{P}$  NMR chemical shift of  $\text{P}_2\text{S}_6^{2-}$  which has not been reliably reported till now. Surprisingly, the  $^{31}\text{P}$  NMR spectrum of  $[\text{nBu}_4\text{N}]_2[\text{P}_2\text{S}_6] \cdot \text{THF}$  dissolved in benzonitrile consists of two signals at a chemical shift of 297.5 ppm and 30.2 ppm (Figure 6).

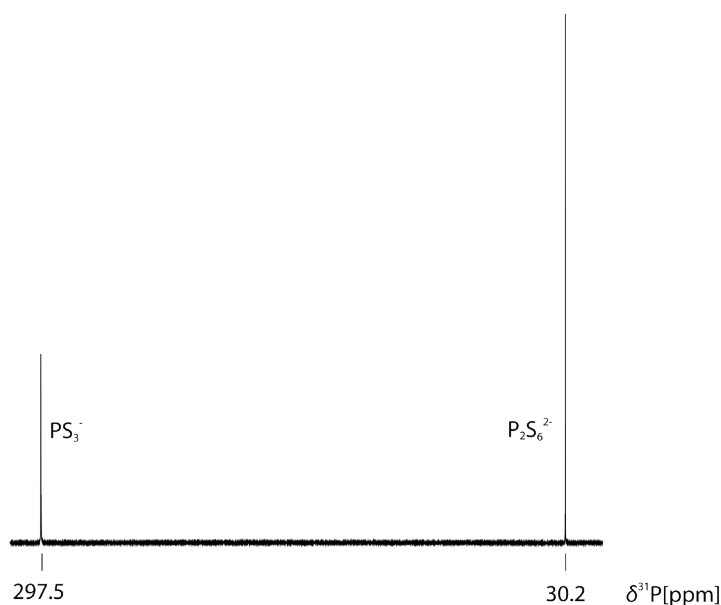
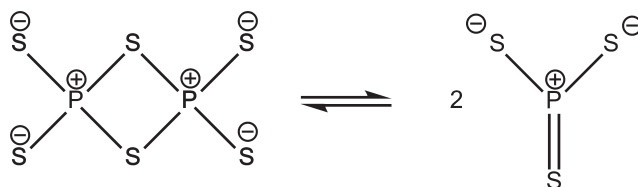


Figure 6. Observed  $^{31}\text{P}$   $\{^1\text{H}\}$  NMR spectrum of  $[\text{nBu}_4\text{N}]_2[\text{P}_2\text{S}_6] \cdot \text{THF}$  dissolved in benzonitrile (0.16 M, 25°C, 4096 scans with PD = 0.5 s, 2 h measuring time,  $\nu_0 = 161.8347$  MHz, broadband  $^1\text{H}$  decoupling, 0.5 Hz line broadening).

The extremely unusual low field shift of 297.5 ppm could also be found in dithioxophosphoranes containing a central phosphorus atom in a similar bonding situation like in the trithiometaphosphate  $\text{PS}_3^-$ . Yoshifuji et al.<sup>14,15</sup> reported the  $^{31}\text{P}$  NMR chemical shift of a dithioxophosphorane to be 298.2 ppm (in  $\text{CDCl}_3$ ). Following the prediction of Brockner that the dimeric trithiometaphosphate anion  $\text{P}_2\text{S}_6^{2-}$  spontaneously dissociates into the monomeric trithiometaphosphate anion  $\text{PS}_3^-$ , the  $^{31}\text{P}$  NMR signal at 297.5 ppm could be assigned to the monomeric trithiometaphosphate  $\text{PS}_3^-$ , while the  $^{31}\text{P}$  NMR signal at 30.2 ppm could be assigned to the dimeric trithiometaphosphate  $\text{P}_2\text{S}_6^{2-}$  (Scheme 6).



Scheme 6: Equilibrium between the monomeric trithiometaphosphate  $\text{PS}_3^-$  and the corresponding dimer  $\text{P}_2\text{S}_6^{2-}$ .

A  $^{31}\text{P}$ ,  $^{31}\text{P}$  EXSY spectrum shown in Figure 7 reveals that – due to the existence of cross peaks between the two signals – interconversion between the trithiometaphosphate and the corresponding dimer is slow on NMR time scale at ambient temperature (Scheme 6). This experimental result is also in agreement with the reported dimer-monomer equilibrium of special dithioxophosphoranes reported in literature.<sup>7</sup>

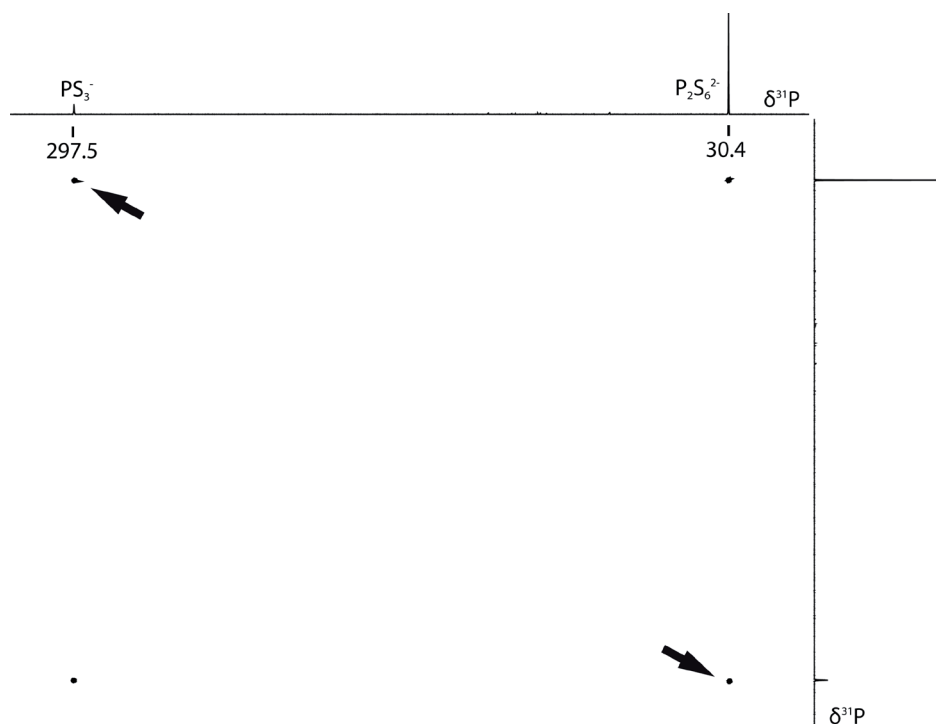


**Figure 7:**  $^{31}\text{P}$ ,  $^{31}\text{P}$  EXSY NMR spectrum of **1** dissolved in propionitrile. Crosspeaks are marked with arrows (0.16 M, 25 °C, matrix 2048 x 2048, mixing time 0.5 sec).

So this is the final proof that a trithiometaphosphate anion  $\text{PS}_3^-$  really exists and is stable in its monomeric form in solution. As it turns out, Roesky had indeed the right feeling that a monomeric trithiometaphosphate anion  $\text{PS}_3^-$  does exist. But the real  $^{31}\text{P}$  NMR chemical shift of this compound is, as expected due to the structural analogy to thioxophosphoranes, shifted to much lower field than reported by Roesky.

This knowledge generates a series of further questions:

- What is the reason for the stability of the  $\text{PS}_3^-$  anion in solution as there is no steric stabilization?
- How can the spontaneous dissociation in solution of  $\text{P}_2\text{S}_6^{2-}$  be explained?
- Which properties does the new anion have?

<sup>7</sup> Beckmann, H.; Großmann, G.; Ohms, G.; Sieler, J. *Heteroat. Chem.* **1994**, *5*(1), 73-83.

## 2.3 Computational results

All calculations were carried out using the Gaussian G03W program code.<sup>8</sup> In order to elucidate the structures, bonding and energies in the gas phase of  $\text{PS}_3^-$ ,  $\text{P}_2\text{S}_6^{2-}$  and  $\text{P}_3\text{S}_9^{3-}$  theoretically, computations were carried out with Becke's B3 three parameter hybrid functional using the LYP correlation functional (B3LYP).<sup>9</sup> For all atoms, Dunning's correlation consistent polarized double-zeta basis set was used (cc-pVDZ) (Table 3).<sup>10,11,12,13</sup> The DFT calculations reproduce the bond angles in the  $\text{P}_2\text{S}_6^{2-}$  and  $\text{P}_3\text{S}_9^{3-}$  anion well, while the P-S bond lengths are overestimated due to the high concentration of negative charge in an isolated anion in the gas phase. Through observed anion-cation interaction in the condensed phase, the concentration of negative charge in the anion could be abated.

**Table 3. Computational results at B3LYP level of theory for the anions  $\text{PS}_3^-$ ,  $\text{P}_2\text{S}_6^{2-}$  and  $\text{P}_3\text{S}_9^{3-}$ .**

	$[\text{PS}_3]^-$	$[\text{P}_2\text{S}_6]^{2-}$	$[\text{P}_3\text{S}_9]^{3-}$
$-E / \text{a.u.}$	1536.138465	3072.174876	4608.142015
$E_{\text{rel.}} / \text{kcal mol}^{-1}$ (per $\text{PS}_3^-$ moiety)	0.0	+ 32.0	+ 57.1
symmetry	$D_{3h}$	$D_{2h}$	$C_{3v}$
NIMAG	0	0	0
$zpe / \text{kcal mol}^{-1}$	3.63	7.97	12.3
		calcul. / expt. <sup>a</sup>	calcul. / exptl. <sup>8</sup>
$d(\text{P-S}_r) / \text{\AA}^b$		2.232 / 2.14	2.227 / 2.129
$d(\text{P-S}_t) / \text{\AA}^c$	1.991	2.016 / 1.97	ax: 2.004 / 1.964 eq: 2.045 / 1.964
$\langle \text{S}_r\text{-P-S}_r \rangle / ^\circ$		89.6 / 91.3	103.2 / 103.7
$\langle \text{S}_t\text{-P-S}_t \rangle / ^\circ$	120.0	118.1 / 117.3	118.3 / 119.7
$\langle \text{S}_r\text{-P-S}_t \rangle / ^\circ$		111.4 / 111.2	$\text{S}_r\text{-P-S}_{t,\text{ax}}$ : 115.2 $\text{S}_r\text{-P-S}_{t,\text{eq}}$ : 101.3
$\langle \text{P-S}_r\text{-P} \rangle / ^\circ$		90.5 / 88.6	115.5 / 111.2

<sup>a</sup> average values; <sup>b</sup>  $\text{S}_r$  = sulfur atom within the ring; <sup>c</sup> terminal sulfur atom.

<sup>8</sup> Gaussian 03, Revision A.1, Frisch, M. J.; Trucks, G. W.; Schlegel, H. B.; Scuseria, G. E.; Robb, M. A.; Cheeseman, J. R.; Montgomery, Jr., J. A.; Vreven, T.; Kudin, K. N.; Burant, J. C.; Millam, J. M.; Iyengar, S. S.; Tomasi, J.; Barone, V.; Mennucci, B.; Cossi, M.; Scalmani, G.; Rega, N.; Petersson, G. A.; Nakatsuji, H.; Hada, M.; Ehara, M.; Toyota, K.; Fukuda, R.; Hasegawa, J.; Ishida, M.; Nakajima, T.; Honda, Y.; Kitao, O.; Nakai, H.; Klene, M.; Li, X.; Knox, J. E.; Hratchian, H. P.; Cross, J. B.; Adamo, C.; Jaramillo, J.; Gomperts, R.; Stratmann, R. E.; Yazyev, O.; Austin, A. J.; Cammi, R.; Pomelli, C.; Ochterski, J. W.; Ayala, P. Y.; Morokuma, K.; Voth, G. A.; Salvador, P.; Dannenberg, J. J.; Zakrzewski, V. G.; Dapprich, S.; Daniels, A. D.; Strain, M. C.; Farkas, O.; Malick, D. K.; Rabuck, A. D.; Raghavachari, K.; Foresman, J. B.; Ortiz, J. V.; Cui, Q.; Baboul, A. G.; Clifford, S.; Cioslowski, J.; Stefanov, B. B.; Liu, G.; Liashenko, A.; Piskorz, P.; Komaromi, I.; Martin, R. L.; Fox, D. J.; Keith, T.; Al-Laham, M. A.; Peng, C. Y.; Nanayakkara, A.; Challacombe, P.; Gill, M. W.; Johnson, B.; Chen, W.; Wong, M. W.; Gonzalez, C.; and Pople, J. A.; Gaussian, Inc., Pittsburgh PA, 2003.

<sup>9</sup> Miehlich, B.; Savin, A.; Stoll, H.; Preuss, H. *Chem. Phys. Lett.* **1989**, *157*, 200.

<sup>10</sup> Woon, D. E.; Dunning Jr., T. H. *J. Chem. Phys.* **1993**, *98*, 1358.

<sup>11</sup> Kendall, R. A.; Dunning Jr., T. H.; Harrison, R. J. *J. Chem. Phys.* **1992**, *96*, 6796.

<sup>12</sup> Dunning Jr., T. H. *J. Chem. Phys.* **1989**, *90*, 1007.

<sup>13</sup> Peterson, K. A.; Woon, D. E.; Dunning Jr., T. H. *J. Chem. Phys.* **1994**, *100*, 7410.

### Lattice energies

As we were able to isolate only the dimeric trithiometaphosphate anion  $P_2S_6^{2-}$  as tetrabutylammonium salt **1** and tetraphenylphosphonium salt **2**, and so were Dimitrov et al., who isolated the  $P_2S_6^{2-}$  anion as tetraphenylarsonium salt in contrast to what has been reported by Roesky et al., we carried out computations of the enthalpies of formation of  $P_2S_6^{2-}$  and  $PS_3^-$  in the solid state.<sup>7c</sup> The enthalpy of formation of  $P_2S_6^{2-}$  (**A**) was computed in literature to be  $\Delta H^\circ(\mathbf{A}) = 62.3 \text{ kcal mol}^{-1}$ .<sup>14,15</sup> Using the data of the X-ray crystal analysis of **1**, the cell volume of compound **1** could be determined to be  $V_{\text{cell}} = 1633.5 \text{ \AA}^3$ . The molecular volume of THF could be calculated using the density of THF ( $\rho(\text{THF}) = 0.889 \text{ g cm}^{-3}$ ) to be  $V_{\text{THF}} = 135 \text{ \AA}^3$ . Therefore, for one formula unit of  $[n\text{Bu}_4\text{N}]_2[\text{P}_2\text{S}_6]$  (**A**) the molecular volume could be estimated to be  $V_{\mathbf{A}} = 749 \text{ \AA}^3$ .<sup>16</sup> According to the Jenkins equation, the lattice energy  $U_L$  for a  $M_2X$  salt could be calculated for **A**:<sup>17,18</sup>

$$U_L = |z_+| |z_-| v (\alpha/(V_M)^{0.33} + \beta) \quad \text{with } V_M \text{ in nm}^3$$

salt	$\alpha$ [kJ/mol]	$\beta$ [kJ/mol]
MX	117.3	51.9
$\text{MX}_2$	133.5	60.9
$\text{M}_2\text{X}$	165.3	-29.8

$$U_L(\mathbf{A}) = 913.0 \text{ kJ mol}^{-1} = 218.2 \text{ kcal mol}^{-1}$$

Assuming that a hypothetical compound  $[n\text{Bu}_4\text{N}][\text{PS}_3]$  **B** possesses exactly half the molecular volume of compound **A**, means  $V_{\mathbf{B}} = 374.5 \text{ \AA}^3$  then the Jenkins equation used above for a MX salt leads to a lattice energy for **B** of  $U_L(\mathbf{B}) = 429 \text{ kJ mol}^{-1} = 102.5 \text{ kcal mol}^{-1}$ .

Now the lattice energies  $U_L$  could be converted into the lattice enthalpies  $\Delta H_L$  using the following equation:<sup>27,28</sup>

$$\Delta H_L(\text{M}_p\text{X}_q) = U_L + [p(n_M/2 - 2) + q(n_X/2 - 2)] RT$$

with  $n_M, n_X$ :

- 3: monoatomic ions
- 5: linear polyatomic ions
- 6: non-linear polyatomic ions

Hence the lattice enthalpy values for **A** and **B** are:

$$\Delta H_L(\mathbf{B}) = 434.0 \text{ kJ mol}^{-1} = 103.7 \text{ kcal mol}^{-1}$$

<sup>14</sup> Klapötke, T. M.; Schulz, A.; Harcourt, R. D. *Quantum Chemical Methods in Main-Group Chemistry*, Wiley: Chichester, 1998.

<sup>15</sup> As  $[n\text{Bu}_4\text{N}]_2[\text{P}_2\text{S}_6] \cdot \text{THF}$  (**1**) is readily available, the computation is based on the results of the X-ray crystal analysis of (**1**).

<sup>16</sup> Aldrich, *Handbuch für Feinchemikalien*, **2007-2008**.

<sup>17</sup> Jenkins, H. D. B.; Roobottom, H. K.; Passmore, J.; Glasser, L. *Inorg. Chem.* **1999**, *38*, 3609.

<sup>18</sup> Jenkins, H. D. B.; Tudela, D.; Glasser, L. *Inorg. Chem.* **2002**, *41*, 2364.

$$\Delta H_L(\mathbf{A}) = 920.4 \text{ kJ mol}^{-1} = 220.0 \text{ kcal mol}^{-1}$$

The enthalpy of the reaction of two  $[n\text{Bu}_4\text{N}][\text{PS}_3]$  (**B**) to form one  $[n\text{Bu}_4\text{N}]_2[\text{P}_2\text{S}_6]$  (**A**) can now be estimated to:

$$\Delta H = + 49.7 \text{ kcal mol}^{-1}.$$

A lattice energy estimation revealed that a cation should have a volume of  $1000 \text{ \AA}^3$ , which means that it should consist of 55–60 non-hydrogen atoms (with the assumption that one non hydrogen atom has a volume of  $18 \text{ \AA}^3$ ).

### Valence bond structures

The VB program package VB2000, version 1.8, was used for all VB calculations employing a full D95 double-zeta basis set. VB2000 is an *ab initio* electronic structure package for performing modern VB calculations; it is based on a highly efficient VB algorithm – the so called algebrant algorithm – and the group function (GF) approach, in which a large molecule is described in terms of its constituent parts physically identifiable “electron groups”. A major feature of VB2000 is the implementation of modern VB theory at *ab initio* level using the algebrant algorithm.<sup>7,27,28,19,20,21,22,23</sup>

The VB method used in this study was the CASVB(6,4) one (*complete active space*) with six VB electrons ( $\pi$  electrons) spread over four  $\pi$  orbitals. The CASVB method implemented in the VB2000 program package generates the weights of all resonance structures. In VB2000 each “structure” becomes a spin-coupling scheme, involving pairs of electrons occupying rather localized, strongly overlapping orbitals. The overlapping orbitals of any bond are expected to bear some similarity to the AOs used in constructing a localized MO. In particular, the  $\pi$ -orbitals used in this study are almost one-center AOs with only a very small degree of “tailing”, *i.e.* spreading onto other atomic centers.

Scheme 7 shows all possible VB structures for the  $\text{PS}_3^-$  anion, which were generated from a CASVB(6,4) calculation with the six  $\pi$ -electrons forming the active VB space (all  $\sigma$  and core electrons were treated with the HF method). As expected, the Hiberty weights of the standard Lewis structures of type **I** are the individually most important contributors to the resonance scheme (Tab. 4). According to investigations made by Schoeller, the set of  $\pi$ -MOs should be composed of the same found for trimethylene methane, thus generating Y aromaticity in  $\text{PS}_3^-$  anion.<sup>24</sup>

<sup>19</sup> Nakamoto, K.; *Infrared and Raman Spectra of Inorganic and Coordination Compounds*, 5<sup>th</sup> ed.; Part A, Wiley: New York, Chichester, 1997, 228.

<sup>20</sup> Li, J.; McWeeny, R. *VB2000*, version 1.7, SciNet Technologies: San Diego, CA, (November 2005).

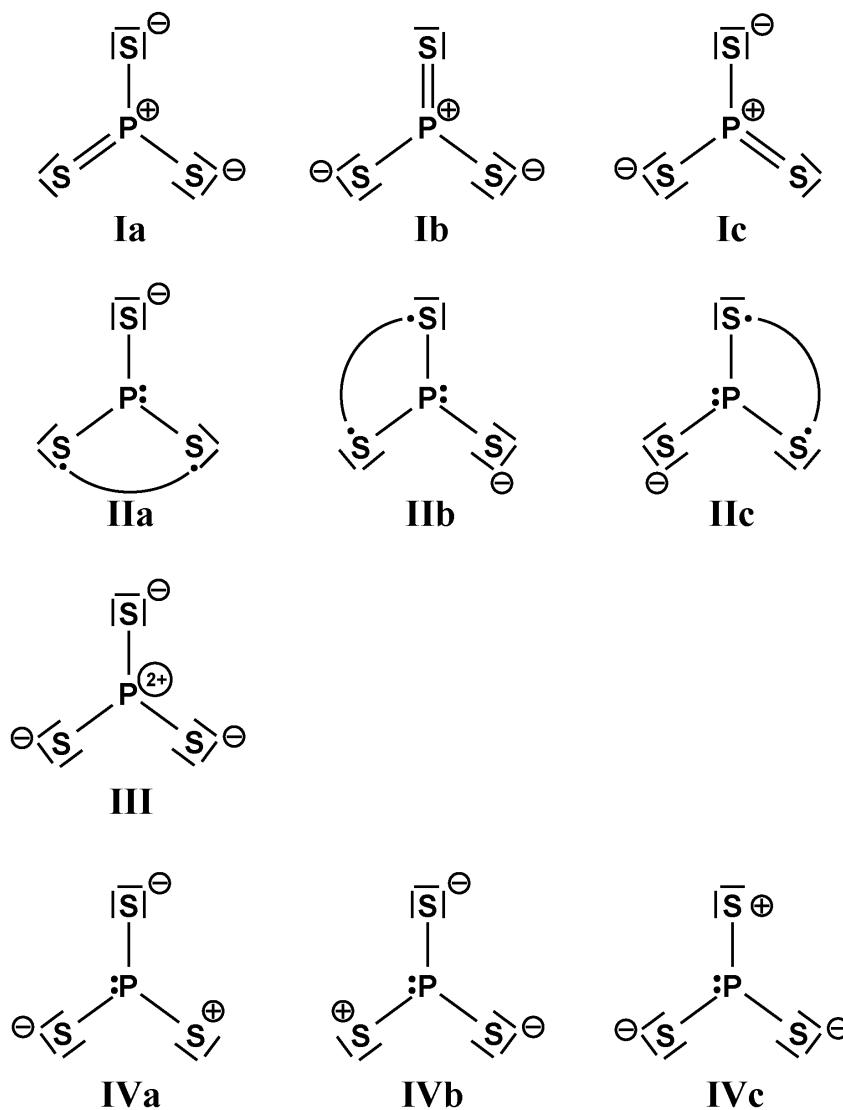
<sup>21</sup> Li, J.; Pauncz, R. *Int. J. Quantum. Chem.* **1997**, *62*, 245.

<sup>22</sup> Li, J.; McWeeny, R. *Int. J. Quantum. Chem.* **2002**, *89*, 208.

<sup>23</sup> McWeeny, R. *Adv. Quant. Chem.* **1999**, *31*, 15.

<sup>24</sup> Schoeller, W. W.; Niemann, J. *Phosphorus, Sulfur and Silicon and Relat. Elem.* **1989**, *46*, 47.

It is also interesting to point out that the Dewar-type (or long bond) structures (II) together with the sextet structure III are important resonance structures, whereas the structures with one sulfur atom carrying a positive charge (IV) are much less important (Tab. 4).



Scheme 7. VB structures for  $\text{PS}_3^-$  generated from a CASVB(6,4) calculation with the six  $\pi$ -electrons forming the active VB space (all  $\sigma$  and core electrons were treated with the HF method).

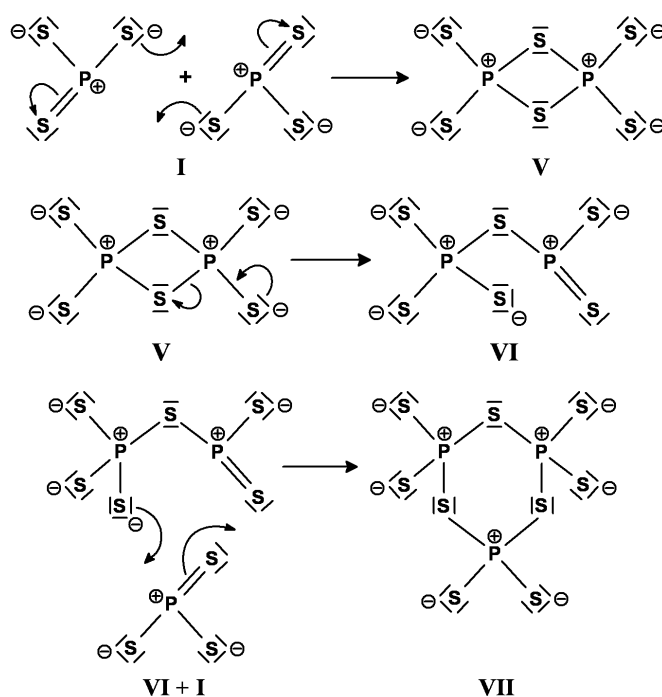
Table 4. Hiberty structural weights<sup>25</sup> of the individual Lewis structures depicted in Scheme 7.

Structure	I	II	III	IV
Hiberty weight	3 x 0.22	3 x 0.07	0.12	3 x 0.001

<sup>25</sup> The Hiberty weights  $W_i$  are defined as follows:  $W_i = C_i^2 / \sum C_i^2$  (where  $C_i$  are the coefficient of the wavefunctions for VB structures I).

Another central question, which has to be answered is why there is a dynamic equilibrium between the monomeric trithiometaphosphate anion  $\text{PS}_3^-$ , which is formed by the spontaneous dissociation of the corresponding dimeric anion  $\text{P}_2\text{S}_6^{2-}$  in solution. This equilibrium can be observed using  $^{31}\text{P}$ ,  $^{31}\text{P}$  EXSY NMR spectroscopy. Dimitrov et al. stated a similar equilibrium for the trimeric trithiometaphosphate anion  $\text{P}_3\text{S}_9^{3-}$  (Scheme 8),<sup>7c</sup> but we were not able to confirm that statement. We rather believe that the formation of the dimeric  $\text{P}_2\text{S}_6^{2-}$  (V) from monomeric  $\text{PS}_3^-$  (I) is straightforward and can easily be explained (Scheme 8). However, the formation of the trimer  $\text{P}_3\text{S}_9^{3-}$  (VII) does not seem to be easily possible from the monomer (I). It is more likely that the trimer (VII) forms from a reaction of the dimer (V) via VI which then reacts with the monomer as shown in Scheme 8.

The quantum chemical calculations showed that the dissociation of the dianion  $\text{P}_2\text{S}_6^{2-}$  into two monoanions  $\text{PS}_3^-$  is facilitated in solution, while in the solid state, due to higher lattice energies, the formation of the dianion  $\text{P}_2\text{S}_6^{2-}$  is favored. Further calculations showed that for a stabilization of the  $\text{PS}_3^-$  anion in the solid state, a cation consisting of at least 50–60 non-hydrogen atoms is necessary.



Scheme 8. Possible VB mechanism for the formation of  $\text{P}_2\text{S}_6^{2-}$  and  $\text{P}_3\text{S}_9^{3-}$ .

## 2.4 Chemical behavior of $\text{PS}_3^-$

Taking into consideration the experiences with neutral dithiooxophosphoranes, a highly electrophilic phosphorus center is to be expected, which should be easily attacked by nucleophiles to form adducts. But as the  $\text{PS}_3^-$  compound is an anion, electrophiles are expected to attack the sulfur atoms to form neutral compounds. Consequently, the trithiometaphosphate anion  $\text{PS}_3^-$  is expected to show an amphoteric acid-base behavior.

To proof this experimentally, the trithiometaphosphate anion was reacted with different nucleophiles ( $\text{F}^-$ ,  $\text{Cl}^-$ ,  $\text{Br}^-$ ,  $\text{I}^-$ ,  $\text{OCN}^-$ ,  $\text{SCN}^-$ ,  $\text{CN}^-$ ) in solution. But in all cases except one, no reaction could be observed. Only in case of  $\text{F}^-$ , three species containing one fluorine atom could be observed in the  $^{31}\text{P}$  NMR spectrum.

In addition, the Mulliken charges of the trithiometaphosphate anion were also calculated. In almost all cases, the effective charge of the central phosphorus atom is less than one. This corresponds to the calculated Mulliken charges for dithiooxophosphoranes reported in literature.<sup>26</sup>

## 2.5 Adduct formation

In the course of the investigation of the reaction condition for the trithiometaphosphate syntheses, we became aware that using polar basic solvents like pyridine or *N*-methylimidazole as reaction medium changes the resonance in the  $^{31}\text{P}$  NMR spectra. The signal at 30.2 ppm caused by the dimeric trithiometaphosphate  $\text{P}_2\text{S}_6^{2-}$  could still be found but no  $^{31}\text{P}$  NMR chemical shift at 297.5 ppm. Instead a new broad signal at higher field depending on the reaction medium used could be identified (Table 5). As already mentioned, the existence of the dimeric trithiometaphosphate  $\text{P}_2\text{S}_6^{2-}$  in the reaction solution always implicates the existence of the monomeric trithiometaphosphate  $\text{PS}_3^-$  due to the spontaneous dissociation of  $\text{P}_2\text{S}_6^{2-}$  in solution. To get more information about the new compound causing the high field shift in the  $^{31}\text{P}$  NMR spectrum, bases were added in stoichiometric amounts to a solution of  $[\text{nBu}_4\text{N}]_2[\text{P}_2\text{S}_6] \cdot \text{THF}$  (**1**), yielding the identical  $^{31}\text{P}$  NMR spectra with a resonance at 30.2 ppm and a broad signal at higher field.

<sup>26</sup> Peräklä, M.; Pakkanen, T. A.; Björkroth, J.-P.; Pohjala, E.; Leiras, O. H. J. *Chem. Soc. Perkin Trans.* **1992**, 2, 1167-1171.

**Table 5.**  $^{31}\text{P}$  NMR chemical shift of the adduct stabilized  $\text{PS}_3^-$ .

base	$\delta^{31}\text{P}$ at 25 °C
4-dimethylaminopyridine	213.5
<i>N</i> -methyl imidazole	254.2
pyridine	223.9

This leads to the assumption that the base coordinates the trithiometaphosphate anion  $\text{PS}_3^-$  forming an adduct. Dimitrov et al.<sup>7c</sup> were the first, who could isolate such adduct stabilized trithiometaphosphates in the solid state. They characterized the compounds using X-ray diffraction methods,  $^{31}\text{P}$ -MAS-NMR spectroscopy and  $^{31}\text{P}$  NMR spectroscopy in solution at different temperatures. They interpreted their results as equilibrium between the adduct stabilized trithiometaphosphate, the free monomeric trithiometaphosphate, the dimeric, and the trimeric trithiometaphosphate (Scheme 9).

**Scheme 9.** Interpretation of the  $^{31}\text{P}$  NMR spectra in solution by Dimitrov et al.

Interestingly, Dimitrov et al. observed in the  $^{31}\text{P}$  NMR spectrum at high temperature (70 °C) a signal at 129-130 ppm, which was assigned to be caused by the adduct stabilized trithiometaphosphate anion and another signal at 226.2 ppm which was assigned to be caused by the free monomeric trithiometaphosphate anion, which is definitely the wrong  $^{31}\text{P}$  NMR chemical shift. This implicates that the equilibrium between the adduct stabilized trithiometaphosphate anion and the free monomeric trithiometaphosphate anion is slow on the NMR time scale even at high temperature.

### *Temperature dependent $^{31}\text{P}$ NMR spectroscopy*

As already mentioned, the equilibrium between the adduct stabilized trithiometaphosphate anion and the free monomeric trithiometaphosphate anion in solution is temperature dependent. We investigated the behavior of **3** dissolved in propionitrile at different temperatures using  $^{31}\text{P}$  NMR spectroscopy. Surprisingly, we were not able to confirm the results of Dimitrov et al.,<sup>7c</sup> who reported that at higher temperatures the resonance for free monomeric trithiometaphosphate anion appears. The  $^{31}\text{P}$  NMR spectra of **3** recorded at different temperatures are shown in Figure 8.

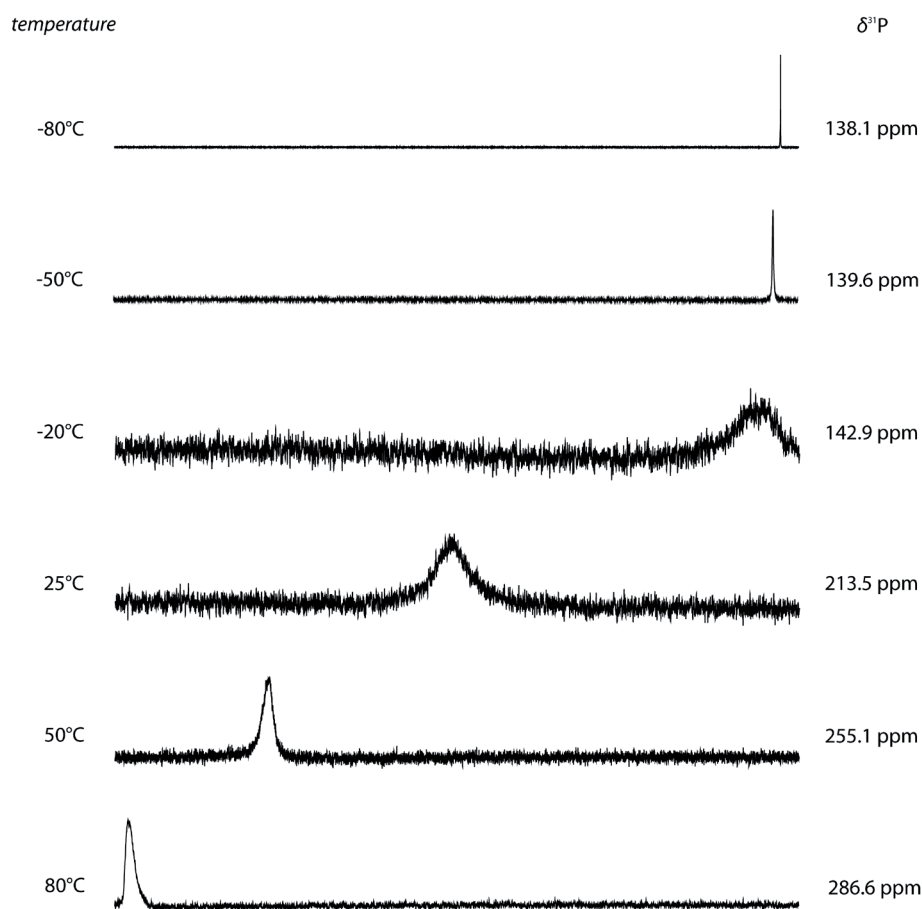
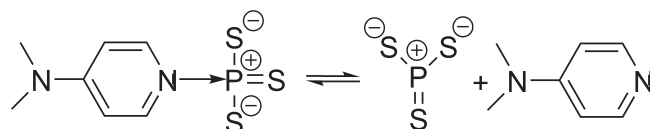


**Figure 8.**  $^{31}\text{P}\{^1\text{H}\}$  NMR spectra of **3** dissolved in propionitrile at different temperatures (0.1 M, 1024 scans with PD = 0.5 s, broadband  $^1\text{H}$  decoupling).

The signal of **3** shifts from high field ( $\delta^{31}\text{P} = 138.1$ ) at low temperature ( $-80\text{ }^\circ\text{C}$ ) to lower field ( $\delta^{31}\text{P} = 286.6$ ) at high temperature ( $80\text{ }^\circ\text{C}$ ). Interestingly, the signal in the  $^{31}\text{P}$  NMR spectrum converges to the  $^{31}\text{P}$  NMR signal observed for the free monomeric trithiometaphosphate anion in propionitrile at 297.5 ppm. As propionitrile has a boiling point at about  $90\text{ }^\circ\text{C}$ , it was not possible to measure  $^{31}\text{P}$  NMR spectra above  $80\text{ }^\circ\text{C}$ . But nevertheless, we came to the conclusion that the resonance observed for **3** in the  $^{31}\text{P}$  NMR spectra measured at different temperatures can be interpreted as averaged signal between the adduct stabilized trithiometaphosphate anion and the free monomeric trithiometaphosphate anion. Depending on the temperature, the equilibrium between these two compound is either on the side of the adduct (at low temperatures) or on the side of the free monomeric trithiometaphosphate anion (at high temperatures) (Scheme 10).



**Scheme 10.** Temperature dependent equilibrium between the adduct stabilized trithiometaphosphate anion and the free monomeric trithiometaphosphate anion.

If *N*-methyl imidazole is added to a solution of **1** in propionitrile and <sup>31</sup>P NMR spectra at different temperatures are measured of this solution, the observed <sup>31</sup>P NMR spectra do not differ significantly from those observed for **3** (Figure 11).

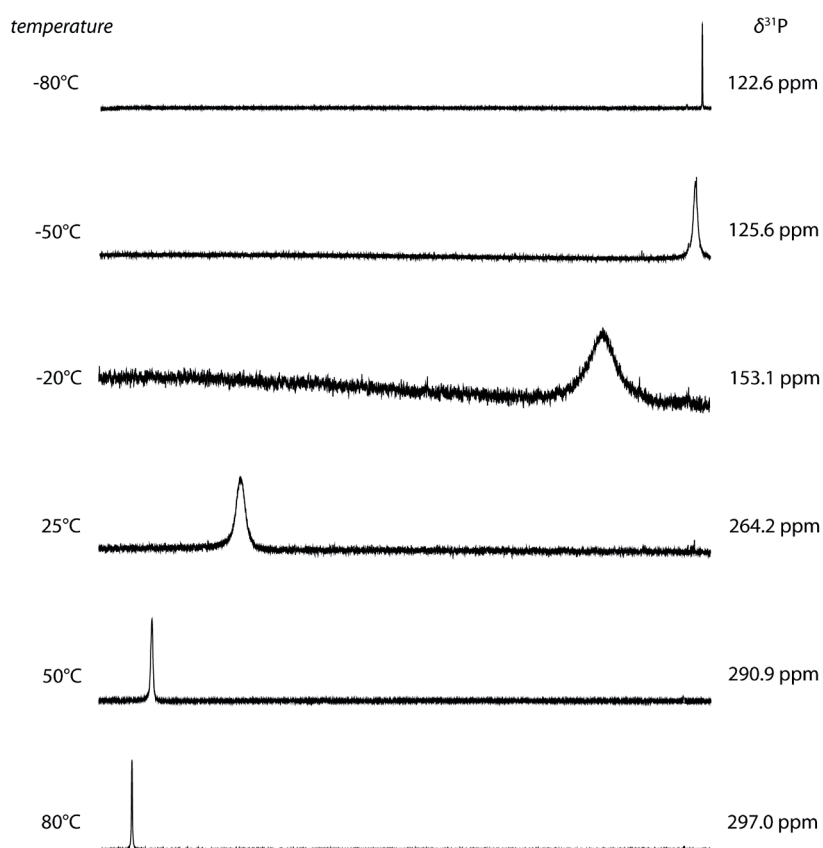
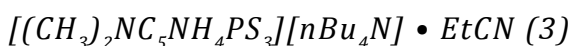


**Figure 9.** <sup>31</sup>P{<sup>1</sup>H} NMR spectra of **1** as *N*-methyl imidazole adduct dissolved in propionitrile at different temperatures (0.1 M, 1024 scans with a PD = 0.5 s, broadband <sup>1</sup>H decoupling).

The <sup>31</sup>P NMR resonance is shifted from high field ( $\delta^{31}\text{P} = 122.6$ ) at low temperatures (-80 °C) to low field ( $\delta^{31}\text{P} = 297.0$ ) at 80 °C. The <sup>31</sup>P NMR chemical shift at 80 °C corresponds to the free monomeric trithiometaphosphate anion  $\text{PS}_3^-$  as already shown before. This is the final evidence for the existence of the temperature dependent equilibrium between the adduct stabilized trithiometaphosphate anion and the free monomeric trithiometaphosphate anion in solution. So obviously, the adduct stabilization in case of the *N*-methyl imidazole stabilized trithiometaphosphate anion

is not so strong compared to **3**, as at 80 °C the equilibrium is almost completely on the side of the free monomeric trithiometaphosphate anion.

In contrast, at -80 °C the equilibrium is almost completely shifted to the side of the adduct stabilized trithiometaphosphate anion in case of **3** as well as in case of the *N*-methylimidazole stabilized trithiometaphosphate anion because the shift of the <sup>31</sup>P NMR signals at -50 °C are almost the same as the <sup>31</sup>P NMR chemical shifts of the signals observed at -80 °C.



To a solution of **1** in propionitrile 4-dimethylaminopyridine was added and after storing the reaction solution at -25 °C, yellow block shaped crystals of **3** could be obtained.  $[(CH_3)_2NC_5NH_4PS_3][nBu_4N] \cdot EtCN$  (**3**) crystallizes in the triclinic space group *P*-1.

The phosphorus atom is coordinated distorted tetrahedral by three sulfur atoms and one 4-dimethylaminopyridine molecule. The three P-S bond lengths are in the range of 198 pm and therefore significantly shorter than a P-S single bond.<sup>1,15</sup> The distance between the phosphorus atom and the nitrogen atom P1-N1 is 188.6(1) pm and therefore significantly longer than a P-N single bond but in the same range as Dimitrov et al. reported for the pyridine adducts.<sup>7c,27</sup> The P-S-P bond angles have an average value of 115.6°. The sum of all three S-P-S angles is 347° indicating only a slight deviation from planarity. In Table 6 some selected bond parameters are summarized.

Table 6. Selected bond parameters of  $[(CH_3)_2NC_5NH_4PS_3][nBu_4N] \cdot EtCN$  (**3**)

Distances [pm]		Bond angles [°]	
S1-P1	198.3(1)	S1-P1-S2	116.2(1)
S2-P1	198.6(1)	S2-P1-S3	114.9(1)
S3-P1	198.4(1)	S3-P1-S1	115.9(1)
N1-P1	188.6(2)	S1-P1-N1	102.7(1)
		S2-P1-N1	101.1(1)
		S3-P1-N1	102.9(1)

<sup>27</sup> Allen, F. H.; Kennard, O.; Watson, D. G.; Brammer, L.; Orpen, A. G.; Taylor, R. J. *Chem. Soc. Perkin Trans. II* **1987**, S1-S19.

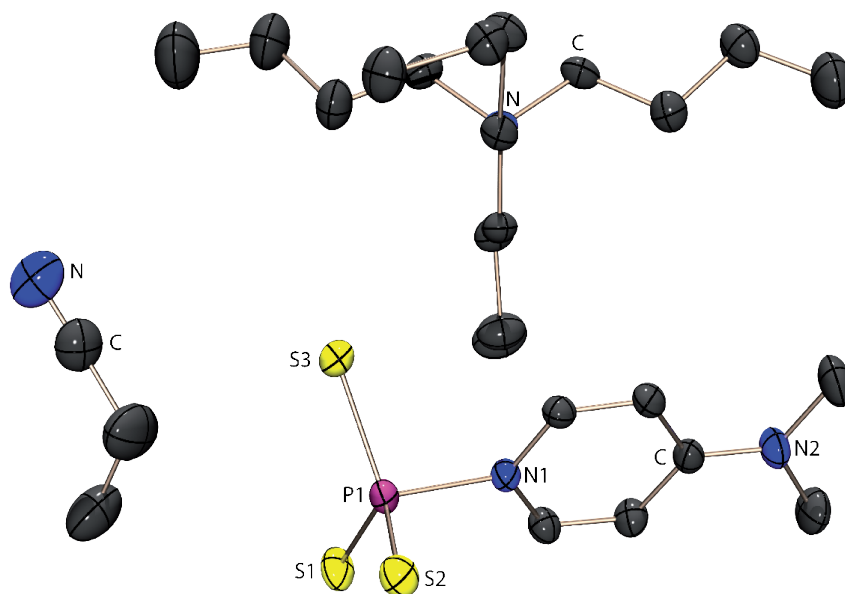


Figure 10. Molecular structure of  $[(\text{CH}_3)_2\text{NC}_5\text{NH}_4\text{PS}_3][n\text{Bu}_4\text{N}] \cdot \text{EtCN}$  (3) in the crystal. Thermal ellipsoids of all non hydrogen atoms are drawn at the 50 % probability level; hydrogen atoms are omitted for clarity. View along  $c$  axis.

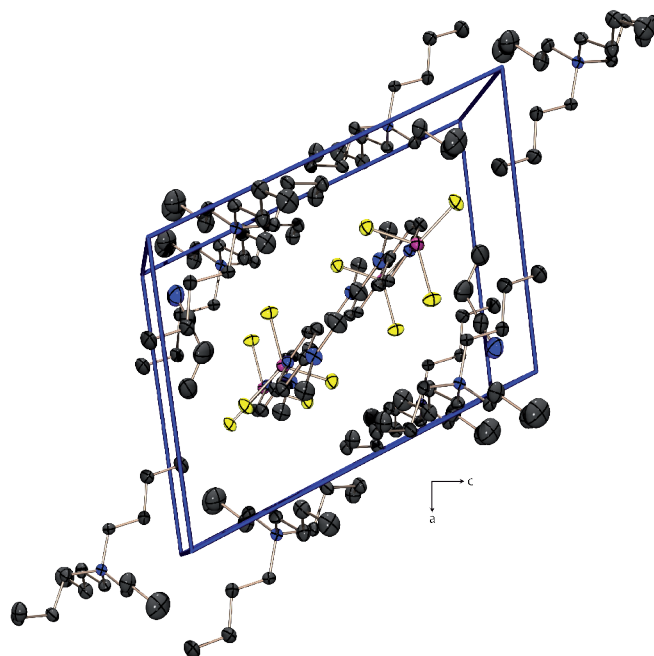


Figure 11. Crystal structure of  $[(\text{CH}_3)_2\text{NC}_5\text{NH}_4\text{PS}_3][n\text{Bu}_4\text{N}] \cdot \text{EtCN}$  (3). Thermal ellipsoids of all non hydrogen atoms are drawn at the 50 % probability level; hydrogen atoms are omitted for clarity. View of the unit cell along the  $b$  axis.

## 2.6 Comparison of the structures of the adduct stabilized trithiometaphosphate $\text{PS}_3^-$

The obtained structural parameters of  $[(\text{CH}_3)_2\text{NC}_5\text{NH}_4\text{PS}_3][n\text{Bu}_4\text{N}] \cdot \text{EtCN}$  (**3**) are compared with those reported in literature by Dimitrov et al.:  $[\text{pyPS}_3][\text{H}_2\text{NMe}_2]$ ,  $[\text{pyPS}_3][\text{H}_2\text{NEt}_2]$  and  $[\text{pyPS}_3][\text{pyH}]$ .<sup>7c</sup>

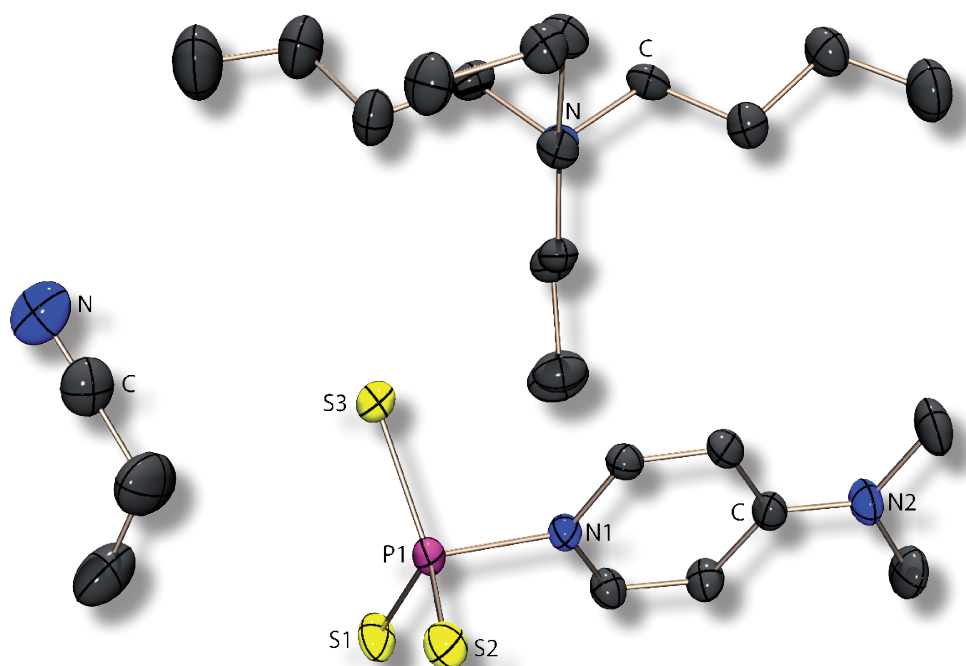
**Table 7.** Comparison of selected bond parameters of all known salts containing the adduct stabilized trithiometaphosphate anion.

	<b>3</b>	$[\text{pyPS}_3][\text{H}_2\text{NMe}_2]$	$[\text{pyPS}_3][\text{H}_2\text{NEt}_2]$	$[\text{pyPS}_3][\text{pyH}]$
P-S bond distances [pm]	198.3(1) 198.6(1) 198.4(1)	197.5(1) 198.4(1) 198.6(1)	197.8(1) 197.8(1) 198.7(1)	198.0(1) 198.6(2) 200.4(1)
average value P-S distances [pm]	198.4	198.2	198.1	199.0
S-P-S bond angles [°]	116.2(1) 114.9(1) 115.9(1)	115.09(4) 115.29(4) 117.67(3)	115.69(5) 116.42(2) 115.69(2)	113.72(2) 116.72(2) 116.41(2)
average value S-P-S bond angles [°]	115.7	116.0	115.9	115.6
$\Sigma$ S-P-S bond angles [°]	347	345.89	347.8	346.85
P-N distance [pm]	188.6(2)	191.5(2)	192.2(2)	190.6(2)

As shown in Table 7, neither the P-S bond lengths nor the S-P-S bond angles vary significantly in all four known salts. Furthermore the central phosphorus atom is only slightly distorted out of the plane, defined by the sulfur atoms in all cases. The P-N distance is somewhat shorter in **3** than in the pyridine stabilized adducts, probably due to the electron donating effect of the dimethylamino group. Another difference between **3** and the pyridine adducts of the trithiometaphosphate anion reported by Dimitrov et al. is the lack of hydrogen bridge bonds between the cation and the anion in **3**. This is in contrast to Dimitrov et al.'s statement that hydrogen bridge bonds between cation and anion provide the essential contribution to stabilize the adduct in the solid state.<sup>7c</sup>

### 3 Conclusion

We were able to contribute new results to the chemistry of the trithiometaphosphate anion  $\text{PS}_3^-$  and complete the work of Brockner, Dimitrov and Roesky by providing a new perspective on that inconspicuous but fascinating  $\text{PS}_3^-$  anion. Quantum chemical calculations reveal that it is impossible to isolate the monomeric trithiometaphosphate anion  $\text{PS}_3^-$  in the crystal by using conventional cations like  $n\text{Bu}_4\text{N}^+$  or  $\text{Ph}_4\text{P}^+$ . The synthesis of other promising cations, which could stabilize the monomeric trithiometaphosphate anion in the crystalline state is currently under work. Additionally, we were able to elucidate the behavior of the adduct stabilized trithiometaphosphate anion in solution. The isolation of **3** reveals that no stabilizing hydrogen bridges between anion and cation are necessary to stabilize the adduct of the trithiometaphosphate anion in the solid state.



## 4 Experimental Section

**General.** All reactions were carried out under inert gas atmosphere using Schlenk techniques. Argon (Messer Griesheim, purity 4.6 in 50 L steel cylinder) was used as inert gas. The glass vessels used were stored in a 130 °C drying oven. Before use, the glass vessels were flame dried in vacuum at  $10^{-3}$  mbar.

The sodium disulfide  $\text{Na}_2\text{S}_2$  was prepared as described in literature and stored in a dry box under nitrogen atmosphere.<sup>28</sup> Elemental sulfur was used as received (Acros Organics).  $\text{P}_4\text{S}_3$  was obtained commercially (Riedel-de H en) and was purified by extraction with  $\text{CS}_2$  before use. The solvents used were dried using commonly known methods and freshly distilled before use. Melting points were determined in capillaries using a B chi B540 instrument and are uncorrected.

**NMR Spectroscopy.** NMR spectra were recorded with a Jeol EX 400 Eclipse instrument operating at 161.997 MHz ( $^{31}\text{P}$ ). Chemical shifts are referred to 85 %  $\text{H}_3\text{PO}_4$  as external standard. All spectra were measured, if not mentioned otherwise, at 25 °C. The %-data correspond to the intensities in the  $^{31}\text{P}$  NMR spectra with respect to the total intensity. The difference to 100 % belongs to not determinable signals.

**X-ray Crystallography.** The molecular structures in the crystalline state were determined using an Oxford Xcalibur3 diffraction instrument equipped with a Spellman generator (voltage 50 kV, current 40 mA) and a Kappa CCD detector with a X-ray radiation wavelength of 0.71073   (MoK $_{\alpha}$ ). The data collection was performed with the CrysAlis CCD software, the data reduction with the CrysAlis RED software.<sup>29,30</sup> The structures were solved with SIR-92, SIR-97 and SHELXS-97 and refined with SHELXL-97 and finally checked using PLATON.<sup>31,32,33,34,35</sup> The absorptions were corrected by SCALE3 ABSPACK multi-scan method.<sup>36</sup> All relevant data and parameters of the X-ray measurements and refinements are given in Table 1.

<sup>28</sup> (a) Thompson, D. P.; Boudjouk, P. J. *Org. Chem.* **1988**, *53*, 2109. (b) Schuster, M. PhD Thesis, LMU Munich, **1999**.

<sup>29</sup> CrysAlis CCD, Oxford Diffraction Ltd., Version 1.171.27p5 beta (release 01-04-2005 CrysAlis171 .NET), (compiled Apr 1 2005,17:53:34).

<sup>30</sup> CrysAlis RED, Oxford Diffraction Ltd., Version 1.171.27p5 beta (release 01-04-2005 CrysAlis171 .NET), (compiled Apr 1 2005,17:53:34).

<sup>31</sup> SIR-92, *A Program for Crystal Structure Solution*; Altomare, A.; Cascarano, G. L.; Giacovazzo, C.; Guagliardi, A. *J. Appl. Cryst.* **1993**, *26*, 343.

<sup>32</sup> Altomare, A.; Burla, M. C.; Camalli, M.; Cascarano, G. L.; Giacovazzo, C.; Guagliardi, A.; Moliterni, A. G. G.; Polidori, G.; Spagna, R. *J. Appl. Crystallogr.* **1999**, *32*, 115.

<sup>33</sup> Sheldrick, G. M. *SHELXS-97, Program for Crystal Structure Solution*; Universit t G ttingen, **1997**.

<sup>34</sup> Sheldrick, G. M. *SHELXL-97, Program for the Refinement of Crystal Structures*; University of G ttingen, Germany, **1997**.

<sup>35</sup> Spek, L. A. *PLATON, A Multipurpose Crystallographic Tool*, Utrecht University, Utrecht, The Netherlands, **1999**.

<sup>36</sup> SCALE3 ABSPACK – *An Oxford Diffraction program (1.0.4,gui:1.0.3)* (C) 2005 Oxford Diffraction Ltd.

**[*n*Bu<sub>4</sub>N]<sub>2</sub>[P<sub>2</sub>S<sub>6</sub>]•THF (1):** P<sub>4</sub>S<sub>3</sub> (4.4 g, 20 mmol), Na<sub>2</sub>S<sub>2</sub> (3.2 g, 40 mmol) and sulfur (3.2 g, 12.5 mmol) in 80 mL of THF were stirred at room temperature. After one day, a yellow solution was obtained. A solution of *n*Bu<sub>4</sub>NBr (25.8 g, 80 mmol) in 20 mL of acetonitrile was added yielding a yellow solution and a white precipitate (NaBr). The NaBr was removed using a G4 frit. The filtrate was stored at -25 °C. Within 24 h, yellow crystals of [*n*Bu<sub>4</sub>N]<sub>2</sub>[P<sub>2</sub>S<sub>6</sub>]•THF formed, which were separated using a G3 frit, washed twice with 10 mL of cold THF and dried under vacuum yielding 15.67 g (6.42 mmol, 32 % with respect to P<sub>4</sub>S<sub>3</sub>) of **1**.

<sup>31</sup>P{<sup>1</sup>H} NMR in THF: δ = 30.2 (P<sub>2</sub>S<sub>6</sub><sup>2-</sup>, 36 %); 79.2 (P<sub>3</sub>S<sub>9</sub><sup>3-</sup>, 6 %); 105.0 (s, 3 %); 107.5 (s, 3 %); 128.8 (P<sub>2</sub>S<sub>7</sub><sup>2-</sup>, 7 %); 297.5 (PS<sub>3</sub><sup>-</sup>, 38 %).

**[Ph<sub>4</sub>P]<sub>2</sub>[P<sub>2</sub>S<sub>6</sub>]•py (2):** P<sub>4</sub>S<sub>3</sub> (880 mg, 4 mmol), Na<sub>2</sub>S<sub>2</sub> (881 mg, 8 mmol) and sulfur (641 mg, 20 mmol) in 40 mL of pyridine were stirred for 24 h at room temperature yielding a yellow solution. Ph<sub>4</sub>PBr (6.708 g, 16 mmol) was added giving a white precipitate (NaBr) which was removed using a G4 frit. The orange filtrate was stored at +4 °C. After five days yellow crystals of [Ph<sub>4</sub>P]<sub>2</sub>[P<sub>2</sub>S<sub>6</sub>]•py were obtained. Yield: 2.83 g (5.2 mmol), m.p.: 173 °C (dec.).

<sup>31</sup>P{<sup>1</sup>H} NMR in pyridine: δ = 128.8 (P<sub>2</sub>S<sub>7</sub><sup>2-</sup>, 11 %); 237.9 (pyPS<sub>3</sub><sup>-</sup>, 83 %).

**[*n*Bu<sub>4</sub>N][[(CH<sub>3</sub>)<sub>2</sub>NC<sub>5</sub>H<sub>4</sub>NPS<sub>3</sub>] (3):** 0.5 g (0.64 mmol) [*n*Bu<sub>4</sub>N]<sub>2</sub>[P<sub>2</sub>S<sub>6</sub>]•THF and 75 mg (0.62 mmol) (CH<sub>3</sub>)<sub>2</sub>NC<sub>5</sub>H<sub>4</sub>N were dissolved in 12 mL propionitrile and stirred at room temperature, yielding a yellow suspension which was refluxed for one hour (90 °C oil bath temperature). The resulting yellow solution was stored at -25 °C. After one week, only few yellow crystals of [*n*Bu<sub>4</sub>N][[(CH<sub>3</sub>)<sub>2</sub>NC<sub>5</sub>H<sub>4</sub>NPS<sub>3</sub>] were obtained. Therefore a yield cannot be determined.

<sup>31</sup>P{<sup>1</sup>H} NMR in propionitrile: δ = 30.2 (P<sub>2</sub>S<sub>6</sub><sup>2-</sup>, 8 %); 128.8 (P<sub>2</sub>S<sub>7</sub><sup>2-</sup>, 7 %), 213.5 (**3**, 69 %), 104.9 (s, 6 %).

**Reactions of PS<sub>3</sub><sup>-</sup> with nucleophiles.** To a solution of PS<sub>3</sub><sup>-</sup> (0.1 M) in propionitrile the corresponding nucleophile (1 eq.) was added at ambient temperature and investigated using <sup>31</sup>P NMR spectroscopy. In case of Cl<sup>-</sup>, Br<sup>-</sup>, I<sup>-</sup>, OCN<sup>-</sup>, SCN<sup>-</sup> and CN<sup>-</sup> only PS<sub>3</sub><sup>-</sup> was observable.

In case of F<sup>-</sup>: <sup>31</sup>P{<sup>1</sup>H} NMR in propionitrile: δ = 149.1 (d, <sup>1</sup>J<sub>PF</sub> = 1.05 kHz, 16 %), 114.9 (d, <sup>1</sup>J<sub>PF</sub> = 1.07 kHz, 2 %), 119.5 (twist-P<sub>2</sub>S<sub>8</sub><sup>2-</sup>, 68 %), 55.5 (chair-P<sub>2</sub>S<sub>8</sub><sup>2-</sup>, 14 %).

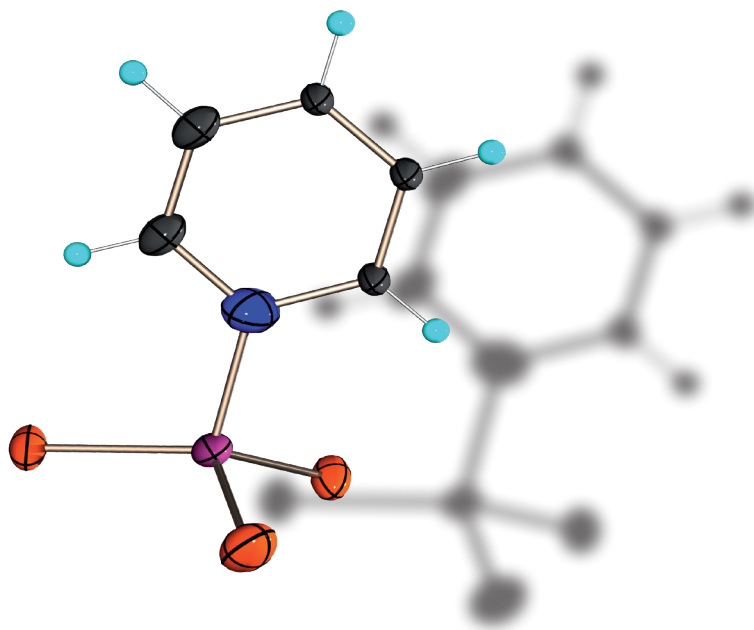
Table 8. Crystal and structure refinement data.

	$[n\text{Bu}_4\text{N}]_2[\text{P}_2\text{S}_6] \cdot \text{THF}$	$[\text{Ph}_4\text{P}]_2[\text{P}_2\text{S}_6] \cdot \text{py} (2)$	$[n\text{Bu}_4\text{N}]$ $[(\text{CH}_3)_2\text{NC}_5\text{H}_4\text{NPS}_3] (3)$
empirical formula	$(\text{C}_{16}\text{H}_{36}\text{N})_6 (\text{C}_{16}\text{H}_{29}\text{N})$ $(\text{P}_2\text{S}_6)_4 \text{C}_4\text{O}$	$\text{C}_{29}\text{H}_{25}\text{NP}_2\text{S}_3$	$\text{C}_{26}\text{H}_{51}\text{N}_4\text{PS}_3$
formula mass	3000.98	545.65	546.86
temp (K)	100	100	200
cryst. size (mm)	0.4 x 0.12 x 0.08	0.3 x 0.3 x 0.25	0.3 x 0.15 x 0.1
cryst. descriptn.	yellow rod	yellow rod	colourless block
cryst. system	triclinic	monoclinic	triclinic
space group	$P-1$	$P2_1/c$	$P-1$
$a$ (Å)	11.1073(8)	9.4174(1)	10.7269(5)
$b$ (Å)	15.4662(11)	12.3123(1)	10.8430(4)
$c$ (Å)	27.2591(19)	23.2297(3)	14.7239(6)
$\alpha$ (deg)	97.892(6)	90	98.584(3)
$\beta$ (deg)	96.433(6)	96.014(1)	102.892(4)
$\gamma$ (deg)	106.977(6)	90	105.500(4)
$V$ (Å <sup>3</sup> )	4378.7(6)	2678.66(5)	1568.40(13)
$Z$	1	4	2
$\rho_{\text{calc}}$ (g cm <sup>-3</sup> )	1.138	1.353	1.160
$\mu$ (mm <sup>-1</sup> )	0.409	0.416	0.308
$F(000)$	1628	1136	598
$\vartheta$ range (deg)	3.71-29.9	3.75-27.00	3.66-27.00
index ranges	$-14 \leq h \leq 14,$ $-19 \leq k \leq 19,$ $-34 \leq l \leq 34,$	$-12 \leq h \leq 12,$ $-15 \leq k \leq 15,$ $-29 \leq l \leq 29$	$-13 \leq h \leq 13,$ $-13 \leq k \leq 13,$ $-18 \leq l \leq 18$
reflcs collcd	48107	28478	17264
reflcs obsd	19039	4832	4416
reflcs unique	11603 ( $R_{\text{int}} = 0.0450$ )	5827 ( $R_{\text{int}} = 0.0287$ )	6817 ( $R_{\text{int}} = 0.0345$ )
$R_1, wR_2$ ( $2\sigma$ data)	0.0428, 0.1013	0.0368, 0.0875	0.0365, 0.0810
$R_1, wR_2$ (all data)	0.0829, 0.1178	0.0483, 0.0950	0.0628, 0.0901
max/min transm	0.8483/1.0000	0.901/0.883	0.970/0.946
data/restr/params	19039/0/818	5827/0/396	6817/0/487
$S$ on $F^2$	0.976	1.052	0.913
larg. diff peak/hole (e/Å)	0.918/-0.815	1.203/-0.416	0.551/-0.285
remarks	the hydrogen atoms of the THF molecule are missing due to the disorder within the molecule.		

## CHAPTER IV

---

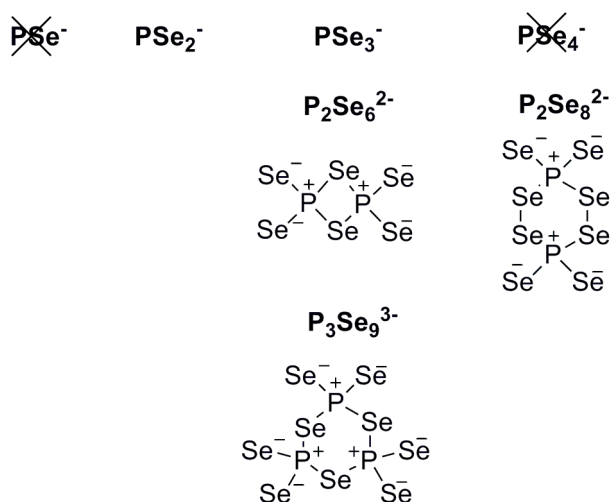
### The Triselenometaphosphate Anion $\text{PSe}_3^-$ : A Synthetic Challenge



*A new synthesis of the triselenometaphosphate anion  $\text{PSe}_3^-$  is presented. Multinuclear NMR spectroscopy ( $^{31}\text{P}$ ,  $^{77}\text{Se}$ ) is used for its characterization. The reaction with nucleophiles like pyridine and N-methylimidazole is investigated. Temperature dependent  $^{31}\text{P}$  NMR spectroscopy is used to examine the equilibrium between the free monomeric triselenometaphosphate anion and its base adducts, in analogy to the corresponding sulfur derivative. In the course of the investigation, the crystal structure of the pyridine adduct of  $\text{PSe}_3^-$  ( $[\text{pyH}][\text{pyPSe}_3]$  (**1**)), is obtained and structurally characterized by single crystal X-ray diffraction. In addition, quantum chemical investigations are carried out to examine the bonding situation in the triselenometaphosphate anion  $\text{PSe}_3^-$  in the gas phase as well as the NMR chemical shift and the Mulliken charges. The structure analysis of  $[\text{pyH}][\text{pyPSe}_3]$  (**1**) is compared with the literature known sulfur analogue  $[\text{pyH}][\text{pyPS}_3]$ .*

## 1 Introduction

Now that the trithiometaphosphate anion  $\text{PS}_3^-$  and its dimer  $\text{P}_2\text{S}_6^{2-}$  have been discussed, let us have a closer look at P, Se anions comprising of a central phosphorus atom in a low coordination number CN (CN = 2, 3). In Scheme 1, the literature known monomers with a central phosphorus atom in a low coordination number ( $\text{PSe}_2^-$ ,  $\text{PSe}_3^-$ ) and the existing oligomers ( $\text{P}_2\text{Se}_6^{2-}$ ,  $\text{P}_3\text{Se}_9^{3-}$ ,  $\text{P}_2\text{Se}_8^{2-}$ ) are shown.<sup>1,2,3,4</sup>



**Scheme 1. Binary phosphorus-selenium anions.**

In 1997, Brockner et al. characterized the formal dimer of the triselenometaphosphate anion  $\text{P}_2\text{Se}_6^{2-}$  by Raman spectroscopy for the first time. Nevertheless, no evidence for the existence of the monomeric triselenometaphosphate anion  $\text{PSe}_3^-$  was found.<sup>1</sup> Indications for the existence of a monomer, dimer and trimer of the triselenometaphosphate anion,  $(\text{PSe}_3^-)_n$  ( $n = 1-3$ ), have been proofed by our group using  $^{31}\text{P}$  and  $^{77}\text{Se}$  NMR spectroscopy.<sup>3</sup>

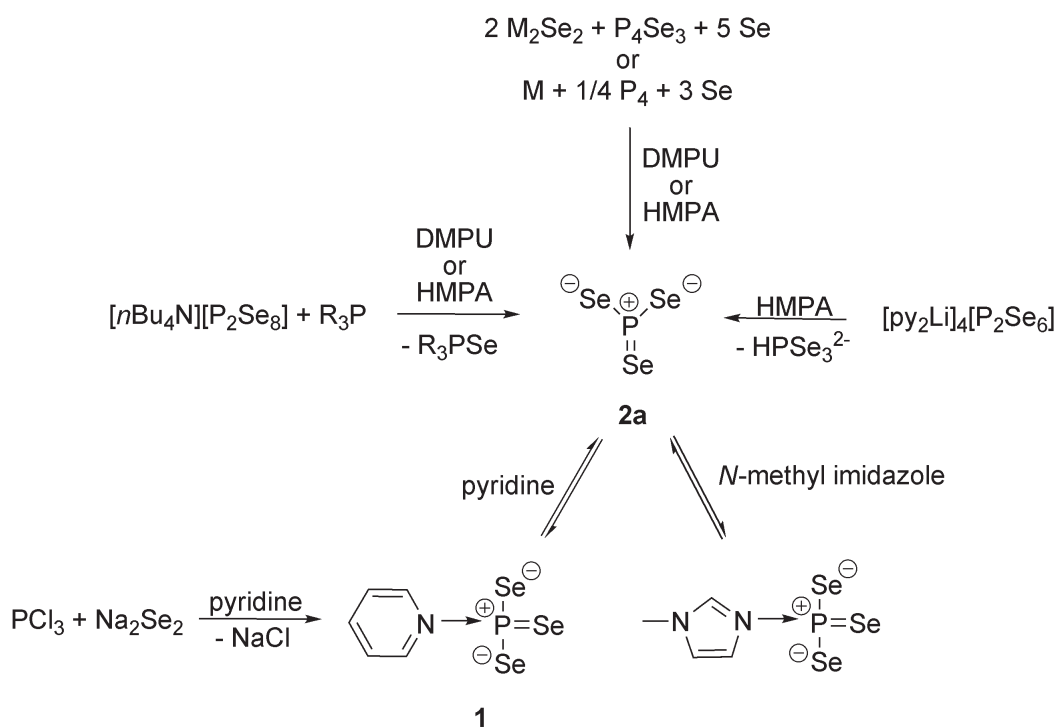
<sup>1</sup> Menzel, F.; Brockner, W.; Ystenes, M. *Vibrational Spec.* **1997**, *14*(1), 59.

<sup>2</sup> O'Neal, S. C.; Pennington, W. T.; Kolis, J. W. *Angew. Chem.* **1990**, *102*(12), 1502.

<sup>3</sup> (a) Karaghiosoff, K.; Schuster, M. *Phosphorus, Sulfur Silicon Relat. Elem.* **2001**, *168*, 117. (b) Schuster, M. *dissertation*, LMU Munich, **1999**.

<sup>4</sup> (a) Zhao, J.; Pennington, W. T.; Kolis, J. W. *J. Chem., Chem. Commun.* **1992**, 265. (b) Rotter, C.; Schuster, M.; Kidik, M.; Schön, O.; Klapötke, T. M.; Karaghiosoff, K. *Inorg. Chem.* **2008**, *632*, 1663.

## 2 Syntheses



Scheme 2. Syntheses of  $PSe_3^-$  and the corresponding *N*-methyl imidazole and pyridine adducts ( $M = Li, Na$ ).

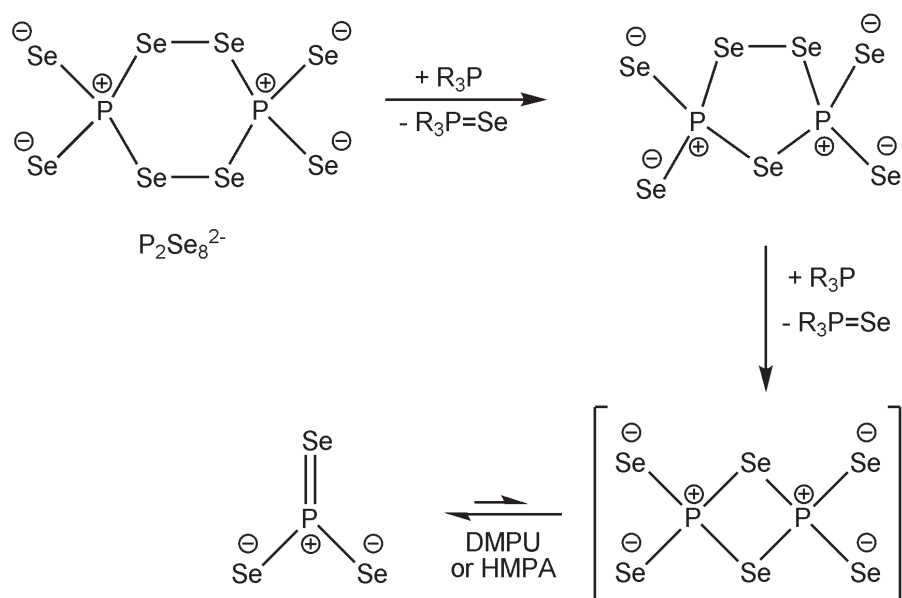
The triselenometaphosphate anion  $PSe_3^-$  (**2a**) could be observed in all polar aprotic solvents shown in Table 1. In case of using  $P_4Se_3, M_2Se_2$  ( $M = Li, Na$ ) as educts or starting from the elements  $P_4, Li/Na$  and selenium, the ideal stoichiometry corresponds to the theoretically needed, which has to be maintained exactly (Scheme 2).<sup>3</sup>

Table 1. Ratio (in mol-%) of  $PSe_3^-$ ,  $P_2Se_6^{2-}$  and  $P_3Se_9^{3-}$  depending on the used solvent. The maximum total proportion (in mol-%) of all three anions in the reaction solution is also given.

solvent	$PSe_3^-$ (2a)	$P_2Se_6^{2-}$ (2b)	$P_3Se_9^{3-}$ (2c)	total proportion
<i>N</i> -methyl imidazole	100 <sup>b)</sup>	0	0	100 <sup>a)</sup>
HMPA	100	0	0	70 <sup>a)</sup>
benzonitrile	100	0	0	19 <sup>a)</sup>
DMPU	98	2	0	80 <sup>a)</sup>
pyridine	90 <sup>b)</sup>	0	10	35 <sup>a)</sup>
THF	70	0	30	30 <sup>a)</sup>
2-methyl pyridine	30	0	70	10 <sup>a)</sup>
acetonitrile	0	0	100	20 <sup>a)</sup>

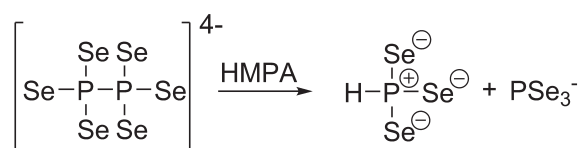
<sup>a)</sup> the percentage ratio of the compounds is determined by using the integrals of the resonances in the <sup>31</sup>P NMR spectra of the corresponding reaction solutions; <sup>b)</sup> as adduct

Alternatively, the triselenometaphosphate  $\text{PSe}_3^-$  is formed on deselenation of  $[\text{nBu}_4\text{N}]_2[\text{P}_2\text{Se}_8] \cdot 2 \text{CH}_3\text{CN}$  using phosphanes  $\text{R}_3\text{P}$  ( $\text{R} = \text{Ph}, \text{C}_2\text{H}_4\text{CN}, \text{nBu}$ ) in DMPU or HMPA (Scheme 2).<sup>3</sup> Therefore, two deselenation steps are required. In the first deselenation of  $\text{P}_2\text{Se}_8^{2-}$ , one endocyclic Se atom is removed, thus a five-membered ring  $\text{P}_2\text{Se}_7^{2-}$  is formed. During the second deselenation, a second selenium atom is removed out of the endocyclic diselenide bridge, forming a four-membered ring  $\text{P}_2\text{Se}_6^{2-}$ , which is the dimer of  $\text{PSe}_3^-$ . In polar solvents like DMPU or HMPA, the equilibrium between  $\text{P}_2\text{Se}_6^{2-}$  and  $\text{PSe}_3^-$  is on the side of the monomeric  $\text{PSe}_3^-$  (Scheme 3).<sup>3</sup>



**Scheme 3.** Formal reaction way of the deselenation of  $\text{P}_2\text{Se}_8^{2-}$  using phosphanes  $\text{R}_3\text{P}$  ( $\text{R} = \text{Ph}, \text{C}_2\text{H}_4\text{CN}, \text{nBu}$ ).

Upon dissolving  $[\text{py}_2\text{Li}]_4[\text{P}_2\text{Se}_6]$  in HMPA, surprisingly, the monomeric triselenometaphosphate anion  $\text{PSe}_3^-$  can be observed in the reaction solution using  $^{31}\text{P}$  NMR spectroscopy. Besides  $\text{P}_2\text{Se}_6^{4-}$   $\text{HPSe}_3^{2-}$  is observable. The ratio of  $\text{PSe}_3^-$ :  $\text{HPSe}_3^{2-}$  is 1 : 1. The more HMPA is added, implying a dilution of the reaction solution, the higher is the observable rate of  $\text{PSe}_3^-$  and  $\text{HPSe}_3^{2-}$  in the  $^{31}\text{P}$  NMR spectrum. In a 0.5 M reaction solution no  $\text{P}_2\text{Se}_6^{4-}$  is observed (Scheme 4).<sup>3</sup>



**Scheme 4.** Formation of  $\text{PSe}_3^-$  on dissolving  $\text{P}_2\text{Se}_6^{4-}$  in HMPA.

A new way of synthesizing the pyridine adduct stabilized  $\text{PSe}_3^-$  anion is starting from  $\text{PCl}_3$  in pyridine with  $\text{Na}_2\text{Se}_2$ , which shows the high building tendency of  $\text{pyPSe}_3^-$  in pyridine.

The  $^{31}\text{P}$  NMR chemical shift of the free monomeric triselenometaphosphate  $\text{PSe}_3^-$  is 212.2 ppm in HMPA (Figure 1). One pair of  $^{77}\text{Se}$  satellites could be observed. The  $^1J_{\text{SeP}}$  coupling constant is  $-788.2$  Hz which is an usual value for one coordinated  $^{77}\text{Se}$  atom. The ratio of the main signal to the corresponding  $^{77}\text{Se}$  satellite pair is 80.5:19.9 thus indicating that three equivalent selenium atoms are bonded to the central phosphorus atom. In the  $^{77}\text{Se}$  NMR spectrum, a doublet at 1251.9 ppm with the same  $^1J_{\text{SeP}}$  coupling constant as in the  $^{31}\text{P}$  NMR spectrum ( $-788.2$  Hz) could be observed for  $\text{PSe}_3^-$  in HMPA.<sup>3</sup>

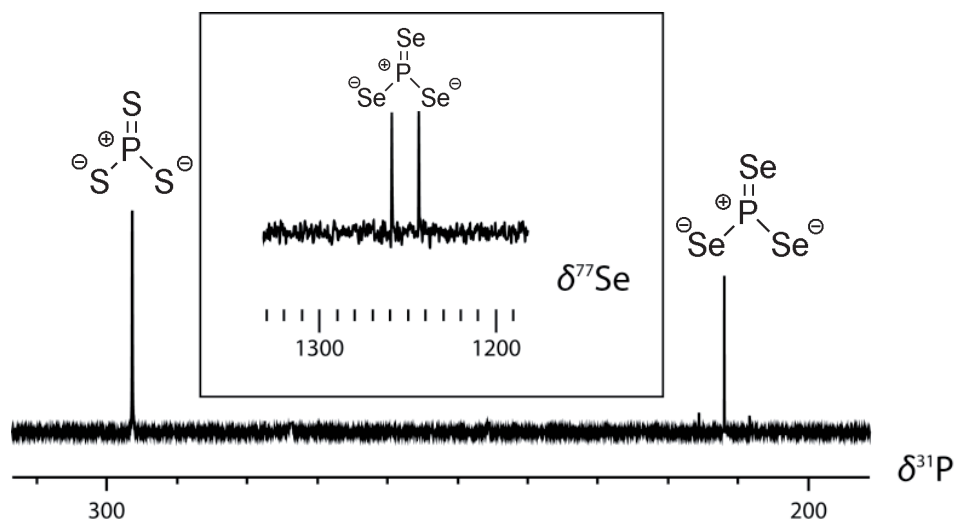


Figure 1.  $^{31}\text{P}$  NMR chemical shift of free monomeric  $\text{PSe}_3^-$  in comparison to the corresponding sulfur analogue  $\text{PS}_3^-$  in HMPA. In the insert black box, the  $^{77}\text{Se}$  NMR spectrum of  $\text{PSe}_3^-$  in HMPA is shown ( $^{31}\text{P}$  NMR spectrum: 1100 scans with a PD = 0.3 s, 15 min measuring time, 0.1 M solution;  $^{77}\text{Se}$  NMR: 50000 scans with a PD = 0.4 s, 12 h measuring time, 0.1 M).

### 3 Crystal and Molecular Structure of [pyH][pyPSe<sub>3</sub>] (1)

The pyridinium salt [pyH][PSe<sub>3</sub>] (**1**) was obtained as block shaped orange crystals in the reaction of PCl<sub>3</sub> with Na<sub>2</sub>Se<sub>2</sub> in pyridine and characterized using single crystal X-ray diffraction. Compound **1** crystallizes in the monoclinic space group *Cc*.

The phosphorus atom is coordinated by three selenium atoms and one pyridine molecule. The P-Se bond distances have an average value of 217 pm and are between the values for a P-Se single bond and those found for the P-Se bond in phosphine selenides.<sup>5</sup> The P1-N1 distance is 185.3(2) pm and therefore significantly longer than the distance for P-N single bond of 176 pm described in literature.<sup>6</sup> The Se-P-Se bond angles have values of 112.4(1)° (Se1-P1-Se2), 114.8(1)° (Se2-P1-Se3) and 115.0(1)° (Se3-P1-Se1). The sum of all three bond angles is 342° which is between a perfect tetrahedral surrounding (324°) and a total planar arrangement (360°) (Table 2).

Remarkably, in contrast to the analogue PS<sub>3</sub><sup>-</sup> salt, no hydrogen bonds could be found between the anion and the cation. The position of the nitrogen atom in the pyH<sup>+</sup> cation could be determined exactly, the position providing the best *wR*<sub>2</sub> value and thermal parameters is shown in Figure 2.

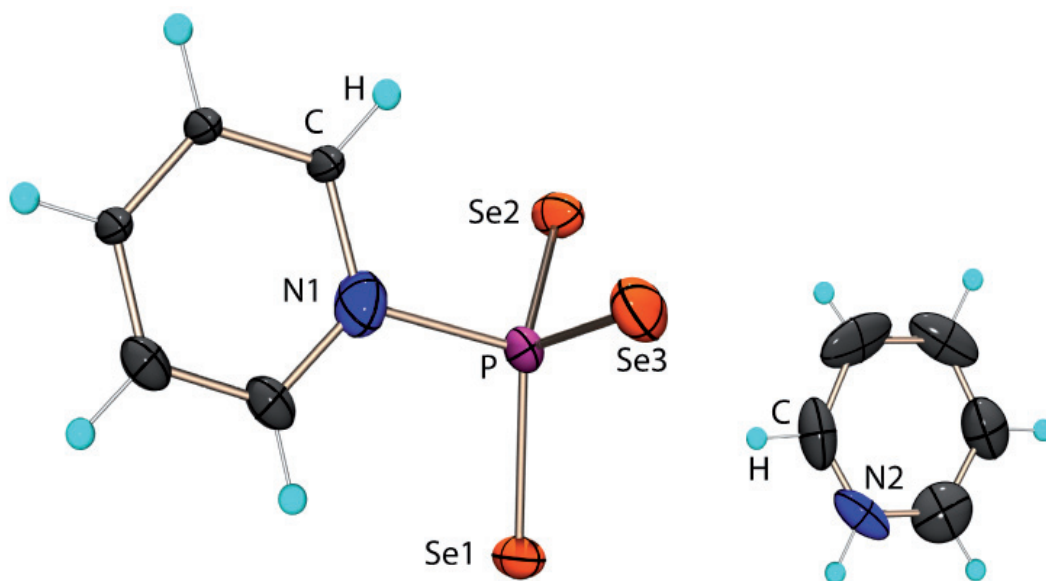


**Figure 2.** Molecular structure of [pyH][pyPSe<sub>3</sub>] (**1**) in the solid state. Thermal ellipsoids of non hydrogen atoms are drawn at the 50 % probability level.

<sup>5</sup> (a) Cordes, A. W., *Selenium*; Zingaro, R. A.; Cooper, W. C. (Ed.), Van Nostrand Reinhold Company: New York, **1974**. (b) Shaw, R. A.; Woods, M.; Cameron, I. S.; Dahlen, B. *Chem. Ind.* **1971**, 151. (c) Grand, A.; Martin, J.; Robert, J. B.; Tordjman, I. *Acta Crystallogr.* **1975**, B31, 2523. (d) Galdecki, Z.; Glowka, M. L.; Michalski, J.; Okruszek, A.; Stec, W. J. *Acta Crystallogr.* **1977**, B33, 2322. (e) Cameron, T. S.; Howlett, K. D.; Miller, K. *Acta Crystallogr.* **1978**, B34, 1639. (f) Codding, P. W.; Kerr, K. A. *Acta Crystallogr.* **1979**, B35, 1261. (g) Romming, C.; Songstad, J. *Acta Chem. Scand.* **1979**, A33, 187.

<sup>6</sup> Holleman, A.; Wiberg, E.; Wiberg, N. *Lehrbuch der anorganischen Chemie*, 102nd ed.; Walter de Gruyter Verlag, Berlin, **2007**.

Table 2. Selected bond parameters of [pyH][PSe<sub>3</sub>] (1)

Distances [pm]		Bond angles [°]	
Se1-P1	217.1(1)	Se1-P1-Se2	112.4(1)
Se2-P1	217.6(1)	Se2-P1-Se3	114.8(1)
Se3-P1	217.3(1)	Se3-P1-Se1	115.0(1)
N1-P1	185.3(2)	Se1-P1-N1	106.9(1)
		Se2-P1-N1	104.3(1)
		Se3-P1-N1	101.8(1)

Within the unit cell, the pyH<sup>+</sup> cations are located between the pyPSe<sub>3</sub> anions and arranged parallel to the pyridine ring of the anion. No other than electrostatic interactions between the cations and the anions can be found in the crystal.

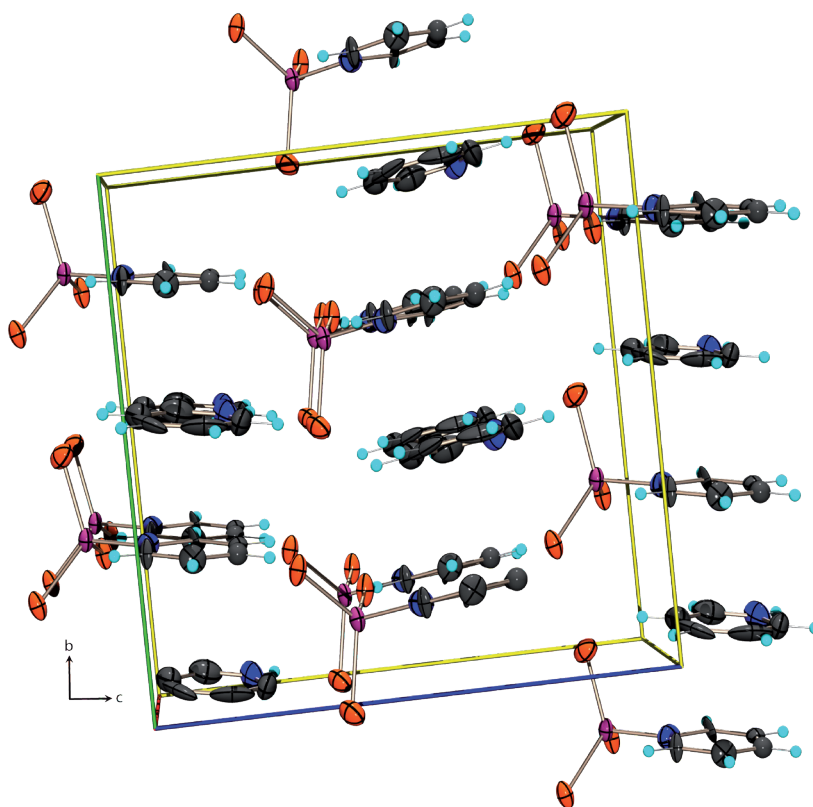


Figure 3. Unit cell of 1. View along *a* axis. Thermal ellipsoids of all non hydrogen atoms are drawn at 50 % probability level.

#### 4 Comparison of the structures of [pyH][pyPSe<sub>3</sub>] and [pyH][pyPS<sub>3</sub>]

The obtained structural parameters of [pyH][pyPSe<sub>3</sub>] (**1**) are compared to those of the analogue sulfur containing salt [pyH][pyPS<sub>3</sub>] in Table 3.

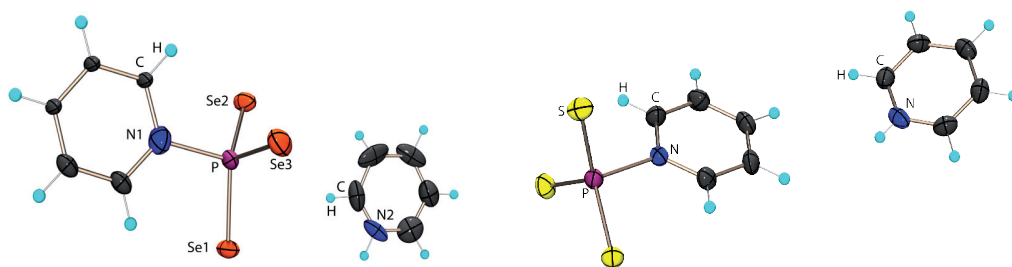


Figure 4. Crystal structures of [pyH][pyPSe<sub>3</sub>] (left) and [pyH][pyPS<sub>3</sub>] (right).

Table 3. Comparison of selected bond parameters of the pyridine adduct stabilized trichalcogenometaphosphate anion [pyH][pyPCh<sub>3</sub>] (Ch = S or Se).

Ch = S or Se	<b>1</b>	[pyH][pyPS <sub>3</sub> ]
P-Ch bond distances [pm]	217.1(1)	198.0(1)
	217.6(1)	198.6(2)
	217.3(1)	200.4(1)
average value P-Ch distances [pm]	217	199.0
Ch-P-Ch bond angles [°]	112.4(1)	113.72(2)
	114.8(1)	116.72(2)
	115.0(1)	116.41(2)
average value Ch-P-Ch bond angles [°]	114.1	115.6
Σ Ch-P-Ch bond angles [°]	342	347
P-N distance [pm]	185.3(2)	190.6(2)

In both cases, the P-Ch bond lengths have an average value, which is in between the values found for P-Ch single bonds and P=Ch double bonds.<sup>5</sup> The Ch-P-Ch bond angles observed in **1** are only slightly smaller than those found in the corresponding sulfur analogue resulting in a slightly bigger deviation from planarity of about 5° in comparison to the sulfur analogue. The most interesting point is the big difference of the P-N distance between **1** (185.3 pm) and [pyH][pyPS<sub>3</sub>] (190.6 pm) of 5 pm.

According to the quantum chemical calculations presented in the previous chapter, equivalent calculations were carried out for the triselenometaphosphate anion PSe<sub>3</sub><sup>-</sup>, in order to elucidate the structure, bonding, energetic situation and NMR chemical shifts of the monomeric triselenometaphosphate PSe<sub>3</sub><sup>-</sup> in the gas phase, where solid states effects are not considered.

## 5 Quantum chemical calculation

The calculations were carried out with the Gaussian 03 program code using different basis sets (pseudo potential ECP28MWB/VTZ<sup>7</sup>, 6-31+G\*\*, aug-cc-pVTZ and aug-cc-pVQZ).<sup>8</sup>

**Table 4. Calculated bond lengths [pm] and angles [°] for  $\text{PSe}_3^-$  in the gas phase.**

	pseudo potential ECP28MWB/VTZ	6-31+G**	aug-cc-pVTZ	aug-cc-pVQZ
$d(\text{P-Se}) / \text{pm}$	220.0	210.4	210.8	210.3
$\angle \text{P-Se-P} / ^\circ$	120	120	120	120
point group	$D_{3h}$	$D_{3h}$	$D_{3h}$	$D_{3h}$

The geometry optimization of  $\text{PSe}_3^-$  yields  $D_{3h}$  symmetry for this anion in all cases, which is in good agreement with the symmetry determined in quantum chemical calculations for the corresponding  $\text{PS}_3^-$ . Also the calculated Se-P-Se bond angles of  $120^\circ$  perfectly confirm the  $D_{3h}$  symmetry of the triselenometaphosphate anion  $\text{PSe}_3^-$  in the gas phase. In case of the calculated bond distances, the all-electron calculations (6-31+G\*\*, aug-cc-pVTZ and aug-pVQZ) give the same value of 210 pm for the P-Se bond, while the pseudo potential ECP28MWB/VTZ calculation gives a value of 220 pm. As the pseudo potential calculation considers relativistic effects, it gives the more reliable value for P-Se bonds (Table 4).

**Table 5. Mulliken charges for  $\text{PSe}_3^-$  and  $\text{PS}_3^-$ .**

	$\text{PSe}_3^-$		$\text{PS}_3^-$	
	P	Se	P	S
pseudo potential ECP28MWB/VTZ	-	-	0.631	-0.544
6-31+G**	0.409	-0.470	-0.015	-0.328
aug-cc-pVTZ	0.308	-0.436	0.631	-0.544
aug-cc-pVQZ	-0.014	-0.329	0.709	-0.570

<sup>7</sup> <http://www.theochem.uni-stuttgart.de/pseudopotentials/index.en.html> (14. Marz 2009).

<sup>8</sup> Gaussian 03, Revision D.01, Frisch, M. J.; Trucks, G. W.; Schlegel, H. B.; Scuseria, G. E.; Robb, M. A.; Cheeseman, J. R.; Montgomery, Jr., J. A.; Vreven, T.; Kudin, K. N.; Burant, J. C.; Millam, J. M.; Iyengar, S. S.; Tomasi, J.; Barone, V.; Mennucci, B.; Cossi, M.; Scalmani, G.; Rega, N.; Petersson, G. A.; Nakatsuji, H.; Hada, M.; Ehara, M.; Toyota, K.; Fukuda, R.; Hasegawa, J.; Ishida, M.; Nakajima, T.; Honda, Y.; Kitao, O.; Nakai, H.; Klene, M.; Li, X.; Knox, J. E.; Hratchian, H. P.; Cross, J. B.; Bakken, V.; Adamo, C.; Jaramillo, J.; Gomperts, R.; Stratmann, R. E.; Yazyev, O.; Austin, A. J.; Cammi, R.; Pomelli, C.; Ochterski, J. W.; Ayala, P. Y.; Morokuma, K.; Voth, G. A.; Salvador, P.; Dannenberg, J. J.; Zakrzewski, V. G.; Dapprich, S.; Daniels, A. D.; Strain, M. C.; Farkas, O.; Malick, D. K.; Rabuck, A. D.; Raghavachari, K.; Foresman, J. B.; Ortiz, J. V.; Cui, Q.; Baboul, A. G.; Clifford, S.; Cioslowski, J.; Stefanov, B. B.; Liu, G.; Liashenko, A.; Piskorz, P.; Komaromi, I.; Martin, R. L.; Fox, D. J.; Keith, T.; Al-Laham, M. A.; Peng, C. Y.; Nanayakkara, A.; Challacombe, P.; Gill, M. W.; Johnson, B.; Chen, W.; Wong, M. W.; Gonzalez, C.; Pople, J. A.; Gaussian, Inc., Wallingford CT, 2004.

## 5.1 Valence bond structures

The VB program package VB2000, version 1.8 was used for all VB calculations employing STO-3G basis set for  $\text{PSe}_3^-$  and additionally the D95 basis set for  $\text{PS}_3^-$ .<sup>9</sup> VB2000 is an *ab initio* electronic structure package for performing modern VB calculations; it is based on a highly efficient VB algorithm – the so called algebrant algorithm – and the group function (GF) approach, in which a large molecule is described in terms of its constituent parts – physically identifiable “electron groups”. A major feature of VB2000 is the implementation of modern VB theory at the *ab initio* level using the algebrant algorithm.<sup>9, 10, 11, 12, 13, 14, 15, 16, 17, 18, 19</sup>

The VB method used in this study was the CASVB(6,4) one (*complete active space*) with six VB electrons ( $\pi$  electrons) spread over four  $\pi$  orbitals. The CASVB method implemented in the VB2000 program package generates the weights of all resonance structures. In VB2000, each “structure” becomes a spin-coupling scheme, involving pairs of electrons occupying rather localized, strongly overlapping orbitals. The overlapping orbitals of any bond are expected to bear some similarity to the AOs used in constructing a localized MO. In particular, the  $\pi$ -orbitals used in this study are almost one-center AOs with only a very small degree of “tailing”, *i.e.* spreading onto other atomic centers.

Figure 4 shows all possible VB structures for the  $\text{PSe}_3^-$  anion, which were generated from a CASVB(6,4) calculation with the six  $\pi$  electrons forming the active VB space (all  $\sigma$  and core electrons were treated with the HF method). As expected, the Hiberty weights of the standard Lewis structures of type **I** are the individually most important contributors to the resonance scheme for  $\text{PSe}_3^-$  (Table 6) in comparison to the already presented ones for  $\text{PS}_3^-$ . It is also interesting to point out that the Dewar-type (or long bond) structures (**II**) together with the sextet structure **III** are important resonance structures for both anions ( $\text{PS}_3^-$  and  $\text{PSe}_3^-$ ) whereas the structures with one chalcogen atom carrying a positive charge (**IV**) is much less important (Table 6).

<sup>9</sup> Li, J.; McWeeny, R. *VB2000*, version 1.7, SciNet Technologies: San Diego, CA, (November 2005).

<sup>10</sup> Li, J.; Pauncz, R. *Int. J. Quantum. Chem.* **1997**, *62*, 245.

<sup>11</sup> Li, J. McWeeny, R. *Int. J. Quantum. Chem.* **2002**, *89*, 208.

<sup>12</sup> McWeeny, R. *Adv. Quant. Chem.* **1999**, *31*, 15.

<sup>13</sup> McWeeny, R. *Proc. R. Soc. Lond.* **1959**, *Ser A253*, 242.

<sup>14</sup> Angyan, J. A. *Theor. Chem. Acc.* **2000**, *103*, 238.

<sup>15</sup> McWeeny, R.; Sutcliffe, B. T. *Proc. R. Soc. Lond.* **1963**, *Ser. A 273*, 103.

<sup>16</sup> Gallup, G. A.; Norbeck, J. M. *Chem. Phys. Lett.* **1973**, *21*, 495.

<sup>17</sup> Hiberty, P. C.; Ohanessian, G. *Int. J. Quantum. Chem.* **1985**, *27*, 245.

<sup>18</sup> Levine, I. N. in *Quantum Chemistry*, vol. I, sect. 15.10, Allyn and Bacon: Boston, **1970**, p 550.

<sup>19</sup> Bachler, V. *Theor. Chem. Acc.* **1997**, *92*, 223.

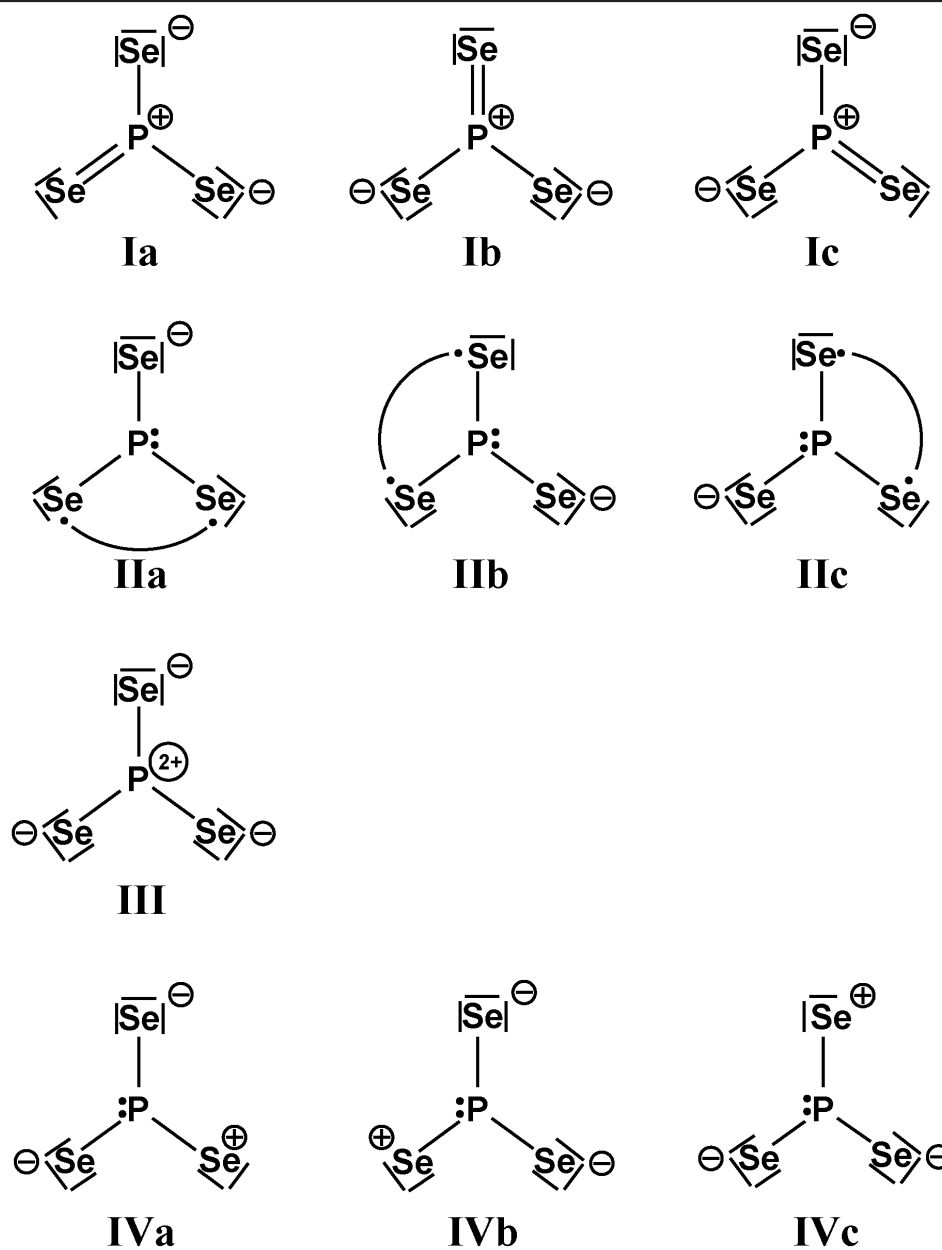


Figure 5. VB structures for  $\text{PSe}_3^-$  generated from a CASVB(6,4) calculation with the six  $\pi$  electrons forming the active VB space (all  $\sigma$  and core electrons were treated with the HF method).

Table 6. Hiberty structural weights of the individual Lewis structures for  $\text{PS}_3^-$  and  $\text{PSe}_3^-$  depicted in Figure 5, calculated at CASVB(6,4)/STO-3G level of theory.<sup>16,17,18,19a,20</sup>

Structure	I	II	III	IV
Hiberty weight for $\text{PS}_3^-$	3 x 0.21	3 x 0.09	0.10	3 x 0.003
Hiberty weight for $\text{PSe}_3^-$	3 x 0.22	3 x 0.07	0.12	3 x 0.003

<sup>20</sup> The Hiberty weights  $W_i$  are defined as follows:  $W_i = C_i^2 / \sum C_i^2$ . (Where  $C_i$  are the coefficients of the wavefunctions for VB structures  $i$ ).

For the  $\text{PS}_3^-$  anion, also a CASVB calculation using the double-zeta D95 basis in order to account for the relatively poor basis set used above were carried out. The results show (Table 7) that the Hiberty weights for the resonance structures of  $\text{PS}_3^-$  remain essentially unchanged which gives credence that also for  $\text{PSe}_3^-$  (for which there is no D95 basis implemented in the VB2000 code) the STO-3G calculated weights are reliable.

**Table 7. Hiberty structural weights of the individual Lewis structures for  $\text{PS}_3^-$  depicted in Fig. 1, calculated at CASVB(6,4)/D95 level of theory.**<sup>16,17,18,19a,21</sup>

Structure	I	II	III	IV
Hiberty weight	3 x 0.22	3 x 0.07	0.12	3 x 0.001

Since the above calculations for  $\text{PS}_3^-$  at the CASVB(6,4) level of theory did not indicate any relevance for structures containing “hypervalent” phosphorus, a VB(6)/3-21G(d) calculation, including explicitly (in addition to the ten structures shown in Figure 5) six further VB structures (using  $d_{z^2}$  orbitals at the P center) with two double bonds between P and S and one single bond between P and S<sup>-</sup> was carried out. It turned out, as already expected from the CASVB calculation, that the three structures with two double bonds each carry a negligible (Hiberty) weight (0.0002).

The calculated  $^{77}\text{Se}$  NMR chemical shifts represent the observed  $^{77}\text{Se}$  NMR chemical shift for the  $\text{PSe}_3^-$  anion quite well. To provide the exactitude of the NMR calculations, the  $^{77}\text{Se}$  NMR chemical shifts of the used reference  $\text{Me}_2\text{Se}$  was also calculated. In Table 8, the calculated isotropic shielding of  $\text{Me}_2\text{Se}$  and  $\text{PSe}_3^-$  as well as the relative  $^{77}\text{Se}$  NMR chemical shifts are summarized and compared to the experimentally observed  $^{77}\text{Se}$  NMR chemical shifts.<sup>21</sup>

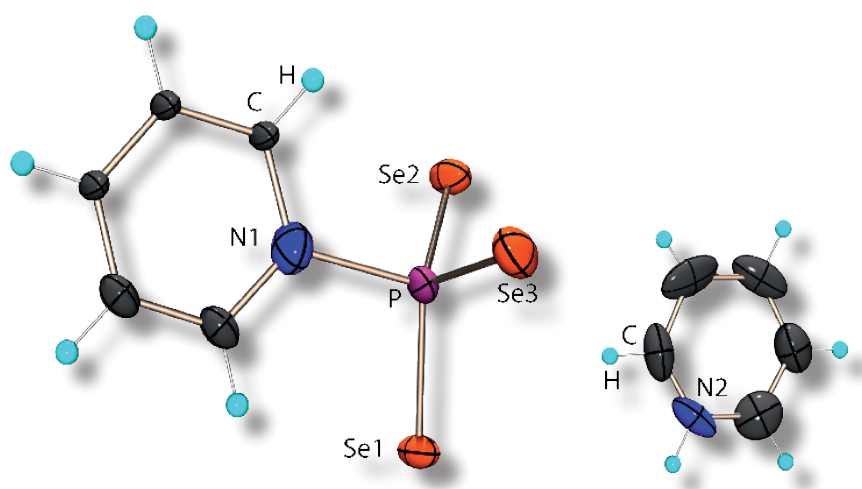
**Table 8. Computed isotropic magnetic shieldings and relative  $^{77}\text{Se}$  NMR chemical shifts (ppm) referenced to  $\text{Me}_2\text{Se}$ .**

	calc. isotropic shielding	rel. shift [ppm]	exptl. reported chem. shift [ppm]
$\text{Me}_2\text{Se}$	1833.9	0	0
$\text{PSe}_3^-$	537.3	1296.6	1251.9

<sup>21</sup>  $^{31}\text{P}$  NMR chemical shifts were also calculated, but differ significantly from the experimental determined ones ( $\Delta\delta = 200$ ).

## 6 Conclusion

The X-ray crystallographic study on [pyH][pyPSe<sub>3</sub>] demonstrates for the first time the existence of the PSe<sub>3</sub><sup>-</sup> anion in the solid state. In addition, quantum chemical calculations were carried out to elucidate the bonding situation, NMR chemical shift and Mulliken charges in the free monomeric triselenometaphosphate PSe<sub>3</sub><sup>-</sup>.



## 7 Experimental Section

**General.** All reactions were carried out under inert gas atmosphere using Schlenk techniques. Argon (Messer Griesheim, purity 4.6 in 50 L steel cylinder) was used as inert gas. The glass vessels used were stored in a 130 °C drying oven and were flame dried in vacuum at  $10^{-3}$  mbar before use.

$\text{Na}_2\text{Se}_2$  was prepared as described in the literature and stored in a dry box under nitrogen atmosphere.<sup>22</sup> Pyridine was dried following known methods.  $\text{PCl}_3$  (Aldrich) was distilled immediately before use.

**NMR Spectroscopy.** NMR spectra were recorded using a Jeol EX 400 Eclipse instrument operating at 161.997 MHz ( $^{31}\text{P}$ ) and 76.321 MHz ( $^{77}\text{Se}$ ). Chemical shifts are referred to 85 %  $\text{H}_3\text{PO}_4$  and  $(\text{CH}_3)_2\text{Se}$  ( $^{77}\text{Se}$ ) as external standards. All spectra were measured, if not mentioned otherwise, at 25 °C. The %-data correspond to the intensities in the  $^{31}\text{P}$  NMR spectra with respect to the total intensity. The difference to 100 % belongs to not determinable signals.

**X-ray Crystallography.** The molecular structure of  $[\text{pyH}][\text{pyPSe}_3]$  in the crystalline state was determined using an Oxford Xcalibur3 diffraction instrument equipped with a Spellman generator (voltage 50 kV, current 40 mA) and a Kappa CCD detector with a X-ray radiation wavelength of 0.71073 Å ( $\text{MoK}_\alpha$ ). The data collection was performed with the CrysAlis CCD software, the data reduction with the CrysAlis RED software.<sup>23,24</sup> The structure was solved with SIR-92 and SHELXS-97 and refined with SHELXL-97 and finally checked using PLATON.<sup>25,26,27,28,29</sup> The absorptions were corrected by the SCALE3 ABSPACK multi-scan method.<sup>30</sup> All relevant data and parameters of the X-ray measurement and refinement are given in Table 9.

<sup>22</sup> (a) Thompson, D. P.; Boudjouk, P. J. *Org. Chem.* **1988**, *53*, 2109. (b) Schuster, M. dissertation, LMU Munich, **1999**.

<sup>23</sup> CrysAlis CCD, Oxford Diffraction Ltd., Version 1.171.27p5 beta (release 01-04-2005 CrysAlis171 .NET), (compiled Apr 1 2005,17:53:34).

<sup>24</sup> CrysAlis RED, Oxford Diffraction Ltd., Version 1.171.27p5 beta (release 01-04-2005 CrysAlis171 .NET), (compiled Apr 1 2005,17:53:34).

<sup>25</sup> SIR-92, **1993**, *A Program for Crystal Structure Solution*; Altomare, A.; Cascarano, G. L.; Giacovazzo, C.; Guagliardi, A. J. *Appl. Cryst.* **26**, 343.

<sup>26</sup> Altomare, A.; Burla, M. C.; Camalli, M.; Cascarano, G. L.; Giacovazzo, C.; Guagliardi, A.; Moliterni, A. G. G.; Polidor, G.; Spagna, R. J. *Appl. Crystallogr.* **1999**, *32*, 115.

<sup>27</sup> Sheldrick, G. M. *SHELXS-97, Program for Crystal Structure Solution*; Universität Göttingen, **1997**.

<sup>28</sup> Sheldrick, G. M. *SHELXL-97, Program for the Refinement of Crystal Structures*; University of Göttingen, Germany, **1997**.

<sup>29</sup> Spek, L. A. *PLATON, A Multipurpose Crystallographic Tool*, Utrecht University, Utrecht, The Netherlands, **1999**.

<sup>30</sup> SCALE3 ABSPACK – *An Oxford Diffraction program (1.0.4,gui:1.0.3)* (C) 2005 Oxford Diffraction Ltd.

---

**[pyH][pyPSe<sub>3</sub>] (1).** Na<sub>2</sub>Se<sub>2</sub> (408 mg, 2 mmol) was suspended in 2 mL of pyridine. PCl<sub>3</sub> (161 μL, 2 mmol) was slowly added during two minutes. The reaction was strongly exothermic yielding a brownish red solution. After one hour at ambient temperature, the reaction mixture was refluxed for two hours. The red brown suspension was centrifuged to remove the red precipitate. The clear orange brown solution was transferred into a NMR tube. After three months, orange crystals of [pyH][pyPSe<sub>3</sub>] were formed and characterized using X-ray crystallography.

<sup>31</sup>P{<sup>1</sup>H} NMR of the reaction solution in pyridine: δ = 206.0 (PCl<sub>3</sub>, 22 %), 200.6 (pyPSe<sub>3</sub>, 3%); 94.1 (py<sub>2</sub>PSe<sub>2</sub><sup>+</sup>, <sup>1</sup>J<sub>SeP</sub> = 817 Hz, 3 %); 44.3 (pyPSe<sub>2</sub>Cl, <sup>1</sup>J<sub>SeP</sub> = 891 Hz, 36 %); 30.5 (s, <sup>1</sup>J<sub>SeP</sub> = 971 Hz, ratio of <sup>77</sup>Se satellites: 6% ≈ 1 Se atom, 8 %); - 11.9 (s, <sup>1</sup>J<sub>SeP</sub> = 816 Hz, ratio of <sup>77</sup>Se satellites: 14.5% ≈ 2 Se atoms, 28 %) ppm.

<sup>77</sup>Se{<sup>1</sup>H} NMR of the reaction solution in pyridine: δ = 701.4 (d, <sup>1</sup>J<sub>SeP</sub> = 816 Hz); 388.4 (pyPSe<sub>2</sub>Cl); 66.3 (d, <sup>1</sup>J<sub>SeP</sub> = 972 Hz).

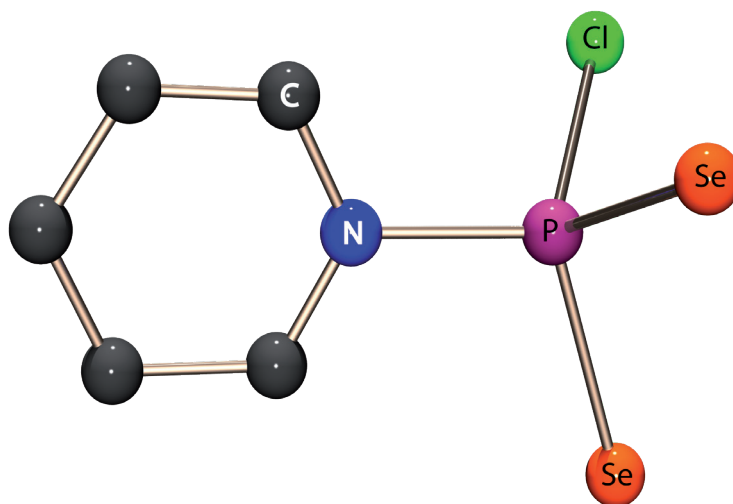
Table 9. Crystal data and structure refinement of 1.

	[pyH][pyPSe <sub>3</sub> ] (1)
empirical formula	C <sub>10</sub> H <sub>11</sub> N <sub>2</sub> PSe <sub>3</sub>
formula mass	427.06
temp (K)	200
cryst. size (mm)	0.15 x 0.15 x 0.05
cryst. descriptn	red plate
cryst. system	monoclinic
space group	<i>Cc</i>
<i>a</i> (Å)	7.7491(7)
<i>b</i> (Å)	13.0902(13)
<i>c</i> (Å)	13.5632(11)
$\alpha$ (deg)	90
$\beta$ (deg)	94.479(8)
$\gamma$ (deg)	90
<i>V</i> (Å <sup>3</sup> )	1371.6(2)
<i>Z</i>	4
$\rho_{\text{calc}}$ (g cm <sup>-3</sup> )	2.068
$\mu$ (mm <sup>-1</sup> )	8.137
<i>F</i> (000)	808
$\vartheta$ range (deg)	4.1327-29.9897
index ranges	-9 ≤ <i>h</i> ≤ 9, -16 ≤ <i>k</i> ≤ 16, -16 ≤ <i>l</i> ≤ 16
reflcns collcd	6811
reflcns obsd	1880
reflcns unique	2688 ( <i>R</i> <sub>int</sub> = 0.0569)
<i>R</i> <sub>1</sub> , <i>wR</i> <sub>2</sub> (2 $\sigma$ data)	0.0358, 0.0643
<i>R</i> <sub>1</sub> , <i>wR</i> <sub>2</sub> (all data)	0.0550, 0.0670
max/min transm	0.307/0.666
data/restr/params	2688/2/132
<i>S</i> on <i>F</i> <sup>2</sup>	0.802
larg. diff peak/hole (e/Å)	0.601/-0.370

## CHAPTER V

---

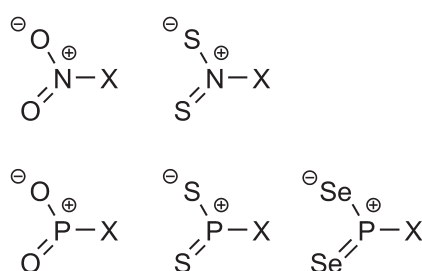
### On the Existence of Dichalcogenophosphoryl Monohalogenides $PCh_2X$ ( $Ch = S, Se, Te; X = Cl, Br, I$ )



*The existence of dichalcogenophosphoryl monohalogenides  $PCh_2X$  ( $Ch = S, Se, Te; X = Cl, Br, I$ ) is investigated. The new syntheses strategy occurred starting from phosphorus trihalogenide ( $PCl_3, PBr_3, PI_3$ ); and sodium dichalcogenide ( $Na_2S_2, Na_2Se_2, Na_2Te_2$ ) in polar aprotic solvents. In addition, the new selenium containing pyridine adducts of  $PSe_2Cl$  and  $PSe_2Br$  can be observed and characterized for the first time using solution NMR spectroscopy.*

## 1 The Problem with $\sigma^3\lambda^5$ Phosphorus

Among the nitrylmonohalogenides and phosphorylmonohalogenides shown in Scheme 1, only the  $\text{NO}_2\text{X}$  ( $\text{X} = \text{F}, \text{Cl}, \text{Br}$ ) are described in literature. The dioxonitrylhalogenides  $\text{NO}_2\text{X}$  are gases under normal conditions (25 °C, 1 bar) and, besides  $\text{NO}_2\text{F}$ , endothermic compounds.<sup>1</sup> Comparing the oxonitrylhalogenid to the isoelectronic nitrate anion  $\text{NO}_3^-$ , the substitution of an oxygen atom through a halogen atom, fluorine, chlorine or bromine, obviously leads to the destabilization of the molecule  $\text{NO}_2\text{X}$ , probably due to the loss of  $\pi$  aromaticity.

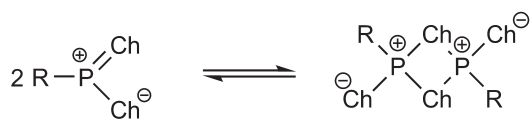


Scheme 1. Lewis formula of  $\text{NO}_2\text{X}$ ,  $\text{NS}_2\text{X}$ ,  $\text{PO}_2\text{X}$ ,  $\text{PS}_2\text{X}$  and  $\text{PSe}_2\text{X}$  ( $\text{X} = \text{F}, \text{Cl}, \text{Br}, \text{I}$ ).

But what is about the dichalcogenylphosphoryl monohalogenides  $\text{PCh}_2\text{X}$ ?

The dichalcogenophosphoryl monohalogenides  $\text{PCh}_2\text{X}$  are metaphosphate derivatives, where the central phosphorus atom has a very unusual bonding situation, as it is planar with the formal oxidation state +V, but has an unsaturated coordination sphere as it is only tricoordinated. So a strong Lewis acidity is to be expected.

The way out of that uncomfortable situation is *dimerisation* (Scheme 2). Großmann observed a monomer-dimer equilibrium for perthiophosphonic acid anhydrides in solution. These compounds have an organic residue R like a phenyl or a methyl group.<sup>2</sup>

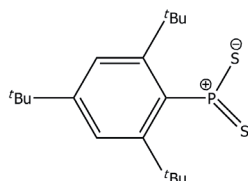


Scheme 2: Dimerisation of metaphosphate derivatives.

<sup>1</sup> Holleman, A.; Wiberg, E.; Wiberg, N. *Lehrbuch der anorganischen Chemie*, 102nd ed.; Walter de Gruyter Verlag, Berlin, 2007.

<sup>2</sup> Beckmann, H.; Großmann, G.; Ohms, G. *Heteroatom Chemistry*, 1994, 5(1), 73-83.

Till now there are only two possibilities known to stabilize the monomeric form: One is described by Yoshifuji et al. where R is a bulky substituent like supermesityl (Scheme 3).<sup>3,4</sup>

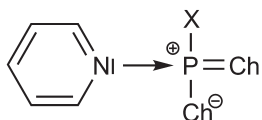


**Scheme 3. Dithioxophosphorane.**

The other possibility is if R is a negatively charged group like  $S^-$  or  $Se^-$ . In the first case the monomeric form is favored due to sterical reasons, while in the second case electronical reasons are responsible for the stabilization of the monomeric form as two anions have to get together during the dimerisation and due to Coulomb interactions this is a disadvantaged process.

So the question was what happens if the negatively charged chalcogen  $Ch^-$  is substituted by a neutral group. And as the halogens are isoelectronic to negatively charged chalcogen anions  $Ch^-$  investigations were made to examine the exchange of chalcogen against halogen atoms.

There are no reports in literature about  $PS_2X$  (as monomer or oligomer), however there are reports about corresponding pyridine adducts  $pyPS_2X$  (Scheme 4).



**Scheme 4: Pyridine adduct stabilized dichalcogenophosphoryl monohalogenides  $pyPCh_2X$ .**

The access to  $PS_2X$  chemistry is represented by  $pyPS_2Cl$ , which is easily prepared starting from  $P_4S_{10}$  and  $PSCl_3$  in pyridine. Starting from  $pyPS_2Cl$  the fluorine derivative can be synthesized, while the bromine analogue is made starting from  $pyPS_2(NMe_2)$  and  $PBr_3$ . In solution an equilibrium between the cation  $py_2PS_2^+ X^-$  and donorstabilized dithiometaphosphoric acid halides  $pyPS_2X$  can be observed (Scheme 5).<sup>5,6,7,8</sup>

<sup>3</sup> Yoshifuji, M.; Toyota, K.; Ando, K.; Inamoto, N. *Chem. Lett.* **1984**, 317-318.

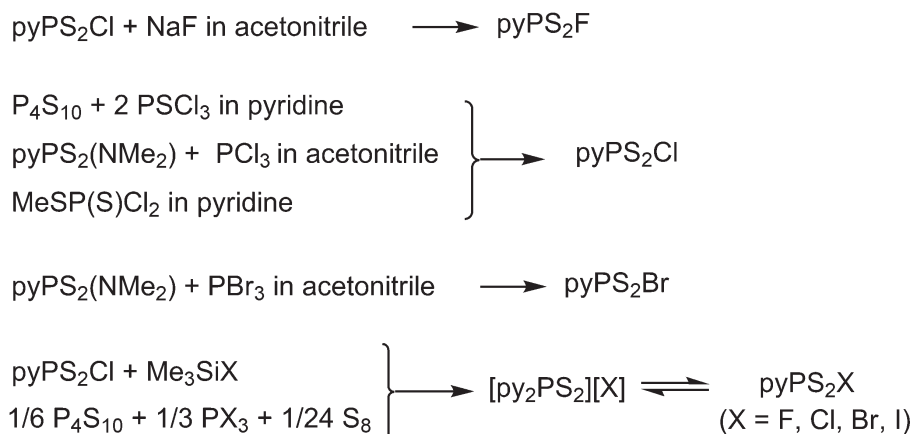
<sup>4</sup> Yoshifuji, M.; Shibayama, K.; Inamoto, N. *Chem. Lett.* **1984**, 603-606.

<sup>5</sup> Meisel, M.; Grunze, H. *Z. anorg. allg. Chem.* **1968**, 360, 277-285.

<sup>6</sup> Fluck, E.; Retuert, P. J.; Binder, H. *Z. anorg. allg. Chem.* **1973**, 397, 225-320.

<sup>7</sup> Costisella, B.; Schulz, J.; Teichmann, H.; Donath, C.; Meisel, M. *Phosphorus, Sulfur Silicon Relat. Elem.* **1990**, 53, 367-371.

<sup>8</sup> Meisel, M.; Lönnecke, P.; Grimmer, A.-R.; Molder-Wulff, D. *Angew. Chem. Int. Ed.* **1997**, 36(17), 1869-1870.



**Scheme 5. Syntheses of literature known pyPS<sub>2</sub>X (X = F, Cl, Br, I).**

As P<sub>4</sub>S<sub>10</sub> is used as educt, no selenium containing compound is described, as the required starting material P<sub>4</sub>Se<sub>10</sub> does not exist. In Table 1 all analytical data of the literature known compounds is summarized.

**Table 1. Analytical data of all literature known pyPS<sub>2</sub>X (X = F, Cl, Br, I).**

Ch	X	NMR data	X-Ray
S	F	$\delta^{31}\text{P} = 112$ <sup>[6]</sup> / $117.5$ <sup>[7]</sup> (in CHCl <sub>3</sub> ) $\delta^{19}\text{F} = 76.5$ <sup>[6]</sup> $^1J_{\text{PF}} = 1144 \text{ Hz}$ <sup>[6]</sup> / $1166 \text{ Hz}$ <sup>[7]</sup> (in CHCl <sub>3</sub> ) $^1J_{\text{PN}} = 20.6 \text{ Hz}$ <sup>[7]</sup>	✗
S	Cl	$\delta^{31}\text{P} = 138$ <sup>[5]</sup> / $97.5$ <sup>[7]</sup> (in CHCl <sub>3</sub> ) $^1J_{\text{PN}} = 24.1 \text{ Hz}$ <sup>[7]</sup>	✓ <sup>[4,9]</sup>
S	Br	$\delta^{31}\text{P} = 65.5$ (in CH <sub>3</sub> CN) <sup>[6]</sup> $^1J_{\text{PN}} = 32.6 \text{ Hz}$ <sup>[8]</sup>	✗
S	I	$\delta^{31}\text{P} = -0.4$ <sup>[8]</sup> $^1J_{\text{PN}} = 36.7 \text{ Hz}$ <sup>[8]</sup>	✗

Therefore the aims of the investigations were:

- Analysis of the bonding situation in pyPS<sub>2</sub>X
- Exceeding the investigation to the corresponding selenium compounds

## 2 New route to $\text{pyPCh}_2\text{X}$ (Ch = S, Se, Te; X = Cl, Br, I)

The easiest and straight forward way to synthesize compounds  $\text{pyPCh}_2\text{X}$  should start from  $\text{PX}_3$  and  $\text{Na}_2\text{Ch}_2$  in pyridine as reaction medium.



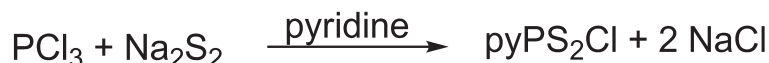
Scheme 6: New synthesis of  $\text{pyPCh}_2\text{X}$ .

The advantages of this reaction way are obvious:

- Possibility to introduce iodine ( $\text{PI}_3$ ), selenium ( $\text{Na}_2\text{Se}_2$ ) or tellurium ( $\text{Na}_2\text{Te}_2$ )
- Formation of only  $\text{NaX}$  as by-product is expected, so purification should be easily made

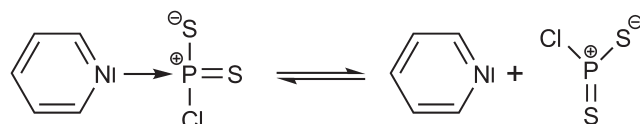
## 3 Reactions of $\text{PX}_3$ with $\text{Na}_2\text{S}_2$ (X = Cl, Br, I)

### 3.1 Reaction of $\text{PCl}_3$ and $\text{Na}_2\text{S}_2$



In the  $^{31}\text{P}$  NMR spectrum of reaction solution of  $\text{PCl}_3$  with  $\text{Na}_2\text{S}_2$  in the stoichiometric ratio of 1:1  $\text{PCl}_3$  can still be observed in quite huge quantities (39 % of the total  $^{31}\text{P}$  intensity). Nevertheless, the  $^{31}\text{P}$  NMR spectrum reveals that the compound  $\text{pyPS}_2\text{Cl}$  is also formed, shows the characteristic  $^{31}\text{P}$  NMR chemical shift of 95.2 ppm (in pyridine; 53 % of the total  $^{31}\text{P}$  intensity). This is in accord with the  $^{31}\text{P}$  chemical shift reported of 97.5 ppm (in  $\text{CHCl}_3$ ).<sup>7</sup> The small difference can be attributed to the different solvents used. In addition, some colourless crystals were isolated after storing the reaction solution at  $-20\text{ }^\circ\text{C}$  for six weeks. The determined cell parameters correspond to those reported in literature for  $\text{pyPS}_2\text{Cl}$ .<sup>9</sup>

Based on the experience with the triseleno- and trithiometaphosphate anion, an equilibrium between the pyridine adduct ( $\text{pyPS}_2\text{Cl}$ ) and free  $\text{PS}_2\text{Cl}$  (and pyridine) might be anticipated (Scheme 7).



Scheme 7: Possible equilibrium between the adduct  $\text{pyPS}_2\text{Cl}$  and the free species  $\text{PS}_2\text{Cl}$ .

<sup>9</sup> Averbuch-Pouchot, M.-T.; Meisel, M. *Acta Crystallogr., Sect. C: Cryst. Struct. Commun.* **1989**, C45, 1937-1939.

However temperature dependent  $^{31}\text{P}$  NMR spectroscopy in the temperature range between  $-40\text{ }^{\circ}\text{C}$  to  $100\text{ }^{\circ}\text{C}$  revealed that this equilibrium is completely on the side of the adduct  $\text{pyPS}_2\text{Cl}$ . Thus,  $\text{PS}_2\text{Cl}$  seems to be less stable than the isoelectronic analogous species  $\text{PS}_3^-$ .

As  $\text{PCl}_3$  was still present in the reaction mixture the amount of  $\text{Na}_2\text{S}_2$  was increased up to a ratio of 1:3. At this stoichiometry no  $\text{PCl}_3$  is observed in the  $^{31}\text{P}$  NMR spectrum anymore. The main product is still  $\text{pyPS}_2\text{Cl}$  (75 % of the total intensity). From the reaction solution at this stoichiometry crystals of  $\text{py}_2\text{P}_2\text{S}_7$  were obtained.

### 3.2 Reaction of $\text{PBr}_3$ and $\text{Na}_2\text{S}_2$



As previously described for the reaction of  $\text{PBr}_3$  with  $\text{Na}_2\text{S}_2$  the first stoichiometry investigated was  $\text{PBr}_3$  and  $\text{Na}_2\text{S}_2$  of 1:1. The  $^{31}\text{P}$  NMR spectrum of the reaction mixture reveals the presence of  $\text{pyPS}_2\text{Br}$  (37 % of the total  $^{31}\text{P}$  intensity) which can thus be obtained using  $\text{PBr}_3$  and  $\text{Na}_2\text{S}_2$  as educts. However  $\text{PBr}_3$  is also still present in the reaction mixture ( $\delta^{31}\text{P} = 220$ ; 16 % of the total  $^{31}\text{P}$  intensity). In addition to  $\text{PBr}_3$  and  $\text{pyPS}_2\text{Br}$  also the signal caused by  $\text{py}_2\text{PS}_2^+$  could be identified at  $\delta^{31}\text{P} = 104.7$  (< 4 % of the total  $^{31}\text{P}$  intensity). This cation was isolated in the crystalline state as  $[\text{py}_2\text{PS}_2]\text{Br}$  salt and identified by its cell parameters using single crystal X-ray diffraction.<sup>10</sup>

The  $^{31}\text{P}$  NMR spectrum of the reaction solution displays two new signals (at 135.8 ppm and 298 ppm) the origin of which remains at the moment mysterious. Temperature dependent  $^{31}\text{P}$  NMR spectroscopy in the range between  $-40\text{ }^{\circ}\text{C}$  and  $0\text{ }^{\circ}\text{C}$  reveals that the signals at  $\delta^{31}\text{P} = 298$  and 135.8 are both shifted to higher field with decreasing temperature ( $\Delta\delta \approx 23$  ppm) and the same is true for the  $^{31}\text{P}$  NMR signal of  $\text{PBr}_3$ . Interestingly the difference between the signals is always the same ( $\Delta\delta = 78$  ppm). Particularly interesting is the signal at  $\delta^{31}\text{P} = 298$ . This corresponds to the signal observed for the  $\text{PS}_3^-$  anion. The presence of  $\text{PS}_3^-$  under the given reaction conditions seems very unlikely, however. The  $^{31}\text{P}$  shift observed for  $\text{PS}_3^-$  in pyridine is 220 ppm, due to the equilibrium with  $\text{pyPS}_3^-$ . In addition, the coexistence of  $\text{PS}_3^-$  and  $\text{PBr}_3$  (a base and an acid) seems improbable. For monomeric  $\text{PS}_2\text{Br}$  a low field  $^{31}\text{P}$  NMR signal would be expected. Further investigations are needed, however, in order to clarify this point.

Increasing the amount of  $\text{Na}_2\text{S}_2$  (ratio 1:3) leads to the formation of only sulfur containing compounds like  $\text{P}_2\text{S}_8^{2-}$ ,  $\text{P}_5\text{S}_{10}^{5-}$  and  $\text{P}_2\text{S}_7^{2-}$ .

<sup>10</sup> Meisel, M.; Lönnecke, P.; Grimmer, A.-R.; Wulff-Molder, D. *Angew. Chem. Int. Ed. Engl.* **1997**, *36*(17), 1869-1870.

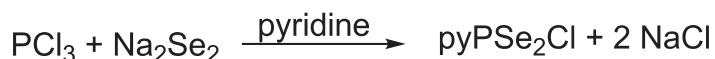
### 3.3 Reaction of $\text{PI}_3$ and $\text{Na}_2\text{S}_2$



$\text{PI}_3$  and  $\text{Na}_2\text{S}_2$  were reacted in pyridine at ambient temperature in the molar ratios 1:1 and 1:3. According to the  $^{31}\text{P}$  NMR spectrum of the reaction solution formation of dithiophosphoryl monoiodide pyridine adduct  $\text{pyPS}_2\text{I}$  does not occur. Instead signals at  $\delta^{31} = 104.7, 119.2$  and  $54.5$  were observed, which can tentatively be assigned to the cation  $\text{py}_2\text{PS}_2^+$  and the anion  $\text{P}_2\text{S}_8^{2-}$ , respectively. This result might be interpreted considering the weak P-I bond, compared to the P-Br and P-Cl bond. Assuming the intermediate formation of  $\text{pyPS}_2\text{I}$  a nucleophilic attack of a second pyridine molecule would be favoured by the weak P-I bond, resulting in the formation of  $\text{pyPS}_2^+$  cation.

## 4 Reaction of $\text{PX}_3$ with $\text{Na}_2\text{Se}_2$ (X = Cl, Br, I)

### 4.1 Reaction of $\text{PCl}_3$ with $\text{Na}_2\text{Se}_2$



Reaction of equimolar amounts of  $\text{PCl}_3$  and  $\text{Na}_2\text{Se}_2$  in pyridine at ambient temperature yields a clear red solution. The  $^{31}\text{P}$  NMR spectrum shows the presence of a considerable amount of unreacted  $\text{PCl}_3$  (22 % of the total  $^{31}\text{P}$  intensity). Main product is the pyridine adduct of  $\text{PSe}_2\text{Cl}$ ,  $\text{pyPSe}_2\text{Cl}$ , which is observed and characterized here for the first time. The identity of  $\text{pyPSe}_2\text{Cl}$  results unambiguously from the pattern of the  $^{31}\text{P}$  NMR signal and is further supported by the  $^{14}\text{N}$  and  $^{77}\text{Se}$  NMR spectra. The  $^{31}\text{P}$  NMR signal (Figure 1) consists of a (1:1:1) triplet and a pair of  $^{77}\text{Se}$  satellites. The triplet is caused by scalar coupling of  $^{31}\text{P}$  with  $^{14}\text{N}$  ( $I = 1$ ) and proves the coordination of pyridine to phosphorus in  $\text{pyPSe}_2\text{Cl}$ .  $^1J_{\text{PN}}$  (44 Hz) is typical for a one bond  $^{31}\text{P}$ ,  $^{14}\text{N}$  coupling. The relative intensity of the  $^{77}\text{Se}$  satellites (12.7 %) corresponds to two selenium atoms bonded to phosphorus.  $^1J_{\text{SeP}} = 892$  Hz is in the same range as found for phosphorus selenides (500 – 1200 Hz).<sup>11</sup> In the  $^{77}\text{Se}$  NMR spectrum a doublet at 388.4 ppm is observed, in a range typical for phosphorus selenides. The P coordinated nitrogen atom gives a signal at – 132.5 ppm.

<sup>11</sup> Karaghiosoff, K. in: *Encyclopedia of Nuclear Magnetic resonance*, Vol. 6 Grant, M.; Harris, R. K. Eds.: Wiley, Chichester, 1996, pp. 3612-3619.

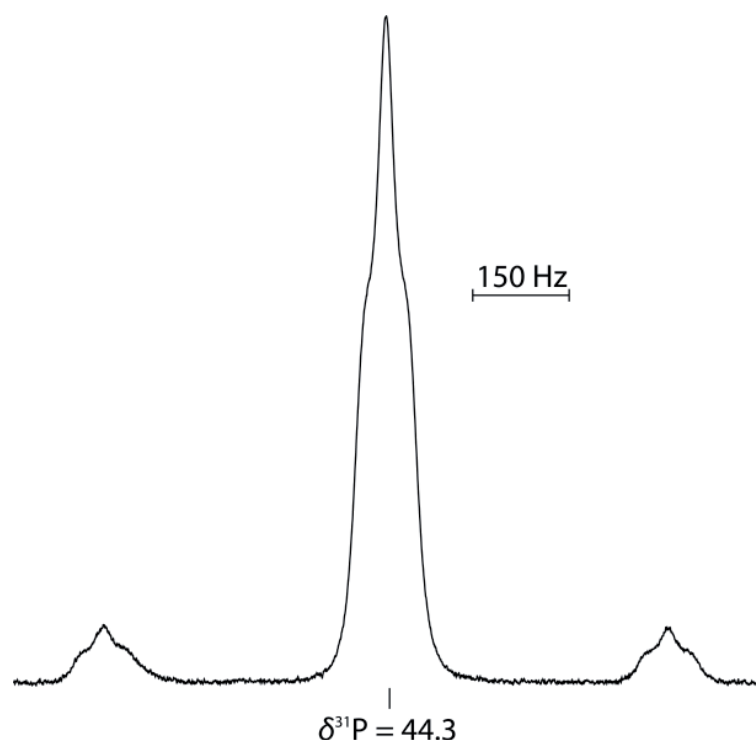


**Figure 1.** Observed  $^{31}\text{P}\{^1\text{H}\}$  NMR spectrum of  $\text{pyPSe}_2\text{Cl}$  in pyridine at  $25^\circ\text{C}$  (0.1 M, 1023 scans with a PD = 0.5 sec, measuring time 28 min,  $\nu_0 = 161.9966$  MHz,  $^1\text{H}$  broadband decoupling).

In addition to the signals of  $\text{PCl}_3$  and  $\text{pyPSe}_2\text{Cl}$  three other signals with one pair of  $^{77}\text{Se}$  satellites each can be observed in the  $^{31}\text{P}$  NMR spectrum: 94.1, 30.5 and  $-11.9$  ppm. The signal at 94.1 ppm (2.5 % of the total intensity) can be attributed to the new cation  $\text{py}_2\text{PSe}_2^+$ . It is formed in much better yield when  $\text{PBr}_3$  is used instead of  $\text{PCl}_3$  (see below).

From the reaction solution red crystals of  $[\text{pyH}][\text{pyPSe}_3]$  were isolated at ambient temperature and were investigated by single crystal X-ray diffraction.

As there is still  $\text{PCl}_3$  in the reaction mixture, the amount of  $\text{Na}_2\text{Se}_2$  has to be increased up to an educt ratio of 1:3 ( $\text{PCl}_3 : \text{Na}_2\text{Se}_2$ ).  $\text{pyPSe}_2\text{Cl}$  could be identified as main product according to the  $^{31}\text{P}$  NMR spectrum of the reaction mixture (58 % of the total intensity). The signal at  $\delta^{31}\text{P} = 94.1$  ppm disappeared completely whereas the total intensity of the signal at  $\delta^{31}\text{P} = 30.5$  ppm increased up to 27 % and that of the singlet at  $\delta^{31}\text{P} = -11.9$  ppm decreased (14 %).

## 4.2 Reaction of $\text{PBr}_3$ with $\text{Na}_2\text{Se}_2$



Addition of  $\text{PBr}_3$  to an equimolar amount of  $\text{Na}_2\text{Se}_2$  in pyridine results in the formation of a clear red solution. The  $^{31}\text{P}$  NMR spectrum shows only two signals at 94.1 ppm and 4.5 ppm, each accompanied by a pair of  $^{77}\text{Se}$  satellites. Main product is  $\text{pyPSe}_2\text{Br}$  (63 % of the total  $^{31}\text{P}$  intensity), the pyridine adduct of  $\text{PSe}_2\text{Br}$ , described and characterized for the very first time. In analogy to the previously described chlorine compound  $\text{pyPSe}_2\text{Cl}$ , the  $^{31}\text{P}$  NMR signal of  $\text{pyPSe}_2\text{Br}$  consists of a 1:1:1 triplet ( $^1J_{\text{PN}} = 36 \text{ Hz}$ ) and one pair of  $^{77}\text{Se}$  satellites ( $^1J_{\text{SeP}} = 851 \text{ Hz}$ ) with a relative intensity of 13 %, indicating the existence of two selenium atoms bonded to the central phosphorus atom (Figure 2).

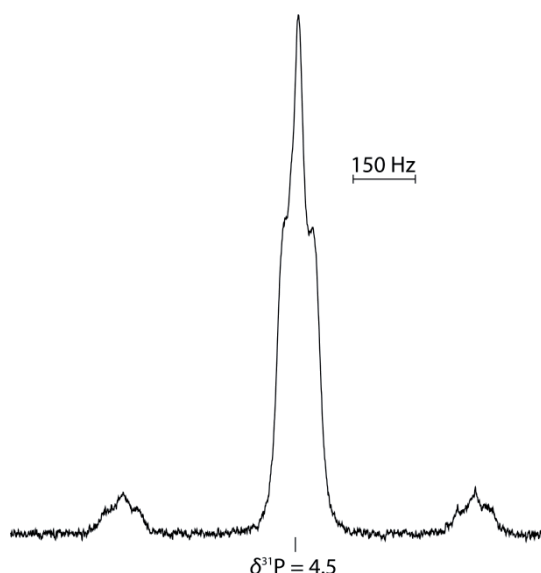


**Figure 2.** Observed  $^{31}\text{P}\{^1\text{H}\}$  NMR spectrum of  $\text{pyPSe}_2\text{Br}$  in pyridine at  $25^\circ\text{C}$  (0.1 M, 4096 scans with a PD = 0.5 sec, measuring time 97 min,  $\nu_0 = 161.8347 \text{ MHz}$ ,  $^1\text{H}$  broadband decoupling).

The singlet at 94.1 ppm, which can also be observed in the reaction of  $\text{PCl}_3$  and  $\text{Na}_2\text{Se}_2$ , is accompanied by one pair of  $^{77}\text{Se}$  satellites with a  $^1J_{\text{SeP}}$  (817 Hz) corresponding to single coordinated selenium atoms, also found in phosphorus selenides.<sup>11</sup> The relative intensity of the  $^{77}\text{Se}$  satellites (16 %) indicates the presence of two selenium nuclei bonded to the phosphorus atom. The signal can be assigned to the bispyridine adduct stabilized  $\text{PSe}_2^+$  cation,  $\text{py}_2\text{PSe}_2^+$ .

**4.3 Reaction of PI<sub>3</sub> with Na<sub>2</sub>Se<sub>2</sub>**

In analogy to the reaction of PI<sub>3</sub> and Na<sub>2</sub>S<sub>2</sub>, only selenium containing compounds like the P<sub>2</sub>Se<sub>8</sub><sup>2-</sup> anion can be observed in the <sup>31</sup>P NMR spectrum. So this synthesis starting from PI<sub>3</sub> is useless so prepare the iodine containing compound pyPSe<sub>2</sub>I.

**4.4 Reaction of PI<sub>3</sub> with Na<sub>2</sub>Te<sub>2</sub>**

The formation of pyPTe<sub>2</sub>I cannot be observed in the <sup>31</sup>P NMR spectrum. Instead the signal of only PI<sub>3</sub> can be identified.

## 5 Conclusion

$PCh_2X$  (Ch = S, Se; X = Cl, Br) can be readily generated by the reaction of  $PX_3$  with  $Na_2Ch_2$  and effectively stabilized as pyridine adducts in solution. The new selenium derivatives  $pyPSe_2Cl$ ,  $pyPSe_2Br$  and  $py_2PSe_2^+$  are prepared and characterized by NMR spectroscopy for the first time. It could be demonstrated that using  $PI_3$  as educt for the syntheses of the corresponding iodine compounds is not suitable as the weak P-I bonds are completely broken by sulfur and selenium atoms. In case of tellurium it has to be recognized that this is too unreactive to break the P-I bond.

It could also be shown that there is no equilibrium between the adduct stabilized dichalcogenophosphoryl monohalogenides  $pyPCh_2X$  and the free monomeric compounds  $PCh_2X$ .

In addition two new compounds can be obtained in the solid state and characterized using X-ray diffraction. They are discussed in separate chapters:  $[pyH][pyPSe_3]$  and  $py_2P_2S_7$ .

**Table 2. Summary of analytical data of the observed compounds.**

	NMR data	X-Ray
$pyPS_2Cl$	$\delta^{31}P = 95.2$ (in pyridine)	✓
$pyPS_2Br$	$\delta^{31}P = 65.5$ (in pyridine)	✗
$pyPS_2I$	not prepareable	
$pyPSe_2Cl$	$\delta^{31}P = 44.3$ (in pyridine) $\delta^{77}Se = 388.4$ $\delta^{14}N = -132.5$ $^1J_{SeP} = 892$ Hz $^1J_{PN} = 44$ Hz	✗
$pyPSe_2Br$	$\delta^{31}P = 4.5$ $^1J_{SeP} = 851$ Hz $^1J_{PN} = 36$ Hz	✗
$pyPSe_2I$	not prepareable	
$pyPTe_2I$	not prepareable	
$py_2PS_2^+$	$\delta^{31}P = 104.7$ (in pyridine)	✓
$py_2PSe_2^+$	$\delta^{31}P = 94.1$ $^1J_{SeP} = 817$ Hz	✗

## 6 Experimental section

**General.** All reactions were carried out under inert gas atmosphere using Schlenk techniques. Argon (Messer Griesheim, purity 4.6 in 50 L steel cylinder) was used as inert gas. The glass vessels used were stored in a 130 °C drying oven. Before use the glass vessels were flame dried in vacuum at  $10^{-3}$  mbar.

The sodium dichalcogenides were prepared as described in the literature and stored in a dry box under nitrogen atmosphere.<sup>12</sup> Pyridine (Aldrich) was dried using commonly known methods.  $\text{PCl}_3$  (Aldrich) was distilled before use.  $\text{PBr}_3$  (Aldrich) was used as received.

**NMR Spectroscopy.** NMR spectra were recorded using a Jeol EX 400 Eclipse instrument operating at 161.997 MHz ( $^{31}\text{P}$ ), 76.321 MHz ( $^{77}\text{Se}$ ) and 28.918 MHz ( $^{14}\text{N}$ ) if not mentioned otherwise. Chemical shifts are referred to 85 %  $\text{H}_3\text{PO}_4$ ,  $(\text{CH}_3)_2\text{Se}$  ( $^{77}\text{Se}$ ) and  $\text{CH}_3\text{NO}_2$  ( $^{14}\text{N}$ ) as external standards. All spectra were measured, if not mentioned otherwise, at 25 °C. The %-data correspond to the intensities in the  $^{31}\text{P}$  NMR spectra with respect to the total intensity. The difference to 100 % belongs to not determinable signals. For low temperature  $^{31}\text{P}$  NMR spectroscopy experiments: The reaction solution was directly used. Samples were measured in the temperature range of  $-40 - 0$  °C at steps of 10°C. The observed signals are listed in the tables below.

**Syntheses.** To a suspension of  $\text{Na}_2\text{Ch}_2$  in pyridine a solution of  $\text{PX}_3$  in pyridine is added slowly at ambient temperature using a dropping funnel. The reaction suspension was allowed to stir for 24 h at room temperature. The used amounts of educts and solvent as well as the NMR analysis are provided in Table 3.

In the case of reaction number 3, a small quantity of colorless crystals of  $\text{pyPS}_2\text{Cl}$  were obtained after storing the reaction solution at  $-20$  °C for two weeks. They were identified by means of single crystal X-ray diffraction by comparison of the unit cell with that reported in the literature.

Similarly in the case of reaction number 4 colorless crystals of  $\text{py}_2\text{PS}_2\text{Br}$  were formed after storing the reaction solution at ambient temperature for 2 days. The compound was identified by means of single crystal X-ray diffraction by comparison of the unit cell with that reported in the literature.

<sup>12</sup> (a) Thompson, D. P.; Boudjouk, P. J. *Org. Chem.* **1988**, *53*, 2109. (b) Schuster, M. *dissertation*, LMU Munich, **1999**.

Table 3. Used amounts of educts and solvent and NMR data.

Rct.	PX <sub>3</sub>		Na <sub>2</sub> Ch <sub>2</sub>		pyridine	NMR data
	V[ml]/m[mg]	n[mmol]	m[mg]	n[mmol]	V [ml]	
	PCl <sub>3</sub> [ml]		Na <sub>2</sub> S <sub>2</sub>			$\delta^{31}\text{P}$
1	0.214	1	110	1	2	205.9 (PCl <sub>3</sub> , 53 %), 95.2 (pyPS <sub>2</sub> Cl, 39 %), 81.2 (s, 4 %), 43.8 (s, 2 %), -10.4 (2 %).
2	0.214	1	220	2	3	205.9 (PCl <sub>3</sub> , 22 %), 95.2 (pyPS <sub>2</sub> Cl, 72 %), 82.3 (s, 3 %), 44.8 (s, 1 %), -9.3 (s, 2 %).
3	0.214	1	330	3	7	104.7 (py <sub>2</sub> PS <sub>2</sub> <sup>+</sup> , 19 %), 95.2 (pyPS <sub>2</sub> Cl, 75 %), 82.3 (s, 3 %), 44.9 (s, 2 %), -18.9 (s, 1 %).
	PBr <sub>3</sub> [ml]		Na <sub>2</sub> S <sub>2</sub>			$\delta^{31}\text{P}$
4	0.092	1	110	1	5	298.0 (s, br, 12 %), 222.7 (PBr <sub>3</sub> , 14 %), 135.8 (s, 23 %), 116.9 (s, 12 %), 104.7 (py <sub>2</sub> PS <sub>2</sub> <sup>+</sup> , 2 %), 97.8 (s, 2 %); 65.5 (pyPS <sub>2</sub> Br, 32 %), 10.0 (s, 2 %), -14.2 (s, 1 %).
5	0.092	1	330	3	7	127.0 (P <sub>2</sub> S <sub>8</sub> <sup>2-</sup> , 9 %), 124.7 (s, 7 %), 119.2 & 54.5 (P <sub>2</sub> S <sub>8</sub> <sup>2-</sup> , 17 %), 95.7 (P <sub>5</sub> S <sub>10</sub> <sup>5-</sup> , 9 %), 93.7 (s, 29 %), 76.5 (s, 9 %), 46.4 (s, 20 %).
	PI <sub>3</sub> [mg]		Na <sub>2</sub> S <sub>2</sub>			$\delta^{31}\text{P}$
6	313	0.76	84	0.76	4	119.2 & 54.5 (P <sub>2</sub> S <sub>8</sub> <sup>2-</sup> , 10 %), 104.7 (py <sub>2</sub> PS <sub>2</sub> <sup>+</sup> , 16 %).
7	500	1.2	396	3.6	8	158.5 (s, br, 18 %), 127.0 (P <sub>2</sub> S <sub>8</sub> <sup>2-</sup> , 2 %), 119.2 & 54.5 (P <sub>2</sub> S <sub>8</sub> <sup>2-</sup> , 52 %), 112.8 (s, 4 %), 104.7 (py <sub>2</sub> PS <sub>2</sub> <sup>+</sup> , 11 %), 95.7 (P <sub>5</sub> S <sub>10</sub> <sup>5-</sup> , 4 %), 86.8 (s, 6 %), 52.2 (s, 3 %).
	PCl <sub>3</sub> [ml]		Na <sub>2</sub> Se <sub>2</sub>			$\delta^{31}\text{P}$ / $\delta^{77}\text{Se}$ / $\delta^{14}\text{N}$
8	0.180	2	408	2	2	$\delta^{31}\text{P}$ = 206.0 (PCl <sub>3</sub> , 22 %), 200.6 (pyPSe <sub>3</sub> , 3 %); 94.1 (py <sub>2</sub> PSe <sub>2</sub> <sup>+</sup> , <sup>1</sup> J <sub>SeP</sub> = 817 Hz, 3 %); 44.3 (pyPSe <sub>2</sub> Cl, <sup>1</sup> J <sub>SeP</sub> = 891 Hz, 36 %); 30.5 (s, <sup>1</sup> J <sub>SeP</sub> = 971 Hz, 8 %); -11.9 (s, <sup>1</sup> J <sub>SeP</sub> = 816 Hz, 28 %) ppm.
9	0.214	1	617	3	7	$\delta^{31}\text{P}$ = 44.3 (pyPSe <sub>2</sub> Cl, 58 %), 30.5 (s, <sup>1</sup> J <sub>SeP</sub> = 973 Hz, 27%), -11.9 (s, <sup>1</sup> J <sub>SeP</sub> = 816 Hz, 14 %). $\delta^{77}\text{Se}$ = 701.4 (d, <sup>1</sup> J <sub>SeP</sub> = 816 Hz), 388.4 (pyPSe <sub>2</sub> Cl), 66.3 (d, <sup>1</sup> J <sub>SeP</sub> = 972 Hz). $\delta^{14}\text{N}$ = -58.8 (pyridine), -132.5 (pyPSe <sub>2</sub> Cl).
	PBr <sub>3</sub> [ml]		Na <sub>2</sub> Se <sub>2</sub>			$\delta^{31}\text{P}$
10	0.092	1	206	1	5	94.1 (py <sub>2</sub> PSe <sub>2</sub> <sup>+</sup> , 37 %), 4.5 (pyPSe <sub>2</sub> Br, 63 %).
11	0.092	1	617	3	7	-56.2 (s, br, 100 %).
	PI <sub>3</sub> [mg]		Na <sub>2</sub> Se <sub>2</sub>			$\delta^{31}\text{P}$ / $\delta^{77}\text{Se}$
12	512	1.24	256	1.24	5	$\delta^{31}\text{P}$ = -2.8 & 87.4 (P <sub>2</sub> Se <sub>8</sub> <sup>2-</sup> , 58 %), -14.7 (P <sub>2</sub> Se <sub>9</sub> <sup>2-</sup> , 25 %), -48.9 (s, br, 17 %).
13	700	1.7	1049	5.1	10	$\delta^{31}\text{P}$ = 54.2 (P <sub>2</sub> Se <sub>6</sub> <sup>4-</sup> , 33 %), -10.4 (s, <sup>1</sup> J <sub>SeP</sub> = 478 Hz, 14 %), -109.9 (PSe <sub>4</sub> <sup>3-</sup> , 53 %). $\delta^{77}\text{Se}$ = 701.6 (PSe <sub>4</sub> <sup>3-</sup> ), 439.7 (s, br), 184.9 (P <sub>2</sub> Se <sub>6</sub> <sup>4-</sup> ).
	PI <sub>3</sub> [mg]		Na <sub>2</sub> Te <sub>2</sub>			$\delta^{31}\text{P}$
14	360	0.87	260	0.87	5	185.5 (PI <sub>3</sub> , 100 %).

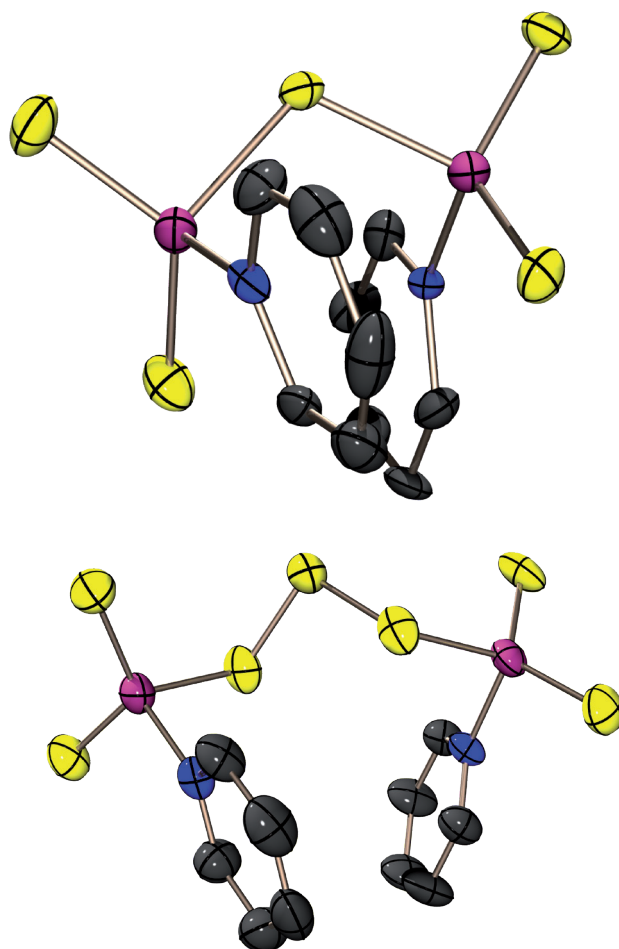
**Table 4. Temperature dependent  $^{31}\text{P}$  NMR spectroscopy of reaction nb. 4 (Table 3).**

T [°C]	$\delta^{31\text{P}}$
-40	273.5 (17.4 %); 194.7 (10.4 %); 114.6 (46.5 %); 102.5 (13.9 %); 67.4 (1.5 %); 65.2 (6.7 %); 9.2 (3.4 %).
-30	281.3 (16.0 %); 203.4 (13.6 %); 122.2 (34.6 %); 114.9 (20.4 %); 67.4 (1.9 %); 65.2 (5.1 %); 9.4 (2.6 %).
-20	288.9 (15.4 %); 207.8 (18.2 %); 125.6 (35.5 %); 115.3 (20.4 %); 67.9 (2.5 %); 65.3 (5.4 %); 9.4 (2.7 %).
-10	291.2 (15.5 %); 211.9 (11.7 %); 128.5 (32.2 %); 115.7 (18.7 %); 68.0 (2.0 %); 65.4 (15.1 %); 9.6 (1.5 %).
0	293.1 (18.3 %); 216.7 (11.9 %); 130.9 (31.9 %); 116.1 (18.5 %); 68.2 (1.8 %); 65.4 (14.8 %); 9.8 (2.7 %).

## CHAPTER VI

---

### Binary Neutral Phosphorus Sulfides $\text{py}_2\text{P}_2\text{S}_5$ and $\text{py}_2\text{P}_2\text{S}_7$

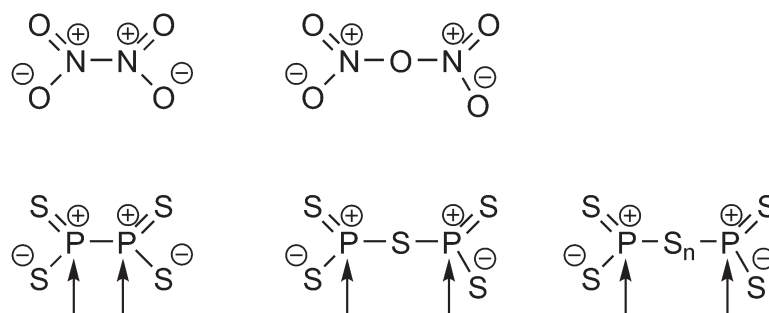


*In course of investigations on dichalcogenylphosphoryl monohalides  $\text{Ch}_2\text{PX}$  ( $\text{Ch} = \text{S}, \text{Se}; \text{X} = \text{Cl}, \text{Br}, \text{I}$ ) a new linear binary stabilized phosphorus sulphide stabilized as the bis(pyridine) adduct  $\text{py}_2\text{P}_2\text{S}_7$  (Millak) was obtained. The compound is formed from the reaction of  $\text{PCl}_3$  and  $\text{Na}_2\text{S}_2$  in pyridine and was characterized using X-ray diffraction,  $^{31}\text{P}$  NMR spectroscopy and quantum chemical calculations.*

*In addition, the already known  $\text{py}_2\text{P}_2\text{S}_5$  (Millikino) was in the solid state and characterized using X-ray diffraction for the first time.*

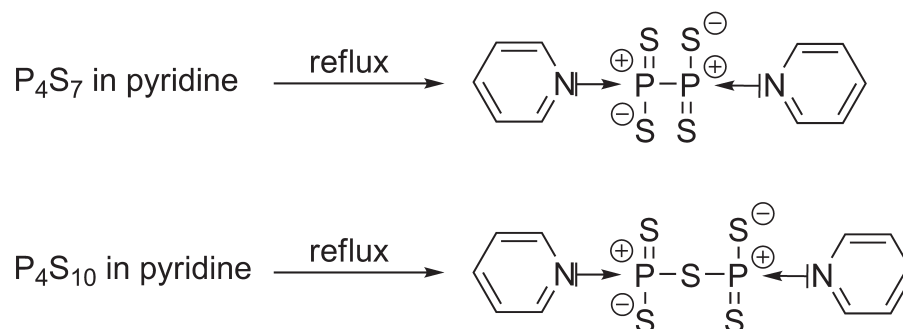
## 1 Introduction

Binary phosphorus sulfides have been known for a long time and belong to the basics of inorganic chemistry, described in every chemistry textbook.<sup>1</sup> Acyclic phosphorus sulfides (comparable to nitrogen oxides) would imply unusually coordinated and bonded phosphorus atoms (either  $\sigma^5\lambda^3$  or  $\sigma^2\lambda^3$  phosphorus atoms), and are not stable at ambient temperature.



Scheme 1. Binary acyclic N,O and P,S compounds.

Some examples illustrating this context are given in Scheme 1. In contrast to the well known dinitrogen tetroxide  $N_2O_4$  and dinitrogen pentoxide  $N_2O_5$ , the corresponding phosphorus sulfides  $P_2S_4$  and  $P_2S_5$  are not stable, due to the presence of  $\sigma^3\lambda^5$  phosphorus atoms. Formally the dimers  $P_4S_8$  and  $P_4S_{10}$  in which phosphorus avoids this unfavourable bonding situation, are known and represent stable molecules. The "monomers" can be however stabilized by complexation (adduct formation) with (a base) pyridine, which fills the electronic gap at  $\sigma^3\lambda^5$  phosphorus. Thus  $py_2P_2S_4$  and  $py_2P_2S_5$  are formed when refluxing  $P_4S_7$  and  $P_4S_{10}$  in pyridine respectively, isolated as stable compounds and characterized by  $^{31}P$  NMR (Scheme 2).



Scheme 2. Literature known bis(py)adduct stabilized phosphorus sulfides.

<sup>1</sup> Holleman, A.; Wiberg, E.; Wiberg, N. *Lehrbuch der anorganischen Chemie*, 102nd ed.; Walter de Gruyter Verlag, Berlin, 2007.

## 2 Results and Discussion

$\text{py}_2\text{P}_2\text{S}_4$  was synthesized by Wolf via refluxing  $\text{P}_4\text{S}_7$  in pyridine. No analytical data is given in the literature for this compound.<sup>2</sup>  $\text{py}_2\text{P}_2\text{S}_5$  was first described by Fluck et al. and characterized using  $^{31}\text{P}$  NMR spectroscopy ( $\delta^{31}\text{P}$  105.5 ppm).<sup>3</sup> Meisel et al. also investigated  $\text{py}_2\text{P}_2\text{S}_5$   $^{31}\text{P}$  NMR spectroscopically ( $\delta^{31}\text{P}$  (crystalline  $\text{py}_2\text{P}_2\text{S}_5$ )  $70\pm 20$ ;  $\delta^{31}\text{P}$  (glassy  $\text{py}_2\text{P}_2\text{S}_5$ )  $103\pm 10$ ).<sup>4</sup> One might think of  $\text{py}_2\text{P}_2\text{S}_5$  being the first member of a series  $\text{py}_2\text{P}_2\text{S}_4(\text{S})_x$  ( $x = 1$ ), due to the tendency of sulfur to form chains. According to the procedure described in literature by Meisel et al., it was possible to obtain  $\text{py}_2\text{P}_2\text{S}_5$  in the solid state as colourless crystals and characterize the compound using single crystal X-ray diffraction.

$\text{py}_2\text{P}_2\text{S}_5$  crystallizes in the triclinic space group  $P-1$ , with two molecules within the asymmetric unit.

The phosphorus atoms are surrounded distorted tetrahedrally by three sulfur atoms and one pyridine molecule. The biggest values for S-P-S angles can be found between the one coordinated sulfur atoms with  $123^\circ$  (Table 1). The S-P-S angles between the one coordinated and two coordinated sulfur atoms are smaller with values around  $102^\circ$ . The P-S-P angles at the two coordinated sulfur atom forming the  $\text{S}_1$ -bridge are  $112.7(2)^\circ$  (P1-S3-P2) respectively  $111.4(2)^\circ$  (P3-S8-P4). The angle sums at the phosphorus atoms are  $341^\circ$ . This indicates a slight deviation from planarity. The P-S distances are within the range expected for P-S single bonds (211 pm) and P=S double bonds (191 pm). The P-N distances are with an average value of 185 pm longer than reported P-N single bonds.<sup>1</sup>

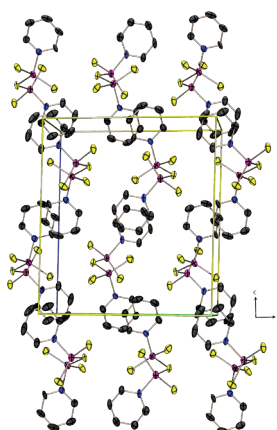


**Figure 1.** Crystal structure of  $\text{py}_2\text{P}_2\text{S}_5$ . View of the unit cell along  $a$  axis. Ellipsoids are drawn at the 50 % probability level. Hydrogen atoms are omitted for clarity.

<sup>2</sup> Wolf, G. U. Patentnummer DD245878, 1987.

<sup>3</sup> Fluck, E.; Binder, H. Z. *Anorg. Allg. Chem.* **1967**, 354(3-4), 114-129.

<sup>4</sup> Meisel, M.; Grunze, H. Z. *Anorg. Allg. Chem.* **1968**, 360, 277-283.

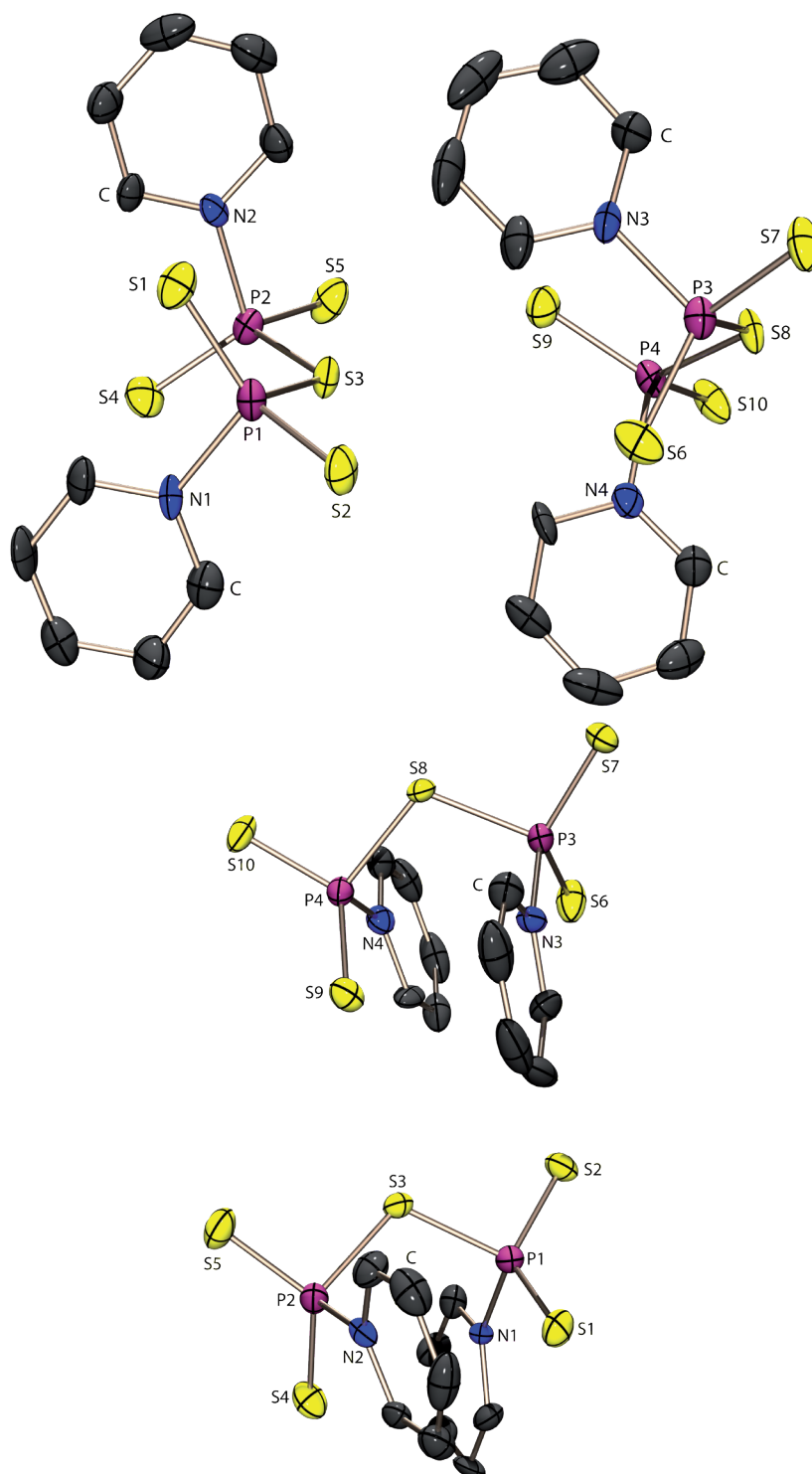


Figure 2. Molecular structure of  $\text{py}_2\text{P}_2\text{S}_5$  shown along the  $a$  axis (upper picture) and along the  $c$  axis. Thermal ellipsoids are set at 50 % probability level. Hydrogen atoms are omitted for clarity.

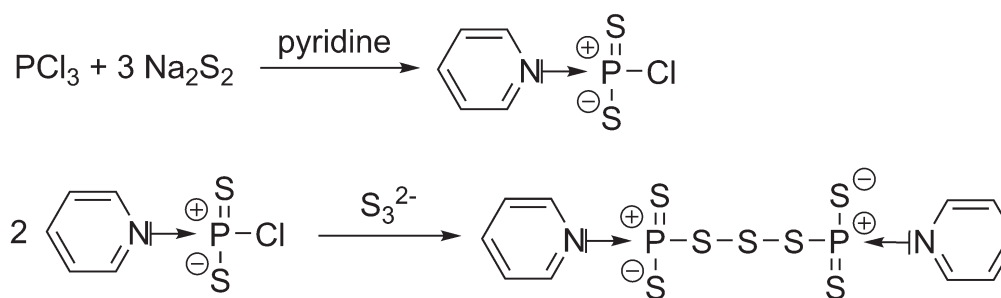
**Table 1. Structural parameters of  $\text{py}_2\text{P}_2\text{S}_5$ .**

Distances [pm]			
P1-N1	186.2(6)	P3-N3	186.5(3)
P1-S1	192.4(3)	P3-S6	211.2(2)
P1-S2	194.2(3)	P3-S7	192.4(1)
P1-S3	211.1(3)	P3-S8	194.0(1)
P2-N2	185.0(6)	P4-N4	185.3(6)
P2-S3	211.8(3)	P4-S8	211.7(3)
P2-S4	193.1(3)	P4-S9	192.3(3)
P2-S5	193.4(3)	P4-S10	193.7(3)
Angles [°]			
S1-P1-S2	123.9(2)	S6-P3-S7	123.6(2)
S2-P1-S3	102.5(2)	S7-P3-S8	103.3(2)
S3-P1-S1	114.9(2)	S6-P3-S8	114.4(2)
S1-P1-N1	106.8(2)	S6-P3-N3	107.4(2)
S2-P1-N1	105.9(2)	S7-P3-N3	105.6(2)
S3-P1-N1	100.0(2)	S8-P3-N3	100.0(2)
P1-S3-P2	112.7(2)	P3-S8-P4	111.4(2)
S3-P2-S4	114.2(2)	S8-P4-S9	114.5(2)
S4-P2-S5	123.6(2)	S9-P4-S10	122.3(2)
S3-P2-S5	103.8(2)	S8-P4-S10	105.2(2)
S3-P2-N2	99.3(2)	S8-P4-N4	99.1(2)
S4-P2-N2	106.6(2)	S9-P4-N4	107.5(2)
S5-P2-N2	106.5(2)	S10-P4-N4	105.5(2)

An alternative synthetic route to bis(pyridine) stabilized phosphorus sulphides might start from a phosphorus trihalide, which is reacted with a polysulfide  $\text{S}_n^{2-}$  ( $n = 2, 3, \dots$ ) in the presence of pyridine. The polysulfide fulfills two functions: it oxidizes the phosphorus (from  $\text{P}^{\text{III}}$  to  $\text{P}^{\text{V}}$ ) and at the same time it provides the sulfur chain, connecting the phosphorus atom. Following this strategy, the new phosphorus sulphide  $\text{P}_2\text{S}_7$  could be prepared and stabilized as the bis(pyridine) adduct.

Crystals of  $\text{py}_2\text{P}_2\text{S}_7$  were obtained in the reaction of  $\text{PCl}_3$  and  $\text{Na}_2\text{S}_2$  in pyridine in a molar ratio of 1:3.

Assuming that the used  $\text{Na}_2\text{S}_2$  contains traces of  $\text{S}_3^{2-}$  anions, the formation of  $\text{py}_2\text{P}_2\text{S}_7$  could be explained as shown in Scheme 2. In the first step the formation of  $\text{pyPS}_2\text{Cl}$  is assumed. Two molecules  $\text{pyPS}_2\text{Cl}$  then further reacts with  $\text{S}_3^{2-}$  like shown in Scheme 3.



Scheme 3. Possible formation of  $\text{PCl}_3$  and  $\text{Na}_2\text{S}_2$  to form  $\text{py}_2\text{P}_2\text{S}_7$ .

$\text{py}_2\text{P}_2\text{S}_7$  was isolated in form of colourless block shaped crystals. Its structure was determined using single crystal X-ray diffraction.  $\text{py}_2\text{P}_2\text{S}_7$  crystallizes in the monoclinic space group  $P2_1/c$ . The molecular structure is depicted in Figure 3.

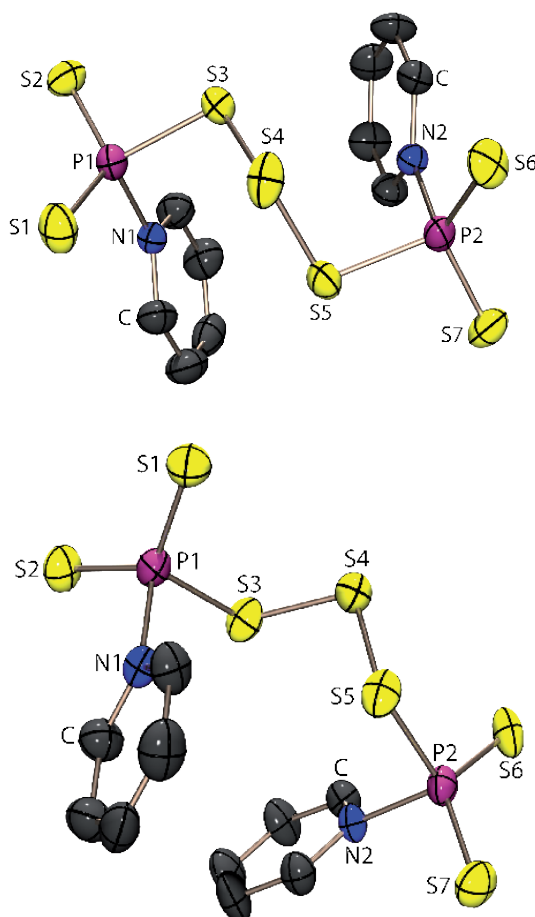
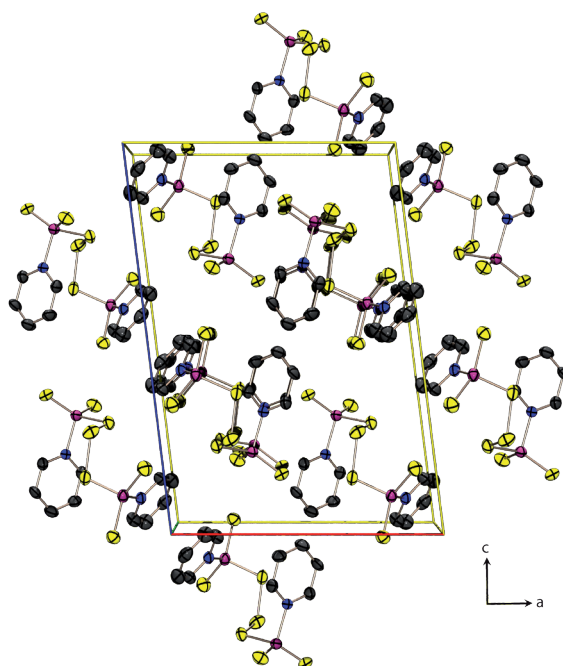


Figure 3. Molecular structure of  $\text{py}_2\text{P}_2\text{S}_7$  shown in two different orientations. Thermal ellipsoids are set at 50 % probability level. Hydrogen atoms are omitted for clarity.



**Figure 4.** Crystal structure of  $\text{py}_2\text{P}_2\text{S}_7$ . View of the unit cell along  $b$  axis. Ellipsoids are drawn at the 50 % probability level. Hydrogen atoms are omitted for clarity.

No interactions between the different molecules in the unit cell were observed (Figure 4).

In  $\text{py}_2\text{P}_2\text{S}_7$  each phosphorus atom is distorted tetrahedrally coordinated by three sulfur atoms and a pyridine molecule. The P-S distances (Table 2) are within the range expected for P-S single bonds (211 pm) and P=S double bonds (191 pm). The P-N distances (Table 2) with 186.9(3) pm (P1-N1) and 186.4(3) pm (P2-N2) are significantly longer than P-N single bonds (176 pm) described in literature. The S-S bond distance in the  $\text{S}_3$  bridge corresponds with 204.2(2) pm (S4-S5) and 206.3(2) pm (S3-S4) very well to the S-S bond distance found in elemental sulfur.

The S-P-S bond angles have values between  $103^\circ$  and  $125^\circ$ . The angle between the three sulfur atoms S3-S4-S5 is  $107^\circ$  thus forming a zick-zack conformation. The corresponding torsion angles P1-S3-S4-S5 [S3-S4-S5-P2] have values of  $84.9(1)^\circ$  [ $90.9(1)^\circ$ ].

The sum of all S-P-S angles for each central phosphorus atom is  $344^\circ$  thus indicating only a slight deviation from planarity for the central phosphorus atoms. This suggests that  $\text{py}_2\text{P}_2\text{S}_7$  might be viewed as the new acyclic phosphorus sulphide  $\text{P}_2\text{S}_7$ , which is stabilized by weak coordination of pyridine to the  $\sigma^{3\lambda^5}$  phosphorus atoms. In order to further investigate this point quantum chemical calculations were performed.

Table 2. Structural parameter of  $\text{py}_2\text{P}_2\text{S}_7$ .

Distances [ $\mu\text{m}$ ]			
P1-N1	186.9(3)	P2-N2	186.5(3)
P1-S1	192.0(1)	P2-S5	211.2(2)
P1-S2	194.0(1)	P2-S6	192.4(1)
P1-S3	212.5(2)	P2-S7	194.0(1)
S3-S4	206.3(2)	S4-S5	204.2(2)
Angles [ $^\circ$ ]			
S1-P1-S2	125.6(1)	S5-P2-S6	114.5(1)
S2-P1-S3	103.4(1)	S5-P2-S7	103.1(1)
S3-P1-S1	113.8(1)	S6-P2-S7	125.5(1)
S1-P1-N1	106.2(1)	S5-P2-N2	97.1(1)
S2-P1-N1	106.1(1)	S6-P2-N2	106.4(1)
S3-P1-N1	98.2(1)	S7-P2-N2	106.3(1)
S4-S3-P1	106.2(1)	S4-S5-P2	104.6(1)
S3-S4-S5	107.6(1)		
Torsion angles [ $^\circ$ ]			
P1-S3-S4-S5	84.9(1)	S3-S4-S5-P2	90.9(1)

### 3 Quantum chemical calculations

In order to elucidate the structure and bonding situation of  $\text{py}_2\text{P}_2\text{S}_7$ , quantum chemical calculations at the MPW1PW91 level of theory using a polarised double-zeta basisset (aug-cc-pVDZ) were carried out, as well as a structure optimization for the hypothetical compound without pyridine  $\text{P}_2\text{S}_7$  (Figure 5). The results for the structure optimization are summarized in Table 3. Interestingly the calculated values for the bond angles of  $\text{P}_2\text{S}_7$  correspond very well to the determined values using single crystal X-ray diffraction. In contrast, the calculated values for  $\text{py}_2\text{P}_2\text{S}_7$  result in longer distances. This suggests that coordination of the pyridine is indeed weak and does not affect the bond lengths within the molecule.

**Table 3. Calculated and experimentally observed distances [pm] and bond angles [°] of  $\text{py}_2\text{P}_2\text{S}_7$  (average values).**

Distances [pm]			
	$\text{py}_2\text{P}_2\text{S}_7$ (obs.)	$\text{P}_2\text{S}_7$ (calc.)	$\text{py}_2\text{P}_2\text{S}_7$ (calc.)
P-N	187	-	196
P-S <sub>oc</sub> <sup>[a]</sup>	193	192	196
P-S <sub>tc</sub> <sup>[b]</sup>	212	213	217
S-S	205	207	208
Angles [°]			
	$\text{py}_2\text{P}_2\text{S}_7$ (obs.)	$\text{P}_2\text{S}_7$ (calc.)	$\text{py}_2\text{P}_2\text{S}_7$ (calc.)
S <sub>oc</sub> -P-S <sub>oc</sub>	126	134	128
S <sub>oc</sub> -P-S <sub>tc</sub>	103/114	107/118	103/115
S3-S4-S5	107	106	105
Torsion angles [°]			
	$\text{py}_2\text{P}_2\text{S}_7$ (obs.)	$\text{P}_2\text{S}_7$ (calc.)	$\text{py}_2\text{P}_2\text{S}_7$ (calc.)
P1-S3-S4-S5	85	85	96
S3-S4-S5-P2	91	85	96

<sup>[a]</sup> oc: one coordinated <sup>[b]</sup> tc: twice coordinated

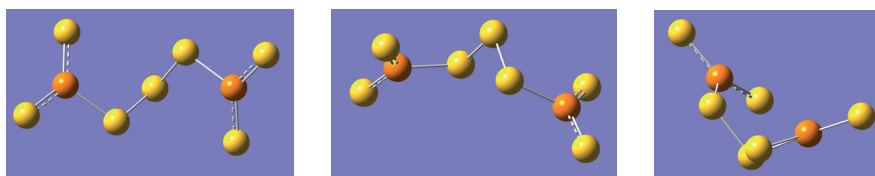


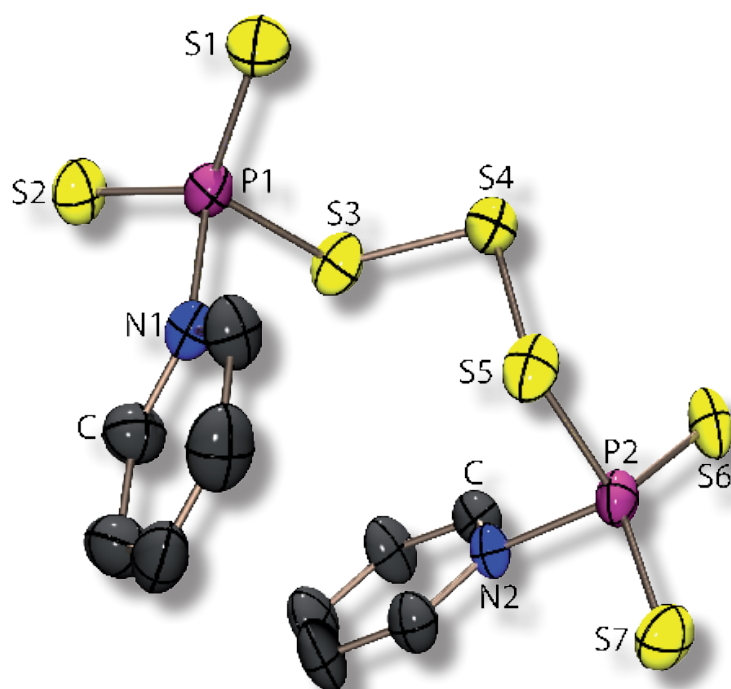
**Figure 5. Optimized structure of  $\text{P}_2\text{S}_7$  showing different orientations.**

In the  $^{31}\text{P}$  NMR spectrum of  $\text{py}_2\text{P}_2\text{S}_7$  a singlet at 82.2 ppm is observed. To support the assignment of the  $^{31}\text{P}$  NMR chemical shift of  $\text{py}_2\text{P}_2\text{S}_7$  quantum chemical calculations at MPW1PW91 level of theory using a polarised double-zeta basisset (aug-cc-pVDZ) for phosphorus were performed. The calculated  $^{31}\text{P}$  NMR chemical shift of 84.2 ppm corresponds very well to the experimentally observed value of 82.2 ppm.

## 4 Conclusion

$\text{py}_2\text{P}_2\text{S}_5$  can be prepared according to the literature procedure and structurally characterized using single crystal X-ray diffraction for the first time. In addition the new  $\text{py}_2\text{P}_2\text{S}_7$  can also be prepared and structurally characterized via single crystal X-ray diffraction.

Due to the calculated and observed structural parameters the present new molecule  $\text{py}_2\text{P}_2\text{S}_7$  can be regarded as bis(py)adduct stabilized neutral, linear, binary phosphorus sulphide  $\text{py}_2\text{P}_2\text{S}_7$  being a new representative of those bis(py)adduct stabilized binary phosphorus sulfides. Also the corresponding  $^{31}\text{P}$  NMR chemical shift could be experimentally determined and justified using quantum chemical calculations.



## 5 Experimental Section

**General.** All reactions were carried out under inert gas atmosphere using Schlenk techniques. Argon (Messer Griesheim, purity 4.6 in 50 L steel cylinder) was used as inert gas. The glass vessels used were stored in a 130 °C drying oven. Before use the glass vessels were flame dried in vacuum at  $10^{-3}$  mbar.

$\text{Na}_2\text{S}_2$  was prepared as described in literature and stored in a dry box under nitrogen atmosphere.<sup>5</sup> Elemental sulfur was used as received (Acros Organics).  $\text{P}_4\text{S}_{10}$  was commercially obtained (Riedel-de Häen).  $\text{PCl}_3$  (Aldrich) was freshly distilled before use, to remove traces of HCl. The used pyridine was dried using commonly known methods and freshly distilled before use.

**NMR Spectroscopy.** NMR spectra were recorded using a Jeol EX 400 Eclipse instrument operating at 161.997 MHz ( $^{31}\text{P}$ ). Chemical shifts are referred to 85 %  $\text{H}_3\text{PO}_4$  as external standard. All spectra were measured, if not mentioned otherwise, at 25 °C. The %-data correspond to the intensities in the  $^{31}\text{P}$  NMR spectra with respect to the total intensity. The difference to 100 % belongs to not determinable signals.

**X-ray Crystallography.** The molecular structures in the crystalline state were determined using an Oxford Xcalibur3 diffraction instrument with a Spellman generator (voltage 50 kV, current 40 mA) and a Kappa CCD detector with a X-ray radiation wavelength of 0.71073 Å (MoK $_{\alpha}$ ). The data collection was performed with the CrysAlis CCD software, the data reduction with the CrysAlis RED software.<sup>6,7</sup> The structures were solved with SIR-92, SIR-97 and SHELXS-97 and refined with SHELXL-97 and finally checked using PLATON.<sup>8,9,10,11,12</sup> The absorptions were corrected by SCALE3 ABSPACK multi-scan method.<sup>13</sup> All relevant data and parameters of the X-ray measurement and refinement are given in Table 4.

<sup>5</sup> (a) Thompson, D. P.; Boudjouk, P. J. *Org. Chem.* **1988**, *53*, 2109. (b) Schuster, M. PhD Thesis, LMU Munich, **1999**.

<sup>6</sup> CrysAlis CCD, Oxford Diffraction Ltd., Version 1.171.27p5 beta (release 01-04-2005 CrysAlis171 .NET), (compiled Apr 1 2005,17:53:34).

<sup>7</sup> CrysAlis RED, Oxford Diffraction Ltd., Version 1.171.27p5 beta (release 01-04-2005 CrysAlis171 .NET), (compiled Apr 1 2005,17:53:34).

<sup>8</sup> SIR-92, **1993**, *A Program for Crystal Structure Solution*; Altomare, A.; Cascarano, G. L.; Giacovazzo, C.; Guagliardi, A. *J. Appl. Cryst.* **26**, 343.

<sup>9</sup> Altomare, A.; Burla, M. C.; Camalli, M.; Cascarano, G. L.; Giacovazzo, C.; Guagliardi, A.; Moliterni, A. G. G.; Polidori, G.; Spagna, R. *J. Appl. Crystallogr.* **1999**, *32*, 115.

<sup>10</sup> Sheldrick, G. M. *SHELXS-97, Program for Crystal Structure Solution*; Universität Göttingen, **1997**.

<sup>11</sup> Sheldrick, G. M. *SHELXL-97, Program for the Refinement of Crystal Structures*; University of Göttingen, Germany, **1997**.

<sup>12</sup> Spek, L. A. *PLATON, A Multipurpose Crystallographic Tool*, Utrecht University, Utrecht, The Netherlands, **1999**.

<sup>13</sup> SCALE3 ABSPACK – *An Oxford Diffraction program* (1.0.4,gui:1.0.3) (C) 2005 Oxford Diffraction Ltd.

---

**py<sub>2</sub>P<sub>2</sub>S<sub>5</sub>·P<sub>4</sub>S<sub>10</sub>** (315 mg, 14.2 mmol) was refluxed in 40 mL of pyridine for 1 h. The orange reaction mixture turned brown when cooling down to ambient temperature and the formation of a colorless crystalline precipitate consisting of **py<sub>2</sub>P<sub>2</sub>S<sub>7</sub>** can be observed. The precipitate was separated and dried in vacuum.

**py<sub>2</sub>P<sub>2</sub>S<sub>7</sub>**. 214 μl (1 mmol) PCl<sub>3</sub> was dissolved in 7 mL of pyridine. After the addition of 330 mg (3 mmol) Na<sub>2</sub>S<sub>2</sub> the yellow reaction suspension stirred over night at room temperature. Afterwards the yellow suspension was filtered to remove the colorless (NaCl) precipitate yielding a yellow solution. 1 ml of the yellow reaction solution was removed and filled into a NMR tube for <sup>31</sup>P NMR spectroscopical investigations. After one day colorless crystals of **py<sub>2</sub>P<sub>2</sub>S<sub>7</sub>** were observed in the NMR tube.

<sup>31</sup>P{<sup>1</sup>H} NMR in pyridine: δ = 113.5 (s, 19.5 %), 95.2 (py<sub>2</sub>PS<sub>2</sub>Cl, 75 %) 82.3 (py<sub>2</sub>P<sub>2</sub>S<sub>7</sub>, 3.5 %), 44.9 (s, 1.5 %), - 18.9 (s, 0.7 %).

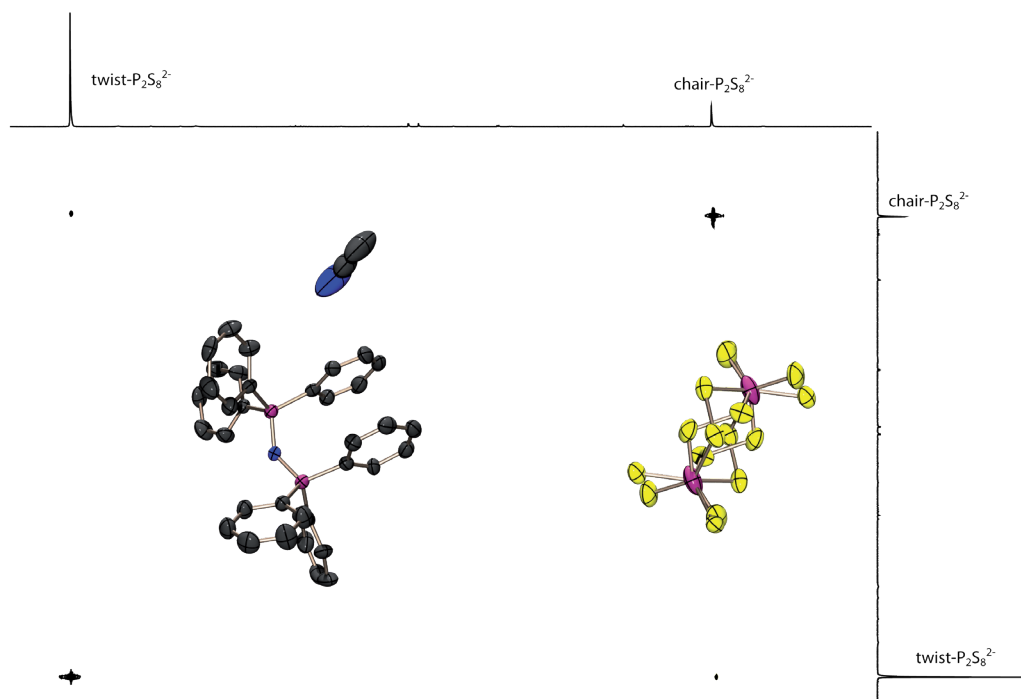
Table 4. Crystallographic and refinement data.

	$\text{pY}_2\text{P}_2\text{S}_5$	$\text{pY}_2\text{P}_2\text{S}_7$
empirical formula	$\text{C}_{10}\text{H}_{10}\text{N}_2\text{P}_2\text{S}_5$	$\text{C}_{10}\text{H}_{10}\text{N}_2\text{P}_2\text{S}_7$
formula mass	380.49	444.63
temp (K)	200	200
cryst. size (mm)	0.3 x 0.05 x 0.05	0.179 x 0.101 x 0.043
cryst. descriptn.	colourless needle	colourless block
cryst. system	triclinic	monoclinic
space group	$P\bar{1}$	$P2_1/c$
$a$ (Å)	9.3013(8)	13.000(3)
$b$ (Å)	12.8702(12)	8.0185(16)
$c$ (Å)	13.2736(13)	17.332(4)
$\alpha$ (deg)	88.536(8)	90
$\beta$ (deg)	87.088(7)	97.68(3)
$\gamma$ (deg)	85.690(7)	90
$V$ (Å <sup>3</sup> )	1582.1(3)	1790.5(6)
$Z$	4	4
$\rho_{\text{calc}}$ (g cm <sup>-3</sup> )	1.597	1.649
$\mu$ (mm <sup>-1</sup> )	0.920	1.051
$F(000)$	776	904
$\vartheta$ range (deg)	4.2043 – 28.9646	3.134 – 25.350
index ranges	-10 $\leq h \leq$ 11, -14 $\leq k \leq$ 15, -15 $\leq l \leq$ 15	-15 $\leq h \leq$ 15, -9 $\leq k \leq$ 9, -20 $\leq l \leq$ 20
reflcs. collcd.	10924	11002
reflcs. obsd.	2759	2316
reflcs. unique	5534 ( $R_{\text{int}} = 0.0760$ )	3259 ( $R_{\text{int}} = 0.0617$ )
$R_1, wR_2$ (2 $\sigma$ data)	0.0644, 0.1465	0.0421; 0.0888
$R_1, wR_2$ (all data)	0.1243, 0.1583	0.0755; 0.0980
max/min transm.	0.759/0.955	0.880/0.956
data/restr./params.	5534/0/343	3259/0/190
$S$ on $F^2$	0.864	1.052
larg. Diff peak/hole (e/Å)	1.073/-0.493	0.375/-0.455



## CHAPTER VII

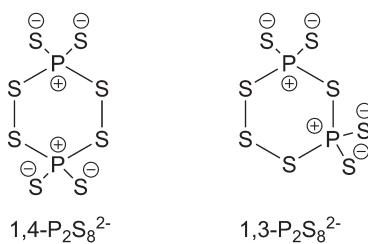
### Some News about $P_2S_8^{2-}$



*The  $P_2S_8^{2-}$  anion is long known in literature. Nevertheless, a characterization using the 2 dimensional  $^{31}P$ ,  $^{31}P$  EXSY NMR spectroscopy is still missing, in order to elucidate if the sixmembered ring contained in  $P_2S_8^{2-}$  is also existing in twist and chair conformation in accordance to the results found for  $P_2Se_8^{2-}$ . In addition a new salt containing the  $P_2S_8^{2-}$  anion could be isolated and characterized using single crystal X-ray diffraction.*

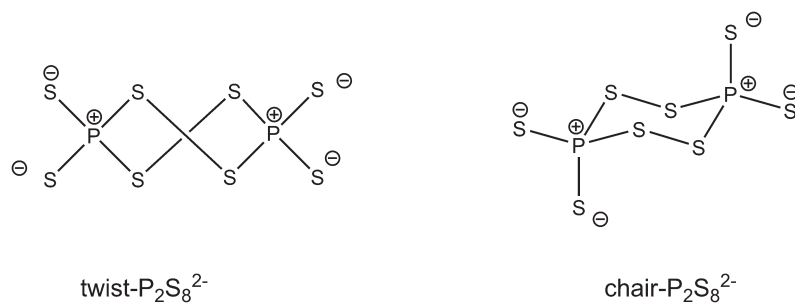
## 1 Introduction

The  $P_2S_8^{2-}$  anion represents an already long known and therefore quite well investigated sulfur rich thiophosphate anion. Two isomers of  $P_2S_8^{2-}$  are known both consisting of a sixmembered ring and exocyclic bonded sulfur atoms. The difference is the connectivity of the atoms within the ring (Scheme 1).<sup>1,2,3</sup>



Scheme 1. Two isomers of  $P_2S_8^{2-}$ .

The  $^{31}P$  NMR chemical shift of the  $1,4-P_2S_8^{2-}$  is reported by Falius et al.<sup>1c</sup> M. Schuster<sup>3</sup> also investigated the  $^{31}P$  NMR chemical shift of  $P_2S_8^{2-}$  and found that in analogy to the  $P_2Se_8^{2-}$  anion<sup>4</sup> two conformers of the  $1,4-P_2S_8^{2-}$  anion are expected: a twist and a chair conformer, which should be in dynamic equilibrium with each other. In fact two signals are observed in the  $^{31}P$  NMR spectrum, when dissolved in an aprotic, polar solvent. Based on the experience with the  $P_2Se_8^{2-}$  anion, M. Schuster assigned the signal at  $\delta^{31}P = 119.5$  to the twist conformer and the signal at  $\delta^{31}P = 55.5$  to the chair conformer.<sup>3</sup> But nevertheless the final proof is still missing, as it has not been possible till now to isolate the twist conformer in the solid state.



Scheme 2. Twist- and chair conformer of  $P_2S_8^{2-}$ .

<sup>1</sup> (a) Dastychova, L.; Sotolarova, M.; Dastych, D.; Taraba, J.; Necas, M.; Prihoda, J. *Polyhedron*, **2007**, *26*, 4250. (b) Katrusiak, A. *J. Mol. Struct.*, **1999**, *125*. (c) Falius, H.; Schliephake, A.; Schomburg, D. *Z. Anorg. Allg. Chem.* **1992**, *611*, 141. (d) Jones, P. G.; Weinkauff, A. *Acta Crystallogr., Sect. C: Cryst. Struct. Commun.*, **1991**, *C47*, 686. (e) Micu-Semeniuc, R.; Popse, S.; Haiduc, I. *Rev. Roum. Chim.*, **1983**, *28(6)*, 605. (f) Minshall, P. C.; Sheldrick, G. M. *Acta Crystallogr., Sect. B: Struct. Sci.*, **1978**, *B34*, 1378.

<sup>2</sup> (a) Hoppe, D.; Pfitzner, A. *Z. Anorg. Allg. Chem.* **2009**, *635*. (b) Gruber, H.; Müller, U. *Z. Anorg. Allg. Chem.* **1997**, *623*, 957.

<sup>3</sup> Schuster, M. *dissertation*, LMU Munich, **1999**.

<sup>4</sup> Rotter, C.; Schuster, M.; Kidik, M.; Schön, O.; Klapötke, T. M.; Karaghiosoff, K. *Inorg. Chem.* **2008**, *632*, 1663.

## 2 Results and Discussion

As already described by M. Schuster the synthesis of  $P_2S_8^{2-}$  is quite straight forward reacting  $P_4S_3$ ,  $Na_2S_2$  and elemental sulfur in the appropriate stoichiometric ratio in an aprotic polar organic solvent like THF or acetonitrile (Scheme 3).



Scheme 3. Synthesis of  $P_2S_8^{2-}$  in solution.

To proof the assumption that a twist conformer of  $1,4-P_2S_8^{2-}$  does exist, and that there is an equilibrium between the twist and chair conformer, a  $^{31}P$ ,  $^{31}P$ -EXSY-NMR experiment was carried out, using a solution of  $Na_2P_2S_8$  in THF. Crosspeaks between the signal at  $\delta^{31}P = 119.5$  and  $\delta^{31}P = 55.5$  revealed that there is indeed an equilibrium between the two species causing these signals (Figure 1).

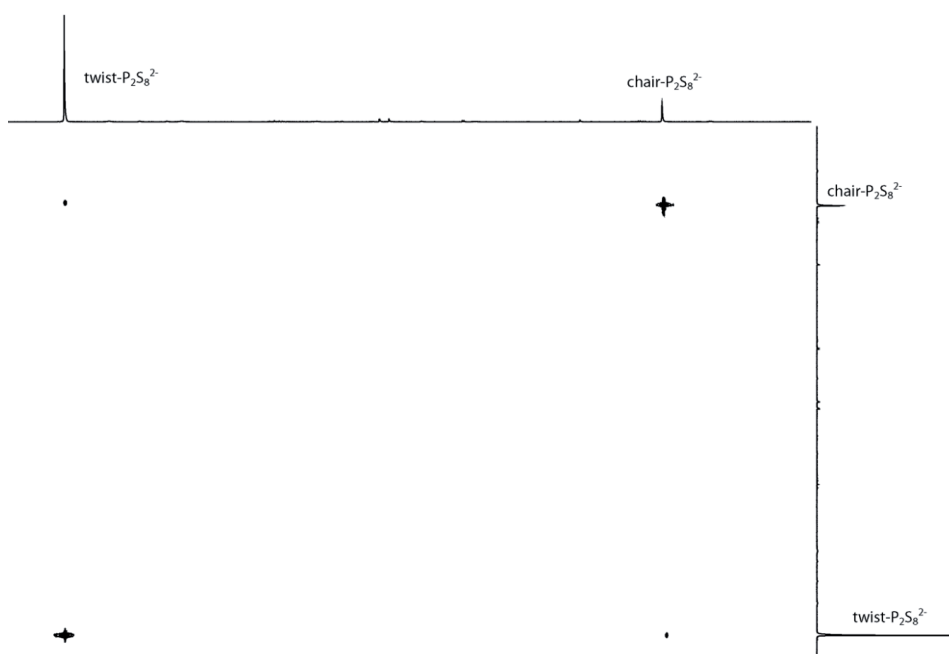
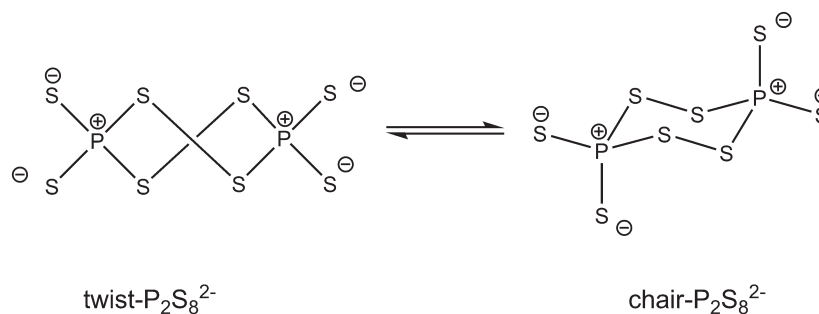


Figure 1.  $^{31}P$ ,  $^{31}P$  EXSY NMR spectrum of  $P_2S_8^{2-}$  dissolved in acetonitrile. (0.1 M, 25°C, matrix 2048 x2048, mixing time 1 sec).

The exchange is slow on the NMR time scale (Scheme 4). The intensity ratio of both signals is 4 : 1 (twist : chair), like already observed for the corresponding selenium compound.



**Scheme 4. Equilibrium of twist and chair conformers of  $P_2S_8^{2-}$ .**

Quantum chemical calculations were carried out at the B3LYP level of theory using 6-311+G(d) basissets in order to elucidate the total energies of twist and chair conformer.<sup>5</sup> The calculations revealed that they are very close together, but the twist conformer is thermodynamically more favoured with a value of  $-2.8$  kcal/mol.

The  $P_2S_8^{2-}$  anion has a very high tendency of formation: it is formed even when stoichiometries are used, which contain less sulfur than needed. Thus the  $P_2S_8^{2-}$  anion is often observed during the synthesis of  $PS_3^-$  as a byproduct.



**Scheme 5. Synthesis of  $PS_3^-$ .**

In course of the investigations to isolate a salt of the  $PS_3^-$  anion in its monomeric form, a new salt containing the  $P_2S_8^{2-}$  anion could be obtained and characterized by single crystal X-ray diffraction.

Colourless crystals of  $[PPN]_2[P_2S_8] \cdot MeCN$  were obtained after the addition of  $PPNCl$  to a reaction solution of  $P_4S_3$ ,  $Na_2S_2$  and sulfur (ratio 1:2:5) in acetonitrile.<sup>6</sup> The salt crystallizes in the monoclinic space group  $C2/c$ .

The crystal of  $[PPN]_2[P_2S_8] \cdot MeCN$  consists of the  $PPN^+$  cations and  $P_2S_8^{2-}$  anions with no significant cation/anion interaction. The  $P_2S_8^{2-}$  anion adopts chair conformation. In the crystal the  $P_2S_8^{2-}$  anions occupy two positions which differ in the positions of the sulfur atoms, while there is almost no difference in the position of the phosphorus atoms. This disorder is shown in Figure 2. Bond lengths and angles are given in Table 1. They do not differ significantly from those of  $P_2S_8^{2-}$  in other salts reported in literature.<sup>1</sup> The disorder of the anions can be explained by the fact, that the cation is very huge and bulky, thus the anion has much space within the crystal and therefore two orientations are possible.

<sup>5</sup> – E/a.u (chair- $P_2S_8^{2-}$ ) = 3868.686151; – E/a.u (twist- $P_2S_8^{2-}$ ) = 3868.690552.

<sup>6</sup> PPN = Bis-(triphenylphosphino)-iminium

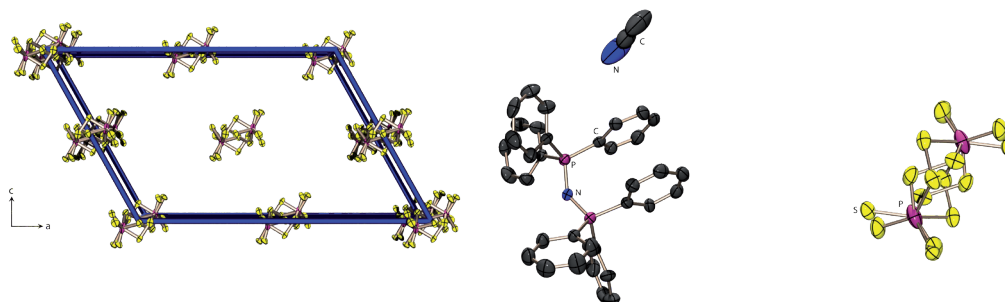


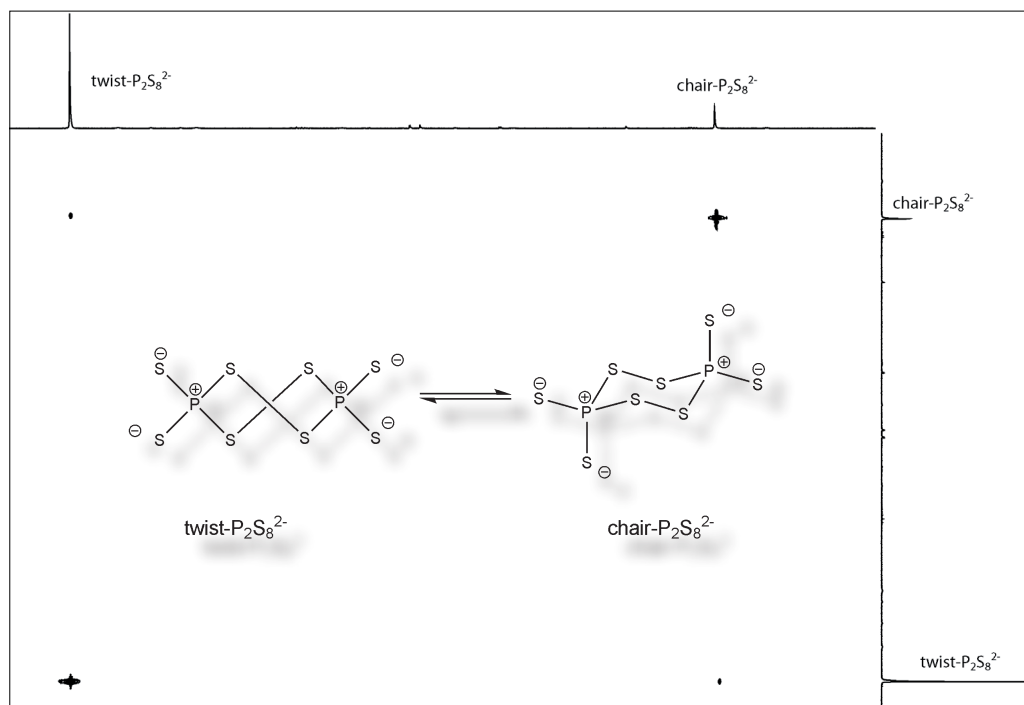
Figure 2. *Right*: molecular structure of  $[PPN]_2[P_2S_8]$  showing the disorder of the  $P_2S_8^{2-}$  anions, view along the  $b$  axis, hydrogen atoms are omitted for clarity, ellipsoids are drawn at 50 % probability level. *Left*: crystal structure of  $[PPN]_2[P_2S_8]$ , view of the unit cell along  $b$  axis, the PPN cation is omitted for clarity, ellipsoids are drawn at the 50 % probability level.

Table 1. Structural details of  $[PPN]_2[P_2S_8] \cdot MeCN$ ,  $i = -x, -y, -z$ .

Distances [pm]			
P3-S1	215.4(3)	P3-S5	191.0(4)
P3-S2	217.3(5)	P3-S6	220.2(3)
P3-S3	208.3(4)	P3-S7	196.5(4)
P3-S4	220.2(4)	P3-S8	168.5(6)
S1-S4( <i>i</i> )	197.8(5)	S6-S7( <i>i</i> )	204.6(5)
Angles [°]			
S1-P3-S2	93.4(2)	S5-P3-S6	80.9(2)
S2-P3-S3	119.1(2)	S6-P3-S7	91.0(2)
S3-P3-S4	107.1(2)	S7-P3-S8	127.8(3)
S1-P3-S4	94.2(2)	S5-P3-S8	113.2(3)
S2-P3-S4	93.1(2)	S6-P3-S8	123.3(3)
S1-P3-S3	139.0(2)	S5-P3-S7	109.9(2)
S4( <i>i</i> )-S1-P3	96.8(2)	S7( <i>i</i> )-S6-P3	100.1(2)
S1( <i>i</i> )-S4-P3	107.2(2)	S6( <i>i</i> )-S7-P3	104.1(2)
S3-P3-S5	33.0(2)	S3-P3-S8	128.6(2)
S3-P3-S6	93.8(2)	S4-P3-S5	139.2(2)
S3-P3-S7	79.4(2)	S4-P3-S6	99.8(2)
S1-P3-S5	113.9(2)	S2-P3-S6	139.3(2)
S1-P3-S6	47.5(2)	S2-P3-S7	116.7(2)
S1-P3-S7	109.1(2)	S2-P3-S8	16.1(2)
S1-P3-S8	78.7(2)	S4-P3-S7	29.8(2)
S2-P3-S5	113.4(2)	S4-P3-S8	100.5(2)

### 3 Conclusion

It could be shown that, according to the results for  $P_2Se_8^{2-}$ ,  $P_2S_8^{2-}$  in fact exists in two conformers, a twist and a chair conformer. The equilibrium between both conformers is relatively slow on the NMR time scale. The high building tendency of  $P_2S_8^{2-}$  could be shown through the isolation of  $[PPN]_2[P_2S_8] \cdot MeCN$  using a stoichiometry with less sulfur than normally needed for the building of  $P_2S_8^{2-}$ . The characterization of  $[PPN]_2[P_2S_8] \cdot MeCN$  occurred using single crystal X-ray diffraction.



## 4 Experimental Section

**General.** All reactions were carried out under inert gas atmosphere using Schlenk techniques. Argon (Messer Griesheim, purity 4.6 in 50 L steel cylinder) was used as inert gas. The glass vessels used were stored in a 130 °C drying oven. Before use the glass vessels were flame dried in vacuum at  $10^{-3}$  mbar.

$Na_2S_2$  and PPNCl were prepared as described in literature and stored in a dry box under nitrogen atmosphere.<sup>7,8</sup> Elemental sulfur was used as received (Acros Organics).  $P_4S_3$  was commercially obtained (Riedel-de Haen), and was purified by extraction with  $CS_2$  before use. The used solvents were dried using commonly known methods and freshly distilled before use.

**NMR Spectroscopy.** NMR spectra were recorded with a Jeol EX 400 Eclipse instrument operating at 161.997 MHz ( $^{31}P$ ). Chemical shifts are referred to 85 %  $H_3PO_4$  as external standard. All spectra were measured, if not mentioned otherwise, at 25 °C. The %-data correspond to the intensities in the  $^{31}P$  NMR spectra with respect to the total intensity. The difference to 100 % belongs to not determinable signals.

**X-ray Crystallography.** The molecular structure in the crystalline state was determined using an Oxford Xcalibur3 diffraction instrument with a Spellman generator (voltage 50 kV, current 40 mA) and a Kappa CCD detector with a X-ray radiation wavelength of 0.71073  (MoK $_{\alpha}$ ). The data collection was performed with the CrysAlis CCD software, the data reduction with the CrysAlis RED software.<sup>9,10</sup> The structure was solved with SHELXS-97 and refined with SHELXL-97 and finally checked using PLATON.<sup>11,12,13,14,15</sup> The absorptions were corrected by SCALE3 ABSPACK multi-scan method.<sup>16</sup> All relevant data and parameters of the X-ray measurement and refinement are given in Table 2.

<sup>7</sup> (a) Thompson, D. P.; Boudjouk, P. J. *Org. Chem.* **1988**, *53*, 2109. (b) Schuster, M. dissertation, LMU Munich, **1999**.

<sup>8</sup> (a) Ruff, J. K.; Schlientz, W. J. *Inorg. Synth.* **1974**, *15*, 84. (b) Chihara, T.; Yamazaki, H. *J. Chem. Soc., Dalton Trans.* **1995**, 1369.

<sup>9</sup> CrysAlis CCD, Oxford Diffraction Ltd., Version 1.171.27p5 beta (release 01-04-2005 CrysAlis171 .NET), (compiled Apr 1 2005,17:53:34).

<sup>10</sup> CrysAlis RED, Oxford Diffraction Ltd., Version 1.171.27p5 beta (release 01-04-2005 CrysAlis171 .NET), (compiled Apr 1 2005,17:53:34).

<sup>11</sup> SIR-92, **1993**, *A Program for Crystal Structure Solution*; Altomare, A.; Cascarano, G. L.; Giacovazzo, C.; Guagliardi, A. *J. Appl. Cryst.* **26**, 343.

<sup>12</sup> Altomare, A.; Burla, M. C.; Camalli, M.; Cascarano, G. L.; Giacovazzo, C.; Guagliardi, A.; Moliterni, A. G. G.; Polidori, G.; Spagna, R. *J. Appl. Crystallogr.* **1999**, *32*, 115.

<sup>13</sup> Sheldrick, G. M. *SHELXS-97, Program for Crystal Structure Solution*; Universitat Gottingen, **1997**.

<sup>14</sup> Sheldrick, G. M. *SHELXL-97, Program for the Refinement of Crystal Structures*; University of Gottingen, Germany, **1997**.

<sup>15</sup> Spek, L. A. *PLATON, A Multipurpose Crystallographic Tool*, Utrecht University, Utrecht, The Netherlands, **1999**.

<sup>16</sup> SCALE3 ABSPACK – *An Oxford Diffraction program* (1.0.4,gui:1.0.3) (C) 2005 Oxford Diffraction Ltd.

**Na<sub>2</sub>P<sub>2</sub>S<sub>8</sub>**: P<sub>4</sub>S<sub>3</sub> (220 mg, 1 mmol), Na<sub>2</sub>S<sub>2</sub> (220 mg, 2 mmol) and elemental sulfur (288 mg, 9 mmol) are suspended in 12 mL of THF. The reaction mixture was stirred over night at ambient temperature. A yellow solution was obtained, from which 0.7 mL were removed and transferred into a 5 mm NMR tube in order to use it for the <sup>31</sup>P,<sup>31</sup>P EXSY NMR experiment.

<sup>31</sup>P{<sup>1</sup>H} NMR in THF: δ = 119.5 (twist P<sub>2</sub>S<sub>8</sub><sup>2-</sup>, 78.0 %), 55.5 (chair P<sub>2</sub>S<sub>8</sub><sup>2-</sup>, 19 %), 115 (s, br, 3 %).

**[PPN]<sub>2</sub>[P<sub>2</sub>S<sub>8</sub>]**: P<sub>4</sub>S<sub>3</sub> (220 mg, 1 mmol), Na<sub>2</sub>S<sub>2</sub> (220 mg, 2 mmol) and elemental sulfur (160 mg, 5 mmol) were suspended in 10 mL of acetonitrile. The reaction mixture was stirred for 24 h at ambient temperature. Then PPNCl (2.154 g, 4 mmol) dissolved in 5 mL of acetonitrile was added. The white precipitate (NaCl) was removed, and the filtrate was stored at room temperature for 24 h. [PPN]<sub>2</sub>[P<sub>2</sub>S<sub>8</sub>] could be isolated as colourless crystals.

<sup>31</sup>P{<sup>1</sup>H} NMR in MeCN: δ = 21.2 (PPN<sup>+</sup>, 65.8 %), 119.5 (twist P<sub>2</sub>S<sub>8</sub><sup>2-</sup>, 2.9 %), 55.5 (chair P<sub>2</sub>S<sub>8</sub><sup>2-</sup>, 0.3 %), -9.2 (s, 10.9 %), 0.85 (s, 10.5 %), 35.4 (s, 2.0 %).

MS (FAB<sup>+</sup>): *m/z* = 538 (PPN<sup>+</sup>, 100 %).

IR: ν [cm<sup>-1</sup>] = 3052 (90), 1587 (95), 1482 (93), 1439 (84), 1284 (85), 1267 (81), 1182 (95), 1162 (97), 1115 (80), 1026 (98), 997 (94), 797 (99), 748 (92), 724 (81), 694 (82), 676 (85), 548 (77), 532 (80), 500 (88).

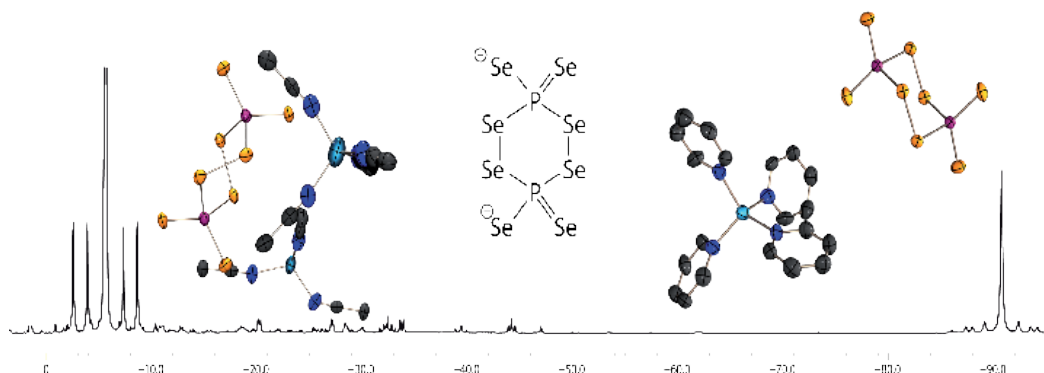
Table 2. Crystal and refinement data.

	[PPN] <sub>2</sub> [P <sub>2</sub> S <sub>8</sub> ]
empirical formula	C <sub>74</sub> H <sub>62</sub> N <sub>3</sub> P <sub>6</sub> S <sub>8</sub>
formula mass	1435.65
temp (K)	200
cryst. size (mm)	0.2 x 0.2 x 0.2
cryst. descriptn.	colourless block
cryst. system	monoclinic
space group	<i>C2/c</i>
<i>a</i> (Å)	32.0246(14)
<i>b</i> (Å)	12.8498(5)
<i>c</i> (Å)	20.2496(8)
$\alpha$ (deg)	90
$\beta$ (deg)	121.295(4)
$\gamma$ (deg)	90
<i>V</i> (Å <sup>3</sup> )	7120.5(5)
<i>Z</i>	4
$\rho_{\text{calc}}$ (g cm <sup>-3</sup> )	1.339
$\mu$ (mm <sup>-1</sup> )	0.431
<i>F</i> (000)	29800
$\vartheta$ range (deg)	3.69-29.99
index ranges	-37 ≤ <i>h</i> ≤ 38, -15 ≤ <i>k</i> ≤ 13, -24 ≤ <i>l</i> ≤ 15
reflcns colcd	14586
reflcns obsd	3237
reflcns unique	6069 ( <i>R</i> <sub>int</sub> = 0.0764)
<i>R</i> <sub>1</sub> , <i>wR</i> <sub>2</sub> (2 $\sigma$ data)	0.0750, 0.1041
<i>R</i> <sub>1</sub> , <i>wR</i> <sub>2</sub> (all data)	0.1617, 0.1347
max/min transm	0.844/1.000
data/restr/params	6069/0/453
<i>S</i> on <i>F</i> <sup>2</sup>	1.041
larg. diff peak/hole (e/Å)	0.551/-0.454



## CHAPTER VIII

### Structural and NMR Spectroscopic Investigations of Chair and Twist Conformers of the $P_2Se_8^{2-}$ Anion



Four salts of the  $P_2Se_8^{2-}$  anion have been prepared, starting from easily available reagents using different reaction strategies including reaction of the elements (Li, Se,  $P_{red}$ ), oxidation of  $P_4Se_3$  with alkalimetal diselenides and elemental selenium, and the use of an ionic liquid as reaction medium. Multinuclear NMR studies show the presence of both chair- $P_2Se_8^{2-}$  and twist- $P_2Se_8^{2-}$  in solution, with twist- $P_2Se_8^{2-}$  being the predominant conformer. The interconversion between the two conformers is slow on the NMR time scale. Structural investigations of the new salts by single-crystal X-ray diffraction reveal that chair- $P_2Se_8^{2-}$  is the conformer mostly found in the solid state. A first structural characterization of twist- $P_2Se_8^{2-}$  is reported. The bonding situation in the  $P_2Se_8^{2-}$  anion as well as the relative stability of the chair, twist, and boat conformers was elucidated by quantum chemical calculations.

## 1 Introduction

In the course of the investigations on chalcogenophosphates my interest was attracted by the anion  $\text{P}_2\text{Se}_8^{2-}$ . This cyclic anion with a six-membered P-Se ring was first synthesized 1992 by J. Kolis et al.<sup>1</sup> The synthesis occurred via the reaction of  $\text{P}_4\text{Se}_4$  glass with an excess of  $\text{K}_2\text{Se}_4$  in DMF:

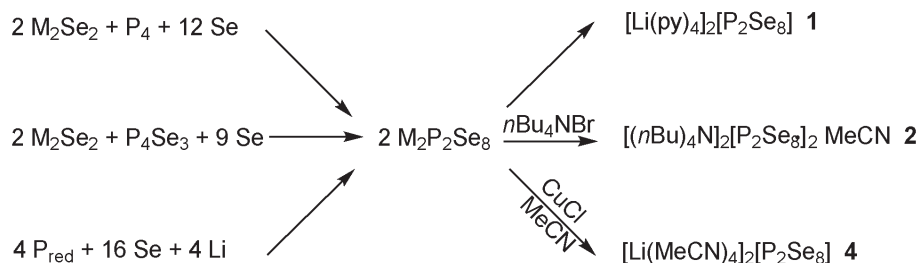


**Scheme 1. Synthesis of  $[\text{Ph}_4\text{P}]_2[\text{P}_2\text{Se}_8]$  according to J. Kolis.**

The  $\text{P}_2\text{Se}_8^{2-}$  anion was isolated as the  $[\text{Ph}_4\text{P}]_2[\text{P}_2\text{Se}_8]$  salt with a yield of 36 %. The compound was characterized using  $^{31}\text{P}$  NMR spectroscopy and single-crystal X-ray diffraction. However, the synthesis of  $\text{P}_2\text{Se}_8^{2-}$  on a large scale by this route is problematic because of the laborious preparation of the starting materials. Here, the synthesis of new salts of the  $\text{P}_2\text{Se}_8^{2-}$  anion starting from easily available materials and its characterization in solution by  $^{31}\text{P}$  and  $^{77}\text{Se}$  NMR spectroscopy as well as in the solid state by single-crystal X-ray diffraction is presented.

## 2 Syntheses

The  $\text{P}_2\text{Se}_8^{2-}$  anion is readily obtained by the oxidation of white phosphorus with an alkali metal diselenide  $\text{M}_2\text{Se}_2$  ( $\text{M} = \text{Li}, \text{Na}$ ) and grey selenium in the appropriate stoichiometric ratio using basic solvents like *N*-methyl imidazole, *N,N*-dimethylpropyleneurea or pyridine. Alternatively,  $\text{P}_4\text{Se}_3$  can be used instead of  $\text{P}_4$  in the reaction with  $\text{M}_2\text{Se}_2$  and grey selenium (Scheme 2). The reactions can be performed on a large scale and yield  $\text{P}_2\text{Se}_8^{2-}$  as the predominating phosphorus-containing species in solution. The use of  $\text{M}_2\text{Se}_2$  has the advantage that common organic solvents like MeCN or THF can also be employed. Exchange of the alkali metal cation by  $n\text{Bu}_4\text{N}^+$  in acetonitrile yields  $[n\text{Bu}_4\text{N}]_2[\text{P}_2\text{Se}_8] \cdot 2\text{MeCN}$  (**2**) as yellow crystals in gram quantities.<sup>2</sup>



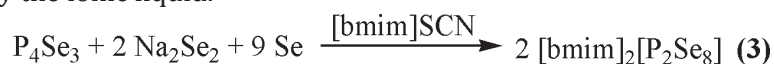
**Scheme 2. Syntheses of new salts with the  $\text{P}_2\text{Se}_8^{2-}$  anion ( $\text{M} = \text{Li}, \text{Na}$ ).**

<sup>1</sup> Zhao, J.; Pennington, W. T.; Kolis, J. W. *J. Chem., Chem. Commun.* **1992**, 265.

<sup>2</sup> (a) Schuster, M. *dissertation*, LMU Munich, **1999**. (b) Rotter, C.; Schuster, M.; Kidik, M.; Schön, O.; Klapötke, T. M.; Karaghiosoff, K. *Inorg. Chem.* **2008**, *47*, 1663.

Lithium salts of the  $P_2Se_8^{2-}$  anion can be readily obtained by reaction of the elements. Heating of red phosphorus together with the stoichiometric amount of lithium and elemental selenium at 240 °C for 24 h results in the formation of an orange-red solid, which readily dissolves in pyridine or acetonitrile. From these solutions, yellow crystals of the lithium salts  $[Li(py)_4]_2[P_2Se_8]$  (**1**) and  $[Li(MeCN)_4]_2[P_2Se_8]$  (**4**) are formed. In the second case, crystallization occurred only after the addition of a small amount of CuCl and yielded a first example of a salt with the  $P_2Se_8^{2-}$  anion in the twist conformation.

Ionic liquids like [bmim]SCN (bmim = 1-butyl-3-methylimidazolium cation) can also be used as a reaction medium of high polarity, which favors the formation of selenophosphate anions. When  $Na_2Se_2$  is reacted with  $P_4Se_3$  and elemental selenium in [bmim]SCN (Scheme 3), orange crystals of the new selenophosphate salt  $[bmim]_2[P_2Se_8]$  (**3**) are isolated in high yield. In this case, the cation of the salt is provided by the ionic liquid.

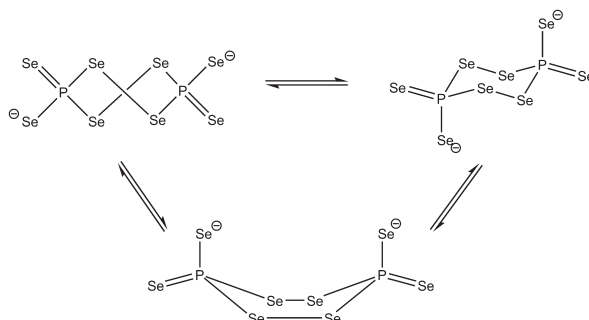


**Scheme 3.** Synthesis of  $[bmim]_2[P_2Se_8]$  in ionic liquid.

The isolated new salts of the  $P_2Se_8^{2-}$  anion are moderately sensitive toward air and moisture and should be stored under an inert atmosphere. They are readily soluble in common organic solvents like acetonitrile, benzonitrile, propionitrile, and pyridine.

### 3 $^{31}P$ and $^{77}Se$ NMR Spectroscopy of the $P_2Se_8^{2-}$ Anion

There are three possible conformations for the six-membered ring in  $P_2Se_8^{2-}$ : chair, boat, and twist conformations (Scheme 4). In contrast to what has been reported in the literature, always two signals (at - 4.5 and - 89.8 ppm) could be observed in the  $^{31}P$  NMR spectrum of  $P_2Se_8^{2-}$ , which are attributed to the twist and the chair conformers, respectively. The ratio between the twist and the chair conformers is 4:1 in all of the solvents investigated. A  $^{31}P$  NMR signal, indicating the presence of a boat conformer, was not observed.<sup>1,2</sup>



**Scheme 4.** Twist (upper left), chair (upper right), and boat (middle) conformations of the  $P_2Se_8$  dianion.

Interconversion between the conformers at ambient temperature is slow on the NMR time scale. The presence of a dynamic equilibrium between the twist and the chair conformers is clearly indicated by  $^{31}P,^{31}P$  exchange NMR spectroscopy (EXSY). In the spectrum (Figure 1) cross peaks between the signals of the two conformers are clearly visible.

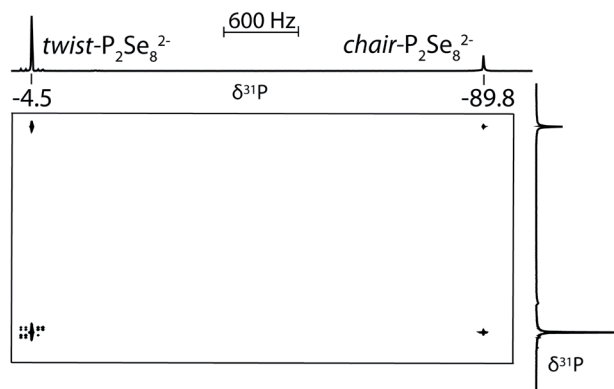


**Figure 1.**  $^{31}P,^{31}P$  EXSY spectrum of  $P_2Se_8^{2-}$  in acetonitrile (0.16 M, matrix 2048 x 1024, mixing time 0.5 sec).

### 3.1 $^{31}P$ NMR Spectra of chair- $P_2Se_8^{2-}$

The  $^{31}P$  NMR signal for the chair conformer of the  $P_2Se_8^{2-}$  anion in acetonitrile was observed at  $-89.8$  ppm (Figure 2). The signal pattern consists of a singlet and three pairs of  $^{77}Se$  satellites. The observed pattern is in accord with the  $C_{2h}$  symmetry of chair- $P_2Se_8^{2-}$ , which implies the presence of two different exocyclic selenium nuclei. The singlet is caused by the isotopomer without  $^{77}Se$  nuclei in the anion. The three pairs of  $^{77}Se$  satellites display an intensity ratio of 2:1:1 and originate from isotopomers with one  $^{77}Se$  nucleus. They all show the typical pattern of the A part of AA'X spectra with  $^3J_{AA'} = ^3J_{PP}$  of 8 Hz. The pair of satellites with the highest intensity is due to the isotopomer with one endocyclic  $^{77}Se$  nucleus ( $^1J_{SeP} = 348$  Hz,  $^2J_{SeP} = 33$  Hz), while the other two pairs of satellites of equal intensity are caused by the isotopomers with a  $^{77}Se$  nucleus in the exocyclic position (axial or equatorial). The corresponding  $^1J_{SeP}$  coupling constants are 604 and 733 Hz.<sup>2</sup>

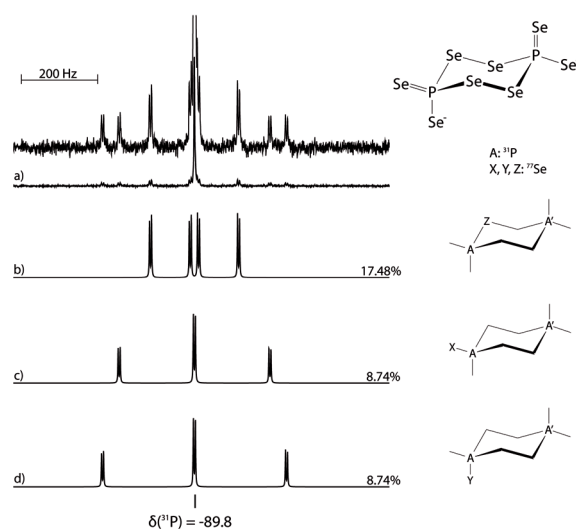


Figure 2.  $^{31}P\{^1H\}$  NMR spectrum of chair- $P_2Se_8^{2-}$ : (a) observed spectrum at  $-20\text{ }^\circ\text{C}$  in acetonitrile (0.16 M, 1200 scans with a PD = 0.5 s, 30 min measuring time,  $\nu_0 = 109.365\text{ MHz}$ , broadband  $^1H$  decoupling, 0.5 Hz line broadening, satellite signals enhanced), (b-d) calculated spectra for the isotomers with one  $^{77}Se$  nucleus.

### 3.2 $^{31}P$ NMR spectra of twist- $P_2Se_8^{2-}$

For twist- $P_2Se_8^{2-}$ , the  $^{31}P$  NMR spectrum shows a singlet at  $-4.5\text{ ppm}$ , which is accompanied by two pairs of  $^{77}Se$  satellites of equal intensity (Figure 3). The two pairs of satellites both display the line pattern typical for the A part of AA'X spectra and are caused by the isotomers with one  $^{77}Se$  nucleus in endocyclic ( $^1J_{SeP} = 372\text{ Hz}$ ) and exocyclic ( $^1J_{SeP} = 659\text{ Hz}$ ) position. The two exocyclic selenium nuclei are isochronous, which is in accord with the twist conformation of the anion. The P,P coupling constant  $^3J_{PP} = ^3J_{AA'}$  is 4 Hz smaller compared to that of chair- $P_2Se_8^{2-}$ .<sup>2</sup>

### 3.3 $^{77}Se$ NMR Spectrum of twist - and chair- $P_2Se_8^{2-}$

In the  $^{77}Se$  NMR spectrum (Figure 4), the signal for the endocyclic selenium atoms of the chair conformer appears at 910 ppm as a doublet of doublets ( $^1J_{SeP} = 348\text{ Hz}$ ). The observed fourline pattern (instead of the anticipated five lines for the X part of AA'X) results from the small P,P coupling constant, which implies only a small deviation from the first-order splitting. For the exocyclic selenium atoms, two doublets at 390 ( $^1J_{SeP} = 733\text{ Hz}$ ) and 242 ppm ( $^1J_{SeP} = 604\text{ Hz}$ ) are observed. On the basis of the quantum chemical calculations (see below), they are assigned to the selenium atoms in axial and equatorial positions, respectively. In the  $^{77}Se$  NMR spectrum of the twist conformer, signals at 762 ppm ( $^1J_{SeP} = 372\text{ Hz}$ ,  $^2J_{SeP} = 33\text{ Hz}$ ) and at 454 ppm ( $^1J_{SeP} = 659\text{ Hz}$ ) are observed for the endocyclic and exocyclic selenium atoms, respectively.<sup>2</sup>

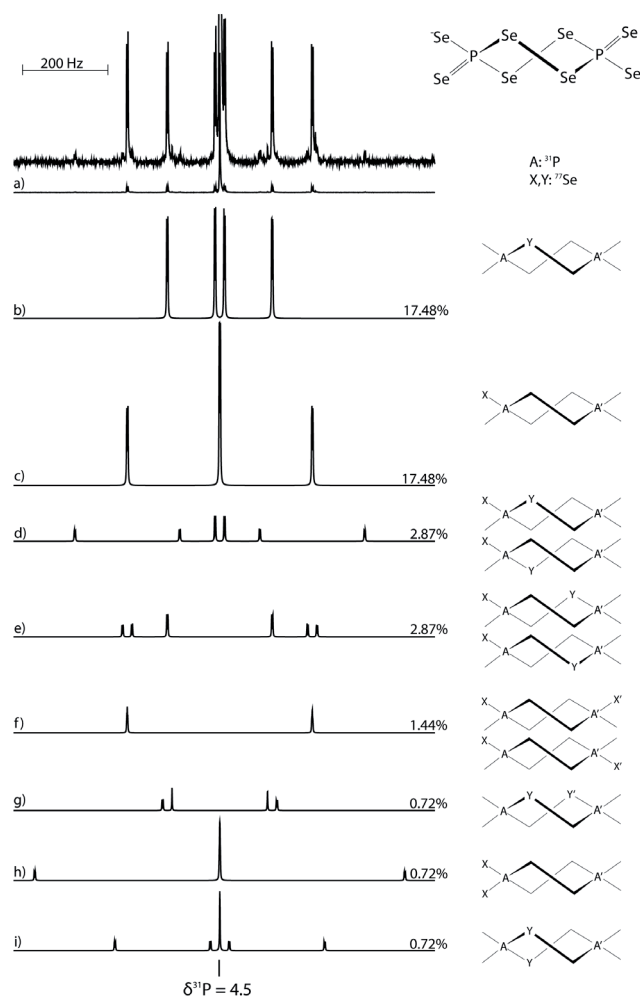


Figure 3.  $^{31}\text{P}\{^1\text{H}\}$  NMR spectrum of  $\text{twist-P}_2\text{Se}_8^{2-}$ : (a) observed spectrum at  $-20\text{ }^\circ\text{C}$  in acetonitrile (0.16 M, 1200 scans with a PD = 0.5 s, 30 min measuring time,  $\nu_0 = 109.365\text{ MHz}$ , broadband  $^1\text{H}$  decoupling, 0.5 Hz line broadening, satellite signals enhanced), (b and c) calculated spectra for the isotopomers with one  $^{77}\text{Se}$  nucleus, (d-i) calculated spectra for the isotopomers with two  $^{77}\text{Se}$  nuclei.

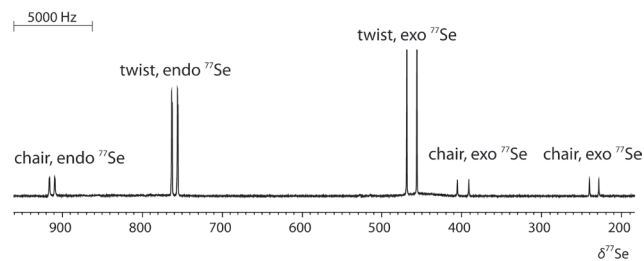


Figure 4.  $^{77}\text{Se}\{^1\text{H}\}$  NMR spectrum of  $\text{twist- and chair-P}_2\text{Se}_8^{2-}$ : observed spectrum at  $20\text{ }^\circ\text{C}$  in *N*-methylimidazol (0.1 M, 92500 scans with a PD ) 0.3 s, 19 h measuring time,  $\nu_0 = 51.525\text{ MHz}$ , broadband decoupling, 2 Hz line broadening).

## 4 Crystal and Molecular Structures of $P_2Se_8^{2-}$ Salts

The structure of the  $P_2Se_8^{2-}$  anion in four different salts was determined using single-crystal X-ray diffraction. In the following section, the structures of the different salts are first discussed individually and are then compared with each other.

### 4.1 $[Li(py)_4]_2[P_2Se_8]$ (**1**)



Block-shaped single crystals of  $[Li(py)_4]_2[P_2Se_8]$  (**1**) suitable for X-ray diffraction were obtained by keeping a pyridine solution of the salt for several days at ambient temperature. The compound crystallizes in the triclinic space group  $P\bar{1}$  with two formula units in the unit cell.

The  $P_2Se_8^{2-}$  anion adopts a chair conformation with  $C_{2h}$  symmetry (Figure 5). The P-Se bond lengths to the exocyclic selenium atoms are with 214.3(1) pm (P1-Se4) and 210.3(1) pm (P1-Se3) between the values for a P-Se single bond and those found for the P-Se bond in phosphine selenides.<sup>3</sup> The endocyclic P-Se distances correspond with 227.6(1) pm (P1-Se1) and 227.4(1) pm (P1(*i*)-Se2) to P-Se single bonds. The Se-Se bond length of 234.2(1) pm is in good agreement with the value expected for a Se-Se single bond.<sup>4</sup> The phosphorus atom is surrounded in a distorted tetrahedral arrangement by four selenium atoms. The endocyclic Se1-P1-Se2(*i*) angle is 104.4(1)°, whereas the exocyclic Se-P-Se angles range between 99° and 124°. Selected structural parameters for the  $P_2Se_8^{2-}$  anion in compound **1** are given in Table 1. The angles at the endocyclic selenium atoms are 103.0(1)° and 102.0(1)°. For the torsion angles P1-Se1-Se2-P1(*i*) and Se2-Se1-P1-Se2(*i*), values of 71.9(1)° and 73.0(1)° are observed.

<sup>3</sup> (a) Cordes, A. W., *Selenium*; Zingaro, R. A.; Cooper, W. C. (Ed.), Van Nostrand Reinhold Company: New York, 1974. (b) Shaw, R. A.; Woods, M.; Cameron, I. S.; Dahlen, B. *Chem. Ind.* **1971**, 151. (c) Grand, A.; Martin, J.; Robert, J. B.; Tordjman, I. *Acta Crystallogr.* **1975**, B31, 2523. (d) Galdecki, Z.; Glowka, M. L.; Michalski, J.; Okruszek, A.; Stec, W. J. *Acta Crystallogr.* **1977**, B33, 2322. (e) Cameron, T. S.; Howlett, K. D.; Miller, K. *Acta Crystallogr.* **1978**, B34, 1639. (f) Coddling, P. W.; Kerr, K. A. *Acta Crystallogr.* **1979**, B35, 1261. (g) Romming, C.; Songstad, J. *Acta Chem. Scand.* **1979**, A33, 187.

<sup>4</sup> Holleman, A. F.; Wiberg, E.; Wiberg, N. *Lehrbuch der Anorganischen Chemie*, 101st ed.; Walter de Gruyter Verlag: Berlin, **1995**.

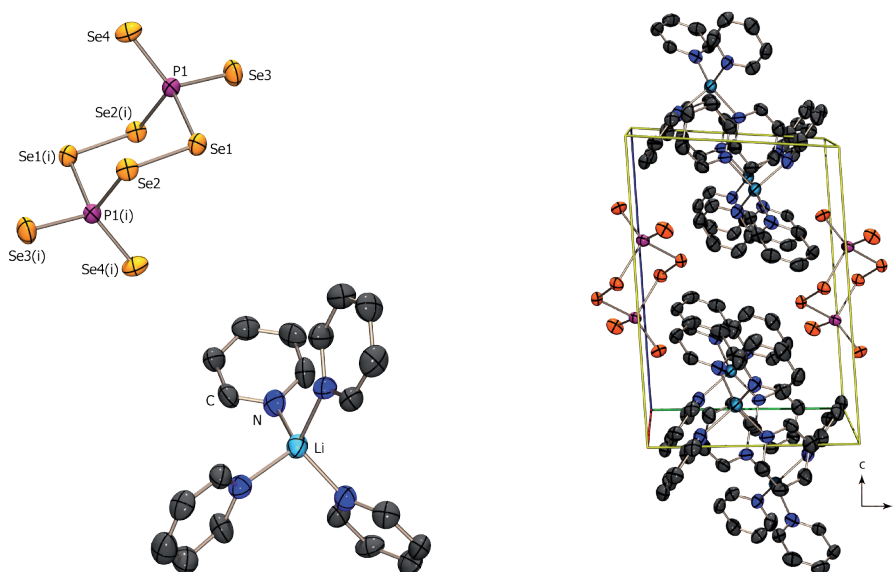


Figure 5. *Left*: Molecular structure of one ion pair in  $[\text{Li}(\text{py})_4]_2[\text{P}_2\text{Se}_8]$  (1) in the crystal. View along the  $b$  axis; ellipsoids are drawn at the 50 % probability level;  $i = 1-x, 1-y, z$ . *Right*: Crystal structure of  $[\text{Li}(\text{py})_4]_2[\text{P}_2\text{Se}_8]$  (1). View of the unit cell along the  $a$  axis; ellipsoids are drawn at the 50 % probability level. In both figures are the hydrogen atoms omitted for clarity.

Table 1. Selected bond lengths (pm) and angles ( $^\circ$ ) of  $[\text{Li}(\text{py})_4]_2[\text{P}_2\text{Se}_8]$  (1).

Bond lengths [pm]			
P1-Se1	227.6(1)	P1-Se3	214.3(1)
P1( <i>i</i> )-Se2	227.4(1)	Se1-Se2	234.2(1)
P1-Se4	210.3(1)		
Bond angles [ $^\circ$ ]			
Se1-P1-Se2( <i>i</i> )	104.4(1)	Se2( <i>i</i> )-P1-Se3	98.96(1)
Se2( <i>i</i> )-P1-Se4	113.69(1)	Se4-P1-Se1	113.2(1)
Se4-P1-Se3	124.2(1)	P1-Se1-Se2( <i>i</i> )	102.0(1)
Se3-P1-Se1	99.7(1)	P1( <i>i</i> )-Se2-Se1	103.0(1)
Torsion angles [ $^\circ$ ]			
P1-Se1-Se2-P1( <i>i</i> )	71.9(1)	Se2-Se1-P1-Se2( <i>i</i> )	-73.0(1)

## 4.2 $[nBu_4N]_2[P_2Se_8] \cdot 2MeCN$ (**2**)

Yellow block-shaped single crystals of  $[nBu_4N]_2[P_2Se_8] \cdot 2 MeCN$  (**2**) were obtained after the addition of tetra(*n*-butyl)ammonium bromide to a solution of  $Na_2P_2Se_8$  in acetonitrile. Compound **2** crystallizes in the monoclinic space group  $P2_1/c$  with four formula units in the unit cell.<sup>2</sup>

The  $P_2Se_8^{2-}$  anion lies on a crystallographic inversion center which is located in the middle of the chair-shaped  $P_2Se_8^{2-}$  ring; therefore, half of the anion is generated by symmetry (Figure 6). The P-Se bond lengths between the phosphorus atom and the axial exocyclic Se atoms (210.8(1) pm) is shorter than that to the equatorial exocyclic selenium atoms (213.5(1) pm). The P-Se distances to the endocyclic selenium atoms are, at 228.0(1) pm, for P1-Se1 and P1(*i*)-Se2 practically identical. The Se-Se distance within the diselenide moiety is 233.5(1) pm (Table 2). Bond lengths and angles of the  $P_2Se_8^{2-}$  anion in compound **2** do not differ significantly from those observed in compound **1**. Again, the largest Se-P-Se angle at phosphorus (123.1(1)°) is that involving both exocyclic selenium atoms. The endocyclic angle Se1-P1-Se2(*i*) is, at 103.3(1)°, smaller. The P1-Se1-Se2 angle within the ring is 102.4(1)°. The two torsion angles are 73.1(1)° (P1-Se1-Se2-P1) and -73.8(1)° (Se2-Se1-P1-Se2).<sup>2</sup>

Two seleniumphosphate anions are centered on the *bc* plane, while six other anions are located at the vertices of the unit cell (Figure 7). There are no other significant interactions in the structure than the electrostatic attraction between the cation and anion. It is worthwhile to mention the loose packing of the ions within the unit cell, and the presence of the acetonitrile solvent molecules in the space between the ions.<sup>2</sup>

**Table 2.** Selected bond lengths (pm) and angles (°) of  $[nBu_4N]_2[P_2Se_8] \cdot 2 MeCN$  (**2**).

Bond lengths [pm]			
P1-Se1	227.9(1)	P1-Se3	210.8(1)
P1( <i>i</i> )-Se2	228.0(1)	Se1-Se2	233.6(1)
P1-Se4	213.5(1)		
Bond angles [°]			
Se1-P1-Se2( <i>i</i> )	103.3(1)	Se2( <i>i</i> )-P1-Se3	113.1(1)
Se2( <i>i</i> )-P1-Se4	101.4(1)	Se4-P1-Se1	100.0(1)
Se4-P1-Se3	123.1(1)	P1-Se1-Se2	102.4(1)
Se3-P1-Se1	113.4(1)	P1( <i>i</i> )-Se2-Se1	102.4(1)
Torsion angles [°]			
P1-Se1-Se2-P1( <i>i</i> )	71.9(1)	Se2-Se1-P1-Se2( <i>i</i> )	-73.0(1)

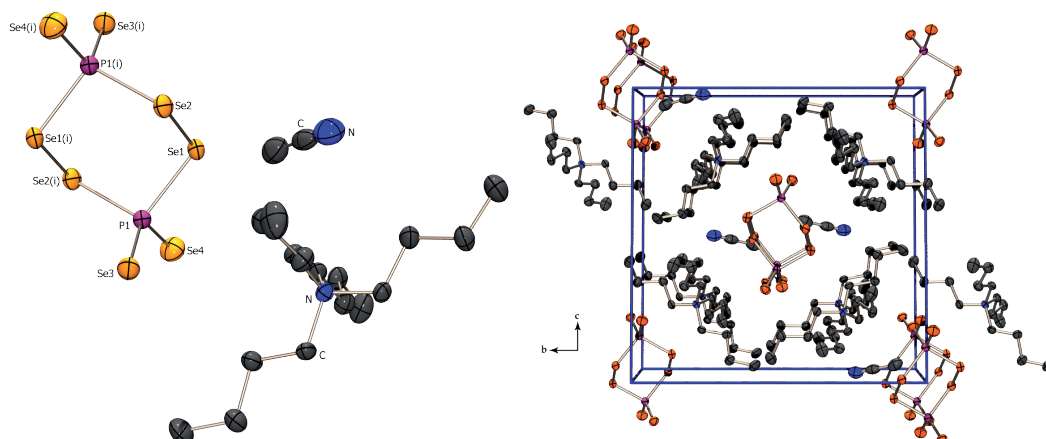


Figure 6. *Left*: Molecular structure of  $[n\text{Bu}_4\text{N}]_2[\text{P}_2\text{Se}_3]\cdot 2 \text{ MeCN}$  (**2**) in the crystal. View along the  $a$  axis; ellipsoids are drawn at the 50 % probability level;  $i = 2 - x, 1 - y, 1 - z$ . *Right*: Crystal structure of  $[n\text{Bu}_4\text{N}]_2[\text{P}_2\text{Se}_3]\cdot 2 \text{ MeCN}$  (**2**). View of the unit cell along the  $a$  axis; ellipsoids drawn at the 50 % probability level. In both figures are the hydrogen atoms omitted for clarity.

### 4.3 $[\text{bmim}]_2[\text{P}_2\text{Se}_8]$ (**3**)

Orange block-shaped single crystals were isolated after one day from a solution containing  $\text{P}_4\text{Se}_3$ ,  $\text{Na}_2\text{Se}_2$ , and grey selenium in 1-butyl-3-methyl-imidazoliumrhodanide  $[\text{bmim}][\text{SCN}]$ . Compound **3** crystallizes in the monoclinic space group  $P2_1/n$  with four formula units in the unit cell.

The  $\text{P}_2\text{Se}_8^{2-}$  anion adopts a chair conformation and is located on a center of inversion; thus, half of the anion is generated by symmetry (Figure 7). The P-Se distances to the axial selenium atoms are with 210.7(1) pm slightly shorter than those to the equatorial exocyclic selenium atoms with values of 213.1(1) pm. The P-Se distances within the ring, Se1-P1 227.7(1) pm and Se2-P1( $i$ ) 228.4(1) pm, as well as the Se-Se distance of 234.4(1) pm fit well to those observed for the other  $\text{P}_2\text{Se}_8^{2-}$  salts (Table 3).

Table 3. Selected bond lengths (pm) and angles ( $^\circ$ ) of  $[\text{C}_8\text{H}_{15}\text{N}_2]_2[\text{P}_2\text{Se}_8]$  (**3**).

Bond lengths [pm]			
P1-Se1	227.7(1)	P1-Se3	210.7(1)
P1( $i$ )-Se2	228.4(1)	Se1-Se2	234.4(1)
P1-Se4	213.1(1)		
Bond angles [ $^\circ$ ]			
Se1-P1-Se2( $i$ )	104.7(1)	Se2( $i$ )-P1-Se3	112.9(1)
Se4-P1-Se2( $i$ )	101.5(1)	Se4-P1-Se1	98.5(1)
Se3-P1-Se4	123.9(1)	P1-Se1-Se2( $i$ )	103.7(1)
Se3-P1-Se1	112.9(1)	Se1-Se2-P1( $i$ )	101.5(1)
Torsion angles [ $^\circ$ ]			
P1-Se1-Se2-P1( $i$ )	71.6(1)	Se2-Se1-P1-Se2( $i$ )	-73.9(1)

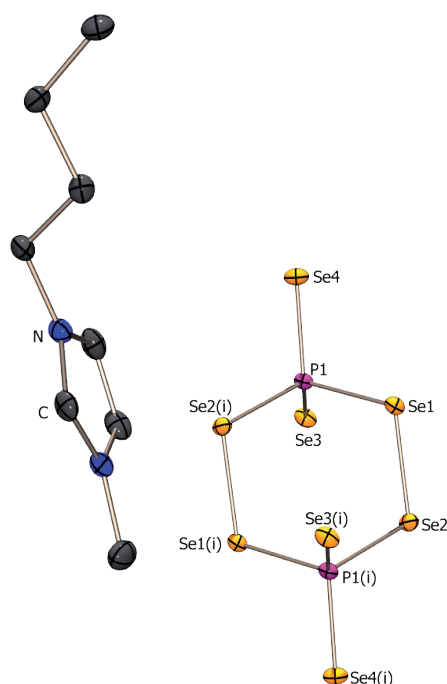


Figure 7. Molecular structure of  $[C_8H_{15}N_2][P_2Se_8]$  (**3**) in the crystal. View along the  $c$  axis; ellipsoids are drawn at the 50 % probability level;  $i = 1-x, 1-y, -z$ . Hydrogen atoms are omitted for clarity.

The phosphorus atom is coordinated in a distorted tetrahedral arrangement by four selenium atoms with the largest Se-P-Se angle ( $123.9(1)^\circ$ ) involving the exocyclic selenium atoms. The Se2-Se1-P1 angle is  $103.7(1)^\circ$ , and the torsion angles adopt values of  $-73.9(1)^\circ$  (Se2-Se1-P1-Se2( $i$ )) and  $71.6(1)^\circ$  (P1-Se1-Se2-P1( $i$ )).

In the crystal, the  $P_2Se_8^{2-}$  anions lie on special positions within the unit cell (Figure 8). Two anions are located in the middle of the  $ab$  plane. Four other anions are placed on the edges of the unit cell along the  $c$  axis at a height of  $c/2$ . Anions and cations are arranged along the  $a$  axis. There are only electrostatic interactions between the cations and the anions.

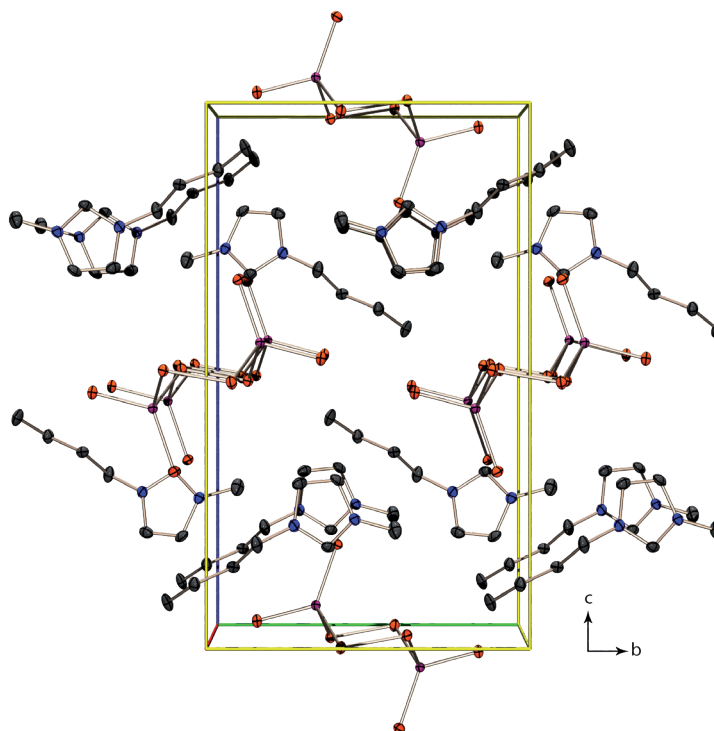


Figure 8. Crystal structure of  $[\text{C}_8\text{H}_{15}\text{N}_2]_2[\text{P}_2\text{Se}_8]$  (**3**). View of the unit cell along the  $a$  axis; ellipsoids are drawn at the 50 % probability level. Hydrogen atoms are omitted for clarity.

#### 4.4 $[\text{Li}(\text{MeCN})_4]_2[\text{P}_2\text{Se}_8]$ (**4**): First Structure of twist- $\text{P}_2\text{Se}_8^{2-}$

In all of the crystal structures of  $\text{P}_2\text{Se}_8^{2-}$  salts investigated so far, the anion was always found to adopt a chair conformation. In contrast, according to NMR spectroscopic investigations, the twist conformer predominates in solution. With  $[\text{Li}(\text{MeCN})_4]_2[\text{P}_2\text{Se}_8]$  (**4**), a first salt with the  $\text{P}_2\text{Se}_8^{2-}$  anion adopting a twist conformation in the solid state was isolated and structurally characterized.

Yellow rod-shaped single crystals of compound **4** were obtained from an acetonitrile solution of  $\text{Li}_2\text{P}_2\text{Se}_8$  after the addition of a small amount of  $\text{CuCl}$  at  $+4$  °C. The crystals have a melting point around  $15$  °C. Compound **4** crystallizes in the orthorhombic space group  $Pbam$  with four formula units in the unit cell.

In the crystal, the  $\text{P}_2\text{Se}_8^{2-}$  anion adopts twist conformation with  $D_2$  symmetry and is located on a 2-fold axis of symmetry, which intercepts the Se-Se bond (Figure 9).

Thus, half of the anion is generated by symmetry. The two P-Se distances to the exocyclic selenium atoms bonded to the same phosphorus atom are with  $212.5(1)$  pm (P1-Se4) and  $212.9(1)$  pm (P1-Se3) very similar (Table 4). The observed values are closer to the distance generally found for phosphine selenides and are significantly smaller than a P-Se single-bond distance.<sup>3,4</sup> The endocyclic P-Se distances are with

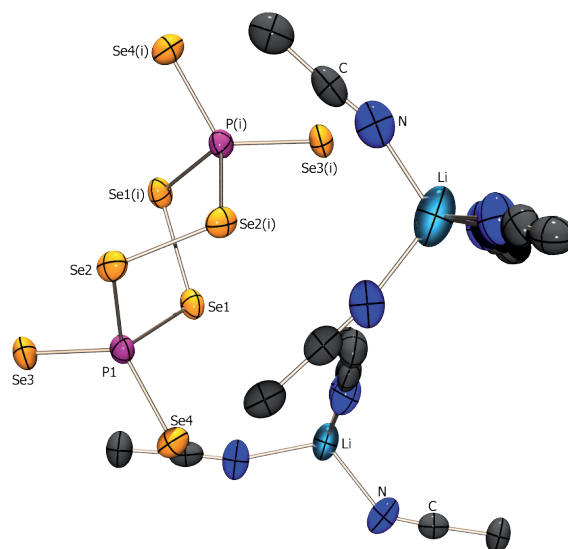


Figure 9. Molecular structure of  $[Li(MeCN)_4]_2[P_2Se_8]$  (4) in the crystal. View along the  $c$  axis; ellipsoids are drawn at the 50 % probability level,  $i = -x, -y, -z$ .

Table 4. Selected bond lengths (pm) and angles ( $^\circ$ ) of  $[Li(MeCN)_4]_2[P_2Se_8]$  (4).

Bond lengths [pm]			
P1-Se1	228.0(1)	P1-Se3	212.9(1)
P1-Se2	228.9(1)	Se1-Se1( <i>i</i> )	232.4(1)
P1-Se4	212.5(1)	Se2-Se2( <i>i</i> )	232.3(1)
Bond angles [ $^\circ$ ]			
Se1-P1-Se2	105.1(1)	Se2-P1-Se3	99.8(1)
Se4-P1-Se2	116.9(1)	Se4-P1-Se1	99.3(1)
Se3-P1-Se4	120.1(1)	P1-Se2-Se2( <i>i</i> )	102.5(1)
Se3-P1-Se1	115.5(1)	P1-Se1-Se1( <i>i</i> )	101.2(1)
Torsion angles [ $^\circ$ ]			
P1-Se1-Se1( <i>i</i> )-P1( <i>i</i> )	88.4(1)	Se1( <i>i</i> )-Se1-P1-Se2	-40.7(1)
P1-Se2-Se2( <i>i</i> )-P1( <i>i</i> )	84.5(1)	Se2( <i>i</i> )-Se2-P1-Se1	-37.2(1)

228.0(1) pm for P1-Se1 and 228.9(1) pm for P1-Se2 typical for P-Se single bonds.<sup>4</sup> The Se-Se distances within the diselenide units are with 232.3(1) pm for Se2-Se2(*i*) and 232.4(1) pm for Se1-Se1(*i*) as expected. The phosphorus atom displays a distorted tetrahedral coordination. The endocyclic angle at phosphorus is 105.1(1) $^\circ$ . As expected, the torsion angles within the ring (88.4(1) $^\circ$  for P1-Se1-Se1(*i*)-P1(*i*), 84.5(1) $^\circ$  for P1-Se2-Se2(*i*)-P1(*i*), -40.7(1) $^\circ$  for Se1(*i*)-Se1-P1-Se2, and -37.2(1) $^\circ$  for Se2(*i*)-Se2-P1-Se1) differ considerably from those observed in the structures of *chair*- $P_2Se_8^{2-}$ .

In the crystal, cations and anions form stacks along the  $c$  axis (Figure 10). The unit cell of compound **4** comprises two complete  $\text{P}_2\text{Se}_8^{2-}$  anions related by a mirror plane to each other, which is oriented orthogonal with respect to the  $c$  axis. Eight more  $\text{P}_2\text{Se}_8^{2-}$  anions are located on the edges of the unit cell along the  $c$  axis. The lithium atoms are tetrahedrally coordinated, each by four acetonitrile molecules.

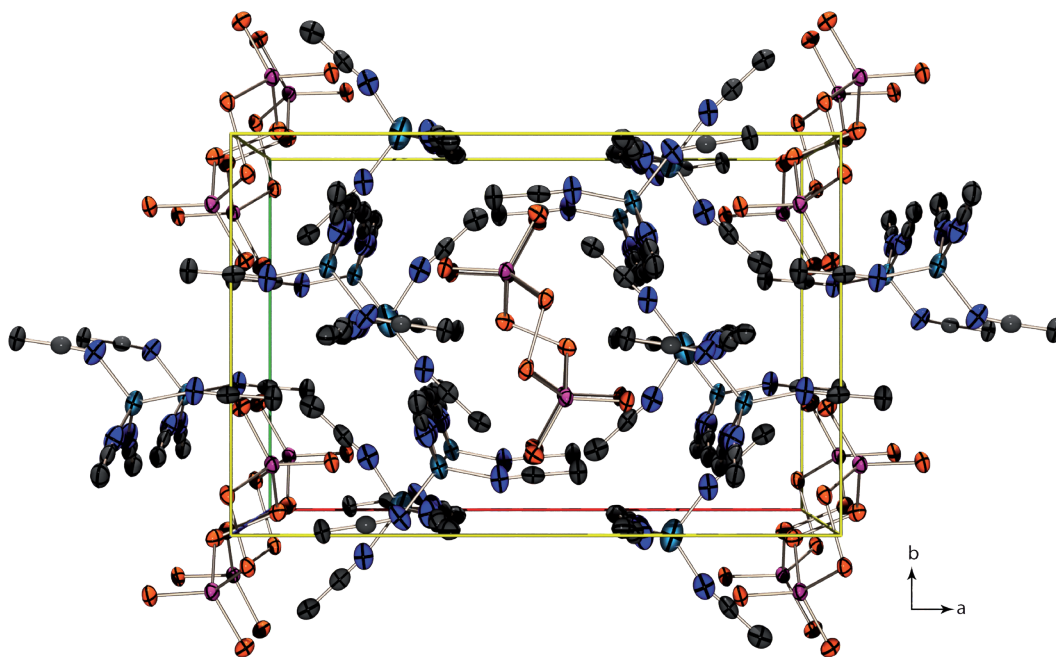


Figure 10. Crystal structure of  $[\text{Li}(\text{MeCN})_4]_2[\text{P}_2\text{Se}_8]$  (**4**). View of the unit cell along the  $c$  axis; ellipsoids are drawn at the 50 % probability level.

#### 4.5 Comparison of the Structures of $\text{P}_2\text{Se}_8^{2-}$ Salts

For a comparison of the structural features of the  $\text{P}_2\text{Se}_8^{2-}$  anion also, the only structurally characterized  $\text{P}_2\text{Se}_8^{2-}$  salt described in the literature so far,  $[\text{Ph}_4\text{P}]_2[\text{P}_2\text{Se}_8]$ , is included.<sup>1</sup> The bond lengths and angles of the  $\text{P}_2\text{Se}_8^{2-}$  anion in all of the salts structurally investigated do not differ significantly. Even in the twist conformation, there are no significant deviations of the bond lengths and angles as compared to those observed for the chair conformation. The  $\text{P}_2\text{Se}_4$  six-membered ring of the  $\text{P}_2\text{Se}_8^{2-}$  anion is remarkable, as to the best of our knowledge, there is only one example in the literature for a comparable six-membered ring with two diselenide units incorporated.<sup>5</sup> The Se-Se distances in this compound, *twist*- $(\text{SiMe}_2\text{Ph})_4\text{C}_2\text{Se}_4$ , are 231.2(1) and 230.9(1) pm and compare well with those found in the  $\text{P}_2\text{Se}_8^{2-}$  salts.<sup>4</sup>

The same applies also to the C-Se-Se-C torsion angles in *twist*- $(\text{SiMe}_2\text{Ph})_4\text{C}_2\text{Se}_4$ , which are with  $-78.7(2)^\circ$  and  $-81.9(2)^\circ$ , in the same range as those found for *twist*- $\text{P}_2\text{Se}_8^{2-}$  in compound **4**.

<sup>5</sup> Klapötke, T. M.; Krumm, B.; Polborn, K.; Scherr, M. *Eur. J. Inorg. Chem.* **2006**, 2937.

## 5 Computational Results

All calculations were carried out using the Gaussian G03W program code.<sup>6</sup> For the  $[P_2Se_8]^{2-}$  anion, both the chair (**A**) and twist (**B**) conformers were observed experimentally by X-ray crystallography. In order to elucidate the structure, bonding, and energetics in the gas phase theoretically, computations were carried out using *ab initio* Hartree–Fock (HF) and hybrid density functional theory (DFT) at the B3LYP level (Becke’s three-parameter hybrid functional, where the nonlocal correlation is provided by the LYP correlation functional, i.e. the correlation functional of Lee, Yang, and Parr).<sup>7,8</sup> Initially, the chair (**A**), twist (**B**), and boat (**C**) conformers were calculated without any symmetry constraints employing an all-electron 3-21G(d) basis set.<sup>9</sup> At this level, the chair and twist conformers were found to be stable minima (NIMAG = 0) on the potential energy hypersurface, whereas the boat conformer was found to optimize to the chair structure. Consequently, all subsequent calculations were performed for the chair and twist conformers in  $C_{2h}$  and  $D_2$  symmetry, respectively, at the HF and B3LYP levels of theory. Calculations employing a D95V basis for phosphorus and a quasirelativistic Stuttgart/Dresden<sup>10</sup> pseudopotential (SDD) for the core electrons of selenium and a double-zeta basis for the valence electrons of Se resulted in optimized structures with overestimated (0.10–0.25 Å) bond lengths.

In order to obtain more reliable structural and thermochemical data, the chair and twist conformers of the  $[P_2Se_8]^{2-}$  anion were then calculated at the B3LYP level of theory using an augmented polarized triple-zeta basis (6-311+G(d)) set for phosphorus and selenium (all-electron calculation).<sup>11</sup> The results are summarized in Table 4.

<sup>6</sup> Frisch, M. J.; Trucks, G. W.; Schlegel, H. B.; Scuseria, G. E.; Robb, M. A.; Cheeseman, J. R.; Montgomery, J. A., Jr.; Vreven, T.; Kudin, K. N.; Burant, J. C.; Millam, J. M.; Iyengar, S. S.; Tomasi, J.; Barone, V.; Mennucci, B.; Cossi, M.; Scalmani, G.; Rega, N.; Petersson, G. A.; Nakatsuji, H.; Hada, M.; Ehara, M.; Toyota, K.; Fukuda, R.; Hasegawa, J.; Ishida, M.; Nakajima, T.; Honda, Y.; Kitao, O.; Nakai, H.; Klene, M.; Li, X.; Knox, J. E.; Hratchian, H. P.; Cross, J. B.; Adamo, C.; Jaramillo, J.; Gomperts, R.; Stratmann, R. E.; Yazyev, O.; Austin, A. J.; Cammi, R.; Pomelli, C.; Ochterski, J. W.; Ayala, P. Y.; Morokuma, K.; Voth, G. A.; Salvador, P.; Dannenberg, J. J.; Zakrzewski, V. G.; Dapprich, S.; Daniels, A. D.; Strain, M. C.; Farkas, O.; Malick, D. K.; Rabuck, A. D.; Raghavachari, K.; Foresman, J. B.; Ortiz, J. V.; Cui, Q.; Baboul, A. G.; Clifford, S.; Cioslowski, J.; Stefanov, B. B.; Liu, G.; Liashenko, A.; Piskorz, P.; Komaromi, I.; Martin, R. L.; Fox, D. J.; Keith, T.; Al-Laham, M. A.; Peng, C. Y.; Nanayakkara, A.; Challacombe, P.; Gill, M. W.; Johnson, B.; Chen, W.; Wong, M. W.; Gonzalez, C.; and Pople, J. A.; *Gaussian 03*, Revision A.1; Gaussian, Inc.: Pittsburgh, PA, 2003.

<sup>7</sup> (a) Roothan, C. C. *J. Rev. Mod. Phys.* **1951**, *23*, 69. (b) Pople, J. A.; Nesbet, R. K. *J. Chem. Phys.* **1954**, *22*, 571. (c) McWeeny, R.; Dierksen, G. *J. Chem. Phys.* **1968**, *49*, 4852.

<sup>8</sup> (a) Lee, C.; Yang, W.; Parr, R. G. *Phys. Rev. B: Condens. Matter Mater. Phys.* **1988**, *37*, 785. (b) Miehlich, B.; Savin, A.; Stoll, H.; Preuss, H. *Chem. Phys. Lett.* **1989**, *157*, 200. (c) Becke, A. D. *J. Chem. Phys.* **1993**, *98*, 5648.

<sup>9</sup> (a) Binkley, J. S.; Pople, J. A.; Hehre, W. J. *J. Am. Chem. Soc.* **1980**, *102*, 939. (b) Gordon, M. S.; Binkley, J. S.; Pople, J. A.; Pietro, W. J.; Hehre, W. J. *J. Am. Chem. Soc.* **1982**, *104*, 2797. (c) Pietro, W. J.; Francl, M. M.; Hehre, W. J.; Defrees, D. J.; Pople, J. A.; Binkley, J. S. *J. Am. Chem. Soc.* **1982**, *104*, 5039. (d) Dobbs, K. D.; Here, W. J. *J. Comput. Chem.* **1986**, *7*, 359. (e) Dobbs, K. D.; Here, W. J. *J. Comput. Chem.* **1987**, *8*, 861. (f) Dobbs, K. D.; Here, W. J. *J. Comput. Chem.* **1987**, *8*, 880.

<sup>10</sup> (a) Dunning, T. H., Jr.; Hay, P. J. In *Modern Theoretical Chemistry*; Schaefer, H. F., III, Ed.; Plenum: New York, 1976. (b) Institut für Theoretische Chemie. <http://www.theochem.uni-stuttgart.de/> (accessed Dec 2007).

<sup>11</sup> (a) McLean, A. D.; Chandler, G. S. *J. Chem. Phys.* **1980**, *72*, 5639. (b) Krishnan, R.; Binkley, J. S.; Seeger, R.; Pople, J. A. *J. Chem. Phys.* **1980**, *72*, 650. (c) Waters, A. J. H. *J. Chem. Phys.* **1970**, *52*, 1033. (d) Hay, P. J. *J. Chem. Phys.* **1977**, *66*, 4377. (e) Raghavachari, K.; Trucks, G. W. *J. Chem. Phys.* **1989**, *91*, 1062. (f) Binning, R. C., Jr.; Curtiss, L. A. *J. Comput. Chem.* **1990**, *11*, 1206. (g) Curtiss, L. A.; McGrath, M. P.; Blauddau, J.-P.; Davis, N. E., Jr.; Radom, L. *J. Chem. Phys.* **1995**, *103*, 6104.

**Table 5. Computational results at the HF/6-311+G(d) and B3LYP/6-311+G(d) level of theory for the chair (A) and twist (B) conformers of  $[P_2Se_8]^{2-}$ .**

	<i>Chair</i> - $[P_2Se_8]^{2-}$ (A)		<i>Twist</i> - $[P_2Se_8]^{2-}$ (B)	
	HF/6-311+G(d)]			
symmetry	$C_{2h}$		$D_2$	
$-E / \text{a.u.}$	19880.11168		19880.112539	
$E_{\text{rel.}} / \text{kcal mol}^{-1}$	+ 0.9		0.0	
	calculated	experimental	calculated	experimental
$d(\text{Se}_{\text{term}}-\text{P}) / \text{\AA}$	2.15 (ax.), 2.17(eq.)	2.10 (ax.), 2.14 (eq.)	2.16	2.13
$d(\text{Se}_{\text{ring}}-\text{P}) / \text{\AA}$	2.31	2.27	2.31	2.29
$d(\text{Se}-\text{Se}) / \text{\AA}$	2.34	2.34	2.33	2.32
$\langle (\text{Se}_{\text{term}}-\text{P}-\text{Se}_{\text{term}}) \rangle / ^\circ$	120.7	124.2	119.0	120.2
$\langle (\text{Se}_{\text{term}}-\text{P}-\text{Se}_{\text{ring}}) \rangle / ^\circ$	113.9 (ax.), 102.1 (eq.)	113.7(ax.), 99.0 (eq.)	102.3, 114.5	99.3, 115.5
$\langle (\text{P}-\text{Se}_{\text{ring}}-\text{Se}_{\text{ring}}) \rangle / ^\circ$	104.9	103.0	102.9	102.6
	B3LYP/6-311+G(d)			
symmetry	$C_{2h}$		$D_2$	
$-E / \text{a.u.}$	19895.465679		19895.469325	
$E_{\text{rel.}} / \text{kcal mol}^{-1}$	+ 2.3		0.0	
	calculated	experimental	calculated	experimental
$d(\text{Se}_{\text{term}}-\text{P}) / \text{\AA}$	2.14 (ax.), 2.18 (eq.)	2.10 (ax.), 2.14 (eq.)	2.17	2.13
$d(\text{Se}_{\text{ring}}-\text{P}) / \text{\AA}$	2.37	2.27	2.37	2.29
$d(\text{Se}-\text{Se}) / \text{\AA}$	2.37	2.34	2.36	2.32
$\langle (\text{Se}_{\text{term}}-\text{P}-\text{Se}_{\text{term}}) \rangle / ^\circ$	122.5	124.2	120.0	120.2
$\langle (\text{Se}_{\text{term}}-\text{P}-\text{Se}_{\text{ring}}) \rangle / ^\circ$	114.5 (ax.), 101.0 (eq.)	113.7, 99.0	100.4, 116.7	99.3, 115.5
$\langle (\text{P}-\text{Se}_{\text{ring}}-\text{Se}_{\text{ring}}) \rangle / ^\circ$	105.6	103.0	104.7	102.6

Both DFT calculations reproduce well the angles in the chair and twist conformers of the  $[P_2Se_8]^{2-}$  dianion (Table 5). Whereas the SDD calculation always overestimated the Se-P and Se-Se bond lengths, the all-electron calculation reproduces the experimentally observed structural parameters reasonably well (Table 5).

It also has to be stressed that all Se-Se and Se-P bond lengths were calculated for the isolated dianion in the gas phase where solid state effects are not taken into account. The fact that both calculations (SDD and all-electron) overestimated to some extent the bond lengths can be explained by the high negative charge concentration for an isolated (gas-phase) dianion, which is not necessarily the case for the condensed

phase where significant cation-anion interactions result in a lowering of the negative charge on the dianion.

It is interesting to point out that the twist and chair conformers are *very* close in their total energies, with the twist conformer being thermodynamically more favorable (after zpe correction) by only 3.3 kcal mol<sup>-1</sup> (B3LYP/SDD calculation) or 2.3 kcal mol<sup>-1</sup> (B3LYP/6-311+G(d)):<sup>12</sup>



$$\Delta H(1) = - 3.3 \text{ kcal/mol (B3LYP/SDD)}, - 2.3 \text{ kcal/mol (B3LYP/6-311+G(d))}$$

The calculated similar relative energies of the twist and chair conformers are consistent with a recent combined theoretical and experimental study on the six-membered  $Se_4C_2$  heterocycle *twist*-(SiMe<sub>2</sub>Ph)<sub>4</sub>C<sub>2</sub>Se<sub>4</sub>.<sup>4</sup> For this system, the twist conformer was calculated to be 1.9 kcal mol<sup>-1</sup> more stable than the chair form.

With the reasonable assumption that  $\Delta S(1) \approx 0$  (no significant change in entropy for the chair to twist conformation change; i.e.,  $\Delta G \approx \Delta H \approx 2.3\text{--}3.3$  kcal mol<sup>-1</sup>), the equilibrium constant for eq 1 can be estimated according to eq 2 to be 2.5–3.7. This indicates that solutions of the chair or twist conformer may often show detectable amounts of the other species present, with the twist concentration being 2.5–3.7 times higher than the concentration of the chair conformer. This is in good accord with the experimental value (see above), which suggests a 1:4 ratio.

$$K = - \exp\{\Delta G/RT\} \approx 2.5\text{--}3.7 \quad (2)$$

The <sup>77</sup>Se NMR chemical shifts differ quite substantially for the chair and twist conformers of the  $[P_2Se_8]^{2-}$  anion. In order to compute the NMR chemical shifts for both species, the isotropic magnetic shieldings were computed using the gauge-independent atomic orbital (GIAO) method implemented in Gaussian03.<sup>5,13</sup> Since the DFT functionals do not include a magnetic field dependence, and therefore the DFT method does not provide systematically better NMR results than Hartree–Fock, the NMR shielding tensors were calculated at the HF/6-311+G(d) level of theory using the GIAO method.<sup>12</sup> Table 6 summarizes the computed isotropic magnetic shieldings. Relative <sup>77</sup>Se NMR chemical shifts (ppm) are referenced to Me<sub>2</sub>Se. Table 5 also contains the experimentally reported and calculated chemical shifts of Me<sub>2</sub>Se, MeSeH, and (CF<sub>3</sub>)<sub>2</sub>Se to provide an assessment of the accuracy of the calculated values.

<sup>12</sup> Klapötke, T. M.; Schulz, A.; Harcourt, R. D. *Quantum Chemical Methods in Main-Group Chemistry*; Wiley: Chichester, U.K., 1998.

<sup>13</sup> (a) Wolinski, K.; Hilton, J. F.; Pulay, P. *J. Am. Chem. Soc.* **1990**, *112*, 8251. (b) Dodds, J. L.; McWeeny, R.; Sadlej, A. J. *Mol. Phys.* **1980**, *41*, 1419. (c) Ditchfield, R. *Mol. Phys.* **1974**, *27*, 789. (d) McWeeny, R. *Phys. Rev.* **1962**, *126*, 1028.

**Table 6.** Computed isotropic magnetic shieldings (GIAO method, HF/6-311+G(d))<sup>5,12</sup> and relative <sup>77</sup>Se NMR chemical shifts (ppm) referenced to Me<sub>2</sub>Se.

	abs. anisotropic shielding	rel. shift, $\delta$ / ppm	exptl. reported chem. shift, $\delta$ / ppm
Me <sub>2</sub> Se	1946	0	0
MeSeH	2031	-85	-115 <sup>15</sup>
(CF <sub>3</sub> ) <sub>2</sub> Se	1308	638	717 <sup>15</sup>
<i>chair</i> -[P <sub>2</sub> Se <sub>8</sub> ] <sup>2-</sup>	1160	786	ring 910
	1564	382	axial 390
	1689	262	equatorial 242
<i>twist</i> -[P <sub>2</sub> Se <sub>8</sub> ] <sup>2-</sup>	1252	694	ring 762
	1534	412	terminal 454

The <sup>31</sup>P chemical shifts are also calculated using the GIAO method at the same level of theory as for the <sup>77</sup>Se NMR shifts (HF/6-311+G(d)). The computed <sup>31</sup>P chemical shifts clearly predict a downfield shift of the twist conformer with respect to the chair conformer of 61 ppm, which is qualitatively in good agreement with the experimentally observed chemical shifts of  $\delta = -89.8$  ppm (chair) and  $\delta = -4.5$  ppm (twist) ( $\Delta\delta = 85$  ppm).

For the chair and twist conformers of the [P<sub>2</sub>Se<sub>8</sub>]<sup>2-</sup> anion, a natural bond orbital (NBO) analysis was performed at the RHF/6-311+G(d) level of theory. The most important natural Lewis structures (according to the NBO analysis) are shown in Figure 8. It is interesting to note that for the chair conformer the four most important (identical) intramolecular donor–acceptor interactions are of the following types:

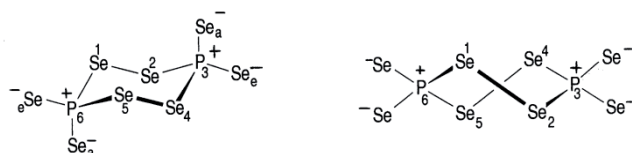
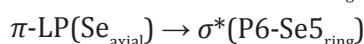
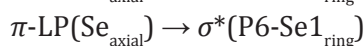
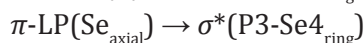
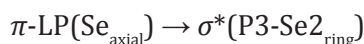


**Figure 10.** Natural Lewis structures for the chair (left) and twist (right) conformers of [P<sub>2</sub>Se<sub>8</sub>]<sup>2-</sup>.



with a donor–acceptor interaction energy of 15.1 kcal mol<sup>-1</sup> each. The fact that the axial terminal Se atoms interact more strongly with the antibonding  $\sigma^*(\text{P-Se}_{\text{ring}})$  bonds than the equatorial terminal Se atoms do is in good accord with the findings for six-membered organic ring compounds in the chair conformation (anomeric effect).<sup>11</sup>

The computed NBO natural charges are summarized in Table 7, and computational details for the chair and twist conformations are given in Table 8.

**Table 7. NBO natural charges for the chair (A) and twist (B) conformers of  $[P_2Se_8]^{2-}$ .**

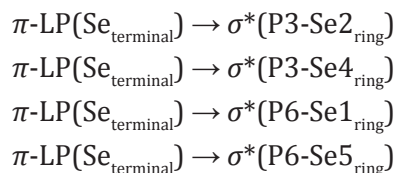
	<i>chair</i> - $[P_2Se_8]^{2-}$ (A)	<i>twist</i> - $[P_2Se_8]^{2-}$ (B)
Se, terminal	axial: -0.62 equatorial: -0.68	-0.66
Se, ring	-0.10	-0.09
P	+0.50	0.50

**Table 8. Computational details for the chair (A) and twist (B) conformers of  $P_2Se_8^{2-}$ .**

	<i>chair</i> - $[P_2Se_8]^{2-}$ (A)	<i>twist</i> - $[P_2Se_8]^{2-}$ (B)
symmetry	$C_{2h}$	$D_2$
$-E$ / a.u.	757.652644	757.657825
$E_{rel.}$ / kcal mol <sup>-1</sup>	+ 3.3	0.0
NIMAG <sup>a</sup>	0	0
$zpe$ <sup>b</sup> / kcal mol <sup>-1</sup>	5.6	5.7
<b><math>\nu</math> IR / Raman / cm<sup>-1c</sup> (intensity)<sup>d</sup></b>		
$d(Se_{term}-P)$ [X-ray] / Å	2.25 (ax.), 2.29 (eq.) [2.10 (ax.), 2.14 (eq.)]	2.27 [2.13]
$d(Se_{ring}-P)$ [X-ray] / Å	2.54 [2.27]	2.54 [2.29]
$d(Se-Se)$ [X-ray] / Å	2.43 [2.34]	2.42 [2.32]
$\angle(Se_{term}-P-Se_{term})$ [X-ray] / °	122.4 [124.2]	120.3 [120.2]
$\angle(Se_{term}-P-Se_{ring})$ [X-ray] / °	114.5 (ax.), 101.8 (eq.) [113.7, 99.0]	101.8, 116.0 [99.3, 115.5]
$\angle(P-Se_{ring}-Se_{ring})$ [X-ray] / °	107.2 [103.0]	106.7 [102.6]
$\nu_{as}(Se_{ring}-Se_{ring})$	234 (2 / 0)	238 (1 / 11)
$\nu_{sym}(Se_{ring}-Se_{ring})$	244 (0 / 9)	250 (0 / 3)
$\nu_{as}(Se_{ring}-P)$	254 (0 / 38)	253 (1 / 14)
$\nu_{sym}(Se_{ring}-P)$	282 (45 / 0)	288 (34 / 4)
$\delta_{as}(Se_{terminal}-P)$	326 (237 / 0)	333 (270 / 6)
$\delta_{sym}(Se_{terminal}-P)$	335 (0 / 17)	343 (0 / 12)
$\nu_{sym}(Se_{terminal}-P)$	428 (168 / 0)	417 (162 / 16)
$\nu_{as}(Se_{terminal}-P)$	429 (0 / 55)	421 (3 / 39)

a) number of imaginary frequencies; b) zero point energy; c) only vibrations with  $\nu > 200$  cm<sup>-1</sup> have been included into the table; d) IR intensities in km mol<sup>-1</sup>; Raman activities in Å<sup>4</sup> amu<sup>-1</sup>.

For the twist conformer, there are again four energetically identical intramolecular donor–acceptor interactions:

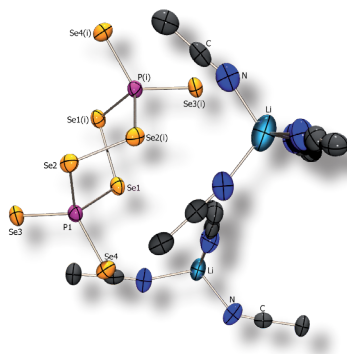


In this case, all four terminal Se atoms donate lone-pair  $\pi$  electron density into the antibonding  $\sigma^*(\text{P-Se}_{\text{ring}})$  bonds, which results in larger ( $116.0^\circ$  and  $116.7^\circ$ ; Table 8)  $\text{Se}_{\text{terminal}}\text{-P-Se}_{\text{ring}}$  angles. The donor–acceptor interaction energies were all calculated to be  $18.5 \text{ kcal mol}^{-1}$  each. The computed NBO natural charges are also summarized in Table 7.

## 6 Conclusion

Starting from readily available reagents and following the synthetic routes described in this study, stable and in common organic solvents soluble salts of the selenophosphate anion  $\text{P}_2\text{Se}_8^{2-}$  become available in preparatively useful quantities. The availability of  $\text{P}_2\text{Se}_8^{2-}$  salts on a large scale opens the door to a systematic study of its coordination chemistry, which might lead to new transition metal selenophosphate based materials prepared by “wet” synthesis under kinetically controlled conditions, and which is under current investigation in our laboratory. The synthetic strategies applied for the synthesis of the  $\text{P}_2\text{Se}_8^{2-}$  salts, and in particular the use of ionic liquids, provide useful methods for the preparation of selenophosphates in general.

The X-ray crystallographic studies on  $[\text{Li}(\text{py})_4]_2[\text{P}_2\text{Se}_8]$ ,  $[\text{bmim}]_2[\text{P}_2\text{Se}_8]$ , and  $[\text{Li}(\text{MeCN})_4]_2[\text{P}_2\text{Se}_8]$  demonstrate the mobility of the system investigated. Small changes in the cation and in the crystallization conditions are sufficient to stabilize the chair conformer of  $\text{P}_2\text{Se}_8^{2-}$  in the solid state, which is found in most cases, although the twist conformer predominates in solution. The results indicate only small energy differences between the conformations of the  $\text{P}_2\text{Se}_8^{2-}$  anion, and this is supported by quantum chemical calculations.



## 7 Experimental Section

**General.** All reactions were carried out under an inert gas atmosphere using Schlenk techniques. Argon (Messer Griesheim, purity 4.6 in 50 L steel cylinder) was used as an inert gas. The glass vessels used were stored in a 130 °C drying oven. Before use, the glass vessels were flame-dried in a vacuum at  $10^{-3}$  mbar.

$P_4Se_3$ , the alkali metal selenides, and 1-butyl-3-methylimidazolium rhodanide were prepared as described in the literature and stored in a dry box under a nitrogen atmosphere.<sup>14,15,16</sup> Elemental selenium and lithium were used as received (Aldrich). The solvents were dried using commonly known methods and were freshly distilled before use.

Melting points were determined in capillaries using a Büchi B540 instrument and are uncorrected.

**NMR Spectroscopy.** NMR spectra were recorded using a Jeol EX 400 Eclipse instrument operating at 161.997 MHz ( $^{31}P$ ), 76.321 MHz ( $^{77}Se$ ), and 155.526 MHz ( $^7Li$ ) and a Jeol GSX 270 Delta Eclipse instrument operating at 109.365 MHz ( $^{31}P$ ) and 51.525 MHz ( $^{77}Se$ ). Chemical shifts are referred to 85 %  $H_3PO_4$  ( $^{31}P$ ),  $(CH_3)_2Se$  ( $^{77}Se$ ), and 0.1 M solution of LiCl in  $D_2O$  ( $^7Li$ ) as external standards. All spectra were measured, if not mentioned otherwise, at 25 °C. The %-data correspond to the intensities in the  $^{31}P$  NMR spectra with respect to the total intensity. The difference to 100 % belongs to not determinable signals. For the simulation of the  $^{31}P$  NMR spectra, the PERCH program package was used.<sup>17</sup>

**X-ray Crystallography.** The molecular structures in the crystalline state were determined using an Oxford Xcalibur3 diffraction instrument equipped with a Spellman generator (voltage 50 kV, current 40 mA) and a Kappa CCD detector with an X-ray radiation wavelength of 0.71073 Å ( $MoK_{\alpha}$ ). The data collection was performed with the CrysAlis CCD software and the data reduction with the CrysAlis RED software.<sup>18,19</sup> The structures were solved with SIR-92, SIR-97, and SHELXS-97 and

<sup>14</sup> (a) Stoppioni, P.; Peruzzini, M. *Gazz. Chim. Ital.* **1988**, *118*, 581. (b) Schön, O. Ph.D. Thesis, LMU Munich, Munich, Germany, 2007.

<sup>15</sup> (a) Thompson, D. P.; Boudjouk, P. *J. Org. Chem.* **1988**, *53*, 2109. (b) Schuster, M. Ph.D. Thesis, LMU Munich, Munich, Germany, 1999.

<sup>16</sup> (a) Dyson, P. J.; Gossel, M. C.; Srinivasan, N.; Vine, T.; Welton, T.; Williams, D. J.; White, A. J. P.; Zigras, T. *J. Chem. Soc., Dalton Trans.* **1997**, 3465. (b) Kamal, A.; Chouhan, G. *Tetrahedron Lett.* **2005**, *46*, 1489.

<sup>17</sup> Laatikainen, R.; Niemitz, M.; Weber, U.; Sundelin, T.; Hasinen, T.; Vepsäläinen, J. *J. Magn. Reson. A* **1996**, *120*, 1.

<sup>18</sup> CrysAlis CCD, version 1.171.27p5 beta (release 01–04–2005 CrysAlis171.NET; compiled Apr 1 2005, 17:53:34); Oxford Diffraction Ltd.: Oxfordshire, U.K.

<sup>19</sup> CrysAlis RED, version 1.171.27p5 beta (release 01–04–2005 CrysAlis171.NET; compiled Apr 1 2005, 17:53:34); Oxford Diffraction Ltd.: Oxfordshire, U.K.

refined with SHELXL97 and finally checked using PLATON.<sup>20,21,22,23,24</sup> The absorptions were corrected by a SCALE3 ABSPACK multiscan method.<sup>25</sup> All relevant data and parameters of the X-ray measurements and refinements are given in Table 8. Further information on the crystal structure determinations has been deposited with the Cambridge Crystallographic Data Centre as supplementary publication numbers 654161 (1), 654159 (2), 654162 (3), and 654160 (4).

**[Li(py)<sub>4</sub>]<sub>2</sub>[P<sub>2</sub>Se<sub>8</sub>] (1).** P<sub>4</sub>Se<sub>3</sub> (1.443 g, 4 mmol), lithium powder (111.1 mg, 16 mmol), and grey selenium (2.842 g, 36 mmol) in 8 mL of pyridine were stirred for 24 h. From the resulting yellow suspension, the solid was separated by filtration using a G4 frit. The yellow solution was stored at room temperature. After three days, yellow crystals of [Li(py)<sub>4</sub>]<sub>2</sub>[P<sub>2</sub>Se<sub>8</sub>] were formed, which were separated by filtration and dried in vacuo. Yield: 2.9 g (90 % with respect to P<sub>4</sub>Se<sub>3</sub>).

Alternatively, red phosphorus (62 mg, 2 mmol), lithium powder (14 mg, 2 mmol), and gray selenium (632 mg, 8 mmol) were heated in a glass flask for 24 h at 240 °C. After cooling to room temperature, the orange-red solid was dissolved in 10 mL of pyridine yielding an orange solution. The solution was stored at room temperature. After five days, yellow crystals of [Li(py)<sub>4</sub>]<sub>2</sub>[P<sub>2</sub>Se<sub>8</sub>] were obtained. Yield: 1.89 g (71 % with respect to P<sub>4</sub>Se<sub>3</sub>).

m.p.: 108 – 110 °C.

<sup>31</sup>P{<sup>1</sup>H} NMR (pyridine): δ = – 89.8 (*chair*-P<sub>2</sub>Se<sub>8</sub><sup>2-</sup>, 21 %), – 4.5 (*twist*-P<sub>2</sub>Se<sub>8</sub><sup>2-</sup>, 79 %).

<sup>77</sup>Se{<sup>1</sup>H} NMR (pyridine): δ = 241.8 (Se<sub>exo</sub>, *chair*-P<sub>2</sub>Se<sub>8</sub><sup>2-</sup>, <sup>1</sup>J<sub>SeP</sub> = 604 Hz), 390.0 (Se<sub>exo</sub>, *chair*-P<sub>2</sub>Se<sub>8</sub><sup>2-</sup>, <sup>1</sup>J<sub>SeP</sub> = 733 Hz), 453.7 (Se<sub>exo</sub>, *twist*-P<sub>2</sub>Se<sub>8</sub><sup>2-</sup>, <sup>1</sup>J<sub>SeP</sub> = 659 Hz), 762.2 (Se<sub>endo</sub>, *twist*-P<sub>2</sub>Se<sub>8</sub><sup>2-</sup>, <sup>1</sup>J<sub>SeP</sub> = 372 Hz, <sup>2</sup>J<sub>SeP</sub> = 33 Hz), 910.0 (Se<sub>endo</sub>, *chair*-P<sub>2</sub>Se<sub>8</sub><sup>2-</sup>, <sup>1</sup>J<sub>SeP</sub> = 348 Hz).

<sup>7</sup>Li{<sup>1</sup>H} NMR (pyridine): δ = 5.5.

**[nBu<sub>4</sub>N]<sub>2</sub>[P<sub>2</sub>Se<sub>8</sub>]·2 MeCN (2).** P<sub>4</sub>Se<sub>3</sub> (1.303 g, 3.6 mmol), Li<sub>2</sub>Se<sub>2</sub> (1.293 g, 7.2 mmol), and grey selenium (2.567 g, 32.5 mmol) in 40 mL of acetonitrile were stirred at room temperature. After three days, a red reaction solution and small amounts of a dark solid (probably unreacted elemental selenium) were obtained. The dark solid

<sup>20</sup> SIR-92, A Program for Crystal Structure Solution: Altomare, A.; Cascarano, G. L.; Giacovazzo, C.; Guagliardi, A. *J. Appl. Crystallogr.* **1993**, *26*, 343.

<sup>21</sup> Altomare, A.; Burla, M. C.; Camalli, M.; Cascarano, G. L.; Giacovazzo, C.; Guagliardi, A.; Moliterni, A. G. G.; Polidori, G.; Spagna, R. *J. Appl. Crystallogr.* **1999**, *32*, 115.

<sup>22</sup> Sheldrick, G. M. *SHELXS-97, Program for Crystal Structure Solution*; Universität Göttingen: Göttingen, Germany, 1997.

<sup>23</sup> Sheldrick, G. M. *SHELXL-97, Program for the Refinement of Crystal Structures*; University of Göttingen: Göttingen, Germany, 1997.

<sup>24</sup> Spek, L. A. *PLATON, A Multipurpose Crystallographic Tool*; Utrecht University: Utrecht, The Netherlands, 1999.

<sup>25</sup> SCALE3 ABSPACK – An Oxford Diffraction program (1.0.4, gui:1.0.3); Oxford Diffraction Ltd.: Oxfordshire, U.K., 2005.

was removed using a G4 frit. A solution of  $nBu_4NBr$  (4.6 g, 14.3 mmol) in 20 mL of acetonitrile was added to the filtrate, and the resulting mixture was stored at room temperature. Within 24 h, yellow crystals of  $[nBu_4N]_2[P_2Se_8] \cdot 2MeCN$  formed, which were separated using a G3 frit, washed with  $3 \times 5$  mL of cold acetonitrile and dried under vacuum. Yield: 5 g (91%, with respect to  $P_4Se_3$ ).

Alternatively,  $P_4$  (1.92 g, 15.5 mmol),  $Li_2Se_2$  (5.32 g, 31.0 mmol), and gray selenium (14.48 g, 186 mmol) in 60 mL of acetonitrile were stirred at room temperature. After five days, a red-brown solution over a dark gray solid (probably unreacted elemental selenium) was formed. The solid was removed by filtration using a G4 frit. Subsequently, a solution of  $nBu_4NBr$  (19.65 g, 60.95 mmol) in 40 mL of acetonitrile was added to the yellow filtrate, and the reaction mixture was stored at room temperature. Within one day, yellow crystals of  $[nBu_4N]_2[P_2Se_8] \cdot 2MeCN$  were formed, which were separated via a G3 frit, washed with  $2 \times 3$  mL of cold acetonitrile and dried under vacuum. Yield: 22.3 g (87 % with respect to  $P_4Se_3$ ).

m.p.: 99-101 °C.

$^{31}P\{^1H\}$  NMR ( $CH_3CN$ ):  $\delta = -4.5$  (*twist*- $P_2Se_8^{2-}$ , 78 %),  $-89.8$  (*chair*- $P_2Se_8^{2-}$ , 22 %).

$^{77}Se\{^1H\}$  NMR ( $CH_3CN$ ):  $\delta = 242.0$  ( $Se_{exo}$ , *chair*- $P_2Se_8^{2-}$ ,  $^1J_{SeP} = 604$  Hz),  $390.0$  ( $Se_{exo}$ , *chair*- $P_2Se_8^{2-}$ ,  $^1J_{SeP} = 733$  Hz),  $453.6$  ( $Se_{exo}$ , *twist*- $P_2Se_8^{2-}$ ,  $^1J_{SeP} = 659$  Hz),  $762.2$  ( $Se_{endo}$ , *twist*- $P_2Se_8^{2-}$ ,  $^1J_{SeP} = 372$  Hz,  $^2J_{SeP} = 33$  Hz),  $910.3$  ( $Se_{endo}$ , *chair*- $P_2Se_8^{2-}$ ,  $^1J_{SeP} = 348$  Hz,  $^2J_{SeP} = 33$  Hz).

Anal. Calcd for  $C_{36}H_{78}N_4P_2Se_8$ : C, 34.79; H, 6.24; N, 4.44. Found: C, 34.83; H, 6.27; N 4.39.

**[bmim] $_2$ [P $_2$ Se $_8$ ] (3).**  $P_4Se_3$  (360 mg, 1 mmol)  $Na_2Se_2$  (815 mg, 4 mmol), and grey selenium (711 mg, 9 mmol) in 1-butyl-3-methylimidazolium thiocyanate (10 mL) were stirred for 12 h at room temperature. During this time, the reagents dissolved completely and an orange solution was obtained. From this solution, orange crystals of  $[bmim]_2[P_2Se_8]$  separated after one day, which were isolated by filtration, washed with 7 mL of cold  $CH_2Cl_2$ , and dried in vacuo. Yield: 261 mg (54 % with respect to  $P_4Se_3$ ).

m.p.: 109-112 °C.

---

**[Li(MeCN)<sub>4</sub>]<sub>2</sub>[P<sub>2</sub>Se<sub>8</sub>] (4)**. P<sub>4</sub>Se<sub>3</sub> (1.443 g, 4 mmol), Li<sub>2</sub>Se (742.7 mg, 8 mmol), and gray selenium (2.21 g, 28 mmol) in 8 mL of acetonitrile were stirred at room temperature for a period of 12 h. The red-brown suspension was filtrated using a G4 frit, and to the orange clear filtrate was added a spatula-point of CuCl. The solution turned red and was stored in the fridge at +4 °C. After one day, [Li(MeCN)<sub>4</sub>]<sub>2</sub>[P<sub>2</sub>Se<sub>8</sub>] separated as yellow crystals. Yield: 1.21 g (58 % with respect to P<sub>4</sub>Se<sub>3</sub>).

m.p.: 14–16 °C.

<sup>31</sup>P{<sup>1</sup>H} NMR (MeCN): δ = - 4.5 (*twist*, 58 %), - 89.8 (*chair*, 14 %) ppm.

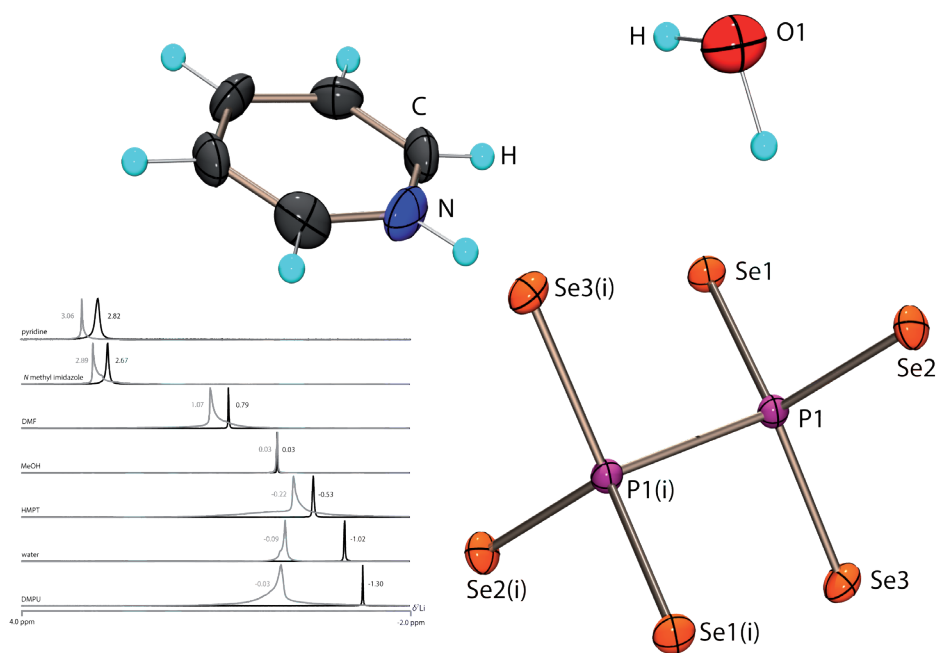
Table 8. Crystal and refinement Data.

	[Li(py) <sub>4</sub> ] <sub>2</sub> [P <sub>2</sub> Se <sub>8</sub> ] (1)	[(nBu) <sub>4</sub> N] <sub>2</sub> [P <sub>2</sub> Se <sub>8</sub> ] · 2 MeCN (2)	[C <sub>8</sub> H <sub>15</sub> N <sub>2</sub> ] <sub>2</sub> [P <sub>2</sub> Se <sub>8</sub> ] (3)	[Li(MeCN) <sub>4</sub> ] <sub>2</sub> [P <sub>2</sub> Se <sub>8</sub> ] (4)
empirical formula	C <sub>20</sub> H <sub>20</sub> LiN <sub>4</sub> PSe <sub>4</sub>	C <sub>36</sub> H <sub>78</sub> N <sub>4</sub> P <sub>2</sub> Se <sub>8</sub>	C <sub>8</sub> H <sub>15</sub> N <sub>2</sub> P <sub>2</sub> Se <sub>4</sub>	C <sub>16</sub> H <sub>24</sub> Li <sub>2</sub> N <sub>8</sub> P <sub>2</sub> Se <sub>8</sub>
formula mass	670.15	1260.67	486.03	1035.93
temp (K)	200	200	100	100
cryst. size (mm)	0.2 x 0.1 x 0.05	0.3 x 0.3 x 0.2	0.25 x 0.2 x 0.15	0.3 x 0.2 x 0.2
cryst. descriptn.	yellow rod	yellow rod	orange block	yellow rod
cryst. system	triclinic	monoclinic	monoclinic	orthorhombic
space group	<i>P</i> -1	<i>P</i> 2 <sub>1</sub> / <i>c</i>	<i>P</i> 2 <sub>1</sub> / <i>n</i>	<i>Pbam</i>
<i>a</i> (Å)	10.1582(8)	9.6284(5)	7.6642(10)	20.0535(6)
<i>b</i> (Å)	10.7716(8)	16.9553 (8)	10.9948(2)	12.1200(5)
<i>c</i> (Å)	12.7499(10)	16.0899(7)	17.0380(3)	15.0831(6)
<i>α</i> (deg)	95.271(6)	90	90	90
<i>β</i> (deg)	94.847(6)	96.875(4)	91.211(2)	90
<i>γ</i> (deg)	114.219(7)	90	90	90
<i>V</i> (Å <sup>3</sup> )	1255.40(17)	2607.8(2)	1435.41(4)	3665.9(2)
<i>Z</i>	2	2	4	4
$\rho_{\text{calc}}$ (g cm <sup>-3</sup> )	1.773	1.605	2.249	1.877
$\mu$ (mm <sup>-1</sup> )	5.922	5.694	10.308	8.081
<i>F</i> (000)	644	1248	912	1936
$\vartheta$ range (deg)	3.98-30.06	4.01-27.50	3.71-27.50	3.76-26.00
index ranges	-14 ≤ <i>h</i> ≤ 14, -15 ≤ <i>k</i> ≤ 15, -17 ≤ <i>l</i> ≤ 17	-12 ≤ <i>h</i> ≤ 12, -22 ≤ <i>k</i> ≤ 22, -20 ≤ <i>l</i> ≤ 20	-9 ≤ <i>h</i> ≤ 9, -14 ≤ <i>k</i> ≤ 14, -22 ≤ <i>l</i> ≤ 22	-24 ≤ <i>h</i> ≤ 24, -14 ≤ <i>k</i> ≤ 14, -18 ≤ <i>l</i> ≤ 18
reflcs collcd	17142	29439	15990	35613
reflcs obsd	2885	4638	2547	3427
reflcs unique	7312 ( <i>R</i> <sub>int</sub> = 0.0792)	5975 ( <i>R</i> <sub>int</sub> = 0.0730)	3287 ( <i>R</i> <sub>int</sub> = 0.0337)	3732 ( <i>R</i> <sub>int</sub> = 0.1607)
<i>R</i> <sub>1</sub> , <i>wR</i> <sub>2</sub> (2 $\sigma$ data)	0.0481, 0.0534	0.0409, 0.0677	0.0281, 0.0715	0.1075, 0.1295
<i>R</i> <sub>1</sub> , <i>wR</i> <sub>2</sub> (all data)	0.1739, 0.0802	0.0649, 0.0770	0.0425, 0.0763	0.1207, 13.42
max/min transm	1.1604/0.7733	1.1938/0.7294	1.0000/0.7163	0.8572/0.4122
data/restr/params	7312/0/271	5975/0/227	3287/0/136	3732/0/190
<i>S</i> on <i>F</i> <sup>2</sup>	0.897	1.060	1.160	1.364
larg. diff peak/ hole (e/Å)	0.556/-0.439	0.616/-0.447	1.176/-0.658	1.535/-0.655



## CHAPTER IX

### A Waterstable Selenophosphate Anion: $P_2Se_6^{4-}$

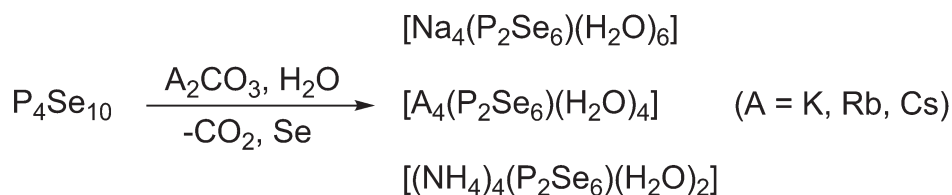


A new structure of the  $P_2Se_6^{4-}$  anion as well as  $^7Li$  NMR spectroscopical investigations on  $[Li(py)_2]_4[P_2Se_6] \cdot 2 py$  are presented. The  $P_2Se_6^{4-}$  anion is remarkably stable in water.

## 1 Introduction

One of the few selenophosphate well known anions is the hexaselenohypodiphosphate anion  $P_2Se_6^{4-}$ . Transition metal salts of this anion (e.g.  $K_2MgP_2Se_6$  or  $Cd_2P_2Se_6$  salts) have been the subject of extensive investigations due to their interesting physical properties like photoconductivity or ferroelectricity. Most of the contributions to the chemistry of the hexaselenohypodiphosphate anion originate from solid state chemistry.<sup>1</sup> Typical syntheses of metal hexaselenohypodiphosphates involve reaction of the elements (the metal, red phosphorus and elemental selenium) at high temperatures resulting in the formation of thermodynamically favoured modifications of the corresponding salts. Alkali metal hexaselenohypodiphosphates and, in particular, the lithium salt are of current interest due to possible ion conductivity. In the case of the lithium salt it might be of interest as a material for lithium ion batteries.<sup>1</sup>

However, no syntheses of metal hexaselenohypodiphosphates in solution have been described in the literature. The only exception is the recently reported reaction of  $P_4Se_{10}$  glass with metal carbonates in water, resulting in the formation of  $[Na_4(P_2Se_6)(H_2O)_6]$ ,  $[A_4(P_2Se_6)(H_2O)_4]$  ( $A = K, Rb, Cs$ ) and  $[(NH_4)_4(P_2Se_6)(H_2O)_2]$  (Scheme 1).<sup>2</sup>



Scheme 1. Synthesis of  $A_4P_2Se_6$  [ $A = Na, K, Rb, Cs, NH_4$ ] according to literature.<sup>1</sup>

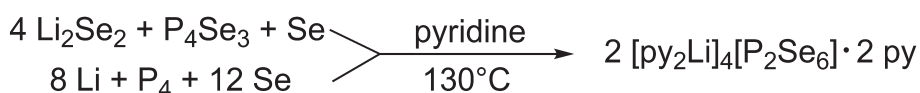
The use of water as reaction medium causes always the formation of toxic  $H_2Se$ . Therefore the development of a general synthesis of metal hexaselenohypodiphosphates in solution, avoiding protic solvents, would be highly desirable. The results of our current investigations in this respect are presented below.

<sup>1</sup> (a) X. Bourdon, A.-R. Grimmer, V. B. Cajipe *Chem. Mater.* **1999**, *11*, 2680. (b) J. D. Breshears, M. G. Kanatzidis *J. Am. Chem. Soc.* **2000**, *122*, 7839. (c) A. Carnabuci, V. Grasso, L. Silipigni *J. Appl. Phys.* **2001**, *90*(9), 4526. (d) P. M. Briggs-Piccoli, K. D. Abney, P. K. Dorhout *J. Nucl. Sci. Technol.* **2002**, *3*, 611. (e) S. Jörgens, A. Mewis, R.-D. Hoffmann, R. Pöttgen, B. D. Mosel *Z. Anorg. Allg. Chem.* **2003**, *629*, 429. (f) S. Jörgens, A. Mewis *Z. Anorg. Allg. Chem.* **2004**, *630*, 51. (g) J. A. Aitken, M. Evain, L. Iordanidis, M. G. Kanatzidis *Inorg. Chem.* **2002**, *41*(2), 180.

<sup>2</sup> Rothenberger, A.; Malliakas, C. D.; Kanatzidis, M. G. *Z. Anorg. Allg. Chem.* **2009**, 635.

## 2 Syntheses

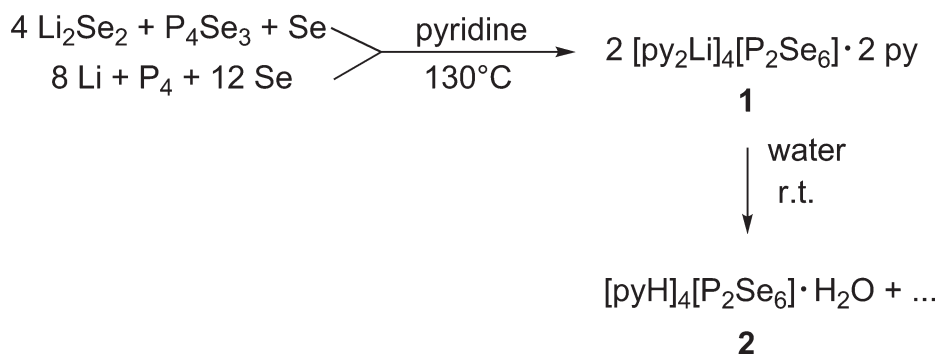
Alkali metal salts of the  $P_2Se_6^{4-}$  anion can be prepared in solution under mild conditions (20 – 130 °C) starting from the corresponding alkali metal diselenide  $M_2Se_2$  ( $M = Li, Na$ ),  $P_4Se_3$  and elemental selenium or alternatively using the elements (the alkali metals, white phosphorus and grey selenium) as educts. A polar and preferably basic solvent like pyridine, *N*-methyl imidazole, THF or DMPU is required (Scheme 2).<sup>3</sup>



Scheme 2. Syntheses of  $P_2Se_6^{4-}$  anion ( $M = Li, Na$ ).

The lithium salt  $[Li(py)_2]_4[P_2Se_6] \cdot 2 py$  is readily obtained in form of yellow crystals on keeping the reaction solution (in pyridine) at ambient temperature over night. The best solvent for **1** is water. In contrast to our expectations the  $P_2Se_6^{4-}$  anion resulted, is remarkably stable towards hydrolysis. A solution of **1** in water shows after three days no indication of hydrolysis in  $^{31}P$  NMR. This unexpected stability is important for the possible use of salts of  $P_2Se_6^{4-}$  in drugs as source of selenium when healing diseases caused by selenium deficiency. It also enabled us to determine the complete  $^{31}P$  and  $^{77}Se$  NMR spectroscopical data of the  $P_2Se_6^{4-}$  anion, which are reported here for the first time (see below).<sup>3</sup>

From the water solution single crystals of the hitherto unknown pyridinium salt  $[pyH]_4[P_2Se_6] \cdot H_2O$ , were obtained. The structure of the salt was determined by single crystal X-ray diffraction (Scheme 3). Compound **2** is remarkably stable in water at +4 °C for several months.



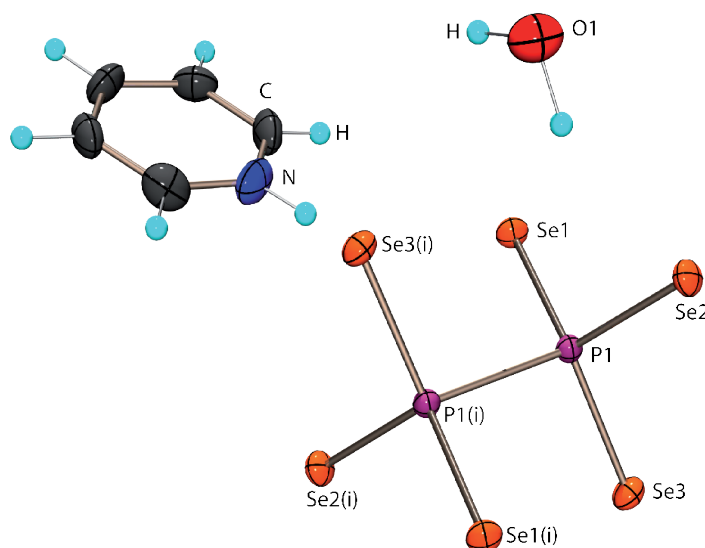
Scheme 3. Syntheses of **1** and **2**.

<sup>3</sup> Schuster, M. *dissertation*, LMU Munich, 1999.

### 3 [pyH]<sub>4</sub>[P<sub>2</sub>Se<sub>6</sub>] • H<sub>2</sub>O (2)

Yellow single crystals of [pyH]<sub>4</sub>[P<sub>2</sub>Se<sub>6</sub>] • H<sub>2</sub>O (**2**) were obtained from a water solution of **1** after 2 days standing at room temperature. Compound **2** crystallizes in the monoclinic space group  $P2_1/c$  with four formula units in the unit cell (Figure 1).

The crystal structure consists of isolated P<sub>2</sub>Se<sub>6</sub><sup>4-</sup> anions and pyH<sup>+</sup> cations (Figure 1). The P<sub>2</sub>Se<sub>6</sub><sup>4-</sup> anion adopts an ethan like conformation. Its structural parameters do not deviate much from those of other salts reported in literature.<sup>1</sup> Despite the presence of water molecules and pyH<sup>+</sup> cations in the crystal no hydrogen bonds were found between the P<sub>2</sub>Se<sub>6</sub><sup>4-</sup> anions and the water molecules or the pyH<sup>+</sup> cations. To the best of my knowledge, this is the first time that the P<sub>2</sub>Se<sub>6</sub><sup>4-</sup> anions are observed in the solid state without any coordination to the cation.

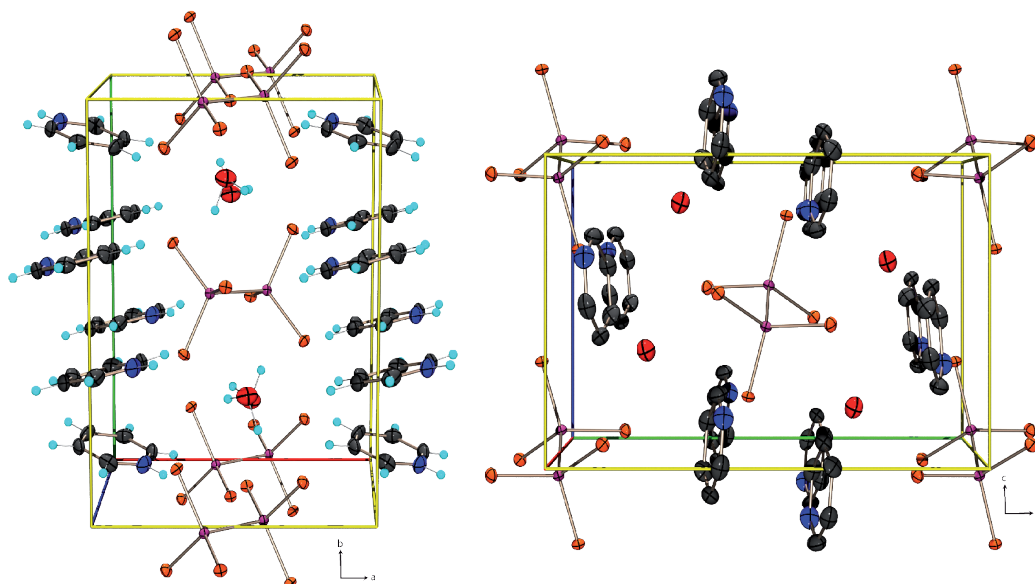


**Figure 1.** Molecular structure of **2** in the crystal. View along *c* axis. Ellipsoids are drawn with 50 % probability level.  $i = 1-x, 1-y, 1-z$ .

There are separated anion – and cation stacks staggered along the *b* axis. The solvent molecule H<sub>2</sub>O is localized between the anion layers. Only electrostatic interactions between the pyH<sup>+</sup> cations and the P<sub>2</sub>Se<sub>6</sub><sup>4-</sup> anions can be observed within the unit cell (Figure 2).

Table 1. Selected bond distances [pm], bond – and torsion angles [°].  $i = 1-x, 1-y, 1-z$ .

Bond lengths [pm]		Bond angles [°]		Torsion angles [°]	
Se1-P1	218.4(1)	Se1-P1-Se2	113.8(1)	Se1-P1-P1( <i>i</i> )-Se1( <i>i</i> )	180.0(1)
Se2-P1	218.5(1)	Se1-P1-Se3	112.2(1)	Se1-P1-P1( <i>i</i> )-Se2( <i>i</i> )	58.3(1)
Se3-P1	217.9(1)	Se2-P1-Se3	110.2(1)	Se1-P1-P1( <i>i</i> )-Se3( <i>i</i> )	-60.5(1)
P1-P1( <i>i</i> )	227.3(1)	Se1-P1-P1( <i>i</i> )	104.9(1)	Se2-P1-P1( <i>i</i> )-Se1( <i>i</i> )	-58.3(1)
		Se2-P1-P1( <i>i</i> )	108.1(1)	Se2-P1-P1( <i>i</i> )-Se2( <i>i</i> )	180.0(1)
		Se3-P1-P1( <i>i</i> )	107.4(1)	Se2-P1-P1( <i>i</i> )-Se3( <i>i</i> )	61.2(1)
				Se3-P1-P1( <i>i</i> )-Se1( <i>i</i> )	60.5(1)
				Se3-P1-P1( <i>i</i> )-Se2( <i>i</i> )	-61.2(1)
				Se3-P1-P1( <i>i</i> )-Se3( <i>i</i> )	-180.0(1)

Figure 2. Unit cell of 2. View along the  $c$  axis (left) and along the  $a$  axis (right, hydrogen atoms are omitted for clarity). Thermal ellipsoids of all non hydrogen atoms are drawn at 50 % probability level.

#### 4 $^{31}\text{P}$ and $^{77}\text{Se}$ Heteronuclear NMR Spectroscopy

The hexaselenohypodiphosphate anion  $\text{P}_2\text{Se}_6^{4-}$  could be characterized via  $^{31}\text{P}$  – and  $^{77}\text{Se}$  NMR spectroscopy in solution. The compound consists of two isochrone phosphorus atoms causing a singlet in the  $^{31}\text{P}$  NMR spectrum for the isotopomer without  $^{77}\text{Se}$  nuclei.<sup>3</sup>

The isotopomer with one NMR active  $^{77}\text{Se}$  nucleus causes an AA'X spin system as the two phosphorus atoms are now magnetically inequivalent. The P,Se coupling constants as well as the P,P coupling constant could be obtained. The  $^1J_{\text{PP}}$  coupling constant is – 210 Hz which is within the range of other known  $^1J_{\text{PP}}$  coupling constants. The  $^1J_{\text{SeP}}$  coupling constant is – 532 Hz which is in between the values for  $^1J_{\text{SeP}}$  coupling constants for one and two coordinated selenium atoms. The  $^2J_{\text{SeP}}$  coupling constant is 9 Hz. Besides the isotopomer with one  $^{77}\text{Se}$  nuclei, the isotopomers with two  $^{77}\text{Se}$  nuclei could also be observed in the  $^{31}\text{P}$  NMR spectrum. The isotopomer where each of the two  $^{77}\text{Se}$  nuclei are bounded to one phosphorus atom cause an AA'XX' spin system. The isotopomer where both  $^{77}\text{Se}$  nuclei are bounded to one phosphorus atom could also be observed in the  $^{31}\text{P}$  NMR spectrum but with less intensity.<sup>3</sup>

The  $^{77}\text{Se}$  NMR spectrum consists mainly of the isotopomer with one  $^{77}\text{Se}$  nuclei (81.31 %) causing the X part of the AA'X spin system. The isotopomer, in which two  $^{77}\text{Se}$  atoms are bonded to two different phosphorus atoms gives the  $^3J_{\text{SeSe}}$  coupling constant which is 11.8 Hz and thus remarkably high.<sup>3</sup>

The  $^{31}\text{P}$  NMR chemical shift of the  $\text{P}_2\text{Se}_6^{4-}$  anion in solutions of compound **1** depends strongly on the solvent used. The phosphorus NMR signal is shifted to lower field in the series of solvents  $\text{H}_2\text{O}$ , MeOH, HMPT, DMPU, pyridine, *N*-methyl imidazole, 2-methyl pyridine and DMF (Table 2).<sup>3</sup>

One reason for this rather huge change in the  $^{31}\text{P}$  NMR chemical shift ( $\Delta\delta = 15$ ) might be the coordination of the lithium cations by the solvent used, which would destroy the  $\text{Li}_4\text{P}_2\text{Se}_6$  clusters found for the solid state. Therefore, the  $^7\text{Li}$  NMR spectra of solutions of compound **1** in different solvents as well as the  $^7\text{Li}$  NMR spectra of LiCl in the same solvents for comparison were measured. First results are presented in Table 2 and Figure 4.

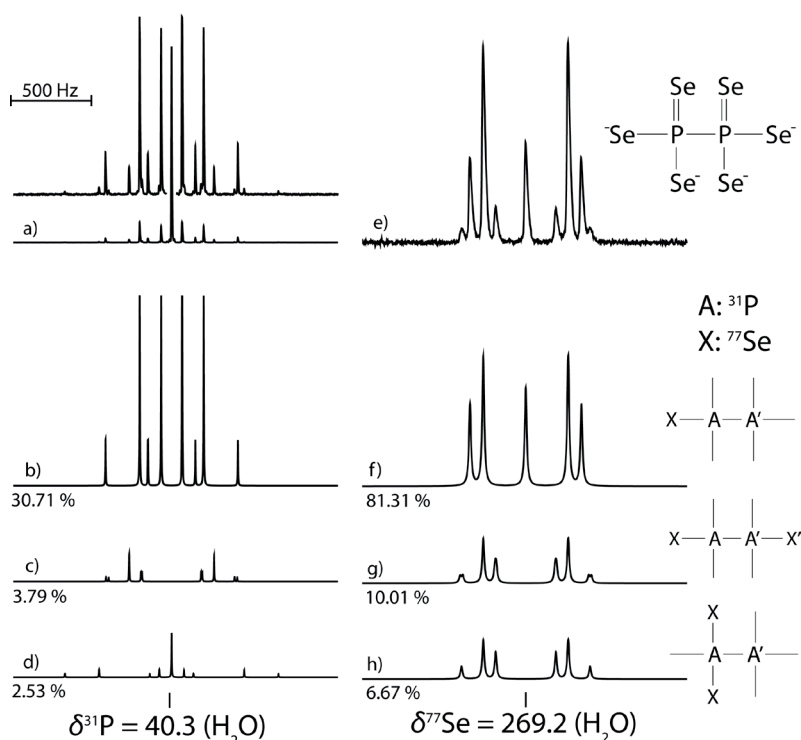


Figure 3.  $^{31}P\{^1H\}$  and  $^{77}Se\{^1H\}$  NMR spectra of  $P_2Se_6^{4-}$ : (a) observed  $^{31}P$  NMR spectrum in  $D_2O$  (0.3 M, 1655 scans, 40 min measuring time); (b) calculated  $^{31}P$  NMR spectrum for the isotopomer with one  $^{77}Se$  nucleus; (c and d) calculated  $^{31}P$  NMR spectra for the isotopomers with two  $^{77}Se$  nuclei; (e) observed  $^{77}Se$  NMR spectrum in  $D_2O$  (0.3 M, 60000 scans, 18 h measuring time); (f) calculated  $^{77}Se$  NMR spectrum for the isotopomer with one  $^{77}Se$  nucleus; (g and h) calculated  $^{77}Se$  NMR spectra for the isotopomers with two  $^{77}Se$  nuclei.<sup>3</sup>

Table 2.  $^{31}P$  and  $^7Li$  NMR chemical shifts of  $P_2Se_6^{4-}$  and  $^7Li$  NMR chemical shifts of  $LiCl$  in different solvents.

Solvent	$\delta^{31}P$	$\delta^7Li$	$\delta^7Li$ (LiCl)	$\Delta\delta^7Li$
water	40.3	-1.02	-0.09	-0.93
HMPT	50.3	-0.53	-0.22	-0.31
DMPU	52.1	-1.30	-0.03	-1.27
pyridine	52.3	2.82	3.06	-0.24
<i>N</i> -methyl imidazole	52.6	2.67	2.89	-0.22
DMF	55.3	0.79	1.07	-0.28

In all cases  $\delta^7Li$  of the salt  $[Li(py)_2]_4[P_2Se_6] \cdot 2 py$  is at higher field compared to  $\delta^7Li$  of  $LiCl$  in the same solvent. The difference  $\Delta\delta^7Li$  are largest in the case of DMPU and water and smallest in the case of *N*-methyl imidazole and pyridine. Further investigations are needed, however, in order to clarify the coordination sphere of the lithium cations of  $[Li(py)_2]_4[P_2Se_6] \cdot 2 py$  in solution.

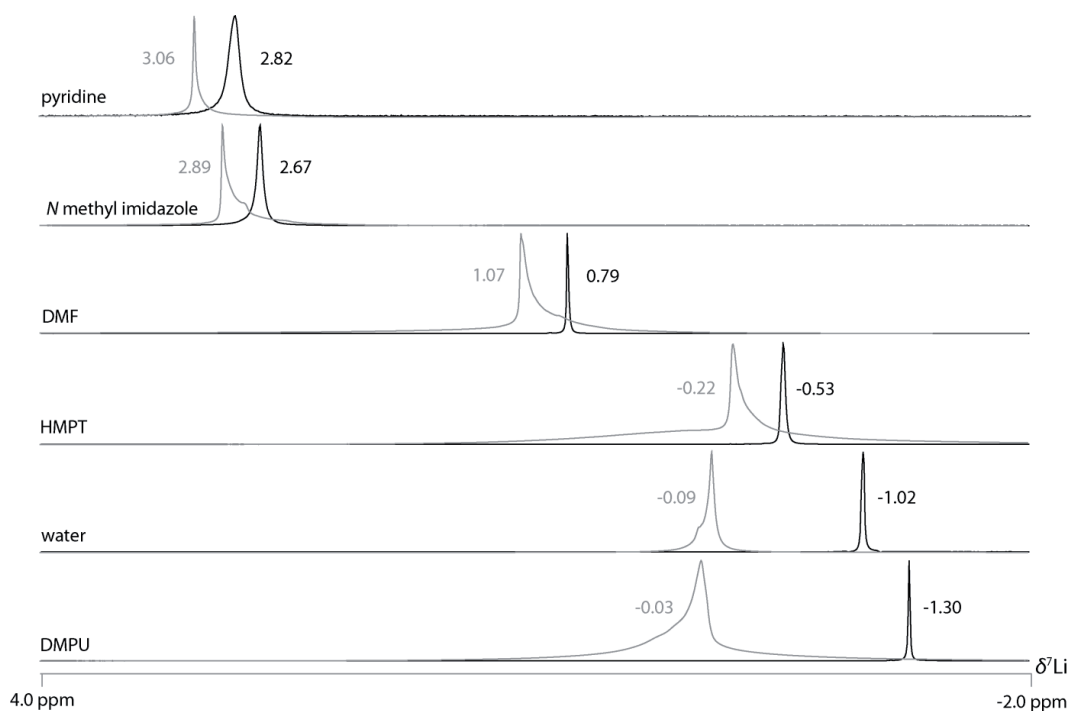
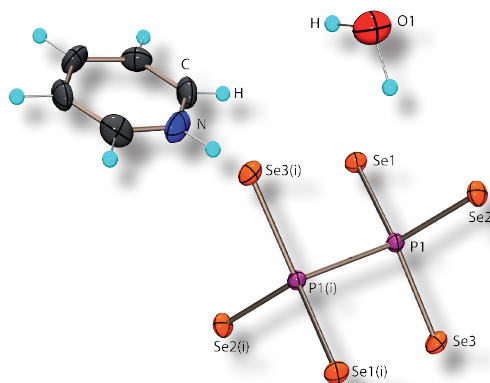


Figure 4. <sup>7</sup>Li NMR spectra of **1** (black) and LiCl (grey) in different solvents.

## 5 Conclusion

Herein a new salt containing the  $P_2Se_6^{4-}$  anion isolated in the solid state as  $[pyH]_4[P_2Se_6] \cdot H_2O$  (**2**) is presented. The compound could be characterized using single crystal X-ray diffraction. **2** is the second example of a salt of the  $P_2Se_6^{4-}$  anion with a non metal cation yielding isolated anions in the solid state which are amazingly stable in water over several months.

In addition, <sup>7</sup>Li NMR spectroscopy was used to examine the behaviour of **1** in different solvents.



## 6 Experimental Section

**General.** All reactions were carried out under inert gas atmosphere using Schlenk techniques. Argon (Messer Griesheim, purity 4.6 in 50 L steel cylinder) was used as inert gas. The glass vessels used were stored in a 130 °C drying oven and were flame dried in vacuum at  $10^{-3}$  mbar before use.

White phosphorus (ThermPhos) was peeled under water, washed with dry THF and dried under vacuum. The alkali metal diselenides were prepared according to a literature procedure and stored in a dry box under nitrogen atmosphere.<sup>4</sup> Elemental selenium (Aldrich) was used as received. The solvents used were dried applying known methods and freshly distilled before use.

**NMR Spectroscopy.** NMR spectra were recorded with a Jeol EX 400 Eclipse instrument operating at 161.997 MHz ( $^{31}P$ ), 76.321 MHz ( $^{77}Se$ ) and 155.526 MHz ( $^7Li$ ). Chemical shifts are referred to 85 %  $H_3PO_4$  ( $^{31}P$ ),  $(CH_3)_2Se$  ( $^{77}Se$ ) and 0.1 M solution of LiCl in  $D_2O$  ( $^7Li$ ) as external standards. All spectra were measured at 25 °C. The %-data correspond to the intensities in the  $^{31}P$  NMR spectra with respect to the total intensity. The difference to 100 % belongs to not determinable signals.

**X-ray Crystallography.** The molecular structure of  $[pyH]_4[P_2Se_6] \cdot H_2O$  in the crystalline state was determined using an Oxford Xcalibur3 diffraction instrument equipped with a Spellman generator (voltage 50 kV, current 40 mA) and a Kappa CCD detector with a X-ray radiation wavelength of 0.71073 Å ( $MoK_{\alpha}$ ). The data collection was performed with the CrysAlis CCD software, the data reduction with the CrysAlis RED software.<sup>5,6</sup> The structure was solved with SIR-92 and SHELXS-97 and refined with SHELXL-97 and finally checked using PLATON.<sup>7,8,9,10,11</sup> The absorptions were corrected by SCALE3 ABSPACK multi-scan method.<sup>12</sup> All relevant data and parameters of the X-ray measurement and refinement are given in Table 3.

<sup>4</sup> P. Boudjouk, D. P. Thompson *J. Org. Chem.*, **1988**, 53, 2109.

<sup>5</sup> CrysAlis CCD, Oxford Diffraction Ltd., Version 1.171.27p5 beta (release 01-04-2005 CrysAlis171 .NET), (compiled Apr 1 2005,17:53:34).

<sup>6</sup> CrysAlis RED, Oxford Diffraction Ltd., Version 1.171.27p5 beta (release 01-04-2005 CrysAlis171 .NET), (compiled Apr 1 2005,17:53:34).

<sup>7</sup> SIR-92, **1993**, *A Program for Crystal Structure Solution*; Altomare, A.; Cascarano, G. L.; Giacovazzo, C.; Guagliardi, A. *J. Appl. Cryst.* **26**, 343.

<sup>8</sup> Altomare, A.; Burla, M. C.; Camalli, M.; Cascarano, G. L.; Giacovazzo, C.; Guagliardi, A.; Moliterni, A. G. G.; Polidori, G.; Spagna, R. *J. Appl. Crystallogr.* **1999**, 32, 115.

<sup>9</sup> Sheldrick, G. M. *SHELXS-97, Program for Crystal Structure Solution*; Universität Göttingen, **1997**.

<sup>10</sup> Sheldrick, G. M. *SHELXL-97, Program for the Refinement of Crystal Structures*; University of Göttingen, Germany, **1997**.

<sup>11</sup> Spek, L. A. *PLATON, A Multipurpose Crystallographic Tool*, Utrecht University, Utrecht, The Netherlands, **1999**.

<sup>12</sup> SCALE3 ABSPACK – *An Oxford Diffraction program* (1.0.4,gui:1.0.3) (C) 2005 Oxford Diffraction Ltd.

---

**[py<sub>2</sub>Li]<sub>4</sub>[P<sub>2</sub>Se<sub>6</sub>] • 2 py (1).** **1** was prepared according to literature.<sup>3</sup> Li<sub>2</sub>Se<sub>2</sub> (1.508 g, 8.77 mmol), P<sub>4</sub>Se<sub>3</sub> (792 mg, 2.19 mmol) and grey selenium (173 mg, 2.19 mmol) were suspended in 30 mL of pyridine. Alternatively, elemental lithium (382 mg, 55.04 mmol), P<sub>4</sub> (853 mg, 6.88 mmol) and grey selenium (6.523 g, 82.61 mmol) were suspended in 60 mL of pyridine. An exothermic reaction was observed. The reaction mixture became green. Afterwards the suspension was refluxed for 2 h (130 °C oil bath temperature). Yellow crystals of **1** were obtained on cooling the reaction mixture to room temperature. The crystals were separated using a G3 frit and washed twice with 5 mL of cold pyridine and twice with 5 ml of diethylether. The yellow crystals of **1** are very sensitive towards light and air. Yield: 2.4 g (40.4 %, 1.7 mmol). For further information concerning the analytical data of compound **1** see reference 3.

**[pyH]<sub>4</sub>[P<sub>2</sub>Se<sub>6</sub>] • H<sub>2</sub>O (2).** 0.2 mmol (135 mg) of [Li(py)<sub>2</sub>]<sub>4</sub>[P<sub>2</sub>Se<sub>6</sub>] • 2 py are dissolved in 2 mL of water. On keeping the solution for 2 days in a closed glass vessel at +4 °C, only few crystals of [pyH]<sub>4</sub>[P<sub>2</sub>Se<sub>6</sub>] • H<sub>2</sub>O were obtained.

Table 3. Crystallographic data.

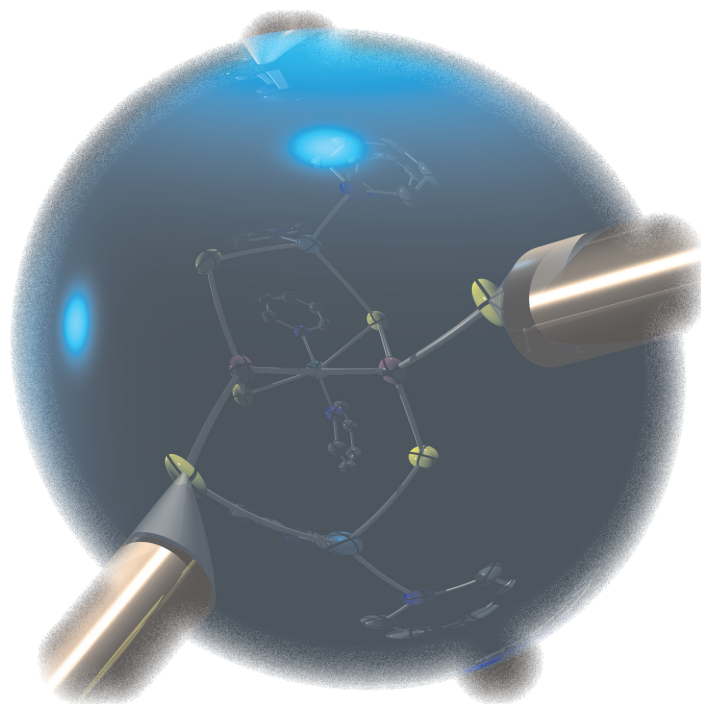
	<b>[pyH]<sub>4</sub>[P<sub>2</sub>Se<sub>6</sub>] • H<sub>2</sub>O (2)</b>
empirical formula	C <sub>20</sub> H <sub>26</sub> N <sub>4</sub> O P <sub>2</sub> Se <sub>6</sub>
formula mass	846.15
temp (K)	200
cryst. size (mm)	0.2 x 0.15 x 0.1
cryst description	yellow block
cryst. system	monoclinic
space group	<i>P</i> 2 <sub>1</sub> / <i>c</i>
<i>a</i> (Å)	9.4755(2)
<i>b</i> (Å)	13.0642(3)
<i>c</i> (Å)	8.4883(2)
α (deg)	90
β (deg)	92.009(2)
γ (deg)	90
<i>V</i> (Å <sup>3</sup> )	1050.12(4)
<i>Z</i>	4
ρ <sub>calcd</sub> (g cm <sup>-3</sup> )	2.315
μ (mm <sup>-1</sup> )	10.610
<i>F</i> (000)	680
θ range (deg)	3.7850-33.3985
index ranges	-8 ≤ <i>h</i> ≤ 11 -16 ≤ <i>k</i> ≤ 16 -10 ≤ <i>l</i> ≤ 9
reflns collected	5237 ( <i>R</i> <sub>int</sub> = 0.0192)
reflns observed	1759
reflns unique	2046
<i>R</i> <sub>1</sub> , <i>wR</i> <sub>2</sub> (all data)	0.0277, 0.0516
<i>R</i> <sub>1</sub> , <i>wR</i> <sub>2</sub> (2σ data)	0.0201, 0.0469
max/min transm	0.346/0.161
data/restr/params	2046/2/112
<i>S</i> on <i>F</i> <sup>2</sup>	1.051
larg. diff peak/hole (e/Å)	0.600/-0.464
comments	The position of the nitrogen atom in the pyH cation could be determined exactly due to the best yielded <i>wR</i> <sub>2</sub> value and thermal parameters for the shown position of the nitrogen atom within the pyridine ring.



## CHAPTER X

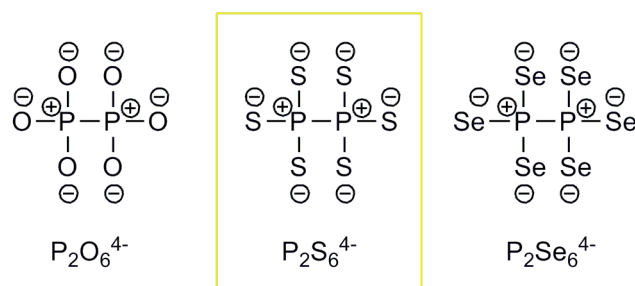
---

### A New Synthesis and Crystal Structure of the Old Hexathiohypodiphosphate $P_2S_6^{4-}$



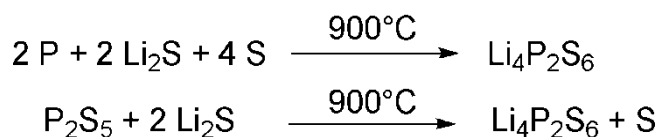
*A new wet chemical synthesis of the hexathiohypodiphosphate anion  $P_2S_6^{4-}$  starting from  $P_4S_3$ ,  $Li_2S$  and elemental sulfur is presented. This reaction in pyridine yields crystals which were analyzed using single crystal X-ray diffraction. The crystals are the hitherto unknown  $[py_2Li]_4[P_2S_6] \cdot 2 py$  compound, which is isostructural to the corresponding selenium compound  $[py_2Li]_4[P_2Se_6] \cdot 2 py$ . A comparison of both structures is presented.*

## 1 Introduction



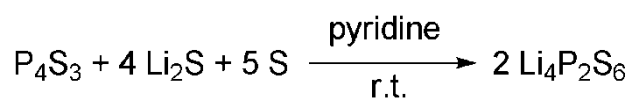
Scheme 1. Known hexachalcogenohypodiphosphate anions  $\text{P}_2\text{Ch}_6^{4-}$  (Ch = O, S, Se).

The hexathiohypodiphosphate anion  $\text{P}_2\text{S}_6^{4-}$  was described first by Falius in 1968.<sup>1</sup> It was synthesized starting from  $\text{PCl}_3$  and  $\text{Na}_2\text{S}$  in water as the sodium salt  $\text{Na}_4\text{P}_2\text{S}_6 \cdot 6 \text{H}_2\text{O}$ . Therefore, the  $^{31}\text{P}$  NMR chemical shift of  $\text{P}_2\text{S}_6^{4-}$  in water was also determined with  $\delta^{31}\text{P} = 110.7$ .<sup>1</sup> From this time on, salts of the hexathiohypodiphosphate anion  $\text{P}_2\text{S}_6^{4-}$  are subject of continuing research (1032 publications using the SciFinder database from 1968-2009) due to its physical properties like semiconductivity, ferroelectricity or luminescence (in dependence on the metal cation used).<sup>2</sup> But in most cases, the compounds are synthesized using common solid state methods.<sup>3</sup> In literature, there is already described another possible synthesis of the lithium salt  $\text{Li}_4\text{P}_2\text{S}_6$  starting from  $\text{Li}_2\text{S}$ , phosphorus and sulfur or  $\text{P}_2\text{S}_5$  in the melt at  $900^\circ\text{C}$  (Scheme 2).<sup>4</sup>



Scheme 2. Solid state synthesis of  $\text{Li}_4\text{P}_2\text{S}_6$ .

The newly developed synthesis starts from  $\text{P}_4\text{S}_3$ ,  $\text{Li}_2\text{S}$  and elemental sulfur and proceeds in pyridine as reaction medium at ambient temperature (Scheme 3).



Scheme 3. Synthesis of  $\text{P}_2\text{S}_6^{4-}$ .

<sup>1</sup> Falius, H. Z. *Anorg. Allg. Chem.* **1968**, 356 (3-4), 189-194.

<sup>2</sup> (a) Mys, O.; Martynyuk-Lototska, I.; Grabar, A.; Vlokh, R. *J. Phys.: Condens. Matter*, **2009**, 21(26), 265401/1-265401/7. (b) Wu, Yuandong, Bensch, W. *J. Solid State Chem.* **2009**, 182(3), 471-478.

<sup>3</sup> (a) Cyin, S. J.; Cyvin, B. N.; Wibbelmann, C.; Becker, R.; Brockner, W.; Parendsen, M. Z. *Naturforsch., A: Phys. Sci.* **1985**, 40A(7), 709-713. (b) Simon, A.; Hahn, H.; Peters, K. *Z. Naturforsch., B: Chem. Sci.* **1985**, 40B(6), 730-732.

<sup>4</sup> Mercier, R.; Malugani, J. P.; Fahys, B.; Douglade, J.; Robert, G. *J. Solid State Chem.* **1982**, 43, 151-162.

## 2 $[py_2Li]_4[P_2S_6] \cdot 2 py$

The salt  $[py_2Li]_4[P_2S_6] \cdot 2 py$  was obtained in excellent yield as yellow crystals from the reaction of  $P_4S_3$ ,  $Li_2S$  and elemental sulfur in pyridine.  $[py_2Li]_4[P_2S_6] \cdot 2 py$  crystallizes in the monoclinic space group  $P2_1/c$ .

It is soluble in highly polar solvents like HMPT, DMPU or water. It is remarkably stable in water over several days. In HMPT and DMPU decomposition takes place.

The molecular structure of  $[py_2Li]_4[P_2S_6] \cdot 2 py$  comprises  $P_2S_6^{4-}$  anions, surrounded by four lithium cations. Each lithium cation is coordinated by two sulfur atoms bonded to the two different phosphorus atoms. The coordination involves for every lithium cation two sulfur atoms of one and one sulfur atom of the other phosphorus atom forming a hetero-norboran skeleton. As a consequence, two of the sulfur atoms bounded to one phosphorus atom are two coordinated, while the third is threefold coordinated. The coordination sphere of the lithium cations is completed by two pyridine molecules, building isolated, neutral  $[py_2Li]_4[P_2S_6]$  clusters, which form the crystal. Two additional uncoordinated pyridine molecules can be found completing the unit cell (Figure 1).

The sulfur atoms of the  $P_2S_6^{4-}$  anion are arranged in a staggered conformation forming an ethane like structure. The P-P bond distance (225.1(1) pm) as well as the P-S bond distances (average value: 202 pm) do not deviate significantly from the bond distances reported in literature for isolated hexathiohypodiphosphate anions like  $Na_4P_2S_6 \cdot 6 H_2O$  or  $K_4P_2S_6 \cdot 4 H_2O$ .<sup>5,6</sup>

The S-Li distances are found with an average value of 247 pm significantly shorter than the S-Li distances in  $Li_4P_2S_6$  (263 pm) described by Mercier et al.<sup>4</sup> In this structure, the coordination number of the lithium cations is six. The lithium cations are surrounded by six sulfur atoms forming a  $LiS_6$  octaeder.<sup>4</sup>

<sup>5</sup> Fincher, T.; LeBret, G.; Cleary, D. A. *J. Solid State Chem.* **1998**, *141*, 274-281.

<sup>6</sup> Gjikaj, M.; Ehrhardt, C. Z. *Anorg. Allg. Chem.* **2007**, *633*, 1048-1054.

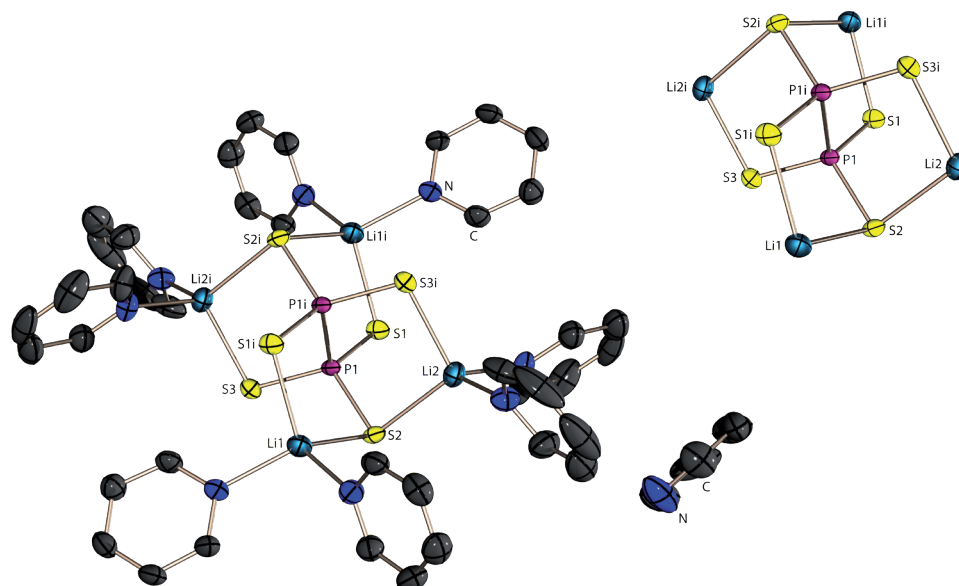


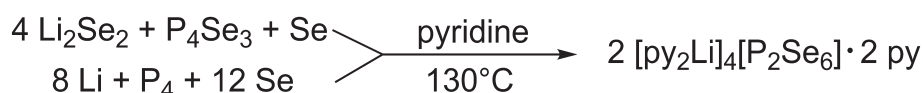
Figure 1. Molecular structure of  $[\text{py}_2\text{Li}_4][\text{P}_2\text{S}_6] \cdot 2 \text{ py}$  in the crystal. Ellipsoids are drawn at 50 % probability level. In the upper right corner the molecular structure is shown without the pyridine molecules. Hydrogen atoms are omitted for clarity.  $i = 1-x, -y, -z$ .

Table 1. Selected bond distances [pm], bond – and torsion angles [°].  $i = 1-x, -y, -z$

Bond lengths [pm]		Bond angles [°]		Torsion angles [°]	
S1-P1	201.2(1)	S1-P1-S2	112.5(1)	S1-P1-P1( <i>i</i> )-S1( <i>i</i> )	-180.0(1)
S2-P1	203.9(1)	S1-P1-S3	114.0(1)	S1-P1-P1( <i>i</i> )-S2( <i>i</i> )	61.0(1)
S3-P1	201.4(1)	S2-P1-S3	111.4(1)	S1-P1-P1( <i>i</i> )-S3( <i>i</i> )	-57.2(1)
P1-P1( <i>i</i> )	225.1(1)	S1-P1-P1( <i>i</i> )	106.7(1)	S2-P1-P1( <i>i</i> )-S1( <i>i</i> )	-61.0(1)
S1-Li1	245.3(2)	S2-P1-P1( <i>i</i> )	103.9(1)	S2-P1-P1( <i>i</i> )-S2( <i>i</i> )	-180.0(1)
S2-Li2	248.8(3)	S3-P1-P1( <i>i</i> )	107.7(1)	S2-P1-P1( <i>i</i> )-S3( <i>i</i> )	61.8(1)
S2-Li2( <i>i</i> )	249.1(3)	P1-S1-Li1	99.8(1)	S3-P1-P1( <i>i</i> )-S1( <i>i</i> )	57.2(1)
S3-Li2( <i>i</i> )	244.1(2)	P1-S2-Li2	93.5(1)	S3-P1-P1( <i>i</i> )-S2( <i>i</i> )	-61.8(1)
		P1-S2-Li1( <i>i</i> )	92.5(1)	S3-P1-P1( <i>i</i> )-S3( <i>i</i> )	180.0(1)
		Li1( <i>i</i> )-S2-Li2	103.1(1)		
		P1-S3-Li2( <i>i</i> )	98.0(1)		

### 3 Comparison of the structures of $[py_2Li]_4[P_2S_6] \cdot 2 py$ and the corresponding selenium compound $[py_2Li]_4[P_2Se_6] \cdot 2 py$

$[py_2Li]_4[P_2Se_6] \cdot 2 py$  was synthesized and characterized first by M. Schuster.<sup>7</sup> The synthesis of  $[py_2Li]_4[P_2Se_6] \cdot 2 py$  proceeds under very mild conditions (20 °C – 130 °C) starting from  $Li_2Se_2$ ,  $P_4Se_3$  or white phosphorus and elemental selenium or starting from the elements in pyridine (Scheme 4) alternatively.<sup>7</sup>



Scheme 4. Syntheses of  $[py_2Li]_4[P_2Se_6] \cdot 2 py$ .

The selenium compound is isostructural to the new salt of the hexathiohypodiphosphate anion  $[py_2Li]_4[P_2S_6] \cdot 2 py$  described previously.

Both hexachalcogenohypodiphosphate anions have an ethan-like structure with a staggered arrangement of the chalcogen atoms. In addition, the coordination spheres of the lithium cations are in both cases formed by two chalcogen atoms and two pyridine molecules. In case of the selenium compound, the Se-Li distances have an average value of 258 pm and are therefore about 10 pm longer than in the thio-analogue (S-Li 247 pm). Nevertheless, the Ch-Li distances correspond in both cases to those found in chalcogenolates where the lithium cation has a coordination sphere similar to the discussed compounds ( $py_2Li$ -Ch) (Table 2).

Table 2. Ch-Li distances in  $[py_2Li]_4[P_2Ch_6] \cdot 2 py$  compared to found distances in chalcogenolates (Ch = S, Se).<sup>8,9,10</sup>

	<i>d</i> (S-Li) [pm]		<i>d</i> (Se-Li) [pm]
$[py_2Li]_4[P_2S_6] \cdot 2 py$	247	$[py_2Li]_4[P_2Se_6] \cdot 2 py$	258
$[py_2Li][PhS]^8$	251; 246	$[py_2Li][PhSe]_2py_2Yb(SePh)_2^9$	257; 269
		$[bipyLi][PhSe]^{10}$	255; 259

<sup>7</sup> Schuster, M. *dissertation*, LMU Munich, 1999.

<sup>8</sup> Banister, A. J.; Clegg, W.; Gill, W. R. *J. Chem. Soc., Chem. Commun.* **1987**, 850-852.

<sup>9</sup> Berardini, M.; Emga, T. J.; Brennan, J. G. *J. Chem. Soc., Chem. Commun.* **1993**, 1537-1538.

<sup>10</sup> Khasnis, D. V.; Buretea, M.; Emge, T. J.; Brennan, J. G. *J. Chem. Soc. Dalton Trans.* **1995**, 45-48.

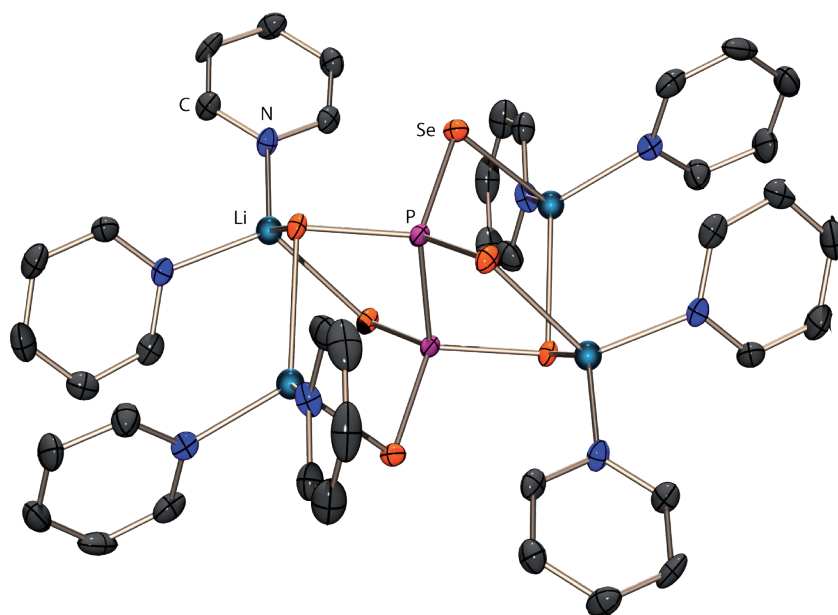


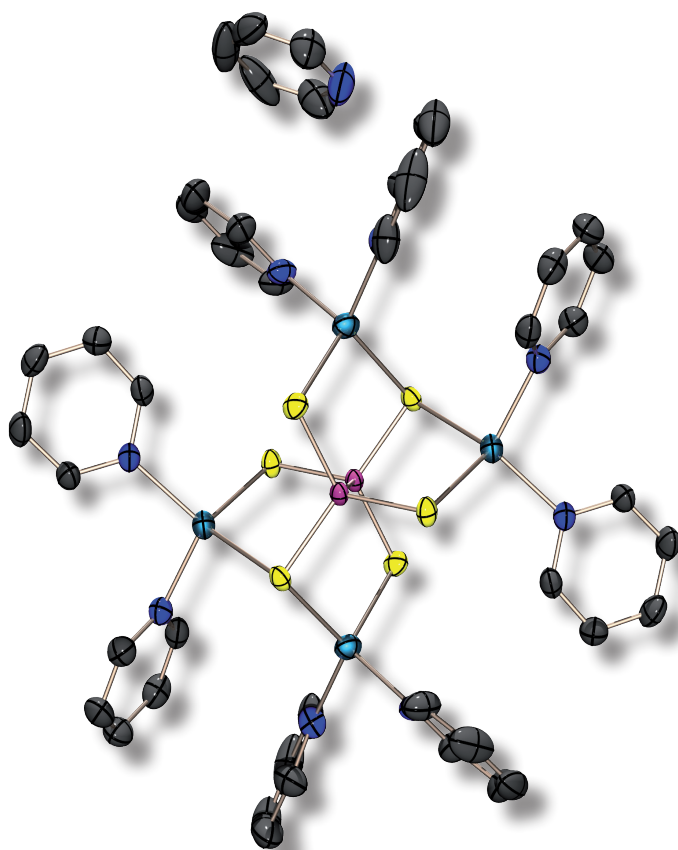
Figure 2. Molecular structure of  $[\text{py}_2\text{Li}]_4[\text{P}_2\text{Se}_6] \cdot 2 \text{ py}$  in the crystal. Ellipsoids are drawn at 50 % probability level. Hydrogen atoms are omitted for clarity.  $i = -x, -y, -z$ .

## 4 Conclusion

It could be shown that starting from  $P_4S_3$ ,  $Li_2S$  and elemental sulfur as educts in pyridine as solvent  $[py_2Li]_4[P_2S_6] \cdot 2 py$  can be prepared in excellent yield. The single crystal X-ray diffraction of the new lithium thiophosphate salt revealed that  $[py_2Li]_4[P_2S_6] \cdot 2 py$  is isostructural to the selenium analogue  $[py_2Li]_4[P_2Se_6] \cdot 2 py$ .

The bond parameters and conformation determined for  $P_2S_6^{4-}$  in  $[py_2Li]_4[P_2S_6] \cdot 2 py$  does not deviate significantly from those reported in literature. The found Li-S distances correspond to S-Li distances in the thiolate  $[py_2Li][PhS]$ . Nevertheless it is the first time that the coordination sphere of the lithium cations is not completed by only  $P_2S_6^{4-}$  molecules.

The stability and solubility of  $[py_2Li]_4[P_2S_6] \cdot 2 py$  in water makes it possible to use this salt as educt for further applications.



## 5 Experimental Section

**General.** All reactions were carried out under inert gas atmosphere using Schlenk techniques. Argon (Messer Griesheim, purity 4.6 in 50 L steel cylinder) was used as inert gas. The glass vessels used were stored in a 130 °C drying oven. Before use the glass vessels were flame dried in vacuum at  $10^{-3}$  mbar.

$\text{Li}_2\text{S}$  was prepared as described in literature and stored in a dry box under nitrogen atmosphere.<sup>11</sup> Elemental sulfur was used as received (Acros Organics).  $\text{P}_4\text{S}_3$  was commercially obtained (Riedel-de Hën), and was purified by extraction with  $\text{CS}_2$  before use. The used solvents were dried using commonly known methods and freshly distilled before use.

**NMR Spectroscopy.** NMR spectra were recorded using a Jeol EX 400 Eclipse instrument operating at 161.997 MHz ( $^{31}\text{P}$ ). Chemical shifts are referred to 85 %  $\text{H}_3\text{PO}_4$  as external standard. All spectra were measured, if not mentioned otherwise, at 25 °C. The %-data correspond to the intensities in the  $^{31}\text{P}$  NMR spectra with respect to the total intensity. The difference to 100 % belongs to not determinable signals.

**X-ray Crystallography.** The molecular structure in the crystalline state was determined using an Oxford Xcalibur3 diffraction instrument with a Spellman generator (voltage 50 kV, current 40 mA) and a Kappa CCD detector with a X-ray radiation wavelength of 0.71073 Å ( $\text{MoK}_\alpha$ ). The data collection was performed with the CrysAlis CCD software, the data reduction with the CrysAlis RED software.<sup>12,13</sup> The structures were solved with SIR-92, SIR-97 and SHELXS-97 and refined with SHELXL-97 and finally checked using PLATON.<sup>14,15,16,17,18</sup> The absorptions were corrected by SCALE3 ABSPACK multi-scan method.<sup>19</sup> All relevant data and parameters of the X-ray measurement and refinement are given in Table 3.

<sup>11</sup> (a) Thompson, D. P.; Boudjouk, P. J. *Org. Chem.* **1988**, *53*, 2109. (b) Schuster, M. PhD Thesis, LMU Munich, **1999**.

<sup>12</sup> CrysAlis CCD, Oxford Diffraction Ltd., Version 1.171.27p5 beta (release 01-04-2005 CrysAlis171 .NET), (compiled Apr 1 2005,17:53:34).

<sup>13</sup> CrysAlis RED, Oxford Diffraction Ltd., Version 1.171.27p5 beta (release 01-04-2005 CrysAlis171 .NET), (compiled Apr 1 2005,17:53:34).

<sup>14</sup> SIR-92, **1993**, *A Program for Crystal Structure Solution*; Altomare, A.; Cascarano, G. L.; Giacovazzo, C.; Guagliardi, A. J. *Appl. Cryst.* **26**, 343.

<sup>15</sup> Altomare, A.; Burla, M. C.; Camalli, M.; Cascarano, G. L.; Giacovazzo, C.; Guagliardi, A.; Moliterni, A. G. G.; Polidori, G.; Spagna, R. J. *Appl. Crystallogr.* **1999**, *32*, 115.

<sup>16</sup> Sheldrick, G. M. *SHELXS-97, Program for Crystal Structure Solution*; Universität Göttingen, **1997**.

<sup>17</sup> Sheldrick, G. M. *SHELXL-97, Program for the Refinement of Crystal Structures*; University of Göttingen, Germany, **1997**.

<sup>18</sup> Spek, L. A. *PLATON, A Multipurpose Crystallographic Tool*, Utrecht University, Utrecht, The Netherlands, **1999**.

<sup>19</sup> SCALE3 ABSPACK – *An Oxford Diffraction program (1.0.4,gui:1.0.3)* (C) 2005 Oxford Diffraction Ltd.

---

**[py<sub>2</sub>Li]<sub>4</sub>[P<sub>2</sub>S<sub>6</sub>] • 2 py.** P<sub>4</sub>S<sub>3</sub> (220 mg, 1 mmol), Li<sub>2</sub>S (184 mg, 4 mmol) and sulfur (160 mg, 5 mmol) in 10 mL of pyridine were stirred at 120 °C for two hours. The reaction suspension turns yellow. After cooling down to room temperature a yellow reaction solution and a yellow precipitate were obtained and separated from each other via centrifugation. The yellow precipitate consists of [py<sub>2</sub>Li]<sub>4</sub>[P<sub>2</sub>S<sub>6</sub>] • 2 py, which is good soluble in water. The yellow solution was stored at ambient temperature. Over night crystals of [py<sub>2</sub>Li]<sub>4</sub>[P<sub>2</sub>S<sub>6</sub>] • 2 py were formed, which were isolated by filtration and dried in vacuum. Yield: 1.07 g (0.99 mmol, 99 % with respect to P<sub>4</sub>S<sub>3</sub>).

<sup>31</sup>P{<sup>1</sup>H} NMR in pyridine of the reaction solution: δ = 233.5 (s, br, 28. %), 122.1 (s, 6.6 %), 113.5 (P<sub>2</sub>S<sub>6</sub><sup>4-</sup>, 17.7 %), 107.2 (s, 10.1 %), 103.1 (s, 7.9 %), 96.3 (s, 7.9 %), 47.2 (s, 3.1 %), 34.2 (s, 3.6 %).

<sup>31</sup>P{<sup>1</sup>H} NMR in water of the yellow precipitate: δ = 111.1 (P<sub>2</sub>S<sub>6</sub><sup>4-</sup>, 100 %).

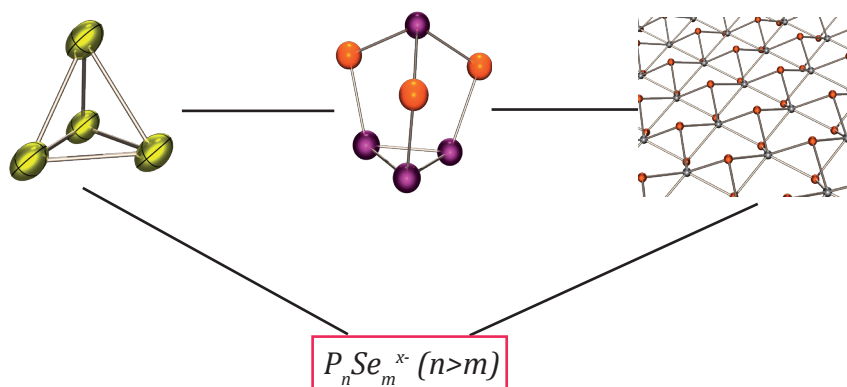
Table 3. Crystal and structure refinement data.

	<b>[py<sub>2</sub>Li]<sub>4</sub>[P<sub>2</sub>S<sub>6</sub>] • 2 py</b>
empirical formula	C <sub>40</sub> H <sub>40</sub> N <sub>8</sub> Li <sub>4</sub> P <sub>2</sub> S <sub>6</sub> • 2(C <sub>5</sub> H <sub>5</sub> N)
formula mass	1073.12
temp (K)	200
cryst. size (mm)	0.3 x 0.3 x 0.25
cryst. descriptn.	colourless block
cryst. system	monoclinic
space group	<i>P</i> 2 <sub>1</sub> / <i>c</i>
<i>a</i> (Å)	10.6899(2)
<i>b</i> (Å)	17.9376(4)
<i>c</i> (Å)	14.5311(3)
$\alpha$ (deg)	90
$\beta$ (deg)	91.524(2)
$\gamma$ (deg)	90
<i>V</i> (Å <sup>3</sup> )	2785.37(10)
<i>Z</i>	2
$\rho_{\text{calc}}$ (g cm <sup>-3</sup> )	1.280
$\mu$ (mm <sup>-1</sup> )	0.346
<i>F</i> (000)	1116
$\vartheta$ range (deg)	4.17-27.00
index ranges	-13 ≤ <i>h</i> ≤ 13, -22 ≤ <i>k</i> ≤ 22, -18 ≤ <i>l</i> ≤ 18
reflcns colcd	46090
reflcns obsd	4681
reflcns unique	6064 ( <i>R</i> <sub>int</sub> = 0.0347)
<i>R</i> 1, <i>wR</i> 2 (2 $\sigma$ data)	0.0298, 0.0751
<i>R</i> 1, <i>wR</i> 2 (all data)	0.0411, 0.0774
max/min transm	0.992/1.000
data/restr/params	6064/0/385
<i>S</i> on <i>F</i> <sup>2</sup>	0.981
larg. diff peak/hole (e/Å)	0.301/-0.288

# CHAPTER XI

---

## Phosphorus Rich Selenophosphates

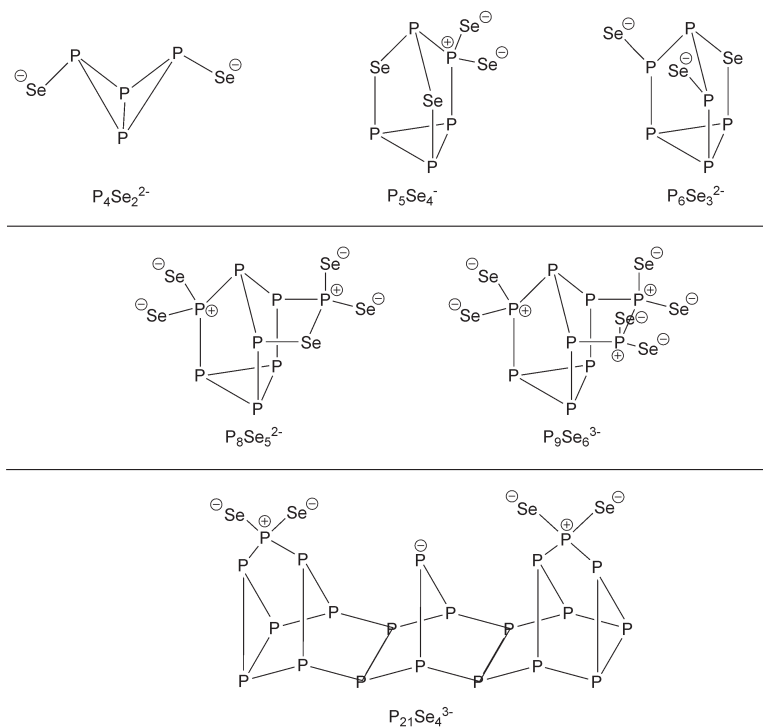


*Phosphorus rich selenophosphates are rarely known in literature till now. As most of the syntheses of selenophosphate anions occur under thermodynamical control, the degradation of the phosphorus frame work is the consequence. Herein two new possibilities are described to synthesize phosphorus rich selenophosphates under kinetical conditions.*

## 1 Introduction

The representatives of binary chalcogenophosphates  $P_nCh_m^{x-}$  reported in the literature comprise mainly chalcogen rich ( $n > m$ ) anions, except  $P_7S_3^-$ , which was reported by Baudler and Floruss and characterized in solution using  $^{31}P$  NMR spectroscopy.<sup>1</sup>

In the case of selenophosphate anions the only known examples of phosphorus rich representatives have been prepared in our group by M. Schuster. He used as educts  $M_2Se$  ( $M = Li, Na$ ),  $P_4Se_3$  or the elements  $P$ ,  $Na$  and selenium and characterized the new anions by  $^{31}P$  and  $^{77}Se$  NMR spectroscopy (Scheme 1).<sup>2</sup> The reaction medium is essential for the synthesis of phosphorus rich selenophosphates, as these compounds can only be observed in highly polar basic solvents like DMPU or *N* methyl imidazole.



Scheme 1. Examples of phosphorus rich selenophosphate anions.

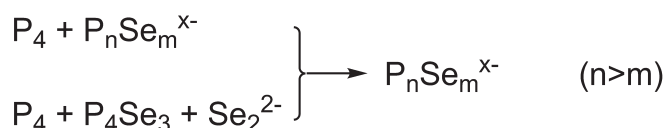
<sup>1</sup> Baudler, M.; Floruss, A. *Z. Anorg. Allg. Chem.* **1994**, 620, 2070–2076.

<sup>2</sup> Schuster, M. *dissertation*, LMU Munich, **1999**.

## 2 A New Route to Phosphorus Rich Selenophosphate Anions $P_nSe_m^{x-}$

Our concept of an alternative synthesis of phosphorus rich selenophosphates anions is based on the straight forward preparation of selenium rich selenophosphate anions as well as on the availability of  $P_4Se_3$  and uses the reactivity of white phosphorus. Reaction of  $P_4$  with selenium rich anions  $P_nSe_m^{x-}$  ( $m > n$ ) might result in a comproportionation to give phosphorus rich anions ( $m < n$ ). Starting from  $P_4Se_3$  in addition to  $P_4$  an anionic species ( $Se^{2-}$ ,  $Se_2^{2-}$ ) is required to furnish the negative charge.

This alternative route is anticipated to proceed also in common organic solvents (THF, pyridine, MeCN) due to the solubility of the tetraalkylammonium salts of e. g.  $P_2Se_8^{2-}$ , which would be an advantage compared to the route developed by M. Schuster (Scheme 2).



Scheme 2. New syntheses of phosphorus rich selenophosphates  $P_nSe_m^{x-}$  ( $n > m$ ).

## 3 Reaction of $P_4$ with $P_4Se_7^{2-}$

To a THF solution of white phosphorus an equimolar amount of  $Na_2P_4Se_7$  was added and the resulting orange yellow suspension was investigated by  $^{31}P$  NMR spectroscopy. The  $^{31}P$  NMR spectrum showed broad signals at 128.9 ppm, 92.4 ppm and -23.2 ppm (13.7 %, 6.3 % and 16.7 % of the total intensity). Interestingly all the white phosphorus had reacted, while  $P_4Se_7^{2-}$  was still present in the reaction solution. In addition the formation of the sixmembered ring  $P_2Se_8^{2-}$  can be observed (Figure 1).

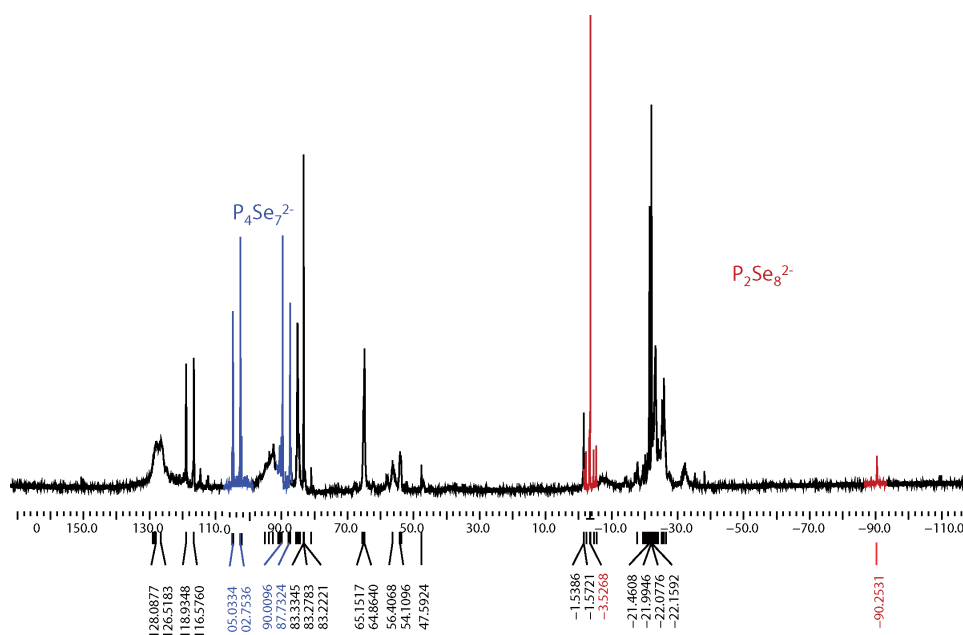


**Figure 1.**  $^{31}\text{P}\{^1\text{H}\}$  NMR spectrum of the reaction solution of  $\text{P}_4$  and  $\text{P}_4\text{Se}_7^{2-}$  in THF at  $25^\circ\text{C}$  (0.1 M; 2048 scans with a PD = 1 s, 73 min measuring time,  $\nu_0 = 161.9966$  MHz, broadband  $^1\text{H}$  decoupling).

The reaction suspension was continued stirring at room temperature for 24 h and again  $^{31}\text{P}$  NMR spectroscopical investigated. The educt signals of  $\text{P}_4\text{Se}_7^{2-}$  could still be observed besides new signals ( $\delta^{31}\text{P} = 116.6$  &  $118.9$ ) which split in the  $^1\text{H}$  coupled  $^{31}\text{P}$  NMR spectrum into quintets. This is most probably due to reaction products with the solvent THF.

As the formation of an orange yellow precipitate was observed, crown ether is added, to increase the solubility of the precipitate, as it is expected, that phosphorus rich selenophosphates are badly soluble in solvents like THF or acetonitrile. But as this does not work properly, the precipitate was separated and solved in pyridine under reflux. The reaction solution turned green, and during cooling down to ambient temperature the color changed to yellow and once again the formation of a yellow precipitate could be observed. The reaction suspension was investigated by  $^{31}\text{P}$  NMR spectroscopy whereas signals corresponding to three compounds can be observed.

At a  $^{31}\text{P}$  NMR chemical shift of  $-19.8$  ppm a singlet with two pairs of  $^{77}\text{Se}$  satellites can be observed. The  $^1J_{\text{SeP}}$  coupling constants correspond with values of 370 Hz and 666 Hz to twice respectively once coordinated selenium atoms.<sup>3</sup> The intensity ratio of the two  $^{77}\text{Se}$  satellite pairs is 1:1. The proportion of the satellites pairs to the total  $^{31}\text{P}$  NMR intensity of the signal is 33 % which leads to the assumption that 4 selenium nuclei are contained in the compound (Figure 2).

<sup>3</sup> Karaghiosoff, K. In *Encyclopedia of Nuclear Magnetic Resonance*; Grant, D. M., Harris, R. K., Eds.: Wiley: Chichester, U.K., 1996; Vol. 6, pp 3612-3619.

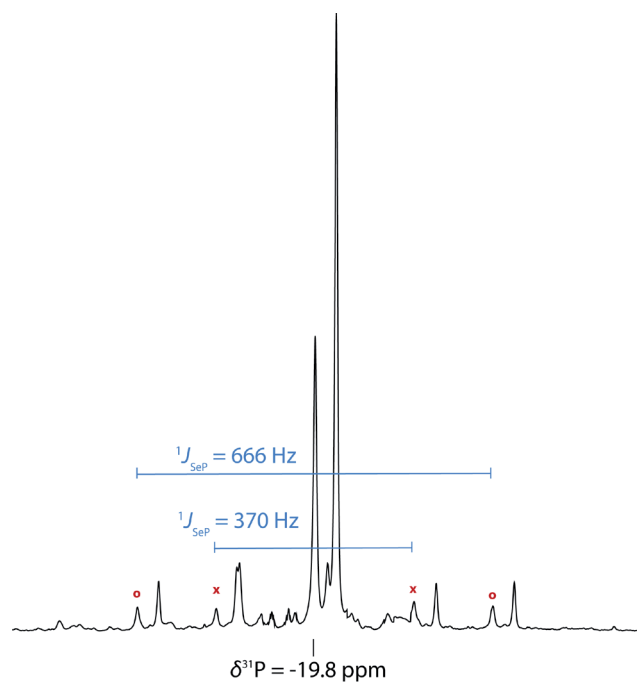


Figure 2.  $^{31}\text{P}\{^1\text{H}\}$  NMR spectrum in pyridine at 25°C. (7429 scans with a PD = 1 s, 266 min measuring time,  $^1\text{H}$  broad band decoupling).

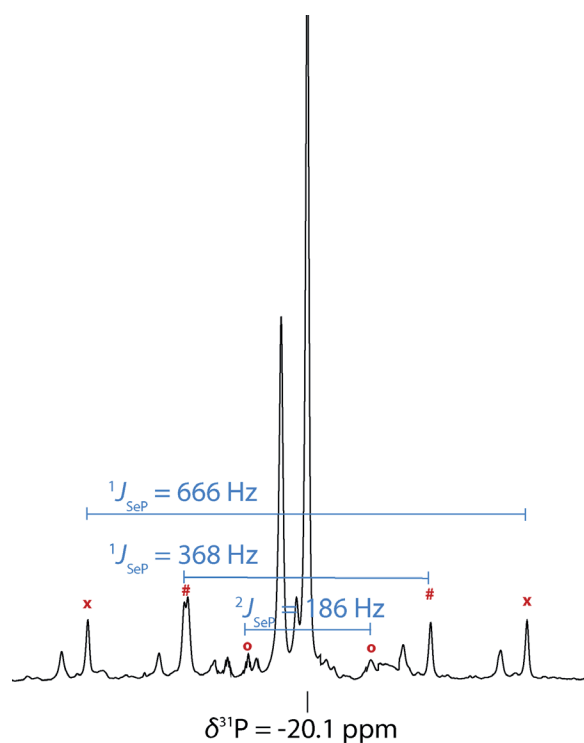


Figure 3.  $^{31}\text{P}\{^1\text{H}\}$  NMR spectrum in pyridine at 25°C (7429 scans with a PD = 1 s, 266 min measuring time,  $^1\text{H}$  broad band decoupling).

The second signal has a  $^{31}\text{P}$  NMR chemical shift of  $-20.1$  ppm and is accompanied by three pairs of  $^{77}\text{Se}$  satellites with an intensity ratio of 1:2:2. The proportion to the total intensity of the  $^{31}\text{P}$  NMR signal is 37 % which implies the existence of 5 selenium nuclei. The two more intense  $^{77}\text{Se}$  satellite pairs have  $^1J_{\text{SeP}}$  coupling constants of 386 Hz and 666 Hz indicating a  $\text{PSe}_4$  surrounding. Due to the existence of the weaker satellite pair with a  $^2J_{\text{SeP}}$  coupling constant of 186 Hz it can be concluded that a P-Se-Se-Se-P motive is existing (Figure 3).

The singlet at  $\delta^{31}\text{P} = -32.4$  is accompanied by two pairs of  $^{77}\text{Se}$  satellites (intensity ratio 1:1) with  $^1J_{\text{SeP}}$  coupling constants of 346 Hz and 669 Hz which corresponds to twice and single coordinated  $^{77}\text{Se}$  nuclei. The proportion of the  $^{77}\text{Se}$  satellites intensity to the total intensity is 23 % thus indicating the existence of three selenium atoms.

Further investigations are in course in order to determine the identity of these compounds.

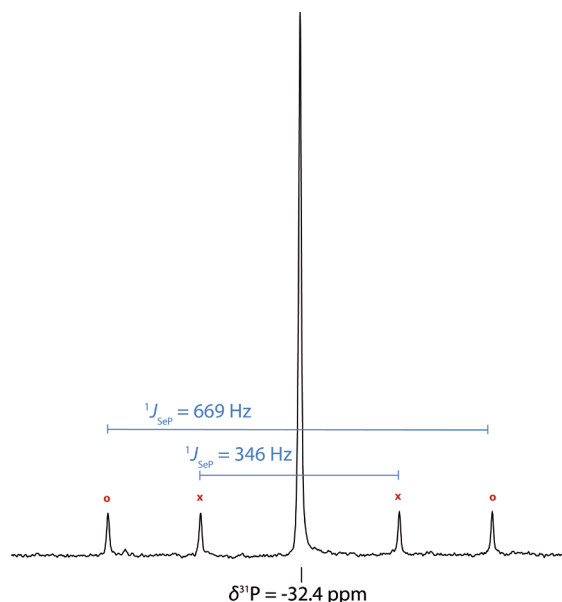
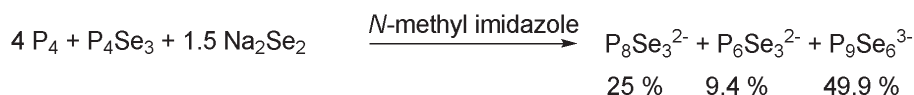
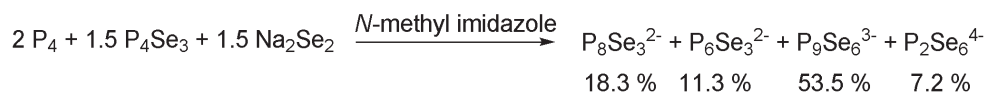


Figure 4.  $^{31}\text{P}\{^1\text{H}\}$  NMR spectrum in pyridine (7429 scans with a PD = 1 s, 266 min measuring time,  $^1\text{H}$  broad band decoupling).

## 5 Reaction of $P_4$ with $P_4Se_3$ and $Na_2Se_2$



**Scheme 3.** Used educt stoichiometries and observed product mixture according to the  $^{31}P$  NMR spectra of the reaction solutions.

As afore mentioned, it has not been investigated till now what products are available using  $P_4Se_3$ ,  $Na_2Se_2$  and  $P_4$  as educts together. It is expected, that new phosphorus rich selenophosphates should be preparable with this educt combination. Due to the experience with the preparation of phosphorus rich chalcogenophosphates *N*-methyl imidazole was used as reaction medium.<sup>2</sup>

All investigated stoichiometries (Scheme 3) provided the same result: It was not possible to observe signals corresponding to hitherto unknown compounds, instead already known<sup>2</sup> but nevertheless mostly phosphorus rich compounds could be observed according to the  $^{31}P$  NMR spectrum:  $P_8Se_5^{2-}$ ,  $P_6Se_3^{2-}$ ,  $P_9Se_6^{3-}$  and  $P_2Se_6^{4-}$  (Figure 5).

Thus it can be concluded that using the syntheses described in Scheme 2, it is not possible to yield new phosphorusrich selenophosphates.

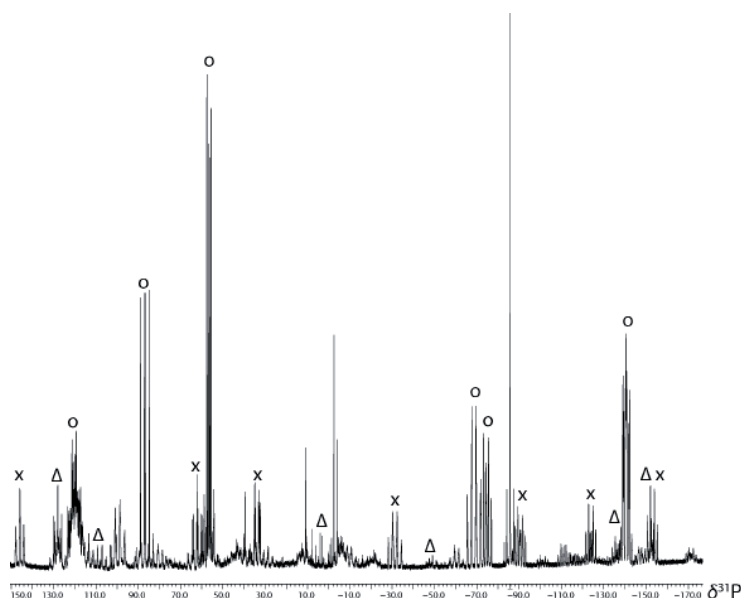
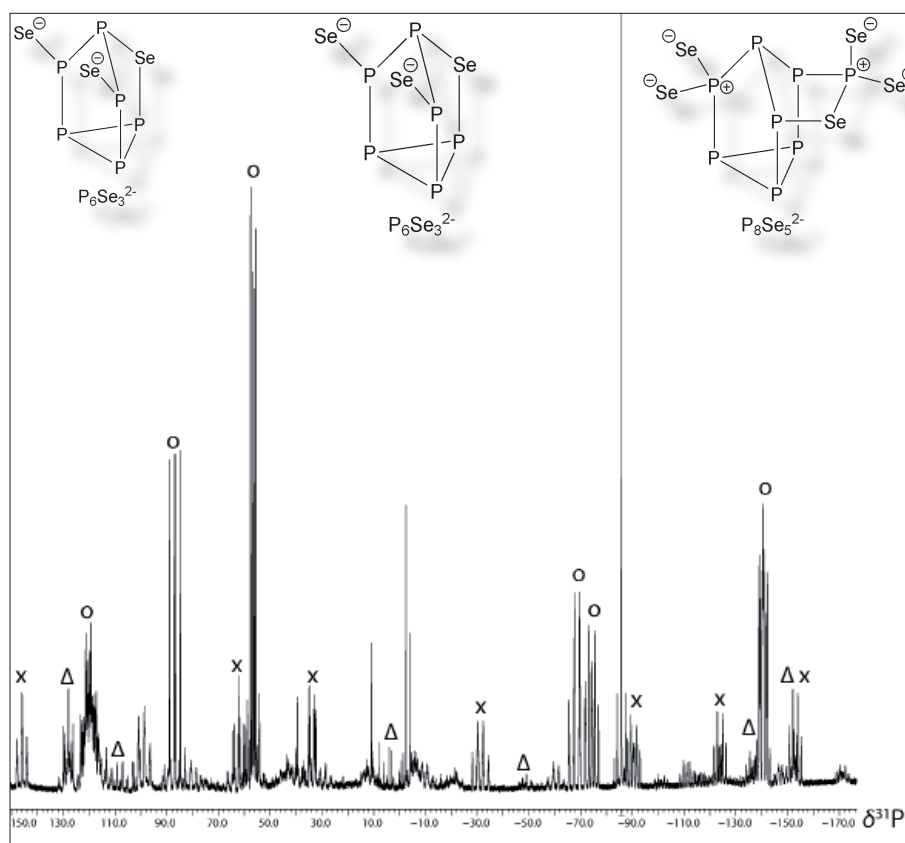


**Figure 5.**  $^{31}P\{^1H\}$  NMR spectrum of the reaction solution ( $4 P_4 + P_4Se_3 + 1.5 Na_2Se_2$ ) (8192 scans with a PD = 0.5 s, 226 min measuring time,  $^1H$  broad band decoupling).  $x = P_8Se_5^{2-}$   $\Delta = P_6Se_3^{2-}$ ;  $o = P_9Se_6^{3-}$ .

## 6 Conclusion

There are indications for the formation of new anions with phosphorus and selenium, in particular when  $P_4Se_7^{2-}$  is used as starting material. This opens the possibility for further investigations in order to identify the products.



## 7 Experimental Section

**General.** All reactions were carried out under inert gas atmosphere using Schlenk techniques. Argon (Messer Griesheim, purity 4.6 in 50 L steel cylinder) was used as inert gas. The glass vessels used were stored in a 130 °C drying oven and were flame dried in vacuum at  $10^{-3}$  mbar before use.

White phosphorus (ThermPhos) was peeled under water, washed with dry THF and dried under vacuum. The sodium diselenide,  $P_4Se_3$ ,  $Na_2P_4Se_7$  and  $Na_2P_2Se_8$  were prepared according to a literature procedure and stored in a dry box under nitrogen atmosphere.<sup>4,5,2</sup> The solvents used were dried applying known methods and freshly distilled before use.

**NMR Spectroscopy.** NMR spectra were recorded with a Jeol EX 400 Eclipse instrument operating at 161.997 MHz ( $^{31}P$ ). Chemical shifts are referred to 85 %  $H_3PO_4$  as external standard. All spectra were measured, if not mentioned otherwise, at 25 °C. The difference to 100 % belongs to not determinable signals. The %-data correspond to the intensities in the  $^{31}P$  NMR spectra with respect to the total intensity. The difference to 100 % belongs to not determinable signals.

### $P_4 + Na_2P_4Se_7$

To a solution of  $Na_2P_4Se_7$  in THF (4.84 mmol), 150 mg (4.84 mmol) white phosphorus was added and stirred at ambient temperature till all  $P_4$  was dissolved. An orange yellow suspension was yielded. 15-crown-5 ether was added to dissolve the precipitate. It was continued stirring for 3 d at room temperature. Still the yellow precipitate could be observed. Therefore the suspension was fritted using a G4 frit to remove the solid. The solid is soluble in pyridine under reflux for 5 h. At higher temperatures the reaction solution turned green, and after cooling down to ambient temperature it turned yellow.

$^{31}P$ - $\{^1H\}$ -NMR (THF):  $P_2Se_8^{2-}$  (chair, 1.8 %),  $P_2Se_8^{2-}$  (twist, 7.2 %),  $P_4Se_7^{2-}$  (16.3 %);  $\delta = 128.9$  (br, 13.7 %), 92.4 (6.3 %), 64.8 (s,  $^1J_{sep} = 930$  Hz, 9.4 %), -21.4 - -23.4 (16.7 %).  
after 24 h:

$^{31}P$ - $\{^1H\}$ -NMR (THF):  $P_2Se_8^{2-}$  (chair, 0.5 %),  $P_2Se_8^{2-}$  (twist, 7.5 %),  $P_4Se_7^{2-}$  (3.5 %),  $\delta = 118.9$  (s, 2.1 %),  $\delta = 116.5$  (s, 2.3 %).

### precipitate in pyridine:

$^{31}P$ - $\{^1H\}$ -NMR:  $\delta = -19.8 - -20.1$  (82.5 %), -32.4 (s, 8.9 %).

<sup>4</sup> Boudjouk, P.; Thompson, D. P. *J. Org. Chem.*, **1988**, *53*, 2109 – 2112.

<sup>5</sup> (a) Stoppioni, P.; Peruzzini, M. *Gazz. Chim. Ital.* **1988**, *118*, 581. (b) Schön, O. dissertation, LMU Munich, Munich, Germany, 2007.

**$2 \text{P}_4 + 1.5 \text{P}_4\text{Se}_3 + 1.5 \text{Na}_2\text{Se}_2$** 

61 mg (1.9 mmol) of  $\text{P}_4$  was dissolved in 5 mL *N* methyl imidazole. Then 348 mg (1.44 mmol)  $\text{P}_4\text{Se}_3$  and 294 mg (1.44 mmol) were added. After stirring at room temperature for 3 h a red solution is obtained.

$^{31}\text{P}$ - $\{^1\text{H}\}$ -NMR (*N* methyl imidazole):  $\text{P}_8\text{Se}_5^{2-}$  (18.3 %),  $\text{P}_6\text{Se}_3^{2-}$  (11.3 %),  $\text{P}_9\text{Se}_6^{3-}$  (53.6 %),  $\text{P}_2\text{Se}_6^{4-}$  (7.2 %).

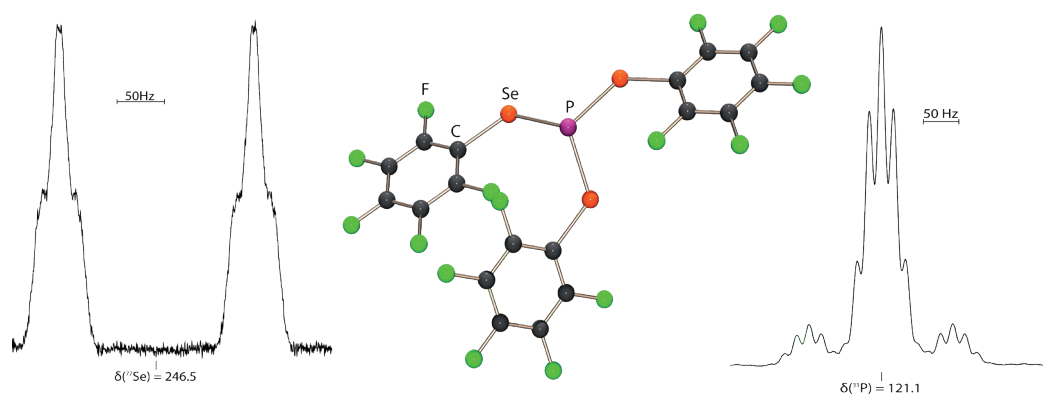
 **$4 \text{P}_4 + \text{P}_4\text{Se}_3 + 1.5 \text{Na}_2\text{Se}_2$** 

White phosphorus (101 mg, 3.16 mmol) was dissolved in 6 mL *N* methyl imidazole and subsequently  $\text{P}_4\text{Se}_3$  (288 mg, 0.79 mmol) and  $\text{Na}_2\text{Se}_2$  (242 mg, 1.18 mmol) were added. The color of the reaction suspension immediately turned into red. After continuous stirring at ambient temperature a clear, red solution is obtained.

$^{31}\text{P}$ - $\{^1\text{H}\}$ -NMR (*N*-MeIm, RT):  $\text{P}_8\text{Se}_5^{2-}$  (25 %),  $\text{P}_6\text{Se}_3^{2-}$  (9.4 %),  $\text{P}_9\text{Se}_6^{3-}$  (49.9 %),  $\delta = -85.8$  (s, 4.2 %).

## CHAPTER XII

### Tris(pentafluorophenylseleno)phosphine ( $C_6F_5Se)_3P$

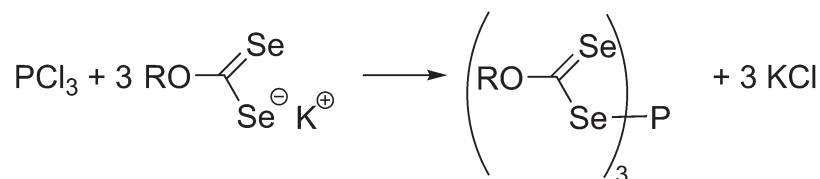


$(C_6F_5Se)_3P$  was obtained by the reaction of  $(C_6F_5Se)_2$  with white phosphorus in THF at ambient temperature. The compound is a new representative of the almost unexplored tris(aryl - or alkylseleno)phosphines  $(RSe)_3P$ . It is the second derivative with a perfluorated organic substituent R bonded to selenium.  $(C_6F_5Se)_3P$  is identified via multinuclear magnetic resonance spectroscopy ( $^{31}P$ ,  $^{77}Se$ ,  $^{19}F$ ).

## 1 Introduction

There are only a few examples known in literature for tris(aryl – or alkylseleno)phosphines and characterization of the known representatives by multinuclear NMR spectroscopy is incomplete.<sup>1,2,3,4,5,6,7</sup>

Rosenbaum was the first who succeeded in synthesizing a trisalkylselenophosphine. He used  $\text{PCl}_3$  and potassiumdiselenoxanthogenate as starting materials.<sup>1</sup>



Scheme 1. Synthesis according to Rosenbaum.

Most of the known tris(aryl – or alkylseleno)phosphines are synthesised using  $\text{PCl}_3$  and an alkali salt of the selenoligand as educts, except Maier, who used white phosphorus and the corresponding organodiselenides as starting materials.<sup>2-5</sup> A full NMR spectroscopical characterization of the described phosphines is missing in most cases, however (Table 1).

Table 1. All known tris(aryl – or alkylseleno)phosphines, the syntheses and analytical characterization.

phosphine	starting materials	analytical methods	NMR chemical shifts [ppm]	coupling constants [Hz]
$(\text{ROCSe}_2)_3\text{P}^1$	$\text{PCl}_3 + \text{ROCSe}_2\text{K}$	elemental analysis	-	
$(\text{MeSe})_3\text{P}^2$	$\text{PCl}_3 + \text{Me}_3\text{SiSeMe}$	NMR	$\delta^1\text{H}$ 2.19	$J_{\text{PH}}$ 6.8, $J_{\text{SeH}}$ 11.3, $J_{\text{CH}}$ 145.4
$(\text{MeSe})_3\text{P}^3$	$\text{P}_4 + (\text{MeSe})_2$	elemental analysis, NMR	$\delta^1\text{H}$ 2.17, $\delta^{31}\text{P}$ 107	$^3J_{\text{PH}}$ 7, $^2J_{\text{SeH}}$ 11, $^1J_{\text{SeP}}$ 233
$(\text{PhSe})_3\text{P}^3$	$\text{P}_4 + (\text{PhSe})_2$	elemental analysis, NMR	$\delta^1\text{H}$ 7.14, 7.5	
$(\text{PhSe})_3\text{P}^5$	$\text{PCl}_3 + \text{NaSeC}_6\text{H}_5$	X-ray structure		
$(\text{CF}_3\text{Se})_3\text{P}^4$	$\text{PBr}_3 + \text{Hg}(\text{SeCF}_3)_2$	IR, NMR	$\delta^{31}\text{P}$ 65.05, $\delta^{19}\text{F}$ 30.4, $\delta^{77}\text{Se}$ 960.0	$^1J_{\text{SeP}}$ 202.5, $^3J_{\text{PF}}$ 14.9
$(\text{CF}_3\text{Se})_3\text{P}^7$	-	NMR	$\delta^{77}\text{Se}$ 541	
$\{\text{Fe}(\text{C}_5\text{H}_4\text{Se})\text{P}[(\text{SeC}_5\text{H}_4)_2\text{Fe}]\}_2$	$\text{PCl}_3 + \text{Fe}(\text{C}_5\text{H}_4\text{Se}-\text{SnMe}_3)_2$	NMR		

<sup>1</sup> Rosenbaum, A. *Journal. für praktische Chemie*, **1968**, 137, 200-205 and references cited therein.

<sup>2</sup> Anderson, J.W.; Drake, J. E.; Hemmings, R. T.; Nelson, D. L. *Inorg. Nucl. Chem. Letters*, **1975**, 11, 233-237.

<sup>3</sup> Maier, L. *Helv. Chim. Acta* **1976**, 59 (28), 252-256.

<sup>4</sup> Darmadi, A.; Haas, A.; Kaschani-Motlach, M. Z. *Anorg. Allg. Chem.* **1979**, 488, 35-39.

<sup>5</sup> Keder, N. L.; Shibao, R. K.; Eckert, H. *Acta Cryst.* **1992**, C48, 1670-1671.

<sup>6</sup> Herberhold, M.; Dörnhöfer, C.; Scholz, A.; G.-X. Jin, *Phosphorus, Sulfur Silicon Relat. Elem.* **1992**, 64, 161-168.

<sup>7</sup> W. Gombler, *Z. Naturforsch., B: Chem. Sci.* **1981**, 36, 535-543.

## 2 Results and Discussion



Scheme 2. Reaction of white phosphorus with  $(\text{C}_6\text{F}_5\text{Se})_2$  in THF.

The new compound  $(\text{C}_6\text{F}_5\text{Se})_3\text{P}$  was obtained by the reaction of white phosphorus with  $(\text{C}_6\text{F}_5\text{Se})_2$  in THF.  $(\text{C}_6\text{F}_5\text{Se})_3\text{P}$  was unequivocally identified using  $^{31}\text{P}$ -,  $^{19}\text{F}$ - and  $^{77}\text{Se}$  NMR spectroscopy. In the  $^{31}\text{P}\{^{19}\text{F}\}$  NMR spectrum of  $(\text{C}_6\text{F}_5\text{Se})_3\text{P}$  a singlet at 121.1 ppm is observed, which is accompanied by a pair of  $^{77}\text{Se}$  satellites ( $^1J_{\text{SeP}} = 205$  Hz, 20 % of the total  $^{31}\text{P}$  signal intensity). The relative intensity of the satellites corresponds to three selenium atoms bonded to phosphorus. When fluorine coupling to phosphorus is allowed, the main signal and the satellites split into a septet due to coupling of phosphorus with the six *o*-fluorine atoms (Figure 1).

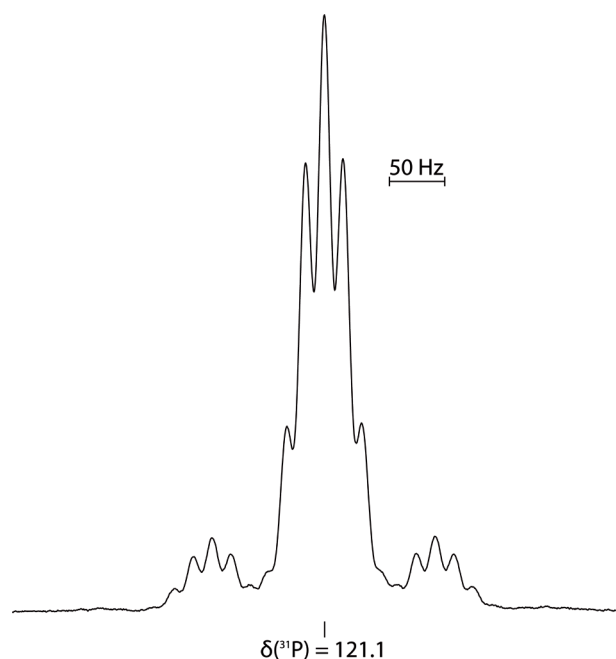
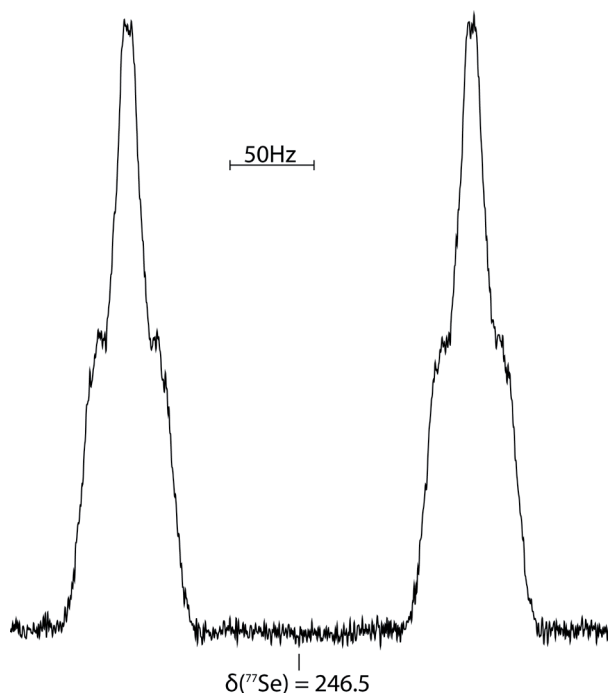


Figure 1.  $^{31}\text{P}\text{-}^{19}\text{F}$  NMR spectrum of  $(\text{C}_6\text{F}_5\text{Se})_3\text{P}$ : observed spectrum at 24°C in THF (0.1 M, 3640 scans with a PD = 0.5 s, 91 min measuring time,  $\nu_0 = 161.9967$  MHz, broadband  $^1\text{H}$  decoupling).

The coupling of the phosphorus atom to the fluorine atoms in meta – and para position is smaller than the line width of the NMR spectrum and therefore cannot be observed. There are three signals for the fluorine atoms in the  $^{19}\text{F}$  NMR spectrum. The  $^{19}\text{F}$  NMR chemical shift of both fluorine atoms in ortho position is -126.9 ppm (doublet) with a  $^3J_{\text{FF}}$  coupling constant to the fluorine atoms in meta position of 22 Hz.

The signal pattern of  $^{19}\text{F}$  atoms located in meta position is a doublet of doublets at a chemical shift of  $-161.8$  ppm. The  $^3J_{\text{FF}}$  coupling constants are  $22$  Hz ( $^{19}\text{F}_{\text{ortho}}-^{19}\text{F}_{\text{meta}}$ ) and  $20$  Hz ( $^{19}\text{F}_{\text{meta}}-^{19}\text{F}_{\text{para}}$ ). The fluorine atom in para position has a NMR chemical shift of  $-151.9$  Hz. The signal splits into a triplet with a  $^3J_{\text{FF}}$  coupling constant of  $20$  Hz. The signal pattern of the  $^{77}\text{Se}$  atoms consists of a doublet of triplets at  $246.5$  ppm. The  $^3J_{\text{SeF}}$  coupling constant is  $20$  Hz (Figure 2).



**Figure 2.**  $^{77}\text{Se}$ - $^{19}\text{F}$  NMR spectrum of  $(\text{C}_6\text{F}_5\text{Se})_3\text{P}$ : observed spectrum at  $24^\circ\text{C}$  in THF (0.1 M, 24184 scans with a PD = 0.5 s, 10.5 h measuring time,  $\nu_0 = 76.3207$  MHz, broadband decoupling).

The  $^{31}\text{P}$  NMR resonance  $(\text{C}_6\text{F}_5\text{Se})_3\text{P}$  is in the same range found for comparable compounds (Table 2), as well as the  $^{19}\text{F}$  NMR resonances. In contrast, the  $^{77}\text{Se}$  NMR signal of  $(\text{C}_6\text{F}_5\text{Se})_3\text{P}$  is shifted to higher field compared to  $(\text{CF}_3\text{Se})_3\text{P}$ .

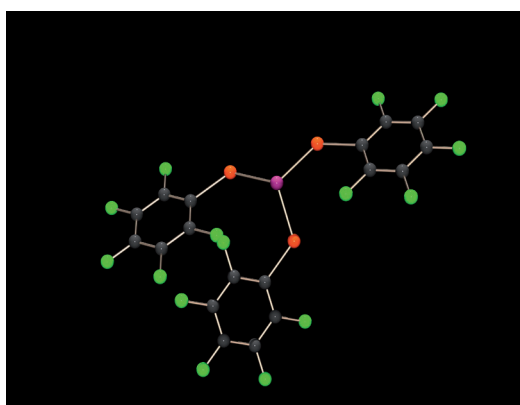
**Table 2. Known tris(aryl – or alkylchalcogeno)phosphines with perfluorinated aryl – or alkyl substituents.**<sup>891011</sup>

phosphine	$\delta^{31P}$	$\delta^{77Se}$	$\delta^{19F}$	coupling constants [Hz]
$(CF_3S)_3P$ <sup>8</sup>	85.0	-	33.5	$^3J_{PF}$ 20
$(CF_3Se)_3P$ <sup>4</sup>	65.5	960.0	-	$^1J_{SeP}$ 202 $^3J_{PF}$ 14.9
$(CF_3Se)_3P$ <sup>7</sup>	-	541	-	-
$(C_6F_5CH_2O)_3P$ <sup>9</sup>	142		-149.1 (o) <sup>a</sup> -167.9 (m) <sup>a</sup> -157.0 (p) <sup>a</sup>	$^3J$ 22.1 <sup>b</sup> $^4J$ 7.7 <sup>b</sup> $^3J$ 20.6 <sup>b</sup> $^4J$ 7.4 <sup>b</sup> $^3J$ 22 <sup>b</sup>
$(C_6F_5O)_3P$ <sup>10</sup>	-		-	-
$(C_6F_5S)_3P$ <sup>11</sup>	-		-130.2 (o) <sup>a</sup> -163.1 (m) <sup>a</sup> -149.2 (p) <sup>a</sup>	$^3J_{FF}$ 20 Hz

a) o = ortho, m = meta, p = para; b) no comment given which coupling constant is meant.

### 3 Conclusions

$(C_6F_5Se)_3P$  is a new representative of the class of tris(aryl-or alkylseleno)phosphines. It is also the second example with perfluorinated substitutes at selenium (Table 2).  $(C_6F_5Se)_3P$  could be unequivocally characterized using  $^{31}P$ -,  $^{19}F$ -, and  $^{77}Se$  NMR spectroscopy.



<sup>8</sup> Haas, A.; Winkler, D. Z. *Anorg. Allg. Chem.* **1980**, 468, 68-76.

<sup>9</sup> Denney, D. B.; Denney, D. Z.; Lin, L.-T. *Phosphorus, Sulfur Silicon Relat. Elem.* **1982**, 13, 1-7.

<sup>10</sup> Furin, G. G.; Krupoder, S. A.; Rezvukhin, A. I.; Kilina, T. M.; Yakobsen, G. G. *J. Fluorine Chem.* **1983**, 22(4), 345-375.

<sup>11</sup> Peach, M. E.; Spinney, H. G. *Can. J. Chem.* **1971**, 49, 644-648.

## 4 Experimental Section

**General.** All reactions were carried out under inert gas atmosphere using Schlenk techniques. Argon (Messer Griesheim, purity 4.6 in 50 L steel cylinder) was used as inert gas. The glass vessels used were stored in a 130 °C drying oven and were flame dried in vacuum at  $10^{-3}$  mbar before use.

White phosphorus (ThermPhos) was peeled under water, washed with dry THF and dried under vacuum. Elemental selenium (Aldrich) was used as received. THF was dried over sodium/benzophenone and freshly distilled before use. The pentafluorophenyldiselenide was prepared according to literature.<sup>12</sup>

**NMR Spectroscopy.** NMR spectra were recorded with a Jeol EX 400 Eclipse instrument operating at 161.997 MHz ( $^{31}\text{P}$ ), 76.321 MHz ( $^{77}\text{Se}$ ) and 376.548 MHz ( $^{19}\text{F}$ ). Chemical shifts are referred to 85 %  $\text{H}_3\text{PO}_4$  ( $^{31}\text{P}$ ),  $(\text{CH}_3)_2\text{Se}$  ( $^{77}\text{Se}$ ) and  $\text{CCl}_3\text{F}$  ( $^{19}\text{F}$ ) as external standards. All spectra were measured at 25 °C.

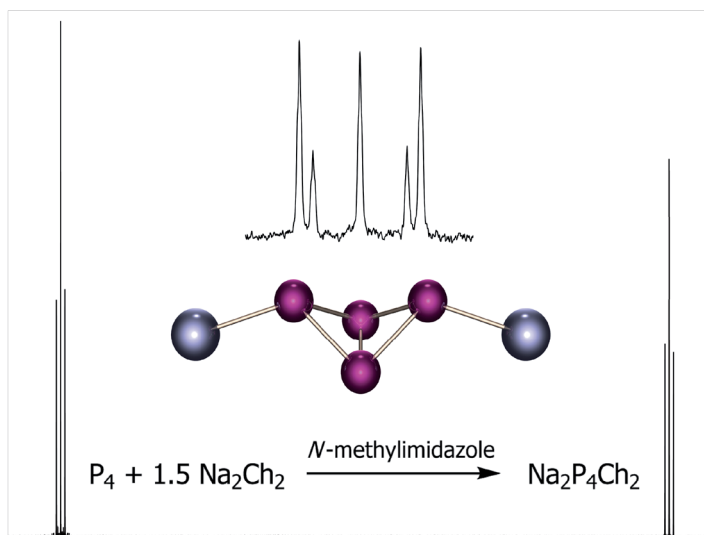
The synthesis of  $(\text{C}_6\text{F}_5\text{Se})_3\text{P}$  was adapted from literature. White phosphorus (0.25 mmol, 8 mg) was solved in 2 mL of THF and pentafluorophenyldiselenide (1.48 mmol, 730 mg) was added in one portion at ambient temperature yielding a clear yellow solution.

The  $^{31}\text{P}$  NMR spectrum of the reaction solution showed two signals at 121.1 ppm ( $(\text{C}_6\text{F}_5\text{Se})_3\text{P}$ , 89 %) and - 526.8 ( $\text{P}_4$ , 11 %).

<sup>12</sup> Klapötke, T. M.; Krumm, B.; Mayer, P. Z. *Naturforsch., B: Chem. Sci.* **2004**, *59*, 547-553.

## CHAPTER XIII

### Do Binary Phosphorus Tellurium Anions Exist?



The first discrete P-Te anion,  $P_4Te_2^{2-}$ , which is readily obtained by oxidation of white phosphorus with  $Te_2^{2-}$  in *N*-methyl imidazole at ambient temperature, is presented. According to the  $^{31}P$  and  $^{125}Te$  NMR spectra, the anion  $P_4Te_2^{2-}$  has a bicyclo[1.1.0]tetraphosphane (“butterfly”) structure with the tellurium atoms in the *exo* positions. The anion is remarkably stable in solution at ambient temperature and disproportionates only slowly with formation of elemental tellurium.  $P_4Te_2^{2-}$  is the first P-Te anion with a bicyclo[1.1.0]tetraphosphane structure. The synthesis of  $P_4Te_2^{2-}$  demonstrates that binary P-Te anions do exist as stable species in solution. Furthermore quantum chemical calculations give an insight into the charge distribution within this anion.

In addition it is possible to observe some new phosphorus rich P-Te compounds after a longer reaction time. The results provide first information on the stability of P-Te anions.

## 1 Introduction

The increasing interest in metal chalcogenophosphates with the heavier chalcogens sulfur and selenium, due to their interesting material properties like ion conductivity or optoelectrical properties, stimulates the search for new and, in particular, phosphorus-rich chalcogenophosphate anions.<sup>1</sup> Surprisingly, while oxo-, thio- and selenophosphate anions are known in literature and are, as in the case of the oxophosphate anions, well investigated, tellurophosphates are practically unknown.

There is only one tellurophosphate anion, which has been described in the literature. Mewis et al. found in crystalline  $\text{BaP}_4\text{Te}_2$  the polymeric anion  $(\text{P}_4\text{Te}_2^{2-})_x$ , which consists of chains of  $\text{P}_6$  rings in the chair conformation with the tellurium atoms covalently bonded to phosphorus in the 1,4 position (Scheme 1, Figure 1).<sup>2</sup>

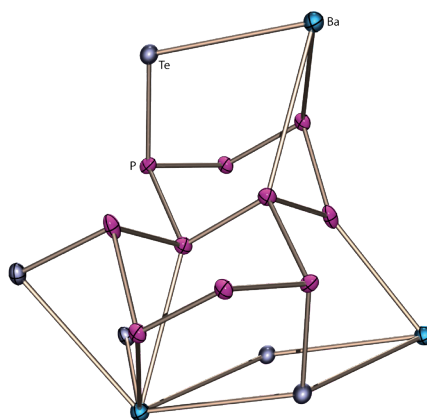
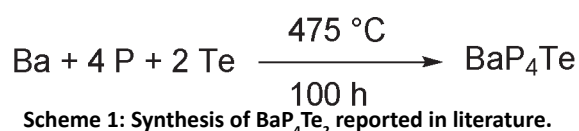


Figure 1. Part of the molecular structure of  $\text{BaP}_4\text{Te}_2$ .

Here, we report the synthesis and multinuclear ( $^{31}\text{P}$ ,  $^{125}\text{Te}$ ) NMR spectroscopic characterization of the new anion  $\text{P}_4\text{Te}_2^{2-}$ , which represents formally the “monomer” of the polymeric  $(\text{P}_4\text{Te}_2^{2-})_x$  and which is the first discrete P-Te anion ever observed. Quantum chemical calculations complete the characterization of  $\text{Na}_2\text{P}_4\text{Te}_2$  with respect to its structure and charge distribution.

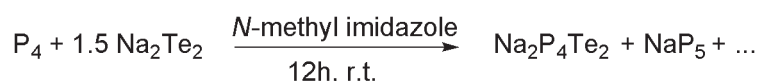
<sup>1</sup> Davies, R. Chalcogen-Phosphorus (and Heavier Congeners) Chemistry. In *Handbook of Chalcogen Chemistry*; Devillanova, F. A., Ed.; RSC Publishing: London, 2007; pp 286–343.

<sup>2</sup> Mewis, A.; Jörgens, S.; Johrendt, D. *Chem.; Eur. J.* **2003**, *9*, 2405–2410.

## 2 Synthesis and NMR analysis of $P_4Te_2^{2-}$

The classical syntheses of metal chalcogenophosphates are mainly the domain of solid-state chemistry. They use the elements as starting materials and involve reactions at high temperatures in the melt, under hydrothermal conditions, or using polychalcogenide fluxes.<sup>3,4,5,6</sup> One synthetic strategy uses reactions in solution at ambient temperature or below, thus making the formation of metastable chalcogenophosphate anions possible. In particular, P-Te anions, which suffer from the weak phosphorus-tellurium bond, should become accessible under these conditions. Chivers et al. have demonstrated that an anionic tellurium atom bonded to a phosphorus atom stabilizes the phosphorus tellurium bond, thus preventing tellurium elimination.<sup>7,8</sup>

In this context, I investigated the reaction of white phosphorus with  $Na_2Te_2$  in *N*-methyl imidazole at ambient temperature. The reaction of  $P_4$  with 1.5 equivalents of  $Na_2Te_2$  is completed within 12 h, yielding a dark purple solution. According to the  $^{31}P$  NMR spectrum, the anion  $P_4Te_2^{2-}$  (**1**) is formed almost quantitatively (98 %; Scheme 2) together with traces (2 %) of  $P_5^-$  ( $\delta^{31}P = 471^9$ ). No other phosphorus-containing species are observed in the solution.



Scheme 2. Synthesis of  $P_4Te_2^{2-}$ .

The stoichiometry (1 : 1.5) as well as the solvent seem to be essential. With less  $Na_2Te_2$ , additional phosphorus-containing products are formed. In less basic solvents than *N*-methyl imidazole, for example in pyridine, only broad  $^{31}P$  NMR signals are observed. The anion  $P_4Te_2^{2-}$  is remarkably stable in *N*-methyl imidazole solution: it can be kept for 1 day in daylight at ambient temperature or for 4 days at 0 °C without detectable decomposition. After a longer period of time, however, the signals of **1** disappear and new broad signals are observed in the  $^{31}P$  and  $^{125}Te$  NMR spectra, most probably due to anions with still higher phosphorus content. This will be discussed in detail later in this chapter.

<sup>3</sup> Chung, I.; Malliakas, C. D.; Jang, J. I.; Canlas, C. G.; Weliky, D. P.; Kanatzidis, M. G. *J. Am. Chem. Soc.*, **2007**, *129* (48), 14996-15006 and references cited therein.

<sup>4</sup> Klingen, W.; Ott, R.; Hahn, H. Z. *Anorg. Allg. Chem.* **1973**, *396*, 271–278.

<sup>5</sup> Krause, W.; Falius, H. Z. *Anorg. Allg. Chem.* **1983**, *496*, 80–93.

<sup>6</sup> Chan, B. C.; Hess, R. F.; Feng, P. L.; Abney, K. D.; Dorhout, P. K. *Inorg. Chem.* **2005**, *44*, 2106–2113 and references cited therein.

<sup>7</sup> Briand, G. G.; Chivers, T.; Parvez, M. *Angew. Chem., Int. Ed.* **2002**, *41*, 3468–3470.

<sup>8</sup> Chivers, T.; Eisler, D. J.; Ritch, J. S. *Dalton Trans.* **2005**, 2675–2677.

<sup>9</sup> Baudler, M.; Düster, D.; Ouzounis, D. Z. *Anorg. Allg. Chem.* **1987**, *544*, 87–94.

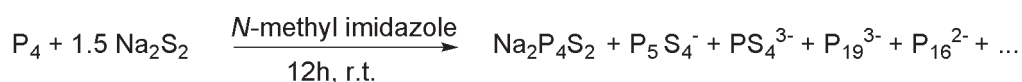
Obviously in the series of anions  $P_4S_2^{2-}$ ,  $P_4Se_2^{2-}$  and  $P_4Te_2^{2-}$ , the phosphorus-tellurium anion **1** seems to be the most stable species under the prevailing reaction conditions.

In case of the selenium analogue, other products like  $PSe_4^{3-}$ ,  $P_2Se_6^{2-}$ ,  $HPSe_3^{2-}$ ,  $HP_2Se_5^{3-}$  and  $P_{19}^{3-}$  were identified using  $^{31}P$  and  $^{77}Se$  NMR spectroscopy (Scheme 3)<sup>10</sup>

$$P_4 + 1.5 Na_2Se_2 \xrightarrow[12h, r.t.]{} Na_2P_4Se_2 + P_2Se_6^{2-} + PSe_4^{3-} + HPSe_3^{2-} + HP_2Se_5^{3-} + P_{21}^{3-} + \dots$$

**Scheme 3. Synthesis of  $P_4Se_2^{2-}$ .**

$P_4S_2^{2-}$  could only be observed in small amounts (4 %) in the reaction solution. Besides  $P_4S_2^{2-}$ ,  $P_4S_5^-$ ,  $PS_4^{3-}$ ,  $P_{19}^{3-}$ ,  $P_{16}^{2-}$  and some protonated species whose identity could not be determined, was identified in the  $^{31}P$  NMR spectrum (Scheme 4).



**Scheme 4. Synthesis of  $P_4S_2^{2-}$ .**

Identity and structure of  $P_4Te_2^{2-}$  result clearly from the  $^{31}P$  and  $^{125}Te$  NMR spectra. They reveal a bicyclo[1.1.0]tetraphosphane (butterfly) structure with the tellurium atoms in the sterically more favorable exo positions (Figure 2).

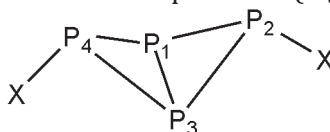


**Figure 2. Bicyclo[1.1.0]tetraphosphane structure. 1, X = Te; 2, X = Se; 3, X = S; 4, X = Cl; 5, X = Br; 6, X = SiMe<sub>3</sub>; 7, X = N(SiMe<sub>3</sub>)<sub>2</sub>.**

The symmetrical bicyclic framework is suggested by the  $^{31}P$  NMR spectrum of  $A_2M_2$  type for the isotopomer without magnetically active tellurium<sup>11</sup> (Figure 3) and is further supported by the satellite pattern for the signal of P-2(4), caused by the isotopomer with one magnetically active  $^{125}Te$  nucleus (A part of the  $A_2M_2X$  spectrum). From the satellite pattern, a large and positive value for the “hidden” coupling constant  $^2J_{PP}$  between the isochronous nuclei P2 and P4 is determined (Table 1), in accord with the exo position of the tellurium nuclei. No signals corresponding to an exo-endo or endo-endo isomer can be detected in the  $^{31}P$  NMR spectrum (Figure 4).

<sup>10</sup> Schuster, M. *dissertation*, LMU Munich, 1999.

<sup>11</sup> natural abundance of  $^{125}Te$  = 7.14 %,  $I = \frac{1}{2}$ .

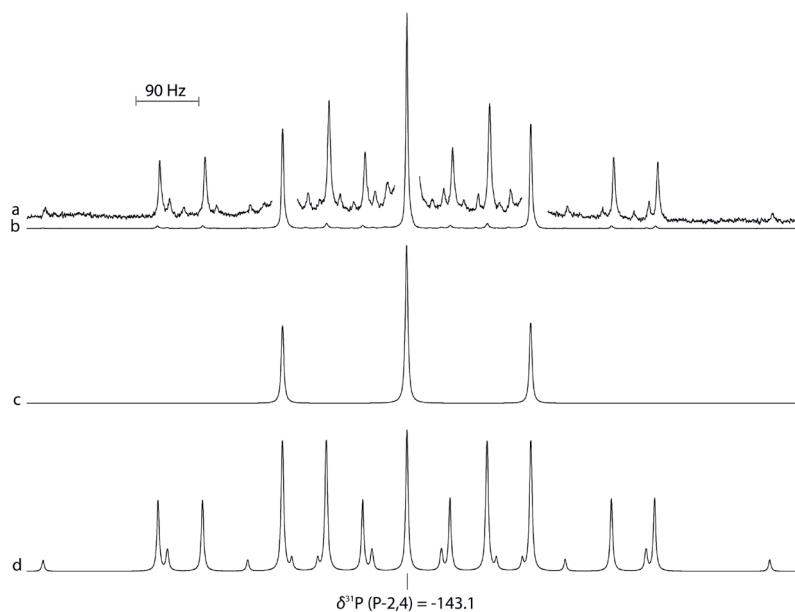


Figure 3.  $^{31}\text{P}$  NMR spectrum of  $\text{P}_4\text{Te}_2^{2-}$  (1). Signal of P2(4), A part of  $\text{AA}'\text{M}_2\text{X}$  spin system: (a) enlarged satellite pattern of the observed spectrum, (b) observed spectrum in *N*-methyl imidazole (9000 scans with relaxation delay of 0.5 s, 274 min measuring time), (c) calculated<sup>12</sup> spectrum for the isotopomer without NMR-active tellurium (86.2 %), (d) calculated spectrum for the isotopomer with one  $^{125}\text{Te}$  nucleus (6.6 %).

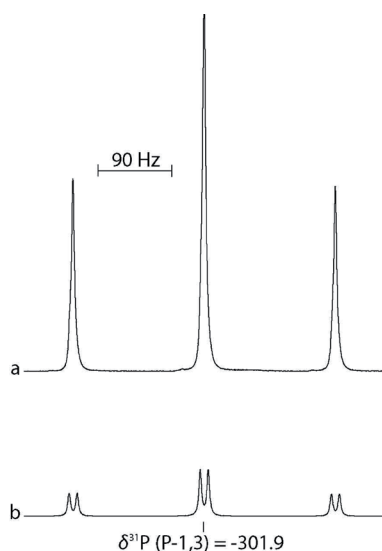


Figure 4.  $^{31}\text{P}$  NMR spectrum of  $\text{P}_4\text{Te}_2^{2-}$  (1). Signal of P1(3), M part of  $\text{AA}'\text{M}_2\text{X}$  spin system: (a) observed spectrum in *N*-methyl imidazole (9000 scans with relaxation delay of 0.5 s, 274 min measuring time), (b) calculated<sup>11</sup> spectrum for the isotopomer with one  $^{125}\text{Te}$  nucleus.

<sup>12</sup> Laatikainen, R.; Niemitz, M.; Weber, U.; Sundelin, T.; Hasinen, T.; Vepsäläinen, J. *J. Magn. Reson., A* 1996, 120, 1–10.

The  $^{125}\text{Te}$  NMR spectrum of **1** (Figure 5) displays the line pattern for the X part of an  $\text{AA}'\text{M}_2\text{X}$  spectrum; each of the five lines expected for the X part of  $\text{AA}'\text{X}$  is further split according to first order into a triplet by coupling with the two magnetically equivalent M nuclei. The  $^2J_{\text{TeP}}$  coupling constant (11 Hz) is small, and for P1(3), the  $^{125}\text{Te}$  satellites overlap with the main signals (Figure 4).

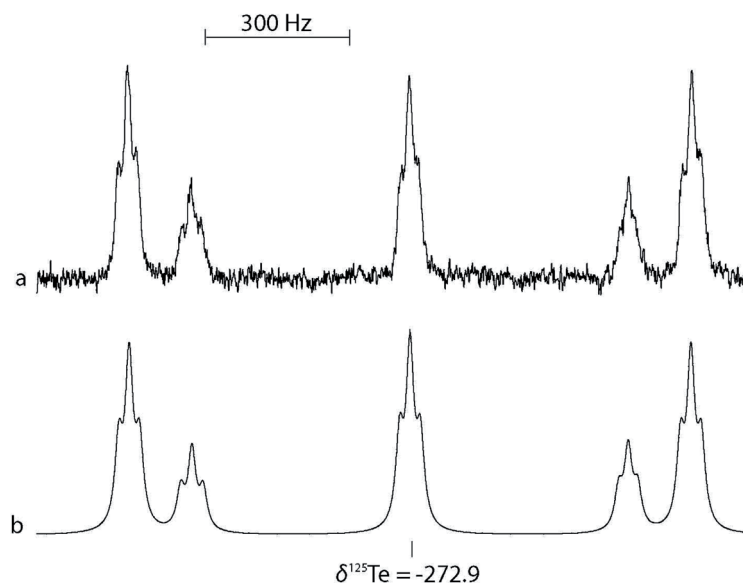


Figure 5.  $^{125}\text{Te}$  NMR spectrum of  $\text{P}_4\text{Te}_2^{2-}$  (**1**). X part of  $\text{AA}'\text{M}_2\text{X}$ : (a) observed spectrum in *N*-methyl imidazole (49740 scans with a relaxation delay of 0.8 s, 25.3 h measuring time), (b) calculated<sup>11</sup> spectrum.

The  $^{31}\text{P}$  NMR data of the new anion  $\text{P}_4\text{Te}_2^{2-}$  fit well to those of the corresponding thiophosphate  $\text{P}_4\text{S}_2^{2-}$  and selenophosphate  $\text{P}_4\text{Se}_2^{2-}$  as well as to those observed for other bicyclo[1.1.0]tetraphosphanes (Table 1). With decreasing electronegativity of the chalcogen the  $^{31}\text{P}$  NMR signals shift to higher field and the value of  $^1J_{\text{PP}}$  decreases. The coupling constant  $^1J_{\text{TeP}}$  in **1** with a value of  $-457$  Hz lies in the expected range and provides a rare example of one-bond P, Te coupling of a trivalent three-coordinated phosphorus atom to a directly bonded anionic tellurium atom.<sup>13</sup>  $^3J_{\text{TeP}}$  in **1** is with a value of  $-138$  Hz remarkably large.

<sup>13</sup> Karaghiosoff, K. In *Encyclopedia of Nuclear Magnetic Resonance*; Grant, D. M., Harris, R. K., Eds.: Wiley: Chichester, U.K., 1996; Vol. 6, pp 3612-3619.

**Table 1. NMR chemical shifts and coupling constants of the new (1) and literature-known (2-8) bicyclo[1.1.0]tetraphosphanes.<sup>14,15</sup>**

		$\delta$ [ppm]	$J$ [Hz]	
<b>1</b> <sup>[a]</sup> (X = Te <sup>-</sup> )	P-2,4	-143.1	$^1J_{PP}$	-180
	P-1,3	-301.9	$^2J_{P2P4}$	168
	Te	-272.9	$^1J_{TeP2(4)}$	-457
			$^2J_{TeP1(3)}$	11
			$^3J_{TeP2(4)}$	-138
<b>2</b> <sup>[a]</sup> (X = Se <sup>-</sup> )	P-2,4	-90.5	$^1J_{PP}$	-206
	P-1,3	-284.0	$^2J_{P2P4}$	181
	Se	-160.0	$^1J_{SeP2(4)}$	-336
			$^2J_{SeP1(3)}$	< 8
			$^3J_{SeP2(4)}$	-51
<b>3</b>	P-2,4	-64.9	$^1J_{PP}$	-222
(X = S <sup>-</sup> )	P-1,3	-271.6		
<b>4</b> <sup>[17]</sup> (X = Cl)	P-2,4	-54.5	$^1J_{PP}$	-215
	P-1,3	-290.4		
<b>5</b> <sup>[17]</sup> (X = Br)	P-2,4	-72.7	$^1J_{PP}$	-203
	P-1,3	-294.4		
<b>6</b> <sup>[14]</sup> (X=SiMe <sub>3</sub> )	P-2,4	-155.0	$^1J_{PP}$	162
	P-1,3	-329.2		
<b>7</b> <sup>[15]</sup> (X=N(SiMe <sub>3</sub> ) <sub>2</sub> )	P-2,4	-79.1	$^1J_{PP}$	222
	P-1,3	-287.3		

<sup>[a]</sup> The signs of the coupling constants result from the iterative fitting of the NMR spectra assuming a negative sign for  $^1J_{PP}$ ,  $^1J_{TeP}$  and  $^1J_{SeP}$ .<sup>12</sup>

A bicyclo[1.1.0]tetraphosphane has been postulated as a reaction intermediate for the nucleophilic degradation of white phosphorus<sup>16,17</sup> and has been shown to be the initial product of the oxidation of white phosphorus with Cl<sub>2</sub> and Br<sub>2</sub>.<sup>18</sup> The formation of the new binary anion **1** implies the oxidative addition of the isoelectronic ditelluride Te<sub>2</sub><sup>2-</sup> to one of the P-P bonds in the P<sub>4</sub> tetrahedron and fits well into this picture.

<sup>14</sup> Cappello, V.; Baumgartner, J.; Dransfeld, A.; Flock, M.; Hassler, K. *Eur. J. Inorg. Chem.* **2006**, 2393–2405.

<sup>15</sup> Niecke, E.; Rüger, R.; Krebs, B. *Angew. Chem.* **1982**, 94(7), 553–554.

<sup>16</sup> Brown, C.; Hudson, R. F.; Wartew, G. A. *Phosphorus, Sulfur Silicon Relat. Elem.* **1978**, 5, 67–80.

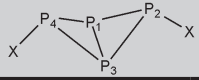
<sup>17</sup> Baudler, M.; Adamek, C.; Opiela, S.; Budzikiewicz, H.; Ouzounis, D. *Angew. Chem.* **1988**, 100, 1110–1111.

<sup>18</sup> Tattershall, B. W.; Kendall, N. L. *Polyhedron* **1994**, 13(10), 1517–1521.

### 3 Quantum chemical calculations

In order to elucidate the structure and charge distribution of  $P_4Te_2^{2-}$  quantum chemical calculations at the MPW1PW91 level of theory using a polarized triple-zeta basis set (aug-cc-pVTZ) for phosphorus and a pseudo potential ECP4GMWB/AVTE for tellurium were carried out.

**Table 2. Calculated and experimentally observed structural parameters for new and literature known bicyclo[1.1.0]tetraphosphanes.<sup>19,20</sup>**

				
Distances [pm]				
	$P_4Te_2^{2-}$ <sup>[a]</sup>	$P_4(P[NiPr_2]_2)$ <sup>[19]</sup>	$P_4(N(SiMe_3)_2)$ <sup>[b, 14]</sup>	$P_4(sMes)_2$ <sup>[d, 20]</sup>
P1-P3	217.36	216.10(12)	212.9	216.6(2)
P1-P4/P2	224.5	221.21(11)/220.70(11)	221.7/222.7	222.3(4)/222.2(3)
P3-P4/P2	224.5	221.76(11)/221.23(11)	222.3/223.0	223.5(7)/223.6(9)
P2-P4	298.4	-	281.0	-
P-Te	246.4	-	-	-
Bond angles [°]				
P1-P4-P3/P1-P2-P3	57.9	58.40(4)/58.55(4)	57.2/57.1	58.1(1)/58.1(1)
P4-P1-P3/P2-P1-P3	61.0	60.93(4)/60.60(4)	61.8/61.5	61.2(1)/61.3(1)
P4-P3-P1/P2-P3-P1	61.0	60.68(4)/60.85(4)	61.0/61.4	60.7(1)/60.6(1)
P4-P1-P2/P4-P3-P2	83.3	80.70(4)/80.46(4)	95.2	80.9(1)/80.4(1)
P-P-X <sup>[c]</sup>	106.4	96.2	107.3	106.9

<sup>[a]</sup> Calculated values, <sup>[b]</sup> Experimentally determined values by X-ray diffraction, <sup>[c]</sup> Averaged values for the experimentally determined angles, <sup>[d]</sup> sMes = super mesityl = 2,4,6-tri-*tert*-butyl phenyl.

The calculated structural parameters (bond distances and angles) of the bicyclo[1.1.0] tetraphosphane framework of  $P_4Te_2^{2-}$  correspond well to those reported in literature for compounds containing the same structural motive (Table 2). The P-P distance of the bridgehead phosphorus atoms P1 and P3 is in all cases shorter, than the distances to the other phosphorus atoms bonded to tellurium. The values for the fold angles are all in the same range. The P-Te distance is calculated to be 246.4 pm in  $P_4Te_2^{2-}$  which is in the same order of magnitude reported for  $BaP_4Te_2$  (246.9 pm). So the geometry optimization corroborates the NMR spectroscopic deduced bicyclo[1.1.0] tetraphosphane framework of  $P_4Te_2^{2-}$ .

In addition the Mulliken charges of the phosphorus and tellurium atoms in  $P_4Te_2^{2-}$  are calculated in order to elucidate the charge distribution within this anion. This is quite an interesting point as the calculated P-Te distance is 246.4 pm indicating a covalent P-Te bonding ( $\Sigma$  covalent radii of P and Te: 247 pm).<sup>21</sup> So it is expected that the negative charge is distributed all over the  $P_4Te_2^{2-}$  molecule. This expectation

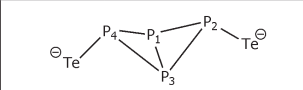
<sup>19</sup> Lapczuk-Krygier, A.; Baranowska, K.; Pikies, J. *Acta Crystallogr., Sect. E: Struct. Rep. Online* **2006**, *64*, o2427-o2440.

<sup>20</sup> Riedel, R.; Hausen, H.-D.; Fluck, E. *Angew. Chem. Int. Ed. Engl.* **1985**, *24*(12), 1056-1057.

<sup>21</sup> Pauling, L. *Die Natur der Chemischen Bindung*, 3rd ed., VCH, Weinheim, **1968**, p. 379.

is confirmed by the calculations. Interestingly, the main part of the negative charge is localized at the tellurium atoms. In contrast, there is only a small amount of the negative charge localized at the bridgehead phosphorus atoms P1 and P3. In Table 3 the calculated Mulliken charges for  $P_4Te_2^{2-}$  in the gas phase are summarized.

**Table 3. Mulliken charges of the phosphorus and tellurium atoms of  $P_4Te_2^{2-}$  in the gas phase.**

		
P1/P3	P2/P4	Te
-0.029	-0.344	-0.627

#### 4 Are there more phosphorus-tellurium anions?

As obviously the only possibility to synthesize P-Te anions is starting from  $P_4$  and  $Na_2Te_2$ , other stoichiometries were examined:

- $P_4 + 2 Na_2Te_2$
- $P_4 + 3 Na_2Te_2$
- $2 P_4 + Na_2Te_2$

In all cases the main product after 24 h is  $P_4Te_2^{2-}$  according to the corresponding  $^{31}P$  NMR spectra. Interestingly, also traces of other phosphorus rich compounds can be identified in the  $^{31}P$  NMR spectra, however. After 24 h only traces of new phosphorus rich compounds could be identified in the  $^{31}P$  NMR spectrum (Figure 5).

After 5 days – the reaction solution was stored in the refrigerator at +4 °C – the signals of  $P_4Te_2^{2-}$  decreased, while the intensity of the signals for the new compounds increased.

After 18 days the signals caused by  $P_4Te_2^{2-}$  disappeared. In the  $^{31}P$  NMR spectrum broad signals appeared and the already observed new ones increased in intensity.

A  $^{31}P$ ,  $^{31}P$ -COSY 45 NMR spectrum revealed cross peaks between the signal groups at  $\delta^{31}P = 168.8, 79.4, -6.0, -113.9, -138.6$  and  $-199.2$  with an intensity ratio of 1:1:1:1:1:1. Therefore, the corresponding new compound must contain six phosphorus atoms obviously arranged in a polycyclic structure. In further investigations the connectivity of the phosphorus atoms has to be determined.

After 4 weeks a further  $^{31}P$  NMR spectrum of the reaction solution was measured. This time no additional signals were observed.

So it can be concluded that the observed P-Te anions are metastable compounds which decompose within several weeks. The same results are found for the other stoichiometries investigated. No further P-Te containing compounds can be identified for sure.

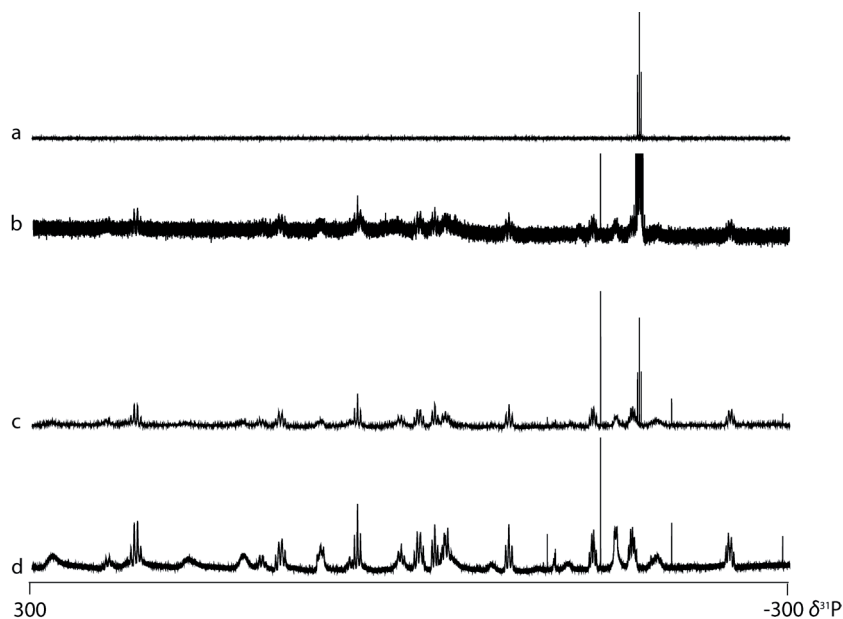


Figure 6. Observed  $^{31}\text{P}$  NMR spectra of the reaction mixture during a period of time in *N*-methyl imidazole: (a) after 24 h; (b) enlarged baseline of the observed  $^{31}\text{P}$  NMR spectrum of the reaction mixture after 24 h; (c) after 5 d; (d) after 18 d.

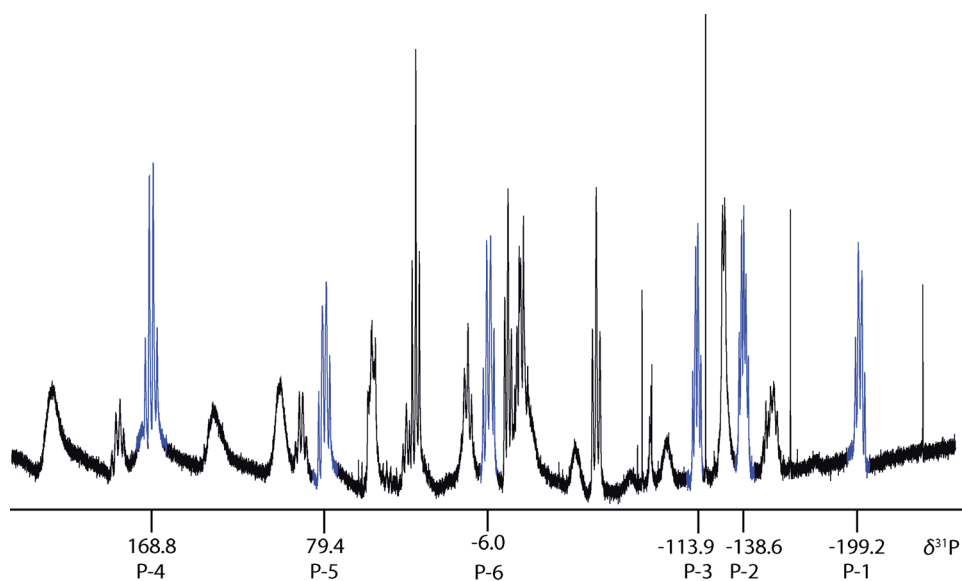
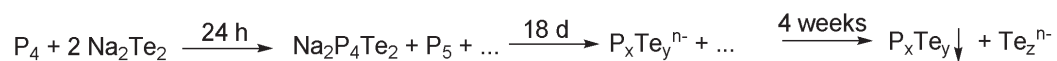


Figure 7.  $^{31}\text{P}$  NMR spectrum of the reaction mixture (32768 scans with a relaxation delay of 0.5 sec., 16.7 h measuring time). Signals which belong to the  $\text{P}_6$  compound are marked in blue.

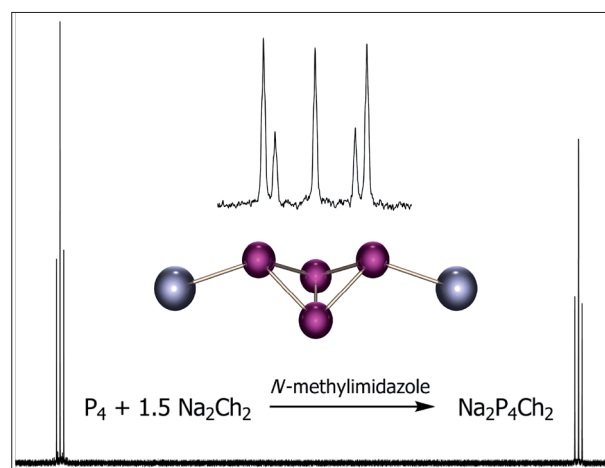


Scheme 5. Decomposition of  $\text{P}_4\text{Te}_2^{2-}$ .

## 5 Conclusion

With the synthesis of the first discrete P-Te anion  $\text{P}_4\text{Te}_2^{2-}$  (**1**) and its full characterization by  $^{31}\text{P}$  and  $^{125}\text{Te}$  NMR spectroscopy, described here, it could be demonstrated that binary phosphorus tellurium anions can exist as stable species in solution. The results suggest the possible existence of further phosphorus-rich P-Te anions like  $\text{P}_6\text{Te}_4^{2-}$ .

The quantum chemical calculations confirm the structure of  $\text{P}_4\text{Te}_2^{2-}$  and elucidate the charge distribution within the  $\text{P}_4\text{Te}_2^{2-}$  anion in the gas phase which is found as expected.



## 6 Experimental Section

**General procedure.** All reactions were carried out under inert gas atmosphere using Schlenk techniques. Argon (Messer Griesheim, purity 4.6 in 50 L steel cylinder) was used as inert gas. All glass vessels used were stored in a 130°C drying oven and were flame-dried in vacuum at  $10^{-3}$  mbar before use.

White phosphorus (ThermPhos) was peeled under water, washed with dry THF and dried under vacuum. The sodium dichalcogenides were prepared according to a literature procedure and stored in a dry box under nitrogen atmosphere.<sup>1</sup> *N*-methyl imidazole (Aldrich) was used as received.

**NMR Spectroscopy.** NMR spectra were recorded with a Jeol EX 400 Eclipse instrument operating at 161.997 MHz ( $^{31}\text{P}$ ), and 126.256 MHz ( $^{125}\text{Te}$ ). Chemical shifts are referred to 85 %  $\text{H}_3\text{PO}_4$  ( $^{31}\text{P}$ ) and  $(\text{CH}_3)_2\text{Te}$  ( $^{125}\text{Te}$ ). All spectra were measured at 25 °C. For the simulation of the  $^{31}\text{P}$  NMR spectra, the PERCH program package was used.<sup>11</sup>

From the resulting reaction solutions a sample was transferred into a 5 mm NMR tube closed with a ground-glass stopper for multinuclear NMR spectroscopic investigations.

**$\text{Na}_2\text{P}_4\text{S}_2$ .** The yellow solution of  $\text{P}_4$  in *N*-methyl imidazole became green after the addition of  $\text{Na}_2\text{S}_2$ . After five minutes stirring at room temperature the reaction solution turned yellow and the formation of an orange-yellow precipitate was observed.

**$\text{Na}_2\text{P}_4\text{Se}_2$ .** After the addition of  $\text{Na}_2\text{Se}_2$  a red brown suspension formed immediately.

**$\text{Na}_2\text{P}_4\text{Te}_2$ .** To a solution of  $\text{P}_4$  (1 mmol) in 5 mL of *N*-methyl imidazole  $\text{Na}_2\text{Te}_2$  (1.5 mmol) was added with stirring at ambient temperature, which was continued for 12 h, thus a purple colored solution could be obtained.

**$\text{P}_4 + 2 \text{Na}_2\text{Te}_2$**

To a solution of  $\text{P}_4$  (2.8 mmol) in 10 mL of *N*-methyl imidazole  $\text{Na}_2\text{Te}_2$  (5.6 mmol) was added at ambient temperature. A dark red colored reaction solution was obtained.

**$\text{P}_4 + 3 \text{Na}_2\text{Te}_2$**

1.98 mmol of white phosphorus were dissolved in 10 mL of *N*-methyl imidazole. 5.95 mmol  $\text{Na}_2\text{Te}_2$  were added at ambient temperature, and a dark red reaction suspension could be obtained.

**$2 \text{P}_4 + \text{Na}_2\text{Te}_2$**

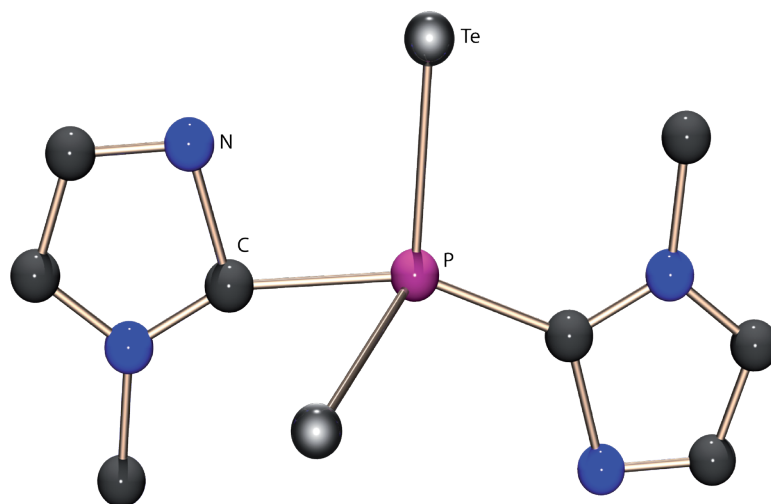
To a solution of white phosphorus (1.46 mmol) in 4 mL of *N*-methyl imidazole  $\text{Na}_2\text{Te}_2$  (0.73 mmol) were added in one portion at room temperature. The reaction mixture turned orange brown.

<sup>11</sup> Boudjouk, P.; Thompson, D. P. *J. Org. Chem.*, **1988**, *53*, 2109 – 2112.

## CHAPTER XIV

---

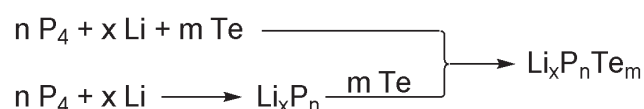
### Some Unexpected Compounds in the Reaction of White Phosphorus, Lithium and Tellurium



*In course of the investigations on the syntheses of new phosphorus tellurium anions in solution starting from the elements white phosphorus, lithium and tellurium in N-methyl imidazole, some new and interesting compounds can be observed. Consequently, the syntheses of these new compounds containing N-methylimidazole were investigated.*

## 1 Introduction

In the course of the investigation on the syntheses of phosphorus-tellurium anions one strategy I tried, was the reaction of the elements white phosphorus, lithium and tellurium in *N*-methyl imidazole or THF as reaction medium (Scheme 1).



Scheme 1. Synthetic strategy for  $\text{Li}_x \text{P}_n \text{Te}_m$ .

In case of *N*-methyl imidazole as reaction medium, I could identify some new and unexpected compounds in the corresponding  $^{31}\text{P}$  NMR spectra. These compounds are described in the present chapter.

## 2 Results and Discussion

White phosphorus, lithium and tellurium in a molar ratio of 1 : 1.6 : 3.1 were stirred in *N*-methyl imidazole for one hour at ambient temperature. A purple solution was obtained. The  $^{31}\text{P}$  NMR spectrum of the reaction solution did not indicate the formation of binary phosphorus-tellurium anions. However, the signals of some new and unexpected species were observed, which are discussed in detail below:

At a  $^{31}\text{P}$  NMR chemical shift of  $\delta = -158.4$  a singlet accompanied by one pair of  $^{125}\text{Te}$  satellites was observed. The value of the  $^1J_{\text{TeP}}$  coupling constant is 1.28 kHz. The intensity ratio of the satellite pair to the total intensity of the signal is 12.2 %, which indicates the presence of two tellurium atoms directly bonded to phosphorus.  $^{31}\text{P}$  chemical shift and  $^1J_{\text{TeP}}$  coupling constant fit well to those of  $[\text{Ph}_2\text{PTe}_2][\text{Li}(\text{THF})_{3.5}(\text{TMEDA})_{0.25}]$  reported by Davies et al.:  $\delta^{31}\text{P} = -123.8$  ppm,  $^1J_{\text{TeP}} = 1.53$  kHz.<sup>1</sup> Based on this similarity the structure **1** of a ditellurophosphonate with two *N*-methyl imidazole moieties bonded to phosphorus via C2 is suggested (Figure 1).

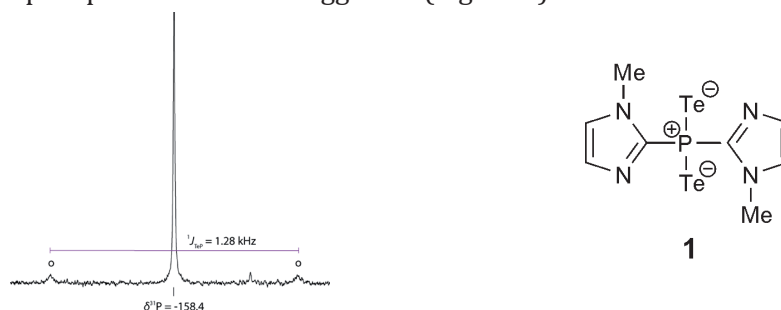


Figure 1.  $^{31}\text{P}\{^1\text{H}\}$  NMR spectrum of **1** in *N*-methyl imidazole. (0.1 M; 29214 scans, 14.9 h measuring time);  $^{125}\text{Te}$  satellites are marked with o.

<sup>1</sup> Davies, R. P.; Martinelli, M. G.; Wheatley, A. E. H.; White, J. P.; Williams, D. J. *Eur. J. Inorg. Chem.* **2003**, 3409.

Another singlet with one pair of <sup>125</sup>Te satellites can be observed at  $\delta^{31}\text{P} = -32.7$ . The  $^1J_{\text{TeP}}$  coupling constant is 1.68 kHz. The intensity ratio of the satellite pair is 8.5 %. Thus it can be concluded that only one tellurium atom directly bonded to phosphorus must be present in the molecule. In addition, one pair of <sup>13</sup>C satellites is clearly visible (Figure 2). The relative intensity of the <sup>13</sup>C satellites can only be roughly estimated (4.2 %) it indicates, however, the presence of more than one carbon atom bonded to phosphorus. Thus, structures **2** and **3** seem possible. The values of  $^1J_{\text{TeP}}$  and  $^1J_{\text{PC}}$  allow distinguishing between the two structures. The value of 1.68 kHz of  $^1J_{\text{TeP}}$  corresponds well to those observed for phosphorus tellurides R<sub>3</sub>P<sup>+</sup>Te<sup>-</sup> (1663 – 2153 Hz)<sup>2</sup>, while for R<sub>2</sub>P<sup>+</sup>Te with a trivalent phosphorus much smaller values are reported, e.g.  $^1J_{\text{TeP}} = 747$  Hz of [Ph<sub>2</sub>P<sup>+</sup>Te][Li(TMEDA)<sub>1.33</sub>(THF)<sub>1.33</sub>] ( $\delta^{31}\text{P} = -32.5$  ppm).<sup>1</sup> In addition, the value of 120 Hz for  $^1J_{\text{PC}}$  indicates clearly the presence of a tetracoordinate phosphorus atom, while for  $^1J_{\text{PC}}$  to a threecoordinate phosphorus again much smaller values are typical (565 – 775 Hz).<sup>1,3</sup> Both coupling constants thus clearly support structure **2** of a phosphorus telluride.

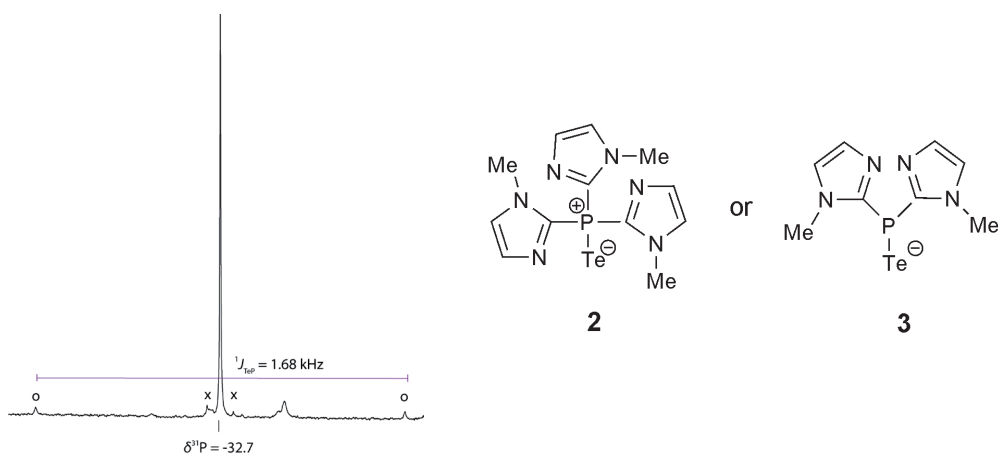


Figure 2. <sup>31</sup>P{<sup>1</sup>H} NMR spectrum of **2** in *N*-methyl imidazole. (0.1 M; 29214 scans, 14.9 h measuring time); <sup>13</sup>C satellites are marked with x; <sup>125</sup>Te satellites are marked with o.

Both compounds discussed above imply reactions of the solvent and *N*-methyl imidazole in position 2 with formation of a P-C bond. In order to put more light on the mechanism of formation of compounds **1** and **2**, the reaction of P<sub>4</sub> with lithium in *N*-methyl imidazole was investigated.

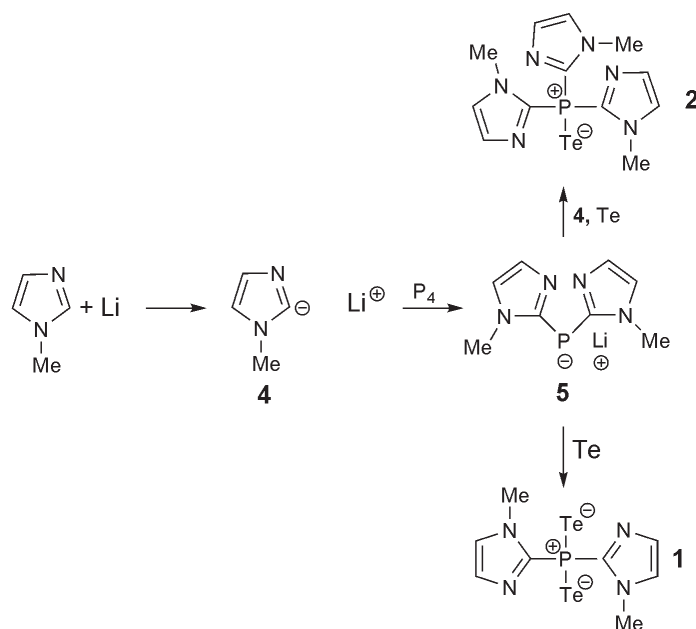
<sup>2</sup> Jones, C. H. W.; Sharma, R. D. *Organometallics*, **1987**, 6(7), 1419-1423.

<sup>3</sup> Bildstein, B.; Sladky, F. *Phosphorus, Sulfur Silicon and Relat. Elem.* **1990**, 47, 341-347.

*Possible reaction mechanism*

The formation of the compounds **1** and **2** described above, can be explained if we assume metallation of *N*-methyl imidazole in 2-position with lithium to compete effectively with the reduction of  $P_4$  to polyphosphides. Metallation of *N*-methyl imidazole in 2-position has been described in literature. Nucleophilic degradation of  $P_4$  by this carbanionic species **4** might lead to the bis(imidazolyl)phosphide **5**, telluration of which should give the anion **1**. Formation of phosphides like **5** by nucleophilic degradation of  $P_4$  has first been described by A. Schmidpeter. The phosphine telluride **2** might result from the oxidative coupling of **4** and **5** (by elemental tellurium) and successive telluration (Scheme 2).

Scheme 2. Reaction scheme of  $P_4$  and lithium in *N*-methyl imidazole.



The observed reaction of lithium with the solvent *N*-methyl imidazole might result from the fact, that white phosphorus, lithium and tellurium were first put into the Schlenk flask and *N*-methyl imidazole was added afterwards. As white phosphorus dissolves quite slowly in *N*-methyl imidazole, lithium would have the chance to react with the solvent before it reacts with phosphorus, due to the only small amounts of  $P_4$  present in solution in the beginning.

Thus,  $P_4$  was first dissolved in *N*-methyl imidazole and then lithium was added. The yellow solution warmed up and its color changed into brownish-red. The  $^{31}P$  NMR spectrum of the reaction mixture is shown in Figure 3.

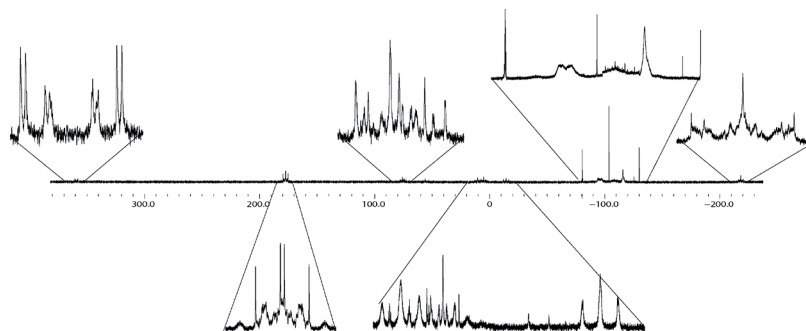


Figure 3.  $^{31}\text{P}\{^1\text{H}\}$  NMR spectrum in *N*-methyl imidazole. (0.1 M; 7507 scans, 3.8 h measuring time).

Three groups of resonances at  $\delta^{31}\text{P} = 177$ ,  $-109.5$  and  $-218$  can be assigned to  $\text{P}_{11}^{3-}$  described by M. Schuster in his dissertation.<sup>4</sup>

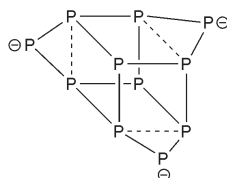


Figure 4. Lewis formula of  $\text{P}_{11}^{3-}$ .

The singlet at a  $^{31}\text{P}$  NMR chemical shift of  $-80.5$  ppm is accompanied by one pair of  $^{13}\text{C}$  satellites. The  $^1J_{\text{PC}}$  coupling constant of 72 Hz indicates a direct bond of the carbon atoms to phosphorus. Thus the  $^{31}\text{P}$  NMR resonance at  $-80.5$  ppm can be attributed to the phosphide **5** (Figure 5).

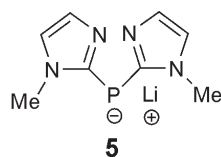


Figure 5. Lewis formula of compound **5**.

In literature there are similar compounds described:  $\text{Ph}_2\text{P}^-$ ,  $\text{PhP}(\text{CN})^-$  and  $(\text{CN})_2\text{P}^-$ .<sup>5,6,7</sup> The corresponding  $^{31}\text{P}$  NMR chemical shifts of these compounds are related to the organic substituents present. The more electron withdrawing the substituent is, the more the  $^{31}\text{P}$  NMR chemical shift is shifted to higher field. Thus, the  $^{31}\text{P}$  NMR chemical shift found for  $(\text{CN})_2\text{P}^-$  is  $-193$  ppm, in contrast to the  $^{31}\text{P}$  NMR chemical shift assigned for  $\text{Ph}_2\text{P}^-$   $-20$  ppm. It can be concluded that *N*-methyl imidazole is an electron donating substituent, but not of that quality like phenyl groups.

<sup>4</sup> Schuster, M. *dissertation*, LMU Munich, 1999.

<sup>5</sup> Fluck, F.; Issleib, K. Z. *Naturforsch. Teil B*, **1965**, *20*, 1123

<sup>6</sup> Schmidpeter, A.; Zirzow, K.-H.; Burget, G.; Huttner, G.; Jibril, I. *Chem. Ber.*, **1984**, *117*, 1695-1706.

<sup>7</sup> (a) Schmidpeter, A.; Zwaschka, F. *Angew. Chem., Int. Ed. Engl.*, **1977**, *16*, 704. (b) Sheldrick, W. S.; Kroner, J.; Zwaschka, F.; Schmidpeter, A. *Angew. Chem.* **1979**, *91*, 998. (c) Sheldrick, W. S.; Kroner, J.; Zwaschka, F.; Schmidpeter, A. *Angew. Chem., Int. Ed. Engl.* **1979**, *18*, 934.

At a chemical shift of  $\delta^{31}\text{P} = 358$  the A-part of an AA'XX' spin system was identified. Signals at such low field are typical for the dicoordinate phosphorus atom in diphosphenes.<sup>8</sup> A similar chemical shift and splitting pattern was also observed for the central two phosphorus atoms in **7**, described by A. Wörner et al.<sup>9</sup> Although the X-part of this system could not yet be identified with certainty, the observed signal strongly indicates the presence of an analogous *N*-methyl imidazole substituted compound in the solution (Figure 6)



Figure 6. *Left*: Lewis structure of compound **6**; *right*: Lewis structure of compound **7**<sup>[9]</sup>.

Elemental tellurium was added to the reaction solution described above to give a dark purple reaction solution. The  $^{31}\text{P}$  NMR spectrum of the reaction solution revealed that the compounds described above have reacted and resonances of new compounds have appeared, as well as the already described resonance of **2**.

In addition signal groups at  $\delta^{31}\text{P} = 100.8, 62, 36, -51, -115, -142$  can be observed, which are most probably due to new binary phosphorus-tellurium anions.

Because of the great interest in the anion **6** attempts were made to synthesize it as the main product. Stoichiometric amounts of white phosphorus, lithium and *N*-methyl imidazole were reacted in THF at ambient temperature. In the  $^{31}\text{P}$  NMR spectrum the following compounds were identified without any doubt:  $(N\text{-MeIm})_2\text{PLi}$  [<sup>10</sup>],  $\text{P}_{11}^{3-}$  and  $\text{P}_5^-$  ( $\delta^{31}\text{P} = 467$ ).<sup>11</sup> The signals of  $[(N\text{-MeIm})_2\text{P}_4]\text{Li}_2$  were not observed.

Also another stoichiometry ( $\text{P}_4 : \text{Li} : N\text{-MeIm} 1:1:1$ ) as well as other reaction conditions ( $-80\text{ }^\circ\text{C}$ ) were applied, according to literature procedure.<sup>8,12</sup> A red reaction solution was obtained and NMR spectroscopically investigated. The products observed are  $\text{P}_5^-$ ,  $\text{P}_{16}^{2-}$  ( $\delta^{31}\text{P} = 60, 39, 6, -34, -132, -172$ )<sup>13</sup> and  $\text{P}_4$ .

I also tried to selectively prepare bis(*N*-methyl imidazolyl)phosphide **5** as the main product. Stoichiometric amounts of  $\text{P}_4$ , lithium and *N*-methyl imidazole were reacted in THF. A green reaction solution was obtained and  $^{31}\text{P}$  NMR spectroscopically investigated. The anion **5** as well as  $\text{P}_7^{3-}$  and other not further identified products, the signals of which split into multiplets in the  $^{31}\text{P}$ - $^1\text{H}$  coupled NMR spectrum were observed.

<sup>8</sup> Schrödel, H.-P.; Schmidpeter, A. *Phosphorus, Sulfur, Silicon Relat. Elem.* **1997**, *129*, 69.

<sup>9</sup> Wiberg, N.; Wörner, A.; Karaghiosoff, K.; Fenske, D. *Chem. Ber. Recueil*, **1997**, *130*, 135.

<sup>10</sup> *N*-MeIm = *N*-methyl imidazole

<sup>11</sup> Baudler, M.; Düster, D.; Ouzounis, D. *Z. Anorg. Allg. Chem.* **1987**, *544*, 87.

<sup>12</sup> Wiberg, N.; Wörner, A. *Eur. J. Inorg. Chem.*, **1998**, *118*, 833.

<sup>13</sup> Baudler, M. *Z. Anorg. Allg. Chem.*, **1985**, *529*, 7.

Attempts were made to isolate the phosphide **5** in the solid state by slow diffusion of diethylether into the reaction mixture. After some days, colorless crystals were obtained and characterized using single crystal X-ray diffraction.

The crystal consists of [Me<sub>2</sub>(O)Si(N-Melm)]Li, which crystallizes in the trigonal space group *R*-3.

The silicium atoms are distorted tetrahedrally coordinated by three carbon and one oxygen atom. The corresponding bond angles range from 113° to 104°. The averaged Si-C bond distances of 187 pm are in accord with literature known values of Si-C single bonds.<sup>14</sup> The Si-O distance is 158 pm long, and therefore in between the values for Si-O single bonds and Si=O double bonds.<sup>15</sup>

The lithium and oxygen atoms in the asymmetric unit are arranged along the *b* axis in a planar fourmembered ring, as the angle sum is 360°. The lithium atoms are tetra coordinated by three oxygen and one nitrogen atom. The coordination sphere of Li1 is built by O1, O2, O1(*i*) and N2; the coordination sphere of Li2 is formed by O1, O2, O2(*ii*) and N3. The distances between the lithium atoms and the oxygen or nitrogen atoms correspond to those found in bis[(μ<sub>2</sub>-benzyl-diethylphosphonato-O,O)-(1,4-diazabicyclo(2.2.2)octane-*N,N'*)-lithium].<sup>16</sup>

Along the *c* axis, the oxygen and lithium atoms are forming two sixmembered rings lying eclipsed one above the other in chair conformation. The two sixmembered ring are formed by O1, Li1, O1(*i*), Li1(*i*), O1(*ii*) Li1(*ii*) respectively Li2, O2, Li2(*i*), O2(*i*), Li2(*ii*), O2(*ii*). As the two sixmembered rings are eclipsed, there is always one lithium atom of the one ring placed over the oxygen atom of the other ring, so there are coordinative interactions between the two rings.

Furthermore, one lithium atom is connected to one neighbored oxygen atom not only through electrostatic interactions, but also due to a N-C-Si bridge, forming a non planar five membered ring (O1, Si2, C2, N2, Li1 and Li2, O2, Si1, C8, N3).

Despite the described interactions and bonds within one molecule, there are no other interactions found between the molecules within the unit cell.

The formation of this compound can be explained by the reaction of ground joint fat containing a polymeric methylated silicon compound.

<sup>14</sup> Allen, F. H.; Kennard, O.; Watson, D. G.; Brammer, I.; Orpen, A. G.; Taylor, R. J. *Chem. Soc. Perkin Trans. II* **1987**, S1.

<sup>15</sup> Holleman, A.F.; Wiberg, F.; Wiberg, N. *Lehrbuch der anorganischen Chemie*, de Gruyter, Berlin **1995**, 101. Auflage

<sup>16</sup> Zarges, W.; Marsch, M.; Harms, K.; Haller, F.; Frenking, G.; Boche, G. *Chem. Ber.* **1991**, *124*, 861.

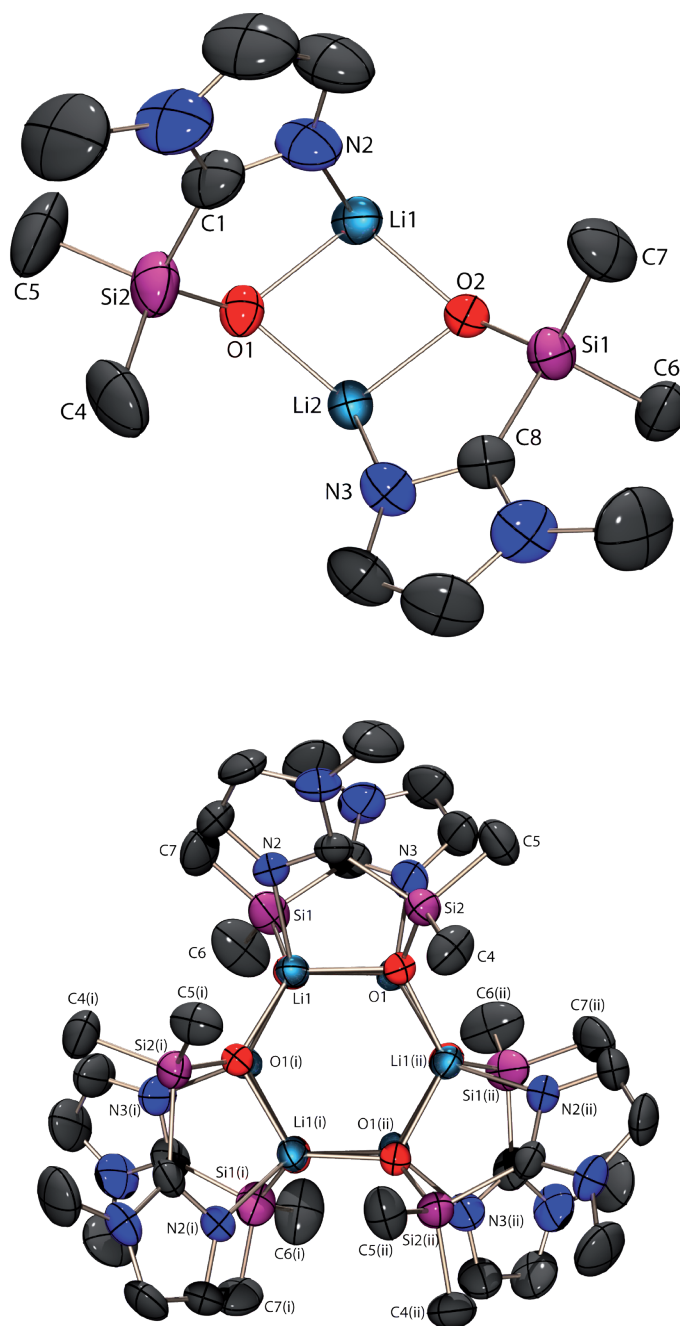


Figure 7. Top: asymmetric unit of [Me<sub>2</sub>(O)Si(N-Melm)]Li, view along *b* axis. Bottom: molecular structure of [Me<sub>2</sub>(O)Si(N-Melm)]Li in the crystal, view along *c* axis, *i* = -*y*, *x*-*y*, *z*, *ii* = -*x*+*y*, -*x*, *z*. Ellipsoids are drawn at the 50 % probability level, hydrogen atoms are omitted for clarity.

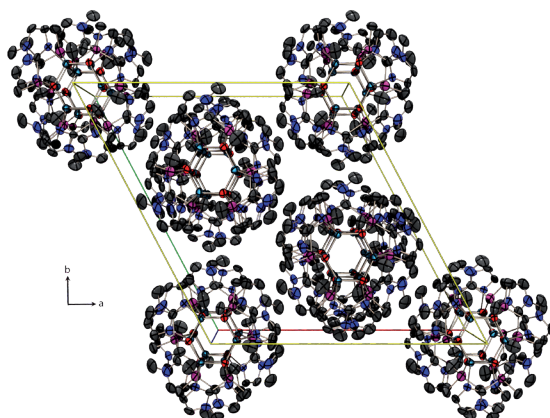


Figure 8. Molecular structure of  $[\text{Me}_2(\text{O})\text{Si}(\text{N-Melm})]\text{Li}$  in the unit cell. View along the  $c$  axis. The ellipsoids are drawn at the 50 % probability level.

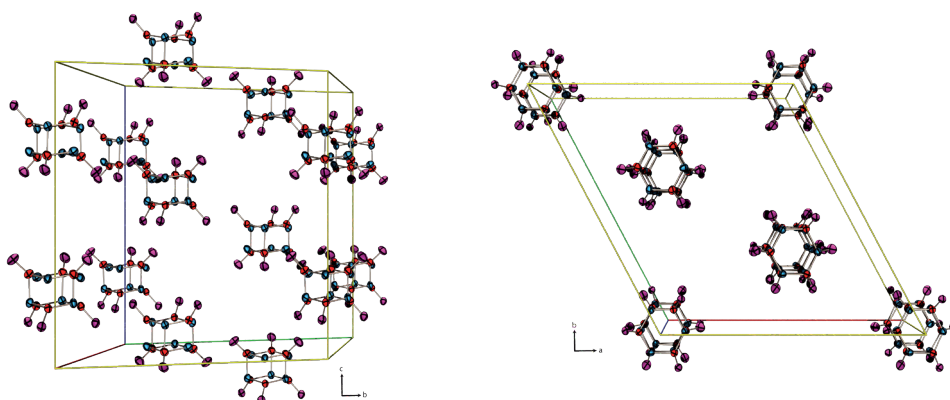


Figure 9. Molecular structure of  $[\text{Me}_2(\text{O})\text{Si}(\text{N-Melm})]\text{Li}$  in the unit cell. View along the  $a$  axis (left) and along the  $c$  axis (right). The ellipsoids are drawn at the 50 % probability level. Hydrogen, nitrogen and carbon atoms are omitted for clarity.

Table 1. Selected bond parameters of  $[(\text{Me}_2(\text{O})\text{Si}(\text{N-Melm}))\text{Li}]_i$ ,  $i = -y, x-y, z$ ,  $ii = -x+y, -x, z$ .

Distances [pm]		Angles [°]		Angles [°]	
Si1-O2	158.4(2)	O1-Si2-C1	104.76(17)	C8-N3-Li2	108.1(3)
Si1-C8	189.9(4)	O1-Li1-O1( <i>i</i> )	120.3(3)	Si1-C8-N3	119.6(2)
Si2-O1	158.3(2)	O1-Li1-O2	99.8(3)	Si1-O2-Li1	137.4(2)
Si2-C1	189.2(5)	O1-Li1-N2	93.8(3)	Si1-O2-Li2	111.33(19)
Si1-C6	185.5(4)	O1( <i>i</i> )-Li1-N2	125.0(4)	Si1-O2-Li2( <i>i</i> )	124.5(2)
Si1-C7	186.9(5)	O1( <i>i</i> )-Li1-O2	98.2(3)	Si2-C1-N2	118.9(3)
Si2-C4	187.2(5)	O1-Li2-O2	100.8(3)	Si2-O1-Li1	112.1(2)
Si2-C5	185.3(5)	O1-Li2-N3	121.1(3)	Si2-O1-Li1( <i>ii</i> )	126.5(3)
O1-Li1	198.3(8)	O1-Li2-O2( <i>ii</i> )	98.8(3)	Si2-O1-Li2	130.2(2)
O1-Li2	194.3(5)	O2-Si1-C8	104.74(14)	Li1-O1-Li2	79.9(3)
O1-Li1( <i>ii</i> )	190.6(7)	O2-Li1-N2	118.4(3)	Li1-O1-Li1( <i>ii</i> )	115.5(3)
O2-Li1	196.6(6)	O2-Li2-N3	94.6(3)	Li1( <i>ii</i> )-O1-Li2	81.7(3)
O2-Li2	197.9(8)	O2( <i>ii</i> )-Li2-N3	120.9(3)	Li1-O2-Li2	79.5(3)
O2-Li2( <i>i</i> )	191.2(8)	O2-Li2-O2( <i>ii</i> )	120.4(3)	Li1-O2-Li2( <i>i</i> )	81.0(2)
N2-Li1	207.8(7)	C1-N2-Li1	109.7(3)	Li2-O2-Li2( <i>i</i> )	114.8(3)
N3-Li2	208.8(6)				

As it is possible to synthesize  $(N\text{-MeIm})_2\text{PLi}$  in solution as main product, the reaction behavior with tellurium is investigated. Therefore  $(N\text{-MeIm})_2\text{PLi}$  is synthesized starting from  $\text{P}_4$ ,  $\text{BuLi}^{17}$  and  $N$ -methyl imidazole in THF, then elemental tellurium is added. So a red reaction suspension is obtained and investigated using  $^{31}\text{P}$  NMR spectroscopy. According to the  $^{31}\text{P}$  NMR spectrum,  $(N\text{-MeIm})_2\text{PLi}$  has abreacted and  $\text{P}_5^-$  and  $\text{P}_7^{3-}$  can be identified as by-products. In addition new signals can be observed, but it is not possible to determine the corresponding compounds:

At  $\delta^{31}\text{P} = -58.7$  a singlet with three pairs of satellites can be identified. The coupling constants are 109, 468 and 871 Hz. The values of the coupling constants are within the range of the values for  $^1J_{\text{TeP}}$  couplings constants (84 - 2290 Hz) reported in literature.<sup>18</sup> Another singlet at  $\delta^{31}\text{P} = -60.4$  is accompanied by two pairs of satellites with values of 143 and 294 Hz. As already mentioned, in both cases it is not possible to suggest structures for the compounds causing these signals. Furthermore, some not interpretable spin systems appear in the spectrum. The  $^{125}\text{Te}$  NMR spectrum shows a singlet at a  $^{125}\text{Te}$  NMR chemical shift of  $-335.0$  ppm.

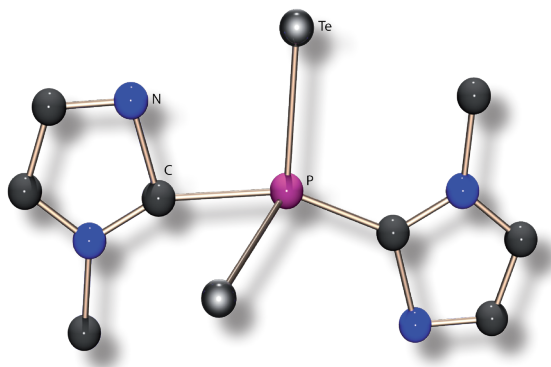
<sup>17</sup> BuLi = butyl lithium

<sup>18</sup> Karaghiosoff, K. In *Encyclopedia of Nuclear Magnetic Resonance*; Grant, D. M., Harris, R. K., Eds.: Wiley: Chichester, U.K., 1996; Vol. 6, pp 3612.

### 3 Conclusion

New reaction products of white phosphorus, lithium, tellurium and *N*-methyl imidazole can be observed and structurally characterized using <sup>31</sup>P NMR spectroscopy. It was also possible to formulate a way of formation of the new compounds.

In addition, the molecular structure of [Me<sub>2</sub>(O)Si(*N*-MeIm)]Li can be determined using single crystal X-ray diffraction.



## 4 Experimental Section

**General procedure.** All reactions were carried out under inert gas atmosphere using Schlenk techniques. Argon (Messer Griesheim, purity 4.6 in 50 L steel cylinder) was used as inert gas. All glass vessels were stored in a 130 °C drying oven and were flame-dried in vacuum at  $10^{-3}$  mbar before use.

*N*-methyl imidazole, tellurium and elemental lithium (Aldrich) were used as received. Butyl lithium (Acros) was used as 2.5 M solution in hexane. White phosphorus (ThermPhos) was peeled under water, washed with dry THF and dried under vacuum.

**NMR spectroscopy.** NMR spectra were recorded using a Jeol EX 400 Eclipse instrument operating at 161.997 MHz ( $^{31}\text{P}$ ), and 126.256 MHz ( $^{125}\text{Te}$ ). Chemical shifts are referred to 85 %  $\text{H}_3\text{PO}_4$  ( $^{31}\text{P}$ ) and  $(\text{CH}_3)_2\text{Te}$  ( $^{125}\text{Te}$ ). All spectra were measured at 25 °C. The %-data correspond to the intensities in the  $^{31}\text{P}$  NMR spectra with respect to the total intensity. The difference to 100 % belongs to not determinable signals.

**X-ray crystallography.** The molecular structure of  $\text{Me}_2(\text{O})\text{Si}(\text{N-MeIm})\text{Li}$  in the crystalline state was determined using an Oxford Xcalibur3 diffraction instrument with a Spellman generator (voltage 50 kV, current 40 mA) and a Kappa CCD detector with a X-ray radiation wavelength of 0.71073 Å. The data collection was performed with the CrysAlis CCD software, the data reduction with the CrysAlis RED software.<sup>19,20</sup> The structures were solved with SIR-92, SIR-97 and SHELXS-97, refined with SHELXL-97 and finally checked using PLATON.<sup>21,22,23,24,25</sup> The absorptions were corrected by a SCALE3 ABSPACK multi-scan method.<sup>26</sup>

<sup>19</sup> CrysAlis CCD, Oxford Diffraction Ltd., Version 1.171.27p5 beta (release 01-04-2005 CrysAlis171 .NET), (compiled Apr 1 2005,17:53:34).

<sup>20</sup> CrysAlis RED, Oxford Diffraction Ltd., Version 1.171.27p5 beta (release 01-04-2005 CrysAlis171 .NET), (compiled Apr 1 2005,17:53:34).

<sup>21</sup> SIR-92, **1993**, *A Program for Crystal Structure Solution*; Altomare, A.; Cascarano, G. L.; Giacovazzo, C.; Guagliardi, A. *J. Appl. Cryst.* **26**, 343.

<sup>22</sup> Altomare, A.; Burla, M. C.; Camalli, M.; Cascarano, G. L.; Giacovazzo, C.; Guagliardi, A.; Moliterni, A. G. G.; Polidori, G.; Spagna, R. *J. Appl. Crystallogr.* **1999**, *32*, 115.

<sup>23</sup> Sheldrick, G. M. *SHELXS-97, Program for Crystal Structure Solution*; Universität Göttingen, **1997**.

<sup>24</sup> Sheldrick, G. M. *SHELXL-97, Program for the Refinement of Crystal Structures*; University of Göttingen, Germany, **1997**.

<sup>25</sup> Spek, L. A. *PLATON, A Multipurpose Crystallographic Tool*, Utrecht University, Utrecht, The Netherlands, **1999**.

<sup>26</sup> SCALE3 ABSPACK - *An Oxford Diffraction program* (1.0.4,gui:1.0.3) (C) 2005 Oxford Diffraction Ltd.

#### 4.1 Syntheses of new P-Te anions outgoing from the elements

##### P<sub>4</sub> + 1.6 Li + 3.1 Te

White phosphorus (267 mg, 8.61 mmol) was dissolved in 10 mL *N*-methyl imidazole. Then elemental lithium (96 mg, 13.79 mmol) and tellurium (3.4 g, 26.69 mmol) were suspended in 25 mL *N*-methyl imidazole and added to the solution of P<sub>4</sub>. The reaction suspension turned red, and heated up a little bit.

<sup>31</sup>P-<sup>1</sup>H-NMR (*N*-MeIm, RT): (*N*-MeIm)<sub>2</sub>P<sup>-</sup>Te<sub>2</sub><sup>-</sup> (11.8 %), (*N*-MeIm)<sub>3</sub>P<sup>-</sup>Te (24.5 %), δ = 120.5 (s, 6.6 %), 27.3 (s, 19.4 %), 20.2 (s, 3.5 %), -2.9 (s, 5.6 %), -10.4 (s, 2.5 %), -38.5 (s, 2.7 %), -115.4 (s, 11.2 %).

<sup>125</sup>Te-<sup>1</sup>H-NMR (*N*-MeIm, RT): δ = 26.3 (s, 86.3 %), -283.3 (s, 11.7 %), -428.1 (s, 1.9 %).

##### P<sub>4</sub> + 1.6 Li + 3.6 Te

140 mg (4.52 mmol) white phosphorus was dissolved in 14 mL *N*-methyl imidazole. 50 mg (7.23 mmol) lithium were added at ambient temperature. The yellow solution turned brownish red and heated up a little bit. Afterwards elemental tellurium (1.2 mL, 8 mmol) was added and the reaction suspension turned dark purple. The suspension was continued stirring at ambient temperature for 24 h.

<sup>31</sup>P-<sup>1</sup>H-NMR (*N*-MeIm, RT): (*N*-MeIm)<sub>2</sub>P<sup>-</sup> (12.7 %), P<sub>11</sub><sup>3-</sup> (33 %), (*N*-MeIm)<sub>2</sub>P<sub>4</sub>Li<sub>2</sub> (1.4 %), δ = -96 (d, 15.9 %), -103.7 (s, 1.98 %), -109.5 (q, 6.8 %), -129.9 (s, 1.7 %).

##### After the addition of tellurium:

<sup>31</sup>P-<sup>1</sup>H-NMR (*N*-MeIm, RT): (*N*-MeIm)<sub>3</sub>P<sup>-</sup>Te (4.5%), δ = 100.8 (t, 8.5 %), 62.0 (t, 2.2 %), 36.0 (t, 1.6 %), 27.4 (s, 8 %), 20.5 (s, 3.4 %), -10.5 (s, 1.2 %), -32.7 (s, 4.5 %), -115 (s, 14 %), -142.0 (m, 6.3 %), -156.5 (s, 4.1 %).

#### 4.2 Syntheses of (N-MeIm)<sub>2</sub>P<sub>4</sub>Li<sub>2</sub>

##### P<sub>4</sub> + 2 Li + 2 *N*-MeIm

White phosphorus (51 mg, 1.58 mmol) were dissolved in 10 mL THF. In another glass vessel, lithium (20 mg, 3.16 mmol) and *N*-methyl imidazole (259 mg, 3.16 mmol) were reacted in 5 mL THF yielding a green solution. This solution is added at once to the solution of white phosphorus. The reactions suspension immediately turned orange.

<sup>31</sup>P-<sup>1</sup>H-NMR (*N*-MeIm, RT): (*N*-MeIm)<sub>2</sub>PLi (10.6 %), P<sub>5</sub><sup>-</sup> (1.4%), δ = -2.46 (quintett, 21.9 %), -98.7 (s, 15.3 %), -176.7 (s, 12.3 %).

**P<sub>4</sub> + Li + *N*-MeIm**

58 mg (1.81 mmol) P<sub>4</sub> were dissolved in 4 mL THF and cooled down to -78°C afterwards. 1.81 mmol (1.81 mL) of an already prepared solution of *N*-MeImLi was added.<sup>27</sup> The suspension turned immediately brownish red.

<sup>31</sup>P-<sup>{1</sup>H}-NMR (THF, -80°C): (*N*-MeIm)<sub>2</sub>PLi (12.7 %), δ = -451.3 (s, 87.3 %).

<sup>31</sup>P-<sup>{1</sup>H}-NMR (THF, RT): P<sub>11</sub><sup>3-</sup> (99.1 %), (*N*-MeIm)<sub>2</sub>PLi (0.5 %), P<sub>5</sub><sup>-</sup> (0.4 %).

**4.3 Syntheses of (*N*-MeIm)<sub>2</sub>PLi****P<sub>4</sub> + 8 Li + 8 *N*-MeIm**

43 mg (1.39 mmol) white phosphorus were dissolved in 10 mL THF. In another flask 71 mg (11.1 mmol) lithium and 911 mg (11.1 mmol) *N*-MeIm were suspended in 5 mL THF. The greenish solution was added to the solution of P<sub>4</sub>, so an orange reaction suspension could be obtained. The reaction mixture was stirred 24 h at ambient temperature and the formation of a yellow precipitate could be observed and removed. So a green solution can be obtained of which 2 mL were transferred into another glass vessel for crystallization and 10 mL diethylether were allowed to diffuse slowly into the reaction suspension. After some days colourless crystals of Me<sub>2</sub>(O)Si(*N*-MeIm)Li could be obtained and analyzed using single crystal X-ray diffraction.

<sup>31</sup>P-<sup>{1</sup>H}-NMR (*N*-MeIm, RT): (*N*-MeIm)<sub>2</sub>PLi (27.9 %), P<sub>7</sub><sup>3-</sup> (18.2 %), δ = 37.1 (q, 11.8 %), -19.7 (t, 10.4 %), -2.9 (s, 5.6 %), -102.3 (t, 10.1 %), -133.4 (s, 21.7 %).

4 days later:

<sup>31</sup>P-<sup>{1</sup>H}-NMR (*N*-MeIm, RT): (*N*-MeIm)<sub>2</sub>PLi (30%), P<sub>7</sub><sup>3-</sup> (43 %), δ = -133.42 (s, 27 %).

**P<sub>4</sub> + 8 Li + 8 *N*-MeIm**

128 mg (4 mmol) white phosphorus were dissolved in 35 mL THF, and then lithium (222 mg, 32 mmol) and 2.63 g (32 mmol) *N*-MeIm were added. The reaction mixture turned red. It was continued stirring at ambient temperature for 24 h yielding a greenish reaction suspension.

<sup>31</sup>P-<sup>{1</sup>H}-NMR (THF, RT): (*N*-MeIm)<sub>2</sub>PLi (23.2 %), P<sub>7</sub><sup>3-</sup> (67.7 %), δ = -133.3 (s, 9.1 %).

After 24 h:

<sup>31</sup>P-<sup>{1</sup>H}-NMR (THF, RT): (*N*-MeIm)<sub>2</sub>PLi (16.7 %), P<sub>7</sub><sup>3-</sup> (65.6 %), δ = 106.6 (m, 5.2 %).

<sup>27</sup> 35 mg (5 mmol) lithium and 398 μL (5 mmol) *N*-methyl imidazole were reacted in 10 mL THF.

#### 4.4 Reaction of (N-MeIm)<sub>2</sub>PLi with tellurium

White phosphorus (80 mg, 2.5 mmol) were dissolved in 7.5 mL THF. In another flask, 319  $\mu$ L (4 mmol) *N*-methyl imidazole and 1.6 mL BuLi were reacted in 8 mL THF. The two solutions were combined, yielding an orange-red solution.

<sup>31</sup>P-{<sup>1</sup>H}-NMR (THF/Hexan, RT): (*N*-MeIm)<sub>2</sub>PLi (44.1 %),  $\delta$  = 53.8 (s, 1.5 %), 32.5 (q, 6.2 %), -16.2 (t, 5.7 %), -109.1 (t, 6 %), -134.4 (s, 35.6 %).

Elemental tellurium (319 mg, 2.5 mmol) were added to the reaction solution at ambient temperature. After one hour, a red solution was obtained, and all tellurium has abreacted.

<sup>31</sup>P-{<sup>1</sup>H}-NMR (THF, RT): P<sub>5</sub><sup>-</sup> (0.2%), P<sub>7</sub><sup>3-</sup> (26.9%),  $\delta$  = 9.5 (q, 6.7 %), -9.5 (m, 15.9 %), -58.7 (s, 6.6 %), -60.4 (s, 3.8 %), -75.5 (t, 8.6 %), -127.2 (m, 6 %), -137.5 (m, 13.2 %).

<sup>125</sup>Te-{<sup>1</sup>H}-NMR (THF, RT):  $\delta$  = -335 (s, 100 %).

Table 2. Crystal and structure refinement data.

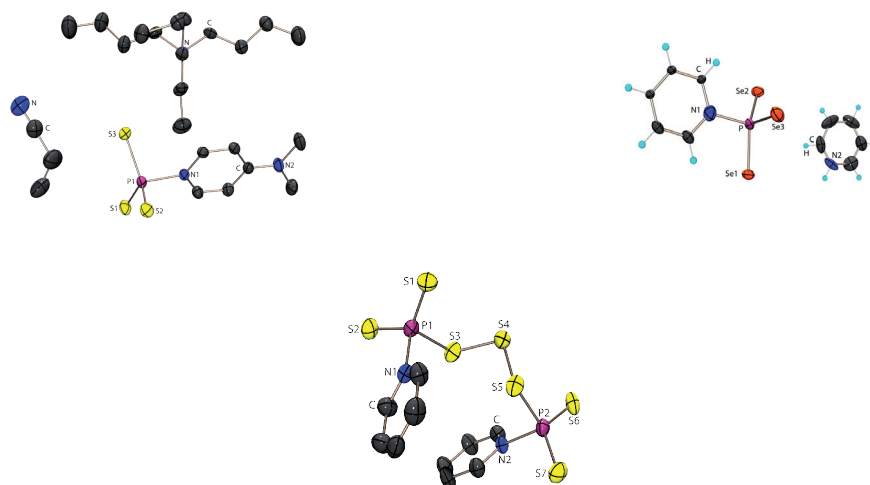
	<b>Me<sub>2</sub>(O)Si(N-Melm)Li</b>
empirical formula	C <sub>36</sub> H <sub>66</sub> N <sub>12</sub> Li <sub>6</sub> O <sub>6</sub> Si <sub>6</sub>
formula mass	973.16
temp (K)	200
cryst. size (mm)	0.2 x 0.15 x 0.1
cryst. descriptn.	colourless block
cryst. system	trigonal
space group	<i>R</i> -3
<i>a</i> (Å)	21.8036(10)
<i>c</i> (Å)	20.6909(8)
<i>V</i> (Å <sup>3</sup> )	8518.6(6)
<i>Z</i>	6
$\rho_{\text{calc}}$ (g cm <sup>-3</sup> )	1.138
$\mu$ (mm <sup>-1</sup> )	0.194
<i>F</i> (000)	3132
$\vartheta$ range (deg)	3.74-23.98
index ranges	-24 ≤ <i>h</i> ≤ 24, -24 ≤ <i>k</i> ≤ 24, -23 ≤ <i>l</i> ≤ 23
reflcs collcd	22172
reflcs obsd	2154
reflcs unique	2966 ( <i>R</i> <sub>int</sub> = 0.0439)
<i>R</i> 1, <i>wR</i> 2 (2 $\sigma$ data)	0.0495, 0.1126
<i>R</i> 1, <i>wR</i> 2 (all data)	0.0822, 0.1337
max/min transm	0.995/1.000
data/restr/params	2966/0/232
<i>S</i> on <i>F</i> <sup>2</sup>	1.055
larg. diff peak/hole (e/Å)	0.265/-0.289

## Conclusion

### 1 $\sigma^3\lambda^5$ - An unusual bonding situation for the phosphorus atom

Trithiometaphosphate  $\text{PS}_3^-$  and triselenometaphosphate  $\text{PSe}_3^-$  anions do exist as monomers in solution and are stable as monomers at ambient temperature. The results in the present thesis definitively put light on the controversies on the existence of  $\text{PS}_3^-$  anion. They also show for  $\text{PS}_3^-$  a low nucleophilicity at phosphorus. So we may call  $\text{PS}_3^-$  as a “heavy nitrate”. It was possible through the synthesis of  $[\text{nBu}_4\text{N}]_2[\text{P}_2\text{S}_6]$  • THF, a soluble salt in organic solvents, to observe an equilibrium between the monomeric  $\text{PS}_3^-$  anion and the corresponding dimer  $\text{P}_2\text{S}_6^{2-}$  in solution. The  $^{31}\text{P}$  NMR chemical shift of  $\text{PS}_3^-$  was determined reliably for the first time. Quantum chemical calculations justify the experimental results.

The stabilization of binary P, S compounds containing  $\sigma^3\lambda^5$  phosphorus atoms in the solid state can be achieved *via* adduct formation with a base like pyridine. The P-N distance gave much longer P-N single bond, which indicates the presence of weak adducts. The isolation of  $\text{py}_2\text{P}_2\text{S}_7$ ,  $\text{py}_2\text{P}_2\text{S}_5$ ,  $[\text{pyH}][\text{pyPS}_3]$  and  $[\text{pyH}][\text{pyPSe}_3]$  in the crystalline state and the NMR spectroscopic identification of  $\text{pyPCh}_2\text{X}$  (Ch = S, Se; X = Cl, Br) is the final evidence for this. In addition, quantum chemical calculations revealed that the double bond rule is set out of order for this kind of compounds with a  $\sigma^3\lambda^5$  phosphorus atom. The examined compounds  $\text{py}_2\text{P}_2\text{S}_5$  and  $\text{py}_2\text{P}_2\text{S}_7$  can therefore be regarded as new bis(pyridine) adduct stabilized neutral binary phosphorus sulfides.



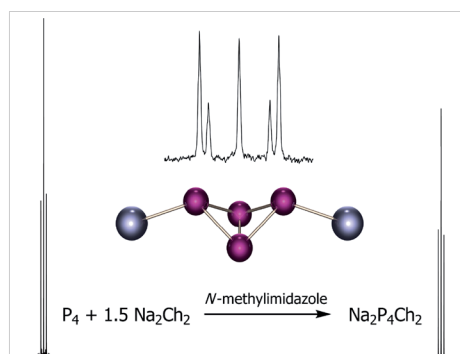
## 2 Alternative syntheses for chalcogenophosphates

The synthesis of chalcogenophosphates at ambient or lower temperature makes it possible to isolate metastable compounds like in the case of twist- $P_2Se_8^{2-}$ , which melts at 15 °C. The use of organic cations like  $Ph_4P^+$  or  $nBu_4N^+$  results in the formation of salts which are soluble in common aprotic organic solvents, like in the case of  $P_2S_6^{2-}$ . In case of the anions  $P_2S_8^{2-}$  and  $P_2Se_8^{2-}$ , consisting of sixmembered rings, it was shown that two conformers - twist- and chair- do exist in solution. There is a dynamic equilibrium between them. The twist conformer is favored in solution, while in the solid state, the chair conformer is isolated.



## 3 New fields of chalcogenophosphate chemistry – a first insight into P, Te anions

Binary P, Te, anions do exist and are stable in solution at ambient temperature. The nucleophilic degradation of white phosphorus in highly polar solvents like *N* methylimidazole with  $Na_2Te_2$  at ambient temperature yields the first P, Te anion  $P_4Te_2^{2-}$  in solution. It is characterized unequivocally by  $^{31}P$  and  $^{125}Te$  NMR spectroscopy. Further investigations revealed that  $P_4Te_2^{2-}$  is just an intermediate during the degradation of white phosphorus, it disproportionate with formation of other phosphorus rich tellurophosphates.







---

## CHRISTIANE ANGELIKA ROTTER

**Geburtsdatum** 13.12.1981  
**Geburtsort** Augsburg  
**Familienstand** ledig  
**Staatsangehörigkeit** deutsch

### Schulbildung

1992 bis 2001	Abitur	Gymnasium Wertingen
1988 bis 1992	Grundschule	Biberbach

### Wissenschaftlicher Werdegang

2007 bis jetzt	Promotion im Fachbereich Anorganische Chemie unter der Anleitung von Prof. Dr. K. Karaghiosoff	Ludwig-Maximilians-Universität München
2005 bis 2006	Studium Chemie Master Thema der Masterarbeit: <i>Systematische Untersuchung der Chalkogenophosphate <math>PX_3^-</math> und <math>P_2X_8^{2-}</math> mit <math>X = S, Se</math></i>	Ludwig-Maximilians-Universität München
2001 bis 2005	Studium Chemie Bachelor	Ludwig-Maximilians-Universität München

### Besuchte Tagungen

April 2009	12 <sup>th</sup> International Seminar: New Trends in Research of Energetic Materials, Pardubice (Tschechien)
März 2009	6 <sup>th</sup> European Workshop on Phosphorus Chemistry, Florenz (Italien): Moderation einer Vortragsreihe

- September 2008      13. Deutscher Fluortag, Schmitten
- März 2008            5<sup>th</sup> European Workshop on Phosphorus Chemistry, Regensburg (Deutschland):  
Vortrag mit dem Thema *New Chalcogenophosphates from White Phosphorus*
- März 2007            4<sup>th</sup> PhD Workshop on Phosphorus Chemistry, Zandvoort (Niederlande): Moderation einer Vortragsreihe

### Auszeichnungen

bester Vortrag (Thema: *New Chalcogenophosphates from White Phosphorus*, Regensburg 2008)

Römer-Preis 2007 für die Masterarbeit (Thema: *Systematische Untersuchung der Chalkogenophosphate  $PX_3^-$  und  $P_2X_8^{2-}$  mit  $X = S, Se$* )

### Publikationen

*An Unusual Binary Phosphorus-Tellurium Anion and its Seleno- and Thio Analogues:  $P_4Ch_2^{2-}$  ( $Ch = S, Se, Te$ ):* C. Rotter, M. Schuster, K. Karaghiosoff; im Druck.

*Structural and NMR Spectroscopic Investigations of Chair and Twist Conformers of the  $P_2Se_8^{2-}$  Anion:* C. Rotter, M. Schuster, M. Kidik, O. Schön, T. M. Klapötke, K. Karaghiosoff; *Inorg. Chem.* **2008**, 47(5), 1663-1673.

